UNIVERSITEIT GENT

FACULTEIT WETENSCHAPPEN
Vakgroep **Geologie en Bodemkunde**

# Proxy versus model-proxy comparison: Holocene climate evolution of the North Atlantic Ocean

*Bernd Rombaut*

Academiejaar 2009–2010

*Scriptie voorgelegd tot het behalen van de graad*
*Van Master in de Geologie*

Promotor: Dr. D. Van Rooij
Co-promotor: Prof. H. Goosse (UCL)
Leescommissie: Prof. M. De Batist, Dr. K. Mertens

**ABSTRACT**

An extensive database was created involving sea surface temperature reconstructions from the Atlantic Ocean of the Holocene period. The records from five different regular applied proxy methods have been included. The five proxies are alkenone unsaturation, Mg/Ca paired with $\delta^{18}O$ (planktonic foraminifera), and faunal assemblages of dinocysts, diatoms and planktonic foraminifera. The first two methods are used to reconstruct annual temperatures, while the faunal methods are used for summer and/or winter temperature reconstructions. There are four parts discussed in this thesis: (1) a comparison between the five proxies; (2) the temperature Holocene and the related oceanic circulation changes; (3) centennial timescale analysis of the data in relation to solar activity; (4) the comparison of proxy data with the ECBILT-CLIO-VECODE model.

A study of the differences in average Holocene temperatures, temperature evolution, and temperature variability between the proxy records reveals that there are some definite trends. Seasonal preference in productivity and growth season is considered to be the best explanation for anomalously high alkenone temperatures records toward higher latitudes. Deviating temperature trends and a lack of seasonal variability in planktonic foraminifera based records (faunal and Mg/Ca) from particularly mid and high latitudes suggest the influence of thermocline temperatures. This is consistent with the analysis that the average dwelling depth for planktonic foraminifera is deeper than for the other proxies. These findings thus suggest that particularly at high latitudes, the interpretation of at least three of the five proxy methods should be reconsidered.

Four distinct Holocene periods could be extracted from the records. A first period between roughly 11,5 and 9,5 ka BP is associated with a lot of temperature variability in the higher latitudes and a warming trend in practically the whole Atlantic region. The temperature increase and high variability have been associated with the start of meridional overturning circulation in the area between Greenland Iceland and Norway area and instability in the thermohaline circulation. The second period occurs between about 9,5 and 8 ka BP. This period is characterized by a small decrease in temperatures in most areas of the North Atlantic region (0,5-1,5°C), while the NW Atlantic experiences a sudden temperature rise. This temperature rise is most distinct (about 6°C) in the area west of the Reykjanes Ridge. A possible cause for this sudden replacement in heat distribution is a northward shift of the Gulf Stream due to high summer insolation and a high temperature gradient between eastern Canada and the warm Atlantic waters. Around 8 ka BP there is again a sudden change in temperature evolution. The 8,2 ka BP event and the initiation of Labrador Sea Water formation are most likely the triggers for this temperature shift (de Vernal et al., 2006). The period between about 8 and 5,5 ka BP is marked by an opposing temperature trend in the North Atlantic compared to the second period. The initiation of Labrador convection and a decrease in summer insolation probably lead to a southward shift of the Gulf Stream (Sachs, 2007). Decreasing summer insolation and the melt

of the last part of the Laurentide Ice Sheet probably lead to the last major reorganization of the oceanic and atmospheric circulation around 5,5 ka BP. The major temperature shift at about 5,5 ka BP could be related to a threshold in the southward shift of the Gulf Stream. The last period between 5,5 ka BP until preindustrial times, is a period of general temperature decrease in practically the whole Atlantic region. The most pronounced temperature decrease during the last 8 kyr is in the NE Atlantic. This and some other changes suggest a trend towards a positive NAO.

Analysis of the centennial variability of the records led to the discovery of periodicities of 150-200 year and about 500 year. Both periodicities indicate a relation with solar activity. The 150-200 year cycle probably corresponds to the ~205 year de Vries cycle. A comparison of the 500 year cycle with solar activity minima also suggests a strong similarity between the two.

The ECBilt-CLIO-VECODE model is able to estimate average temperature changes over a broad latitudinal band, but it fails picking up local changes. The fact that the model does not simulate the southward shift in the Gulf Stream, probably leads to the anomalously high temperatures in the Atlantic region between particularly 50 and 60°N. From all the models in the PMIP2 database, only the CSIRO-Mk3L-1.1 model seems to simulate the southward shift in the Gulf Stream.

AKNOWLEDGEMENTS

The development of the extensive database could be achieved thanks to data obtained from the PANGAEA and WDC-A databases, and via personnel communication with several researchers. Therefore I would like to thank An de Vernal and Julian Sachs.

Finally I also want to thank my promotor, Dr. David Van Rooij, for his constructive comments.

# INDEX

## Introduction

The North Atlantic region has been proven to be one of the key areas concerning global climate change (Bianchi and McCave, 1999; Sachs, 2007). The Gulf Stream, North Atlantic Current and its extensions form a strong and complex current system (Krauss et al., 1990; Mann, 1967), and are globally the main contributors to poleward heat transport (Macdonald and Wunsch, 1996). Although many studies have been devoted to this current system, the effect of climate change on these surface currents and the other way round are still not known in detail. This keeps the North Atlantic region very interesting for further analysis.

This study focuses on temperature evolution during the Holocene (11,7-0 ka BP). Several proxies and models have been used to reconstruct the Holocene climate. The most applied and reliable proxies are the alkenone biomarker, Mg/Ca in combination with oxygen isotopes, and the counting and statistical analysis of microfossils like dinocysts, foraminifera and diatoms (Birks, 2008). During the last decade a lot of Holocene climate simulating models have been developed and assembled in a database thanks to the foundation of the Paleoclimate Modeling Intercomparison Project (PMIP). The focus in this study is mainly on the ECBilt-CLIO-VECODE model (Renssen et al., 2004). This model includes an atmospheric, sea ice-ocean and vegetation component, but still lacks a dynamic ice sheet model.

Most of the studies find a similar general trend concerning the Holocene climate of the North Atlantic Ocean. In the early stages most proxy data provide evidence of a thermal optimum (10-8 ka BP) (Andreev et al., 2001; Duplessy et al., 2001; Kaufman et al., 2004; Koc et al., 1996; MacDonald et al., 2000; Marchal et al., 2002), which suggests a slightly delayed response to the maximum in high latitude summer insolation at 11 ka BP (Berger et al., 1978; Koc and Jansen, 1994). At northern high latitudes, and especially in northwest Canada, this optimum seems to occur much later (7-4 ka BP) (CAPE_project_members, 2001; Kaplan et al., 2002; Kaufman et al., 2004; Korhola et al., 2000; Levac et al., 2001a). The major delay of the Holocene maximum is explained by the influence of the albedo effect due to the remains of ice sheets and changes in vegetation. After this optimum there is a general, slow cooling trend, which shows considerable variability in the long-term trend. Cooling events seem to appear at millennial to centennial timescales (Dahl and Nesje, 1996; Duplessy et al., 2001; Korhola et al., 2000; Voronina et al., 2001). There is still a degree of uncertainty whether these cooling events are synchronous throughout the circumpolar region.

The first aim is to compare the different data from several proxies in the same oceanic settings, and draw conclusions concerning recurring deviations in temperature trends between the proxies. This analysis gives better insight in how to interpret the records of different proxies. A next step in this study is to divide the Holocene in several periods, with regards to major and widespread temperature shifts. These periods are then thoroughly analyzed relative to transition period and temperature trend.

The consequences of these findings on the current system and the North Atlantic Oscillation (NAO) are considered next. Special attention is hereby given to temperature changes in the Gulf Stream/North Atlantic Current region and Mediterranean Sea A third goal is to discuss how insolation (millennial timescale), solar variability and ice rafted debris (centennial timescale) affected temperatures during the Holocene. Regarding centennial variability, temperature records have initially been screened on periodicity. A final intention is the analysis of the differences between proxy records and the model output from the ECBilt-CLIO-VECODE model in particular. In addition, synthesis maps from different models predicting the mid Holocene temperature change are briefly compared in order to see which model(s) perform better. Examining differences between model output and proxy based data can contribute to improve models. The general idea of this study is to get a better understanding of the Holocene temperature evolution in the Atlantic region on millennial and centennial timescales.

This is the first study that combines data from the five most used temperature proxies in the Atlantic region. Comparing proxy data on this is important for a better understanding of the general differences between each of the proxies. Another innovating part in this study is the detailed comparison of records on a centennial timescale with regards to solar activity and ice rafted debris reconstructions. This analysis might lead to a better understanding of rapid climate changes in the North Atlantic region.

A few conventions are made. The first ones are with respect to the age and dating of events or periods. All ages are in calibrated year before present (BP). Periods are in kyr (1000 year time span), and fixed ages are in ka (1000 year ago). A second convention is on the timing of early, mid and late Holocene. These periods are loosely defined as 11,5-9,5 (early Holocene – EH), 9,5-5,5 (mid Holocene – MH) and 5,5-0 ka BP (late Holocene – LH).

Mind that a list of abbreviations is available in Appendix 1. All data tables related to this work are too much to integrate in this thesis, therefore they are all available on a CD-rom.

The first part of this thesis contains an extended literature study in which the oceanographic setting, the different proxies, the Holocene climate evolution in the Atlantic region and (paleo)climate modeling are thoroughly discussed. A second section considers the origin of the data, the construction of the database and the applied methods and software to obtain the results. In a next part a presentation of the data and a comparison of the different calibration/transfer function methods used for a same proxy are briefly analyzed. The fourth section contains the results including deflecting temperature trends between the different proxies, Holocene temperature evolution on a millennial and centennial timescale, and a comparison between model output and proxy data. The discussion of these results covers a fifth part. Finally, the conclusions are presented in the conclusion.

# I Literature Study

## 1. Oceanographic setting

### 1.1 Geographical setting

The collected data are reconstructed sea surface temperatures from sediment cores situated in the Atlantic Ocean (fig 1). Also Mediterranean Sea and Arctic Ocean records are included. The Atlantic Ocean is connected with the Arctic Ocean through the Denmark Strait, Greenland Sea, Norwegian Sea and Barents Sea. Labrador Sea and Davis Strait form gateways to the Hudson Bay and the Baffin Bay in the northwest Atlantic. The eastern and western sides are enclosed by continents that have an important role in orchestrating the ocean currents. The Strait of Gibraltar connects the Atlantic with the Mediterranean Sea. Other seas that are associated with the Atlantic, and mentioned further are the North Sea and Baltic Sea in the northeast Atlantic, the Gulf of Mexico and Caribbean Sea in the west equatorial area, the Gulf of Guinea in the east equatorial region, and finally the Irminger Sea in the central North Atlantic south of the Denmark Strait.

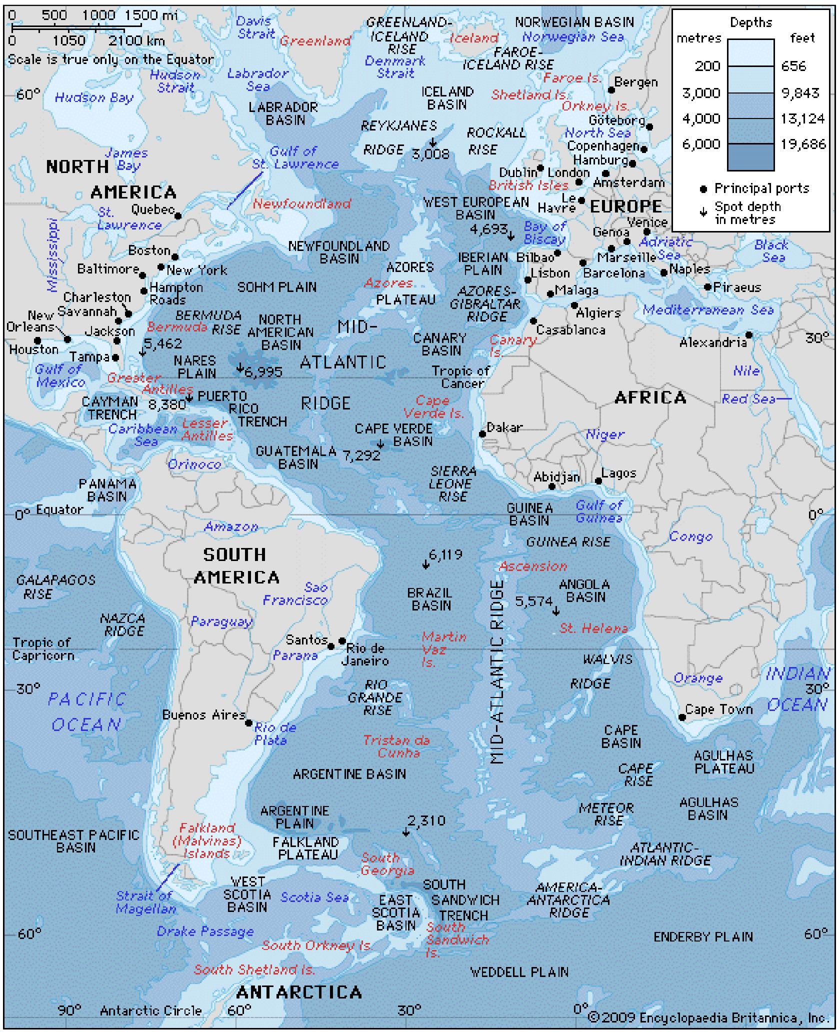


**Fig. 1: The Atlantic Ocean, with depth contours and submarine features (Encyclopedia Britannica)**

## 1.2 Today's ocean characteristics

Salinity and temperature differences in ocean waters are the two most important characteristics in driving the deep ocean circulation, while wind is the main forcing driving the ocean surface currents. It is useful to have an idea of modern temperature and salinity across the Atlantic, as these will not have changed majorly during the Holocene and can be used as a reference. The average 2009 sea surface temperatures and sea surface salinities are presented in figures 2 and 3.

Annual temperatures vary mainly with latitude and current systems, and range from less than −2°C to about 28°C. Maximum temperature regions lay north of the equator, and extend more northward on the western side of the Atlantic, while minimum values are found in the polar areas. Temperatures decrease fastest in the mid latitudes. The Atlantic is the saltiest of the three major oceans in the world. The salinity of the surface waters in the open ocean ranges from about 33 to 37 PSS (3,3-3,7%). These high salinity levels are very important with respect to the thermohaline circulation (Bryan, 1986).

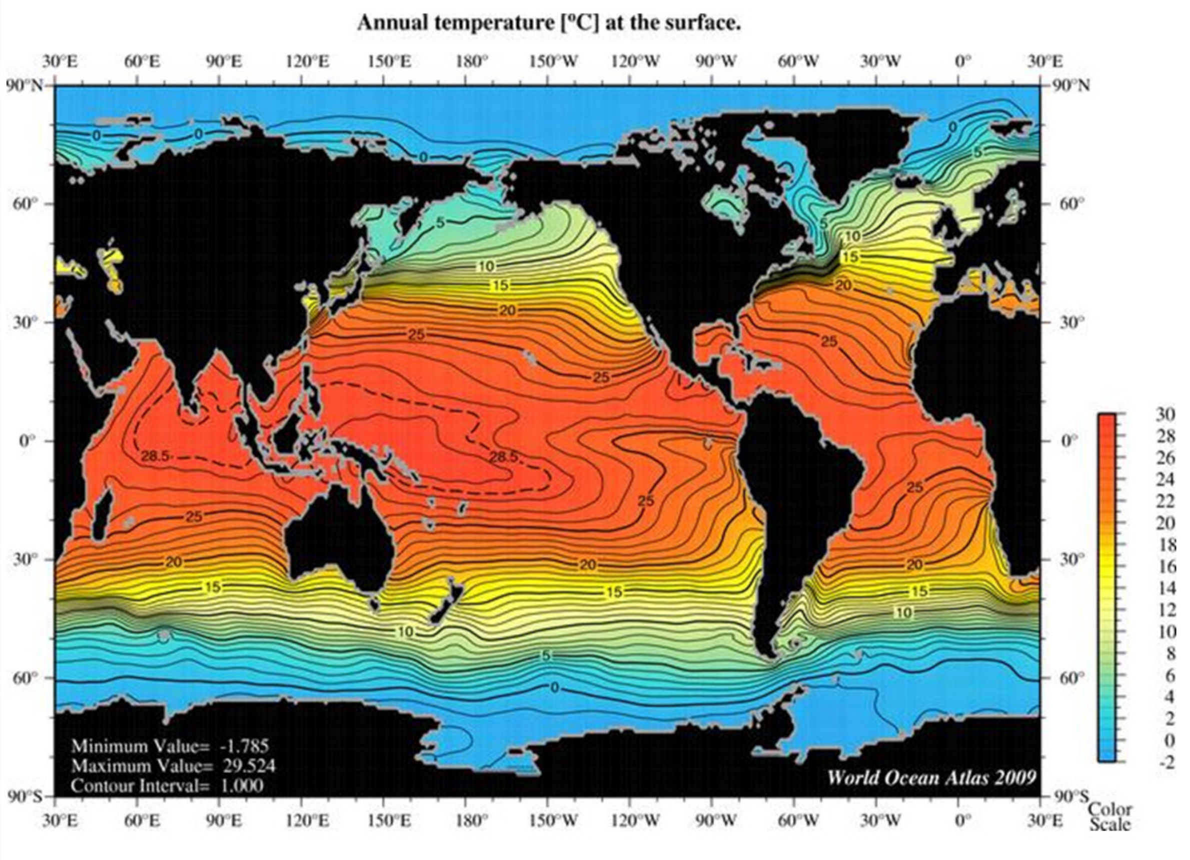


**Fig. 2: National Oceanographic Data Center (World Ocean Atlas 2009) Annual SST's of 2009**

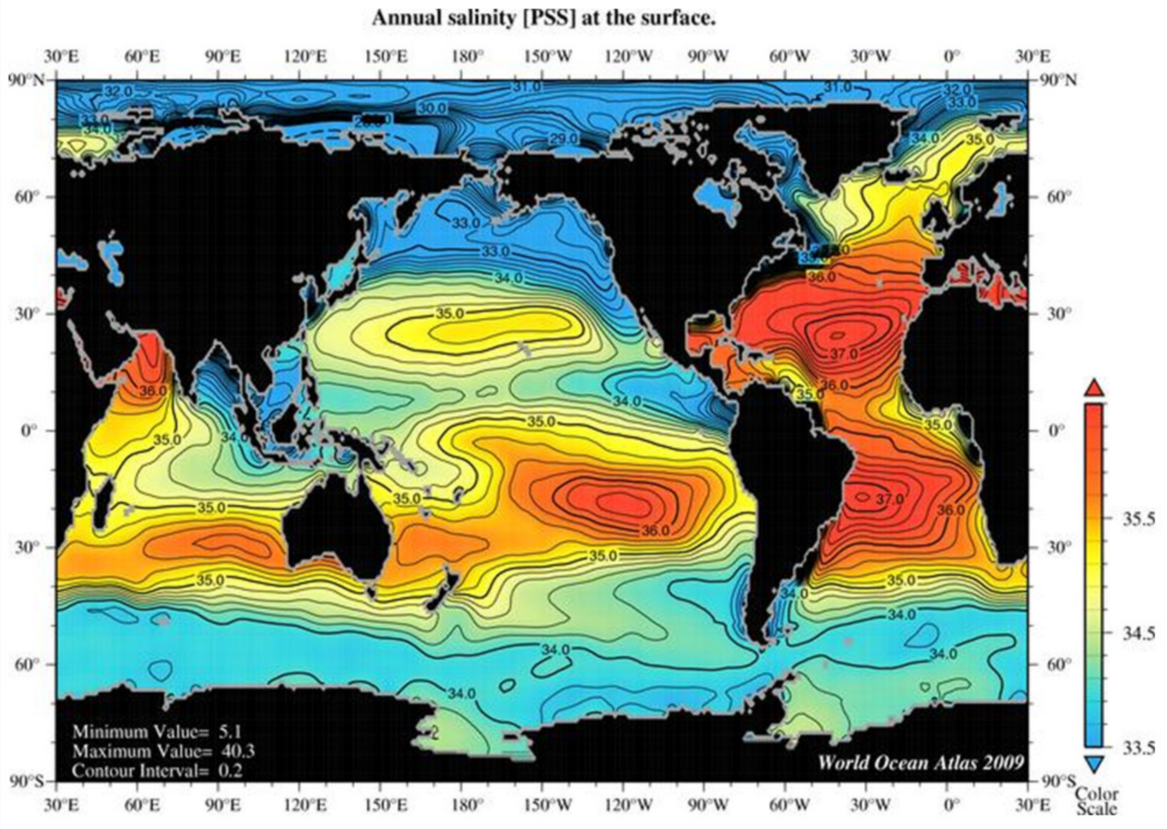


**Fig. 3: National Oceanographic Data Center (World Ocean Atlas 2009) Annual SSS's of 2009**

## 1.3 Ocean circulation

### *1.3.1 Surface circulation*

The surface waters are most valuable for paleoclimate analysis as they are a good measure for atmospheric conditions. This study will analyze reconstructed surface temperature data, notwithstanding that it is also possible to draw some conclusions on changes in the deeper water masses.

There are several "warm and cool" ocean surface currents crossing the Atlantic. Currents are not river-like, but are forming meanders and eddies, or split into filaments (Wilkes, 1859). Due to density differences and wind patterns, upwelling and sinking exists in certain regions of the ocean. The combination of horizontal and vertical motion creates oceanic gyres. The surface currents of the anticyclonic subtropical gyres can be divided in two types. The western boundary currents, which are fast, intense, deep and narrow, and the eastern boundary currents which are slow, wide shallow and diffuse. Besides the anticyclonic subtropical gyres, there are also cyclonic subpolar gyres.

A map of the Atlantic Ocean surface currents is shown in figure 4. As temperatures are strongly influenced by these currents, particularly in the high latitudes, a brief summary is given on the most important currents. These include the warm Gulf Stream, North Atlantic Current (and its different branches and extensions) and the cold Greenland Currents and Labrador Current. Information on the other currents is available in the database.


**Fig. 4: Currents of the Atlantic Ocean. (Adapted from J. Bartholomew, Advanced Atlas of Modern Geography, McGraw-Hill, 3d ed., 1957)**

*a) Gulf Stream and North Atlantic Current System (fig. 4 and 5)*

The Gulf Stream (GS) System is an extensive western boundary current playing an important role in the poleward transfer of heat and salt. The Gulf Stream begins south of Cape Hatteras (central US coast), where the Florida Current ceases to follow the continental shelf. The Gulf Stream bifurcates around 38,5°N 44°W (Mann, 1967). One branch forms the North Atlantic Current curving north along the continental slope, and turning east between 50° and 52°N. The other branch is called the Azores Current, and flows southeast towards the Mid-Atlantic Ridge. The region of the Gulf Stream's branch point is highly dynamic and subject to rapid change, which is linked to outbursts of Labrador Current water (Krauss and Ning, 1987) leading to extensive mixing at the end of the Gulf Stream.

The North Atlantic Current (NAC) branch represents the bulk of the Gulf Stream continuation past its branch point. The NAC is strengthened by mixing interactions of the Gulf Stream and Labrador Current. The North Atlantic Current goes on to feed some of the major subarctic currents completing the poleward transport of tropical waters. The NAC bifurcates at 47°N, 41°W with waters from the eastern flank heading northeast and from the western flank heading northwest (Krauss et al., 1987).

The Irminger Current (IrC), located above the western slope of the Reykjanes Ridge, branches from the North Atlantic Current at about 26°W (Bersch et al., 1999). The current is deflected north when it is west of the ridge crest and south when it is east of it (Bersch, 1995). Southward flow variability indicates that there is a relatively strong temporal variability of the IrC in crossing the ridge (Bersch, 1995). Krauss (1995) found that it branches along the Reykjanes Ridge between 60°N and 62°N. Waters from the eastern side of the ridge move towards the Norwegian Sea. Water west of 28°W travels toward the Greenland continental slope and is eventually advected by the East Greenland Current. As the eastern branch encounters the Rockall Plateau at about 24°W, the Irminger Current flows westward and enters the Iceland Basin.

The North Icelandic Current (NIC) is a small, but important extension from the Irminger Current on the North Icelandic shelf. This region is sensitive to interactions of warm Atlantic waters, advected by the Irminger Current (IrC), and cold Arctic and Polar waters advected by the East Icelandic (EIC) and East Greenland Currents (EGC) (Hansen and Østerhus, 2000; Hopkins, 1991). This is a region of strong east-west hydrographic gradients, characterized by seasonal and spatial variations in the physical properties of the surface waters, sea-ice distribution and deep water formation.

The slow moving North Atlantic Drift Current (NADC) is an extension of the North Atlantic Current located between about 50°-64°N and 10°-30°W. It is a shallow, widespread and variable wind-driven warm surface current, slowly spilling into the Nordic Seas. As the NADC forms the boundary between the cold, subpolar region and the warm, subtropical gyre of the Northeastern Atlantic, it is included in the Subarctic or Subpolar Front (Bischof et al., 2003). The current is unique in that it transports warm waters to latitudes higher than in any other ocean, thereby producing the moderate climate of Europe and western Scandinavia (Bigg et al., 1996; Giraudeau et al., 2000). Because of the rapid advection of the North Atlantic gyre, the temperature of the surface waters of the NADC almost always exceeds that of both surrounding waters and the overlying atmosphere (Rossby, 1996). The NADC is thought to have been established as early as 13,4 ka BP, although with periods of decadal-scale variations of heating and cooling (Koç et al., 1993).

The eastern side of the NADC is often referred to as the Slope Current (SC). The SC flows along the British Isles continental slope from south of Porcupine Bank to the Faroe-Shetland Channel (Hackett and Røed, 1998). Sherwin et al. (1999) state that numerous studies have suggested that the Slope Current flowing through the Faroe-Shetland channel carries most of the heat that enters the Nordic Seas.

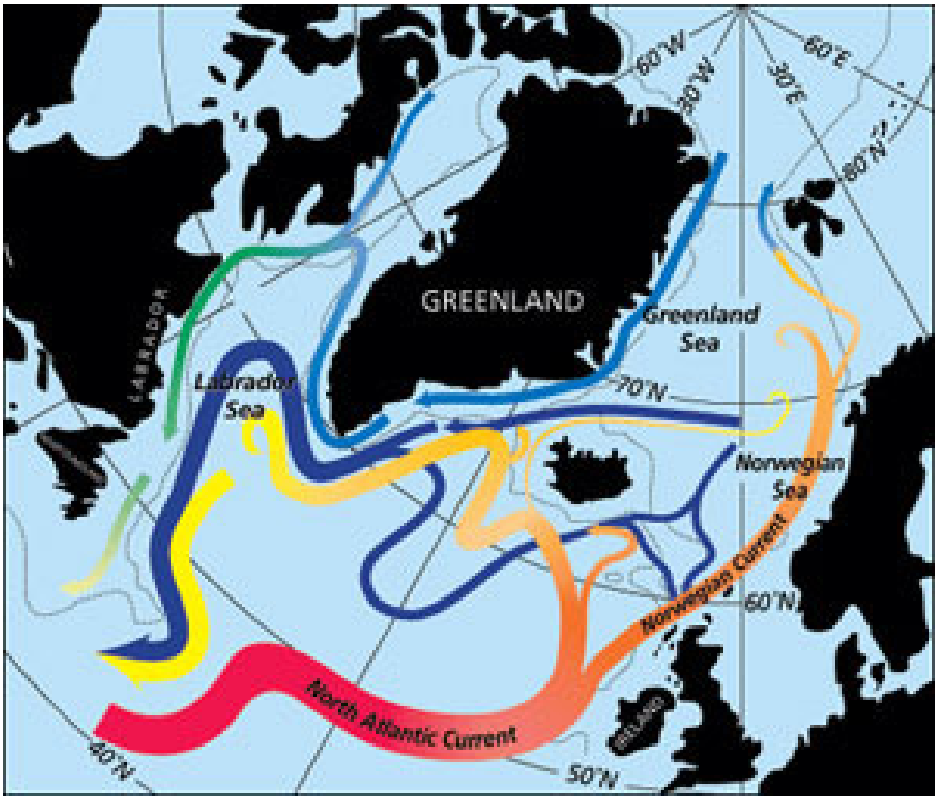


**Fig. 5: Pathways associated with the transformation of warm subtropical waters into colder subpolar and polar waters in the northern North Atlantic. Along the subpolar gyre pathway the red to yellow transition indicates the cooling to Labrador Sea Water, which flows back to the subtropical gyre in the west as an intermediate depth current (yellow). (Jack Cook, Woods Hole Oceanographic Institution)**

The Norwegian Current (NC) flows northward along the west coast of Norway. The Norwegian Current has a western boundary formed by a southward inflow of Atlantic Water (Haugan et al., 1991) creating a front between the cold, low-salinity Norwegian Current and the warmer, more saline Atlantic Water. The origin of the cold, low-salinity waters being the Baltic Sea., North Sea, and Norwegian rivers and fjords (Haugan et al., 1991; Sætre, 1999).

The West Spitsbergen Current (WSC) is the northernmost extension of the Norwegian Atlantic Current, and can express considerable variation in temperature. It flows poleward through the eastern Fram Strait along the western coast of Spitsbergen (Perkin and Lewis, 1984). Being the only deep-water connection between the Arctic Ocean and the world ocean, the Fram Strait is an important site for the exchange of mass, heat, and salt (Perkin and Lewis, 1984). The WSC carries warm Atlantic waters north into the Arctic Ocean (Saloranta and Haugan, 2004). The Fram Strait is the northernmost permanently ice-free ocean area in the world (Haugan, 1999).

*b) The cold Greenland Currents and Labrador Current (fig. 4 and 5)*

The East Greenland Current (EGC) transports recirculating Atlantic Water, Arctic Ocean water masses, and >90% of the ice exported from the Arctic Ocean southward (Woodgate et al., 1999). Consequently the EGC is an important link between the Arctic Ocean and the North Atlantic Ocean. With its high surface current velocities, the EGC carries sea ice and Polar Water out of the Arctic Ocean through Fram Strait, acting as the main freshwater sink for the Arctic Ocean (Schlichtholz and Houssais, 1999). In addition to the cold, low-salinity surface water from the Greenland Sea, the EGC is also fed by warm and saline water from the south via the Norwegian Atlantic Current. This suppresses ice formation in the current because the addition of saline water to this region of intense cooling destabilizes the water column (Aagaard et al., 1985).

The West Greenland Current (WGC) flows north along the shelf and shelf break of the west coast of Greenland. It transports fresh and cold (-2°C) water from the Nordic seas (Cuny et al., 2002). The WGC also transports small icebergs north of 60°N, and primarily north of 70°N into Baffin Bay. Many icebergs are transported south, through the Davis Straits, by the Labrador Current and either recirculate in the Labrador Sea or end up melting in the North Atlantic shipping lanes. At the north Labrador Sea the current bifurcates. Part of the current continues to flow along the Greenland coast, and the remainder proceeds westward to join the Labrador Current (Cuny et al., 2002). The WGC exhibits variability in its salinity. Anomalies occur on a decadal time scale (Dickson et al., 1984).

The Labrador Current (LaC) is a continuation of the Baffin Current flowing southeastward from Hudson Strait (60°N) along the continental slope (therefore also called slope waters) to the Tail of the Grand Banks (43°N) (Smtih et al., 1937). The Labrador Current forms the front over the continental shelf between the cooler, fresher Baffin Bay waters and the warmer, saltier open ocean waters. There is also a cyclonic circulation east of the current and north of 54°N bordered by the North Atlantic Current in the South and the West Greenland Current in the East (Lazier and Wright, 1993).

### *1.3.2. Deep ocean circulation*

The Atlantic Ocean includes four major water masses and a smaller one at different depth levels and with different density or salinity and temperature characteristics (fig. 6). The central waters constitute the surface waters, and are divided in a northern and southern part. The surface water circulation and currents will be discussed below. The deep water masses are the Antarctic Intermediate Waters (AAIW) flowing until depths of about 1500 m, the North Atlantic Deep Water (NADW) mainly flowing at depths from about 1000 to 4000 m and the Antarctic Bottom Water (AABW) flowing at greater depths. At about 35°N, there is a smaller water mass running into the North Atlantic Deep Water coming from the Mediterranean, which is called the Mediterranean Overflow Water (MOW). The flow in deep water masses is driven by density differences, and is called thermohaline circulation (THC). This THC works as a conveyor belt transporting large water masses towards the poles, and therefore aids the wind driven circulation. For the North Atlantic Drift, the conveyor belt is the main driving mechanism pulling warm water northward.

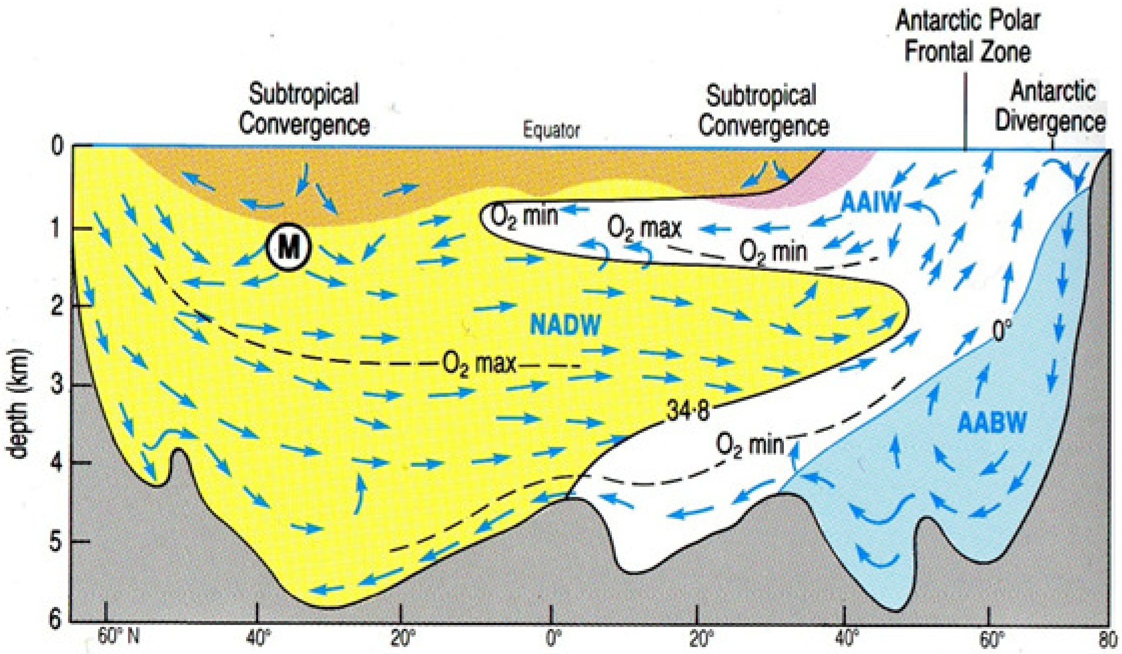


**Fig. 6: Meridional cross-section of the Atlantic Ocean, showing movement of the major water masses; water with salinity greater than 34,8 is shown yellow, and water warmer than 10 °C is shown pink/orange (Brown et al., 2001)**

The NADW is the major and most important deep water mass of the Atlantic. This water mass has two major surface sources of deep water formation, the GIN area (main source) forming the North-East Atlantic Deep Water and Labrador Sea, forming the North-West Atlantic Deep Water or Labrador Sea Water. The water in the GIN area is the densest in the world ocean with temperatures below 0 °C and salinities of ~34,9 practical salinity units (psu), ideal for deep convection. The sinking in the GIN area occurs on a line very near to the East Greenland Polar front. The location of the dominant sinking places on this SW-NE oriented zone is variable, and depends on the southward heat transport and the concurrent atmosphere dynamics. Under the right conditions, a third region of deep water formation can develop in the West Irminger Sea (Pickart et al., 2003). Ice formation and fresh water influx in the Baffin Bay and Labrador Sea through the Davis Strait and their effect on atmosphere dynamics play an important role in creating this deep water formation spot. This deep water is also considered Labrador Sea Water as it sinks to the same depths. The Greenland Sea water is denser than the Labrador Sea water implying that the Labrador Sea Water overlays the North-East Atlantic Deep Water. These deep waters are transported south towards the other pole, surging there to the surface (Rhein et al., 1995).

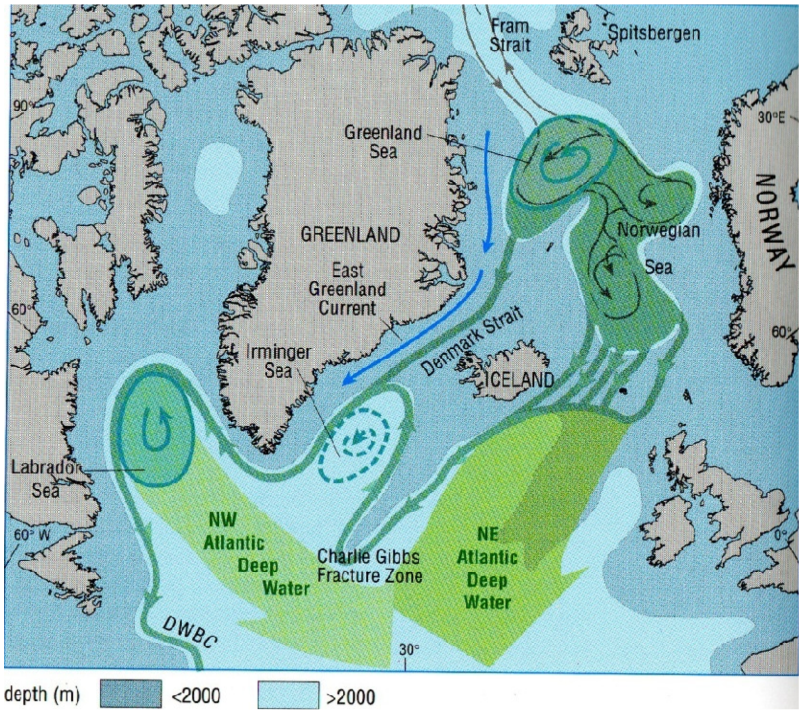


**Fig. 7: Map showing the cyclonic gyres in Greenland and Labrador Seas, which are the main areas for deep water formation in the Northern Hemisphere; the dashed cyclonic arrow is a less important region of deep water formation, in the Irminger Sea; DWBC = Deep Western Boundary Current; the broad green arrows indicate the two types of North Atlantic Deep Water, North-East Atlantic Deep Water, formed in the Greenland Sea, overlain by the less dense North-West Atlantic Deep Water, formed in the Labrador Sea and therefore also called Labrador Sea Water; the smaller green arrows form the overflow areas (Brown et al., 2001)**

## 1.4 Relation to climate

The climate of the Atlantic Ocean and adjacent land areas is influenced by the temperatures of the surface waters and the dynamics of the atmosphere, which are intimately connected. Major indicators for the atmosphere dynamics are the so called teleconnections. Two indices exist for the North Atlantic region: North Atlantic Oscillation (NAO) and Arctic Oscillation (AO). Both indices are closely related to each other. In this study, only the more common NAO is considered (fig. 8).

The NAO is the dominant mode of sea level pressure variability in the North Atlantic region (Hurrel, 1995). The NAO index, defined as the sea level pressure difference between the Azores High and the Icelandic Low (Rogers, 1984), describes the steepness of a north-south atmospheric pressure gradient across the North Atlantic Ocean. Winter weather patterns throughout the North Atlantic basin have historically been affected by changes in the NAO (Hurrell and Van Loon, 1997). Commonly when there is high pressure at the Azores, there will be low pressure at Iceland and the other way round. A positive NAO means that there is a large pressure difference between the Icelandic and Azores region, and is associated with strong westerlies. During a negative NAO there is no significant pressure difference, which is linked with a reorganization of the jet stream and associated changes in regional temperatures and storm tracking (Hurrel et al., 2001).

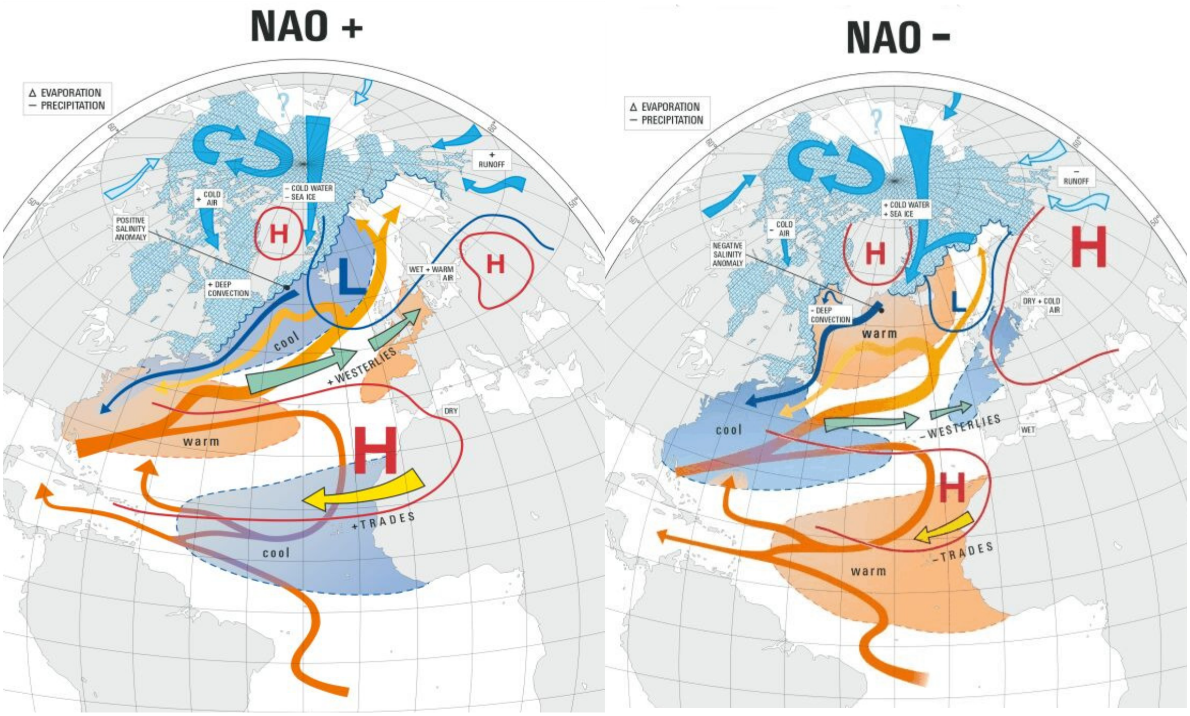


**Fig. 8: Temperature, pressure, wind, sea ice, ocean current and precipitation changes related to a positive and negative NAO phase (KLIMET, Grüppe fur Klimatologie/Meteorologie, Geography, University of Bern, Switzerland)**

# 2. Proxy analysis

## 2.1 Introduction

The first objective in this project is to find as much temperature reconstructions as possible from sediment cores in the Atlantic Ocean. Temperature proxies, along with dating methods, are the keys to palaeotemperature reconstruction. The use of these temperature proxies from sediment cores evolved quickly over the last 50 year. This can be attributed to the growing interest in the past climate to predict climate changes in the future. This study will concentrate on the millennial scale climate variation during the Holocene. Therefore it is necessary to apply proxies, which can give detailed quantitative temperature estimates. Sedimentation records have to meet certain conditions. A substantial and continuous deposition is needed during the Holocene period, the sediment may not have experienced any mixing and has to be deposited in situ (e.g. Argentine Basin SST reconstructions with alkenones 2-6 °C colder due to strong current transport (Benthien and Müller, 2000). In the North Atlantic away from the continental margins, the average deposition rates are ~2-4 cm $ka^{-1}$(Balsam and McCoy, 1987), and on continental margins average rates are of order 10 cm $ka^{-1}$. It is also important to be careful during the coring as the whole core has to stay perfectly intact.

The possible proxies for this research can be divided in two groups, the ones based on calibration methods, which are the biomarkers and geochemical based methods and the ones based on transfer functions through species counting of certain microfossil groups. For the moment, there is only one biomarker that has been regularly used for temperature reconstructions, the alkenones. A second biomarker is $TEX_{86}$ based on the relative distribution of membrane lipids of marine non-thermophilic crenarchaetoa (Kim et al., 2008; Schouten et al., 2007). Its use has been mostly restricted to lakes, but recently some publications on marine cores were published (Castañeda et al., 2010). Element ratios from planktonic foraminifera and corals are also used as a palaeothermometer. These include Mg/Ca and Sr/Ca ratios, and are paired with $\delta^{18}O$. The transfer function based methods are applied to several microfossil groups including foraminifera, diatoms and dinocysts as most important ones.

Records of five different proxies are gathered in this thesis. Two calibration based methods on alkenones and Mg/Ca (paired with $\delta^{18}O$) and three transfer function based methods on dinocysts, planktonic foraminifera and diatoms. The reasons to pick these five instead of other palaeothermometers are that for each of these proxies at least 9 records are available and that the accuracy of all five methods is in the same range.

## 2.2 $C_{37}$ alkenone lipid biomarker as SST proxy

a. Intoduction

The existence of alkenones, which are long-chain unsaturated methyl and ethyl ketones with 37 to 39 C-atoms, is first described by Volkman et al. (1980). Alkenones are in fact the most common biomarkers produced by some algae of the class Haptophyceae. They are first discovered in *E. huxleyi* (Fig. 5), belonging to the coccolitophorids, and later on in four other species of the Isochrysidales (Prymnesiophyta), which do not bear coccoliths (Marlowe et al., 1984; Marlowe et al., 1984b). The dominant species are *Emiliania huxleyi* and *Geophyrocapsa oceanica* (Conte et al., 1995; Volkman et al., 1980). Alkenones have the characteristic to survive deposition in a recognizable form. Thus, they can be considered as chemical fossils (Eglinton and Calvin, 1967). Given their phytoplanktonic source, the alkenones originate from somewhere in the euphotic zone.

a. (E,E)-15,22-heptatriacontadien-2-one ($C_{37:2}$)

b. (E,E,E)-8,15,22-heptatriacontatrien-2-one ($C_{37:3}$)

c. (E,E,E,E)-8,15,22,29-heptatriacontatetraen-2-one ($C_{37:4}$)

**Fig. 9: The three alkenone strains, with two, three and four double bonds**

b. Alkenone calibration and precision

SSTs can be derived from $C_{37}$ alkenones (fig. 9), thanks to the $U^{k}_{37}$ index (Brassel et al., 1986). This index stands for the relation between di- and tri-unsaturated $C_{37}$ alkenones, which is related to the coccolithophorids growth temperature, and is defined by the following formula:

$$U^{k}_{37} = C_{37:2} - C_{37:4} / C_{37:2} + C_{37:3} + C_{37:4}$$

Because $C_{37:4}$ is not common outside locations in the high latitudes and some coastal sites this index was soon simplified to the $U^{k'}_{37}$ index (Prahl and Wakeham, 1987). In the Nordic Seas it has been suggested that it is more appropriate to use a calibration based on the original $U^{k}_{37}$ index(Bendle and Rosell-Melé, 2004), but for the lower latitudes the simplified calibration is used.

$$U^{k'}_{37} = C_{37:2} / C_{37:2} + C_{37:3}$$

The calibration of the $U^{k'}_{37}$ index was initially based on laboratory measurements, afterwards confirmed by several studies on marine surface sediments (60°N-60°S; 0-29°C) using annual mean temperatures at 0 m depth from a climatological database (Müller et al., 1998), and further studies around the world (Conte et al., 2006). The best linear correlation found by Müller et al. (1998) between $U^{k'}_{37}$ and SST in the tropical to subpolar eastern South Atlantic (149 sites) was determined using annual mean SST from 0-10 m water depth ($U^{k'}_{37}$ = 0,033 T + 0,069, $r^2$ = 0,981, with a standard error of ± 1°C (± 0,032 $U^{k'}_{37}$ units)). In the other oceanic regions (370 sites) ($U^{k'}_{37}$ = 0,033 T + 0,044, with a standard error of ± 1,5°C (± 0,050 $U^{k'}_{37}$ units)) the relationship was almost identical to the *E. huxleyi* calibrations ($U^{k'}_{37}$ = 0,033 T + 0,043) of Prahl and Wakeham (1987).

Rosell-Melé et al. (1995) reported that despite reworking of organic matter prior to its burial, and different populations of alkenone producing coccolithophorids, core tops from the eastern North Atlantic show seasonal linear correlations between $U^{k'}_{37}$, and SST across a range of temperatures of coccolithophorid habitats. These findings proved once again the usefulness of alkenones as a temperature proxy.

It is important to perform more measurements of Haptophyte algae and their alkenone production rate at different biogeographical regions to construct more detailed calibration curves (2001; Conte et al., 1998b). The alkenone signal is most accurate during phases with rapid sedimentation (Thomsen et al., 1998).

c. Advantages and disadvantages

There are three main reasons why the alkenones are valuable as a proxy. They are present throughout all ocean waters (Marlowe et al., 1990), the alkenone temperature signal in sediments is very robust (Grimalt et al., 2000; Teece et al., 1998) and they occur persistently throughout the stratigraphic record (Marlowe et al., 1990).

Another advantage is that core-top calibrations of various biogeographical settings are strongly linear, which suggest less species dependency than calibrations with culture experiments. Also variations in growth rate of algae and nutrient availability doesn't seem to significantly affect the $U^{k'}_{37}$ results (Müller et al., 1998). Evolution and/or extinction cannot have an impact on the alkenone ratio, because this study is limited to the Holocene. There is no systematic trend detected with the $CO_2$ water concentration variability, despite large changes in the content of alkenones per cell (Riebesell et al., 2000).

Although that alkenones are a very good temperature proxy, some remarks have to be made when analyzing results. Findings from laboratory experiments clearly show that the absolute value for $U^{k'}_{37}$

recorded in sediments is not exclusively determined by growth temperature or by export of a signal from cells productive at the sea surface (Prahl et al., 2003).

Anomalies between measured temperatures and $U^{k'}_{37}$-based temperatures (Conte and Eglinton, 1993; Sikes and Volkman, 1993) have been attributed to either the sensitivity of $U^{k'}_{37}$ to environmental and/or physiological parameter(s) (Conte et al., 1995) or to variations in the abundance of $C_{37}$ alkenone isomers among different algal species (Marlowe et al., 1984b).

An experiment from Conte et al. (1998a) with *E. Huxleyi* and *G. Oceanica* strains between temperatures of 6-30°C revealed that there is a reduction in slope of the calibration < 12°C and > 21°C, which means that the adaptation to temperatures is limited at the extremes of its growth temperature range. The genetic and physiological differences ratify the importance to examine the natural variability of these strains and to improve the temperature calibrations. Old data (pre 1998) might underestimate temperatures > 24°C (tropics and subtropics), because a linear trend is used for the temperature calibration (Conte et al., 1998a).

Seasonality in production and/or thermocline production, and differential degradation of $C_{37:2}$ and $C_{37:3}$ seem to affect the sedimentary alkenone signal. The core-top alkenone integrated production temperature is compared with annual mean SSTs. $U^{k'}_{37}$ is found to be consistently higher than predicted from SST, which becomes more pronounced with decreasing SSTs. The seasonality of the so-called algae blooms can have this influence. Once or twice a year there is a maximum in export fluxes of alkenones and the timing of these maxima differs between different oceanic regions. Along with a surface cooling trend there is a change in the seasonal timing and/or duration of the growth period of alkenone producers (Marchal et al., 2002).

Because the current calibration is empirically derived, it does not reflect any spatial and temporal variations of the production of alkenones in the oceans. Although the calibration provides an approximately global signal of alkenone accumulation in bottom sediments, it should be handled carefully, because several studies revealed that in certain contexts or regions it is faulty to derive absolute temperatures from the above calibration (2006; Conte et al., 1995; 2001).

The estimation of advected alkenones is very important, which means that it is necessary to determine the sedimentary origin wherever possible and that one should be careful when interpreting the alkenone contents in sediments, because the age and source can sometimes vary significantly in the same horizont (e.g., up to 7,000 yr difference in Bermuda Rise drift sediments (Ohkouchi et al., 2002)). Also asynchronies between alkenone-derived SSTs and other temperature proxies should be carefully investigated (Sachs et al., 2000).

In regions where a complex food web efficiently retains biogenic material in the upper pelagic layer, the originally imprinted alkenone signal can be altered. Strong deviations from the surface signal occur in areas with high resuspension fluxes and nepheloid layers due to increased contributions of particles with long residence time. These effects are particularly significant at high latitudes (> 60°) with low in-situ temperatures and areas with enhanced flow condition (Thomsen et al., 1998).

d. Conclusion

Although there is still space for improvement, the alkenone temperature calibration seems to be very useful in most oceanographic settings during the Holocene.

## 2.3 Mg/Ca paleothermometry on planktonic foraminifera

a. Introduction

Oxygen isotope measurements in foraminifera depend on both temperature and the isotopic composition of the water, which limits their utility for reconstructing past ocean temperatures. Only recently the potential of Mg/Ca in planktonic foraminifera and Sr/Ca in corals as recorders of SSTs has been realized. A serious advantage of these carbonate-based thermometers is the possibility of coupling with $\delta^{18}O$, which provides a novel way to adjust for temperature dependency of carbon and isolate the record of $\delta^{18}O_{water}$ (Barker et al., 2005). This $\delta^{18}O_{water}$ can be used to reconstruct evaporation-precipitation changes and gives information about changes in continental ice volume (Lear et al., 2000).

Element-to-calcium ratios in $CaCO_3$ minerals depend on two factors, which are the corresponding element-to-calcium activity ratios of the ocean water and the distribution coefficients of these elements between the carbonate mineral and seawater respectively (Rosenthal et al., 2006). At equilibrium, the partitioning constant between the two mineral phases depends on temperature as the substitution of Mg into calcite is associated with a change in heat thus also temperature. The substitution of Mg into calcite is an endothermic reaction, and thus the Mg/Ca ratio of calcite will increase with increasing temperature (Rosenthal et al., 1997).

b. Temperature calibrations with Mg/Ca of Planktonic Foraminifera

The extent of temperature dependence of Mg uptake into planktonic foraminifera has been determined using three sorts of approaches: the culture-based calibrations (Lea et al., 1999; Russell et al., 2004); Russell et al., 2004), sediment trap calibrations (Anand et al., 2003) and core top calibrations (Elderfield and Ganssen, 2000). Mg/Ca calibrations are expressed as an exponential dependence of temperature as follows:

$$\text{Mg/Ca (mmol}^{-1}) = Be^{AT}$$

Where A is the exponential constant, B the pre-exponential constant (determines the absolute temperature and is species specific (Anand et al., 2003), but is also affected by diagenetic overprints (Lohmann, 1995; Rosenthal and Lohmann, 2002) and T is temperature in °C

In the first method planktonic foraminifera grow under controlled laboratory conditions, where temperature is fixed. This technique suggests a temperature sensitivity of 9,7 ± 0,9 % per °C. The second method involves measurements of planktonic foraminifera from sediment trap time-series characterized by high seasonal SST variability and provides a temperature sensitivity of 9 ± 0,3% per °C. In the last technique Elderfield and Ganssen (2000) analyze fossil foraminifera from surface sediments, and after a re-evaluation by Rosenthal and Lohmann (2002) the temperature sensitivity is 9,5 ± 0,5% per °C. Offsets in Mg/Ca among individual species in culture and field studies suggest the need for single-species calibration (Rosenthal et al., 2006). Mg/Ca ratios are more accurate in estimating relative changes in temperature than absolute temperatures, due to local biases.

c. Pairing $\delta^{18}O$ and Mg/Ca records

After the first calibrations for planktonic and benthic foraminifera (Rosenthal et al., 1997), the coupling of Mg/Ca and $\delta^{18}O$ became instantly very popular as it offers some advantages in comparison with other paleoceanographic methods. Previously interpretations of foraminiferal oxygen isotope records were limited, because the $\delta^{18}O$ composition of carbonates depends on both the temperature and the isotopic composition of the water in which the test was formed. The effect of each of these variables could not be determined, until the discovery of the Mg/Ca thermometry as an independent proxy for the actual temperature at which the test precipitated. Now it was possible to adjust the $\delta^{18}O_{calcite}$ for temperature and calculating $\delta^{18}O_{water}$. The following calibration of the isotopic composition of the seawater from foraminiferal $\delta^{18}O_{calcite}$ is widely used:

$$\delta^{18}O_{water} = 0,38 + (T - 16,5 + 4,8 \text{ x } \delta^{18}O_{calcite})/4,8$$

where T is the Mg/Ca based temperature in °C and the factor 0,27 converts the calcite standard units of PDB to water units based on the SMOW. Due to a strong covariance between $\delta^{18}O_{water}$ and surface salinity (Craig and Gordon, 1965), changes in evaporation/precipitation can be constructed and by inference salinity (Mashiotta et al., 1999; Stott et al., 2004).

The potential of this combined $\delta^{18}O$ and Mg/Ca records has been already demonstrated in many studies (Elderfield and Ganssen, 2000; Elderfield et al., 2002). On the basis of the average $\delta^{18}O$ and Mg/Ca offsets observed between different species, (Skinner and Elderfield, 2005) conclude that many of the temperature calibrations that are currently proposed for both of these proxies are inconsistent.

d. Remarks

Inter-species variability in Mg/Ca is largely correlated with calcification depth as shallow dwellers have high Mg/Ca ratios and deep dwellers relatively low Mg/Ca (Rosenthal and Boyle, 1993). There is significant variability in the Mg distribution within and among foraminifera tests as these foraminifera grow layers at several depths. So the whole test Mg/Ca composition, used for temperature reconstructions, represents a weighted average of calcite layers formed at different depths/temperatures (Lohmann, 1995).

Among specimens of the same species there might also be variability in test composition. Particularly shell size has a serious effect on Mg/Ca ratios. In most species Mg/Ca increases with increasing test size, possibly because smaller specimens calcify faster than larger ones (Elderfield and Ganssen, 2000). The impact of biomineralization processes on the Mg content of foraminiferal shells is discussed by Erez et al. (2003) and Bentov and Erez (2005; Bentov and Erez, 2006). Also growth season or depth habitat can be factors of Mg/Ca variability among different morphotypes of the same species.

Studies also reveal large compositional variability within individual chambers and within the test as a whole (Anand, 2005; Brown and Elderfield, 1996; Gehlen et al., 2004). Shallow dwelling species tend to have more homogeneous composition than deep dwelling species (larger extent of vertical migration), thus suggesting that temperature exerts a significant control on intra-test variability (Eggins et al., 2003).

Studies show a weak normal relationship between planktonic foraminiferal Mg/Ca and seawater salinity (Lea et al., 1999; Nürnberg et al., 1996) and an inverse relationsip with pH (Lea et al., 1999; Russell et al., 2004). Also dissolution seems to affect the Mg/Ca composition of planktonic foraminifera. This could be deduced from the correlation between Mg/Ca and depth of the seafloor form which the tests were collected, thus suggesting alteration by post-depositional dissolution on the seafloor (Savin and Douglas, 1973). There is also a systematic decrease in Mg/Ca ratios likely caused by preferential dissolution of Mg-rich calcite, which might be more susceptible to dissolution (Brown and Elderfield, 1996). Dissolution is the main secondary cause for the Mg/Ca variation, with potential errors of more than 0,5°C. Calculations show that the saturation horizon for Mg-rich parts of tests may be elevated by several hundred meters compared with normal calcite (Brown and Elderfield, 1996). Various approaches have been used to account for dissolution effects (Dekens et al., 2002; Rosenthal and Lohmann, 2002). Other biases introduced by Mg-rich gametogenic calcification and contaminant phases limit confidence in Mg/Ca-based reconstructions (Hastings et al., 1998).

e. Conclusion

Mg/Ca ratios is one of the most recent temperature proxies. Although that it already delivers some good temperature reconstructions, the maximum potential of this paleothermometer has not been reached yet.

## 2.4 Transfer functions as SST proxy

### *2.4.1 Introduction and history*

Early on microfossil assemblages proved to be very important in paleoceanography as a reconstruction tool for climatic or oceanographic parameters. The tracing of SSTs in the past is mostly performed, using transfer functions. An accurate identification of species and counting of taxa, or presence/absence of specific taxa are required to do adequate statistical analysis as transfer functions convert the counting of different species of microfossils, which are linked to a favorite living temperature or other paleoceanographic proxy, to a past SST. Sachs et al. (1977) defined transfer function procedures as methods producing calibrated quantitative estimates of some parameters of the environment, or methods that permit quantitative estimates of ocean or climate parameters using paleontological data. Mostly the present day distribution is compared with the corresponding distribution of climate variables determinant for the distribution of a specific species.

John Murray, participant of the Challenger Expidition (1872-1875) found that planktonic foraminifera are omnipresent on the seafloor and that species composition is linked to the temperature of the waters in which they lived (Murray, 1897). In 1935, Schott, was the first to count species within the fossil assemblages on the seafloor from sediments of the Meteor Expidition (1925-1927) [*Schott*, 1935]. Parker [1958] was the first to plot warm- and cold-water faunal percentages as a function of depth in core. It was only in 1969 that the first genuine transfer function method appeared (Berger, 1969). Three year later, Webb and Bryson (1972), used transfer functions in a paleoclimatic context for the first time.

Whatever the algorithms and techniques used, all transfer functions start with three databases and most of them work in three steps. There is (1) the modern database that displays the chosen fossil species present in core-top sediments, (2) the modern parameter database that gives quantitative values of surface properties extracted from *in situ* measurements and the (3) fossil species database that includes census counts of the same species in down-core samples. The three methodical steps are a calibration step (compares the modern species database with the modern parameter database to detect species-environment relationships between the two sets), a comparison step (correlates fossil database to the modern database to detect similarities between the two sets) and an estimation step (produces the quantitative estimate based on the two first steps) (Crosta et al., 2007) (fig. 10). Each technique is dependent upon, but differently affected by, the quality of the three databases. The quality of the databases is determined by taxonomy, core-top coverage and the extraction of modern parameters.

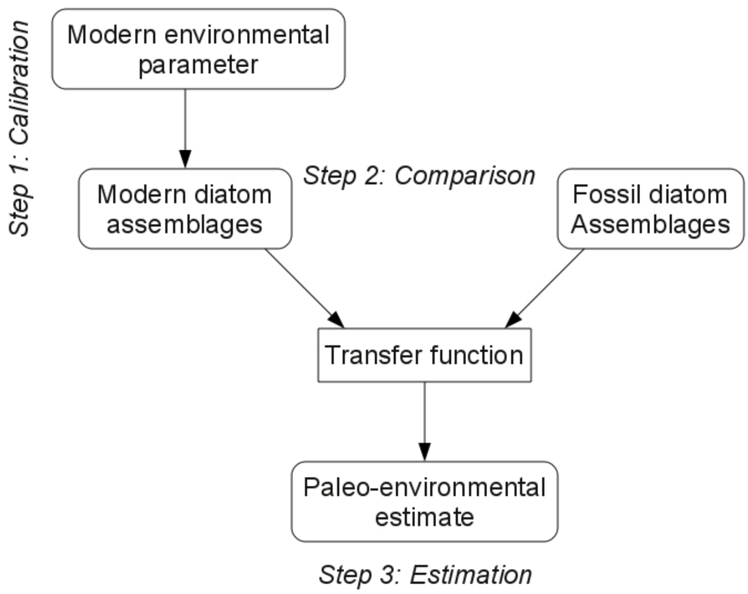


Fig. 10: Schematic protocol of a transfer function highlighting the databases and the three-step mathematical technique (Crosta et al., 2007)

### *2.4.2 Methods based on calibration*

Transfer function models and methods based on calibrations imply some assumptions. First, the climate is the ultimate cause of changes in the paleobiological data. The ecological properties of the included species in the data has not changed between the period analyzed and the present time. A last condition is that the modern observations have to contain all the necessary information to interpret the fossil data.

The most simple and firstly used transfer function is the weighted-average optimum temperature method of Berger (1969). This technique uses the following formula:

$$T_{est} = \Sigma\ (p_r\ .\ t_i)\ /\ \Sigma\ p_i$$

where $p_i$ the proportion of species i and $t_i$ = optimal temperature for species i.

This method is univariate, so the precision is not ideal. Therefore, some other, more complex transfer functions were developed. A breakthrough came with the so-called Imbrie-Kipp multi-variate transfer function method (Imbrie and Kipp, 1971).

The calibration methods can be divided in three subgroups: the ordination-based methods, the generalized models and non-parametric models.*Ordination based methods*

These methods sort multi-dimensional data points along one or several axes to visualize their structure. There are different ordination techniques, which can be divided in two groups, the indirect gradient analysis (ordination along hidden variables) and direct gradient analyses (gradient in relation to environmental variables). The first group includes principal component analyses (PCA) and correspondence analysis (CA), the second includes partial least square analyses (PLS), canonical correlation analysis (CCA) and the methods derived from weighted average and partial least square.

PCA is one of the earliest ordination methods and forms the basis of the Imbrie & Kipp method (Imbrie and Kipp, 1971). The variance in the species data set is maximized, but because this does not guarantee the maximized variance of the climatic variables, it is accompanied by multiple regression, which projects the climate on the species space. This method has been mainly applied to marine diatoms and siliceous microfossils. Compared to PCA, CA is more suitable with species assemblages, because unimodal relationships replace linear relationships between species and climate parameters (ter Braak, 1985).

The PLS analyses aims at finding a linear combination to maximize the covariance with the environmental parameter. This method differs from PCA as the interpretation of the components is linked to the predictand to be reconstructed, whereas in PCA the components must be calibrated inductively on the predictor. There are two possibilities of generalization to several predictands: maximize the sum of the correlations of each predictand (redundancy analysis (ter Braak and Prentice, 1988) or maximize the correlation between a linear combination of the predictors and a linear combination of the predictands, which allows the deduction of the relationships of the predictands in relation to the predictors (Fritts et al., 1971). WA-PLS regression is related to CA as PLS is related to PCA. The generalization of several predictands is provided by canonical correspondence analysis (CCA) (ter Braak, 1986; ter Braak, 1987). The WA-PLS method has been mainly used on diatoms and planktonic foraminifera.

#### *2.4.2.2 Generalized models and non-parametric methods*

There are two generalized models, the general linear model and generalized additive model (Guisan et al., 2002). Because they are not used frequently for palaeoceanographic purposes, they will not be discussed. A regularly applied non-parametric method is the artificial neural networks (ANN). It seems to be an excellent approach for a large class of non-linear problems (Walczak and Wegscheider, 1994). ANN uses a black box approach, which allows very close data fitting, but also implies that it is very hard to analyze the causality between input and output variables and to find the proper structure of the network. An ANN consists of a number of simple and interconnected processors called neurons. An input signal passes these neurons to reach output variables (environmental). A major issue for the ANN method is the number of iterations needed for correct calibration and reconstruction. It is needed to stop the iterations before overestimation (Guiot et al., 1996; Malmgren and Nordlund, 1996). This method is frequently used in a multi-model approach.

### *2.4.3 Methods based on similarity*

These methods are based on the comparison of past assemblages with modern assemblages. The mutual climatic range methods consider only the occurrence in terms of presence/absence, and are therefore not accurate enough to estimate past SSTs and will not be discussed. Another and better alternative is the analogue based approach (Hutson, 1980). This method has no strict calibration, but instead relies on the comparison between assemblages. For these analogue methods, it is necessary to have extensive sets of modern assemblages as there is no calibration allowing extrapolation. The analogue-based approach has two main advantages. Several environmental variables can be reconstructed at the same time and no assumption is made of the relationship between taxon abundance and environmental gradients. In the 1990s this method became more and more popular.

#### *2.4.3.1 Modern analogue technique*

With the modern analogue technique (MAT), environmental data are interpolated at the sampling sites as with the calibration methods. According to the taxa sensitivity against the different environmental variables to be reconstructed, they are given a certain weight. The most responsive taxa have the greatest influence upon the choice of analogues. An appropriate distance measure is required in order to adopt the degree of analogy between fossil and modern assemblages. The smaller the distance the greater is the degree of analogy between the two samples. The degree of analogy is mostly expressed in percentages. The MAT method is now a standard method often compared with other ones. One of the major studies performed with this method was on dinocyst assemblages (Guiot and de Vernal, 2006).

#### *2.4.3.2 Constrained analogues*

There is a major problem of wrong analogues in the case of fossil assemblages characterized by a limited number of taxa, which are ubiquitous and represent a wide range of environmental conditions. There are two main approaches for constrained analogue methods. One is to reject all the assemblages from other biomes even if the distance with fossil assemblages is very low. The second approach uses paleoclimatic information derived from independent proxies. The disadvantage of this last approach is that the independent paleoclimate proxies are no longer available for comparison (Guiot and de Vernal, 2006).

Pflaumann et al. (1996) developed a method with an implemented constraint related to the geographical distance from the fossil site, in addition to the distance between several spectra (modern

**analog technique** with similarity index: SIMMAX method). This approach seems to be very useful to reconstruct the Holocene, but not for glacial periods.

#### *2.4.3.3 Response surfaces*

The response surface analogue technique (RSAT) re-maps the taxa into an environmental space using the modern data set. The main method applied is the quantitative environmental response surfaces, where surfaces are fitted to the abundance values of each taxon used for reconstruction (Bartlein and Colin, 1986; Huntley, 1994). There are two main advantages with the RSAT approach. The variation of taxa independent of climate is smoothed, so the response surface is flat and contributes little to the choice of analogues. Also each type of climate is evenly represented, which improves the value of the confidence interval.

The revised analogue method (RAM) proposed by Waelbroeck et al. (1998) uses gridded assemblages in addition to raw assemblages, which provides a better shaped data set. The gridded samples are obtained by interpolation in the climatic space (more flexible than a surface). RAM is very useful to improve the reconstructions of SSTs at cold and warm ends of the temperature range. It is frequently used in multiproxy approaches.

### *2.4.4 Comparing the different methods: which ones perform best*

The method that performs least is the I&K method (Imbrie and Kipp, 1971). PLS, WA-PLS and GAM produced already better results, but lack accuracy for cold and warm data sets. There are three methods which provide rather good results for whole data sets: MAT, RAM and ANN (Hayes et al., 2005; Peyron and de Vernal, 2001; Waelbroeck et al., 1998). RAM outperforms MAT on the extreme data sets, but in general they yield results of similar quality. Also ANN seems to give similar results as MAT and RAM. Therefore these three are the best methods for a multi-method approach, but also WA-PLS is often used.

### *2.4.5 Conclusion*

Transfer methods are powerful methods that translate complex biological assemblages into simple abiotic parameters. A multi-method approach of at least three methods is advised, so that it is possible to remove outliers and use the average values (Kucera et al., 2005). Transfer functions are most useful to constrain or validate paleoclimatic models.

## 2.5 Transfer functions on planktonic foraminifera

a. Introduction

Forams are single celled organisms protected by a shell or test variously composed of secreted organic matter (tectin), secreted minerals (calcite, aragonite or silica) or of agglutinated particles (Boersma and Silva, 1983). These tests consist of one (unilocular) or more chambers (multilocular), which are interconnected with a foramen. These tests can be very abundant in sediments. They comprise over 55% of Arctic biomass and over 90% of deep sea biomass (Armstrong and Brasier, 2005c).

The two major ecological factors on planktonic foraminifera are temperature and salinity. There are about 100 species of living planktonic foraminifera, which is comparable with the species living during the Holocene. These foraminifera are small (mostly 50-200 µm) and short lived (about one month). The tests are adapted to retard sinking. The planktonic foraminifera can be divided into three groups according to their living depth: a shallow group (<50 m), an intermediate group (between 50 and 100 m) and a deeper group (>100 m). The distribution of the foraminifera is bipolar (Armstrong and Brasier, 2005c). Subpolar and polar populations can be distinguished by a predominance of left- or right-handed coiling. Planktonic foraminiferal densities can be very high around the margins of oceanic gyres. The use of forams is limited by the occurrence of the lysocline or calcite compensation depth (CCD). The CCD is the depth where calcite dissolves. This CCD limits the area of research to places with a maximum depth of 3000 m (Armstrong and Brasier, 2005c).

b. Transfer function method for planktonic forams

Within the CLIMAP project there is a consensus on how to handle these ooze samples (CLIMAP_Project_members, 1976). The developed method involves the counting of 300-500 specimens in random subsamples of the >150 µm fraction. This method is far from perfect, but relatively easy to carry out. The size limit biases the assemblage composition, especially towards the poles because of a decreasing foram size (Schmidt et al., 2004). That is why in some studies at higher latitudes smaller size fractions are taken into account. Also the quality of the data relies on correct identification. Most of the species are easy to recognize, but there are some that look alike (e.g. *G. bulloides* and *G. falconensis*). (Fig. 11)

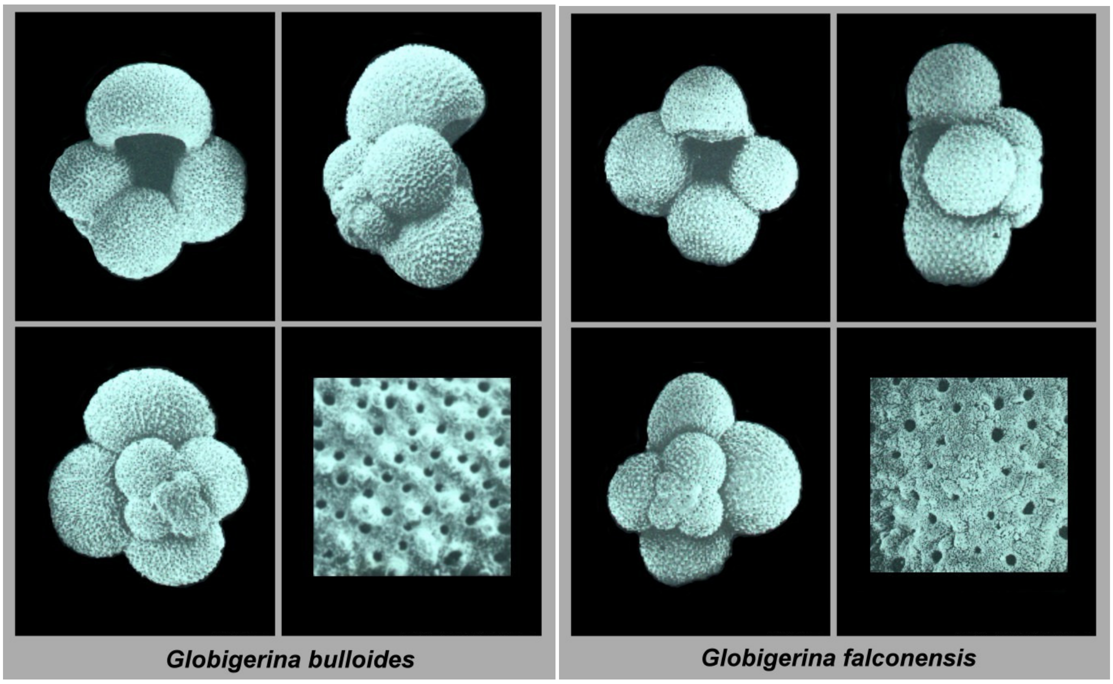


**Fig. 11: Microscopic views of *G. bulloides* and *G. falconensis*. The difference between the two can only be seen in the microscopic texture of the tests**

The counted subsamples can then be converted to temperatures using a transfer function method. The CLIMAP project used the Imbrie-Kipp transfer function method (Imbrie and Kipp, 1971), but this as we know today, this method has not the greatest accuracy. There has been a recent revival in foram transfer functions, thanks to the development and application of new computational techniques applied to data of the Last Glacial Maximum (LGM) (Kucera et al., 2005). This multi-technique approach managed to lower the prediction errors to below 1 °C. It's also possible to derive other environmental variables from foraminifer transfer functions (e.g. reconstruct calcite saturation of glacial bottom waters (Anderson and Archer, 2002) and reconstruct paleoproductivity).

c. Remarks

The narrow temperature ranges of living planktonic foraminifer species make them a very good proxy for paleoclimate (Armstrong and Brasier, 2005c). Also the easiness to determine different species is very useful for fast and accurate counting to determine past temperatures via transfer functions.

A boundary condition for the collected sediments is that they have to be deposited above the CCD in order to contain foraminifera. One gram of deep-sea calcareous ooze normally contains thousands of specimens suitable for quantitative analyses (larger than 150 µm). Planktonic forams are extremely sensitive to surface waters, particularly SSTs (Morey et al., 2005). Therefore they are very useful as temperature proxy. Secondary influences may include an ecotone effect (tends to separate high latitude faunas in environments with seasonal varying pycnocline, from low-latitude faunas in environments with a permanent pycnocline), salinity and nutrient or fertility gradient.

Shell-weight measurements were carried out on planktonic foraminifera from coretop depth transects in the three major oceans to investigate calcite dissolution above the lysocline (de Villiers, 2005). Foraminifera deposited in sediments overlain by supersaturated bottom water undergo considerable dissolution at the sediment–water interface and the calcite saturation state at the interface is considerably offset from that of the bottom water. Also, the extent of exposure to undersaturated conditions at the interface is not constant as it tends to increase towards the surface ocean, where the organic matter flux is higher. de Villiers (2005) proposes that the benthic layer at the sediment–water interface represents a zone of undersaturation through which the foraminifera pass, and that the residence time of foraminifera within this zone of intense organic matter respiration is long enough to result in significant decreases in shell weight. de Villiers (2005) postulates that this dissolution effect needs to be included in the transfer function.

Regarding to temperature- and other proxies, it is assumed that each morphospecies of planktonic foraminifera represents a genetically continuous species with a unique habitat. A recent study discovered that hidden genetic diversity among modern planktonic foraminifera has significant effects on paleoproxies derived from their tests. Kucera and Darling (2002), gathered all available data on genetic diversity, which suggest that cryptic genetic diversity is common among modern planktonic foraminifera, but the total number of cryptic genetic types per morphospecies is limited and the distribution is not random. A model example, where they split *G. bulloides* into three genetic types, led to a reduction in the 1 °C (Malmgren et al., 2001) prediction error rate. They concluded that genetic diversity among planktonic foraminifera may become more of an advantage than a disadvantage to paleoproxies. The only problem for now is to distinguish these genetic types in the fossil record.

d. Conclusion

Transfer functions on planktonic foraminifera have been the most important temperature proxy for several tens of year, but during the last few year other temperature proxies, and then in particular the alkenone biomarker, took over. Still, the precision of this method is rather good.

## 2.6 Transfer functions on dinocysts

a. Introduction

Dinoflagellates are second most important primary producers in the world, and because of their carotenoid pigments, they form the famous red tides during blooming populations (Armstrong and Brasier, 2005b). About 2000 species have been discovered in modern marine waters. Thus dinoflagellates show high species diversity, but they also show a high variability in morphology (fig.

12) and adaptation to a wide range of environments (Sournia, 1995), particularly temperature. Although dinoflagellates can move vertically, they only inhabit the shallow surface layer, because most of them cannot cross the pycnocline (Levandowsky and Kaneta, 1987). Most of them have a very complicated life cycle. During sexual reproduction, some species form diploid cells protected with cysts, which let them survive during a dormancy period (Fensome et al., 1993). Some species form calcareous cysts, and about 10-20% of the species produce cysts of the highly resistant organic diosporin, which is found in the fossil record (Dale, 1976; Head, 1996). The chemical macromolecular composition varies with different taxons (Fensome et al., 1993; Kokinos et al., 1998; Versteegh and Blokker, 2004). The so-called dinocysts measure typically 15 to 100 µm in diameter. There is a general consistency between the distribution of cyst-forming dinoflagellates in surface waters and dinocysts in sediments, but they are not in perfect correspondence (Dodge and Marshall, 1994). Despite that dinocysts are found everywhere in high concentrations, there is a clear decrease of species from the tropics to the poles.

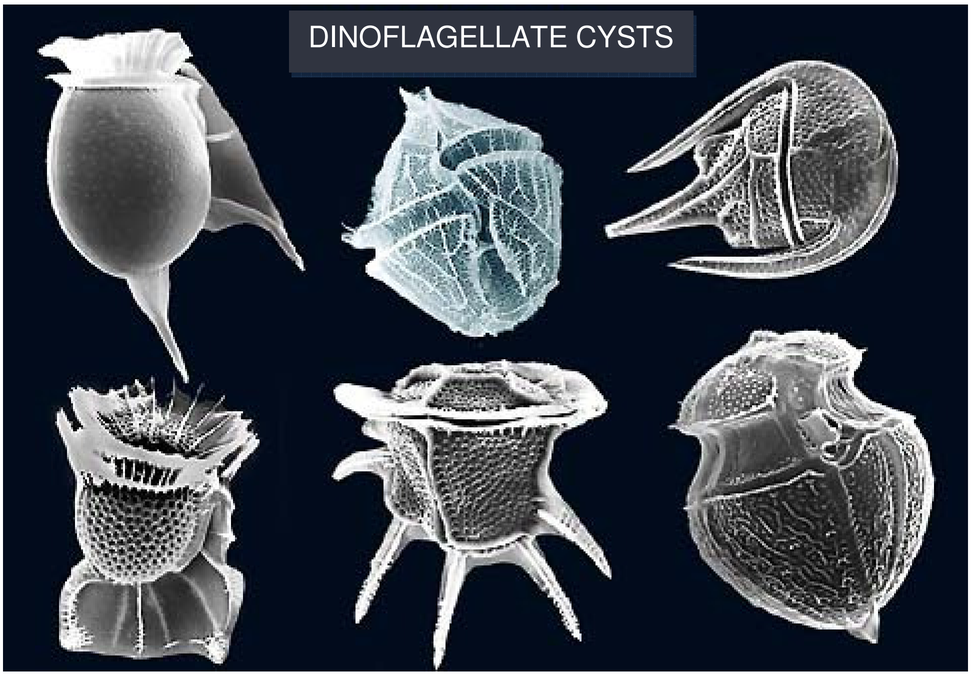


**Fig. 12: Some examples of different species of dinoflagellate cysts. These indicate a lot of inter-species variability, which make them easy to recognize and count.**

b. <u>Transfer function method for dinocysts</u>

Dinocysts can be used for different hydrographic parameters. Apart from temperature they can also be used to determine salinity, sea-ice cover, indicator of sea level and productivity. The last two decades there has been an increase in studies using dinocysts. The best transfer function method to reconstruct these oceanographical parameters is the modern analogue technique (de Vernal et al., 1994). This method has been used particularly to estimate the SSTs in summer and winter, salinity and sea ice cover in the North Atlantic (de Vernal et al., 1993; 2001; 1996; 1994; Eynaud et al., 2002; Hillaire-

Marcel et al., 2001; Levac et al., 2001; Solignac et al., 2004), Arctic and subarctic seas (de Vernal et al., 2005; Levac and De Vernal, 1997; Levac et al., 2001; Voronina et al., 2001), the northeastern North Pacific and Southern Ocean.

Because of co-variance among the above parameters, regression-based techniques such as the Imbrie and Kipp (1971) method or artificial neural networks have to be used with much caution (de Vernal and Marret, 2007). The relationship between assemblages and a given parameter and the equation describing this relationship, may differ significantly depending upon the initial calibration set. The analogue techniques and their variants appear more appropriate than calibration approaches. However, they can also yield faulty results. One potential problem concerns false analogues, notably when assemblages are characterized by the dominance of ubiquitous taxa.

The use of the best-analogue technique with a new dinocyst database, including 677 samples, permits quantitative reconstruction of sea-surface conditions at the scale of the northern North Atlantic and the Arctic domain. The degree of reliability of transfer functions can be evaluated from validation tests. The error of prediction calculated from modern assemblages is ±1.3 °C and ±1.8 °C for the temperature of February and August (de Vernal, 2001).

In the North Atlantic for example, the inventory of dinocysts that occur in Quaternary deposits include about 100 taxa (de Vernal et al., 1992). Only a total of 27 taxa is considered for statistical treatments. Such a number of taxa is relatively low as compared to the one used for diatom data treatment in subpolar basins (Koç et al., 1993). However, it is similar to the number of foraminifer taxa used for transfer functions at comparable latitudes (Imbrie and Kipp, 1971; Pflaumann et al., 1996), and it is higher than the number of coccolith taxa included in databases representative of middle to high latitudes of the North Atlantic.

c. Remarks

Fossil dinocysts contain dinosporin, which is very resistant (Armstrong and Brasier, 2005b). They are most abundant along continental margins. Because they are well preserved, unlike calcareous or silicic matter, the study of dinocysts in the field of paleoceanography and paleoecology during Late Cenozoic is very interesting. Another advantage is that dinocyst data also provide access to sea-surface reconstructions in neritic or epicontinental environments, where most other micropaleontological indicators of a pelagic production are rare. Such is the case, for example, in Hudson Bay, the Gulf of St. Lawrence and on the shelf off Labrador (de Vernal et al., 1993; Levac and De Vernal, 1997). Most taxa are also characterized by a relatively narrow range with respect to temperature, salinity and/or seasonal duration of sea-ice cover (de Vernal et al., 1997). The concentration of dinocysts in sediments decrease rapidly offshore, which makes them complementary to open ocean tracers, such as calcareous dinoflagellates (Vink, 2004; Vink et al., 2002), coccoliths (Winter et al., 1994) and planktonic forams (Bé and Tolderlund, 1971).

The relationship between dinocysts and SST is most probably season-dependant. Dinoflagellates encystment occurs most frequently during summer, which means that dinocyst assemblages are mainly related to summer SSTs (Matthiessen et al., 2005). This has to be taken into account when interpreting the results. At high northern latitudes in the Atlantic Ocean, there seems to be a relation between dinocyst assemblages and seasonality, explained by the difference between the warmest and coldest months. Seasonality plays probably a major role in dinoflagellate distribution, ecology and cyst production.

The relatively high species diversity, often more than 10, in the polar bioclimatic domain is a peculiarity of the dinoflagellate cyst assemblages as compared to planktonic foraminifer or coccolith assemblages. From this point of view, the dinoflagellate cyst database is particularly accurate for the reconstruction of hydrographic conditions in high latitude marine environments (de Vernal et al., 1997).

With dinocysts it is possible to reconstruct various parameters in addition to temperature. This is really an advantage compared to other paleoceanographic proxies, but it can also be a disadvantage because co-variance does occur in some marine environments, particularly in the open North Atlantic Ocean, where there is generally co-variance of seasonal SSTs, of SST versus salinity, and there is a relationship between sea-ice cover and SSTs. Also, near-shore areas, epicontinental seas and estuaries tend to have large differences between summer and winter SSTs, due to low thermal inertia as a result of stratification of a buoyant low salinity surface layer. The conclusion of the above is that the interdependency between hydrographic parameters depends a lot upon the marine setting. Apart from SSTs, SSSs and ice cover, dinocyst assemblages can also be used for the reconstruction of productivity and nitrates (Devillers and de Vernal, 2000).

Beyond the degree of precision that is defined on the basis of calibration and validation exercises, there are uncertainties. One concerns the fact that the fossil assemblages analyzed may have no modern analogue(Marret et al., 2001). Another uncertainty concerns the paleoceanographical conditions that may be out of the range of the modern data set that is represented in the reference data banks (de Vernal et al., 1997). Moreover, the combination of parameters that control the modern biogenic production and species distribution may have been different on the time scale of aimed paleoceanographical reconstructions.

The nutrient availability and the structure of plankton populations have an influence on dinoflagellate and thus cyst assemblages. This is why it can possibly have an effect on the relationship between paleoceanographic conditions and the dinoflagellates.

d. Conclusions

Dinocysts are complementary with other microfossils in many respects. They are very resistant, because they are composed of refractory organic matter. Dinoflagellates are found everywhere, but in far larger concentrations along continental margins than in open ocean environments opposing to most other microfossils. The well preserved dinocysts permit reconstructions from the study of marine sediments in spite of the dissolution that may affect calcium carbonate or silicate microfossils such as those in Baffin Bay (de Vernal et al., 1994). The relatively high species diversity in polar seas makes it one of the only tracers for paleocenographical research in Arctic areas. The possibilities with dinocysts as a tracer are still developing and improving. Transfer functions constitute a powerful tool in paleoceanography that require careful use depending upon the regional context and the ecology of organisms (de Vernal et al., 1997).

## 2.7 Transfer functions on diatoms

a. Introduction

Diatoms are unicellular algae lacking a flagella. Their cell wall is silicified forming a frustule with two valves. These frustules can be found in the fossil record and they may accumulate in diatomite. Diatoms live in almost all kinds of aquatic and semi-aquatic environments that are exposed to light (Armstrong and Brasier, 2005a). They are the dominant marine primary producers and play an important role in carbon, silica and nutrient budget of the modern ocean. Diatom taxonomy is based on the shape and ornamentation of the frustules. The classification of Simonsen (1979) is still the most accepted. About 285 genera and 12,000 species have been recognized (Round et al., 1990).

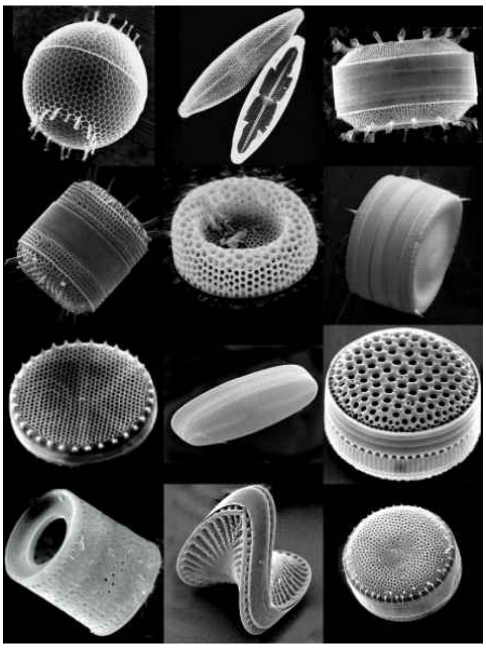

**Fig. 13: Mircoscopic view of different species of pennate (elliptical) and centric (circular) diatoms.**

Diatoms ranges in size from 1 to 2000 µm in length, but most species are between 10 and 100 µm (Armstrong and Brasier, 2005a). The diatoms can be divided in two groups: the pennate diatoms (elliptical), which are mobile thanks to the production of mucus, and the centric diatoms (circular), which are non-motile (fig. 13). The opaline silica frustules contain two halves, which are the epivalve and hypovalve. The region of overlap of these two halves is the girdle. This girdle is important for identification. The valve surface is covered with tiny pores called punctae. Arrangement of the punctae in lines gives rise to striae.

Centric diatoms live mostly as plankton in marine water, especially at subpolar and temperate latitudes, while the pennate diatoms inhabit the other niches and are of less interest in this study. Diatoms are very abundant in regions of upwelling, because these zones are rich in silica, phosphate, nitrate and iron. They are limited to the photic zone (<200 m) as they require light.

b. <u>Transfer function method for diatoms</u>

Diatoms are ideal for providing past sea surface temperature estimates through transfer functions (Birks and Koç, 2002). Generally reduced data sets of 20 to 40 diatom species are used to estimate temperatures. The advantage to work with reduced species data sets compared to raw data sets is that the high variability of the diatom assemblages is smoothed (Racca et al., 2004). Similarly, although it is possible to work on limited surface sample data sets, it may be best to work on extended data sets that cover broader modern conditions, hence reducing the possibility of nonanalog conditions.

Like with most temperature proxies, the SST accuracy derived from diatom assemblages of surface sediments is a bit less than 1 °C. A study on diatoms in the Labrador Sea for example, provides estimates with accuracies of 0.93ºC (August) and 0.64ºC (February) for temperature (De Sève, 1999).

c. <u>Remarks</u>

Diatoms are extremely sensitive to physical and chemical conditions, which makes them important as past environment reconstructors (Armstrong and Brasier, 2005a). Especially at high latitudes or at great water depth, diatoms are very important, because of the lack of calcareous microfossils in these places. They can even live under sea-ice as they can survive at low light levels thanks to a large set of pigments allowing them to capture a wide range of wavelengths.

Diatoms are found mainly in cold, nutrient-rich regions where silicic acid is not limiting, such as the polar regions, the coastal and equatorial upwelling systems, and in the coastal areas. Carbonate organisms outcompete the diatoms in other regions as they require less nutrients. Although there is not a real diatom zonation for the world ocean, clear zonation patterns have been identified in specific areas.

Fast reproduction allows diatoms to build a very high biomass, which will eventually form diatomite, if the preservation process is sufficient. This diatomite is ideal for climate reconstructions.

The relationships between abiotic and biotic factors on diatom distribution in surface waters are poorly understood, which might lead to biases. It is generally accepted that SSTs (Neori and Holm-Hansen, 1982), sea-ice conditions (Horner, 1985), macro- and micronutrient levels (Fitzwater et al., 1996), stability of the surface water layer (Leventer, 1991), salinity (esp. in coastal regions and regions of the Arctic Ocean influenced by sea-ice, due to strong salinity gradients) (Licursi et al., 2006), light levels and grazing are the most important factors on diatoms distribution.

The major processes determining diatom flux to the seafloor are sedimentation type (Schrader, 1971; Smetacek, 1985), lateral transport (Leventer, 1991), and dissolution in the water column and at the water-sediment interface (Kamatani et al., 1988; Shemesh et al., 1989). Although that only 1-10% of the diatoms reach the sediment (Ragueneau et al., 2000), the residual sedimentary assemblages are still indicative of surface conditions in different oceanic regions (Koç and Schrader, 1990; Pokras and Molfino, 1986) and can therefore be used to reconstruct oceanographic and climate changes (Koç et al., 1993; Pokras and Molfino, 1986).

### d. Conclusion

Diatoms are very sensitive to environment parameters and live in subpolar regions where they are a perfect alternative for calcareous microfossils as these calcareous microfossils practically do not exist in these regions.

## 2.8 Radiocarbon dating of sediment cores

Radiocarbon dating is the most powerful dating method for the Holocene. It is very accurate and can be performed in almost every deep see deposit, thanks to the presence of carbon. Nevertheless there are several problems when applying $^{14}C$ techniques on marine records (fig. 14). There is the need for calibration of the $^{14}C$ timescale, the potential variability in marine$^{14}C$ reservoir ages and age biases resulting from variable fluxes of $^{14}C$ to the sediment together with differential mixing due to sediment bioturbation.

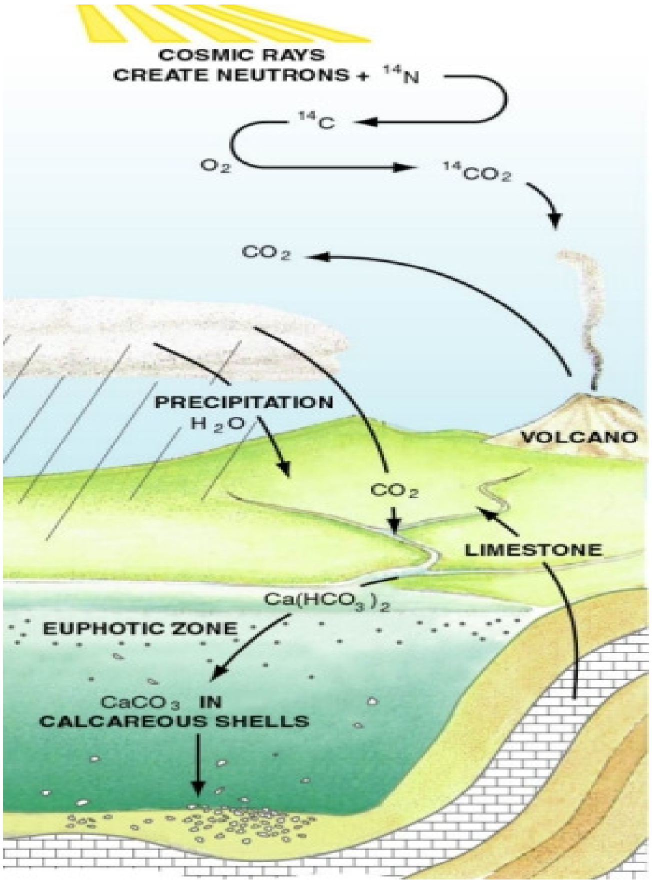


**Fig.14: The $^{14}C$ cycle indicates that a lot of processes are involved, and thus can have an effect on $^{14}C$ values**

### *2.8.1 Calculation of $^{14}C$ ages*

The $^{14}C$ is produced by cosmic radiation interacting with atmospheric nitrogen. It is mixed in the atmosphere as $^{14}CO_2$. $^{14}C$ dating is based on the radioactive decay law:

$$t = 1/\lambda * \ln (N_0/N_t) = 1/\lambda * \ln (A_0/A_t)$$

where $\lambda$ is the decay constant of $^{14}C$; $N_t$ and $A_t$ is the remaining $^{14}C$ concentration (N) or activity (A); and $N_0$ and $A_0$ are the initial $^{14}C$ concentration and activity. The $^{14}C$ decay constant was measured accurately and reached a consensus with a half life of 5730±40yr (Godwin, 1962).

The $^{14}C$ activity (depletion) of a sample relative to the standard is given by:

$$\delta^{14}C = ((A_{sample}/A_{standard}) - 1)) * 1000$$

where $\delta^{14}C$ is the standard-corrected $^{14}C$ activity per mil; $A_{semple}$ is the original measured activity; and $A_{standard}$ is 95% of the NBS oxalic acid standard. TO obtain correct $^{14}C$ dates, it is important that the measured $^{14}C$ activity is corrected for isotopic fractionation. The correction can be determined by measuring the abundance of the stable isotope $^{13}C$ and comparing it with the $^{13}C$ of the source material.

### *2.8.2 Measurement techniques*

The $^{14}C$ activity can be measured in two ways, either by counting the carbon ions using accelerator mass spectrometry (AMS) or detecting its radioactive decay (radiometric techniques). The advantage with AMS is that it has a far higher sensitivity and a shorter measurement time (1 hour). The advantage with radioactive decay is that only uses a minute fraction of the $^{14}C$ atoms present in a sample.

### *2.8.3 Contamination/Sample Materials*

The age resolution of radiocarbon dating is in the order of a few decades and can be considered as very good. A bigger problem is the potential of contamination, either before sampling or in the laboratory. In the laboratory this can be prevented by taking some precautions (van Klinken and Hedges, 1998).

The samples in which $^{14}C$-activity is measured form as follows. Atmospheric $CO_2$ dissolves and reacts within seawater to form carbonic acids and dissociate into bicarbonate and carbonate ions. The total of all marine aquatic carbonate species is referred to as dissolved inorganic carbon (DIC). The dated carbonate material, which is formed by marine fauna in the mixed layer, is assumed to be in equilibrium with the seawater. The main uncertainty comes from the variation of the marine reservoir composition. Therefore a correction database has been constructed, which allows to estimate apparent ages. Estimating DIC age and reservoir corrections requires caution. Foraminifera, corals and mollusks are mainly used to determine the $^{14}C$ age, because they are widespread and contain the necessary carbonate. If due to low productivity or lack of preservation, the $^{14}C$ dating is impossible with macrofossils, the pool of organic carbon can be used when biomarkers can be isolated in the organic carbon.

### 2.8.4 *Calibration of the radiocarbon timescale*

$^{14}C$ ages assume that initial $^{14}C$ concentrations remains constant during history, but studies show that this is not the case. As a result of changing $^{14}C$, radiocarbon ages differ significantly from calendar ages. The changing $^{14}C$ can be contributed either to changes in the $^{14}C$ production in the atmosphere (function of geomagnetic field and solar variability (Stuiver and Braziunas, 1993) or the distribution of $^{14}C$ between different reservoirs in the global carbon cycle (primarily deep ocean ventilation (Siegenthaler and Sarmineto, 1993). Marine-based calibration back to 50 ka have been provided by $^{14}C$ and $^{230}Th$-dated coral results with irregular sample spacing (Fairbanks et al., 2005) and at higher resolution from sediments of the Cariaco Basin (Hughen et al., 2004).

The most recommended calibration database for marine data is the MARINE04 database, which extends until 26 cal ka BP (Hughen et al., 2004).

### 2.8.5 *Marine $^{14}C$ reservoir age*

The residence time of $^{14}C$ in the deep ocean, with respect to gas exchange with the atmosphere, is in the order of several hundred to 1600 yr (Broecker and Peng, 1982). Stratified surface waters at low latitudes are well equilibrated with the atmosphere, and therefore have typically lower reservoir ages than at high latitudes, where older water outcrops at the surface.

### 2.8.6 *Bioturbation and abundance effects*

Flaws in apparent $^{14}C$ ages can occur through the combined effects of bioturbation and abrupt changes in $^{14}C$-carrier abundances and size (Bard, 2001; Broecker et al., 1999). There are some ways to overcome these problems. The most important one is to select cores with high sedimentation rates and high and steady foraminiferal fluxes. It is also useful to date only the samples occurring within peaks in foraminiferal abundance (Broecker et al., 1999).

Differential dissolution can also lead to biases. Shallower dwelling species have thinner shells and dissolution would preferentially remove these species and bias the sample toward older ages. A solution would be to restrict dating to species with narrow depth ranges, but in high-latitude marine environments this isn’t possible because the lack of species.

Another problem are the highly variable environmental and sedimentological conditions with respect to shallow marine settings. These environments have their specific problems regarding $^{14}C$ dating.

# 3. The Holocene climate

## 3.1 Intro

In this climate summary, the focus will be on climate reconstructions of marine sediments on a centennial to millennial timescale. The reconstruction of past climates and certainly the Holocene is an indispensable resource to help to predict the future climate as we can learn a lot from the natural climate variability since the last glaciations (Hay et al., 1997). In the last couple of decades, the knowledge of the Holocene climate has increased significantly due to new and improved techniques, and research in many geographic areas leading to more details, new ideas and conceptual breakthroughs. The Holocene has generally been a period of overall relative stability, compared to the last glacial (Alley, 2000; Bradley, 1999).

Some important problems still remain to reconstruct the Holocene climate.

1. The most critical problems are the temporal and spatial patterns of Holocene climate changes in chronology (Birks, 2008)
2. There are often diverse interpretations for the observed changes
3. The climatic sensitivity of different types of organisms
4. Problems in understanding and quantifying interactions with external forcing factors

## 3.2 Climate projects focused on proxy data

In 1971, Imbrie and Kipp (1971) developed transfer functions to reconstruct quantitatively summer and winter SSTs and SSSs from fossil foraminiferal assemblages, which was widely used in the CLIMAP (Climate Mapping, Analysis and Prediction) project (1976) that studied the climate of the Last Glacial Maximum (LGM) (21 ka BP). One year after CLIMAP, also the COHMAP (Co-operative Holocene Mapping Project) was founded (Cohmap, 1988). Here the basic idea was to simulate past climates every 3 ka during the past 18 kyr. After CLIMAP and COHMAP projects, a next project on Holocene climate reconstruction, PAGES (Past Global Changes), was launched in 1991. Its goal is to study and reconstruct Holocene climate history using a variety of records along broad-scale transects. This project still runs today. A summary can be found in Alverson et al. (2003)

## 3.3 Proxies

A variety of proxies exist that can be used for Holocene climate reconstruction. These proxies can be divided in two major groups. The first group consists of the proxies used for continental Holocene climate reconstruction. It includes as most important: lake sediment proxies (mainly pollen, microfauna and biomarkers), speleothems, tree rings and ice core records. All these proxies can be used for temperature reconstructions. Pollen, speleothems and tree rings are also useful to reconstruct precipitation. Important continental tracers are tree line changes with respect to glacier advances and retreats (Denton and Karlén, 1973) and sediment characteristics related to lake level fluctuations (Bowler, 1976; Bradbury et al., 1981).

The second group contains the proxies that predict changes in the marine Holocene climate coming from marine cores. Concerning temperature reconstructions, the most important ones have been thoroughly discussed in the previous section. Most of these proxies are also extensively used for salinity and sea ice cover reconstructions. An important tracer in the North Atlantic Ocean is ice rafted debris (IRD). These IRDs are hematite-stained grains, Icelandic volcanic glass and detrital carbonates coming from icebergs transported by the cold Greenland Currents, East Icelandic Current and Labrador Current, and therefore indicating the amount of ice melt in the Arctic (Bond et al., 1997).

## 3.4 Atlantic Holocene climate evolution and ocean current changes

### *3.4.1 General climate evolution*

*Younger Dryas*

The Holocene starts after a fast temperature rise of several degrees at the end of the Younger Dryas (YD). This warming can be detected in many temperature records and is dated at ±11,5 ka BP (Gulliksen et al., 1998; Hughen et al., 2000; Taylor et al., 1997). The temperature rise is linked to a reinvigoration of the Atlantic MOC, and thus a strengthening of the thermohaline circulation (McManus et al., 2004). The YD-Holocene transition is also associated with a reduced inflow of Irminger Current waters to the North Icelandic Shelf and with an abrupt resumption of the African Monsoon (Garcin et al., 2007; Knudsen et al., 2004). The temperature rise in Greenland is estimated to be 5-10°C and is associated with an increase in precipitation (Alley, 2000). Also in the Mediterranean region, and in the North and Norwegian Sea, a temperature rise of the same magnitude occurs (Hald et al., 2007).

*Early Holocene*

The so-called Pre-Boreal oscillations, which are cold spells during the early Holocene (9,2 ka BP, between 10,2 and 10,4 ka BP, 10,8 and 10,9 ka BP, and 11,3 and 11,5 ka BP), indicate that this was a period of high climate variability (Andresen and Bjorck, 2005; Björck et al., 2001; Schwander et al., 2000). This high variability has been related to regular fresh water influxes due to the melting of residual glaciers and of sea-ice from the glacial period. The melting itself occurred under the influence of increased summer insolation (Berger et al., 1978) and of variance in solar activity, which lead consequently to alternating periods of weak and strong thermohaline circulation (Bauch et al., 2001; Björck et al., 2001). This is also emphasized by the high seasonality differences (de Vernal et al., 2006) and nutrient-rich cool waters in the South Icelandic Basin during the early Holocene (Eynaud et al., 2004). The modern oceanographic sea surface circulation was established around 10,2 ka BP (Knudsen et al., 2004). During the early Holocene, the rise in temperature is significantly damped by the ice albedo effect in regions where glaciers are still present (Kaufman et al., 2004; Levac, 2001). In other North Atlantic regions the existence of an early-mid Holocene optimum is present (de Vernal et al., 2006; Duplessy et al., 2001; Marchal et al., 2002). Especially along the main SW-NE axis of the North Atlantic Current occur positive anomalies up to 6°C above present (de Vernal et al., 2006). These positive anomalies are sustained until 7,5-8,5 ka BP.

*Mid Holocene*

The mid Holocene, also referred to as the Holocene Thermal Maximum (HTM), is the warmest period during the interglacial, especially at intermediate to high latitudes (de Vernal et al., 2006; Duplessy et al., 2001; Duplessy et al., 2005; Eynaud et al., 2004; Kim et al., 2004; Koc and Jansen, 1994; Marchal et al., 2002; Sarnthein et al., 2003). Many planktonic foraminifera records though indicate an earlier Holocene maximum (Hald et al., 2007; Marchal et al., 2002). In the tropics, this climate optimum is less marked, nonexistent or even colder (wind driven upwelling) according to alkenone data (Kim et al., 2004). The thermal maximum is delayed to 6 ka in the Labrador Sea (fig. 15), probably related to the late degradation of the Laurentide Ice Sheet and to changes in vegetation (Andersen et al., 2004; Hall et al., 2004). In the central NA, the early HTM seems to be only distinct in which marine proxy data are summer and ocean surface related (Moros et al., 2004). IRD and temperature records suggest that increased polar water supplies on the east Greenland shelf during the mid Holocene were mostly deflected towards the northern Iceland shelf and did not efficiently reach the south of Greenland (Moros, 2006; Solignac et al., 2008). A decoupled dynamics of the western branch of the IrC and of the NIC could be the cause of such a discrepancy (Solignac et al., 2008). In northern Africa, this period is known as the African Humid Period due to an intense monsoon system.

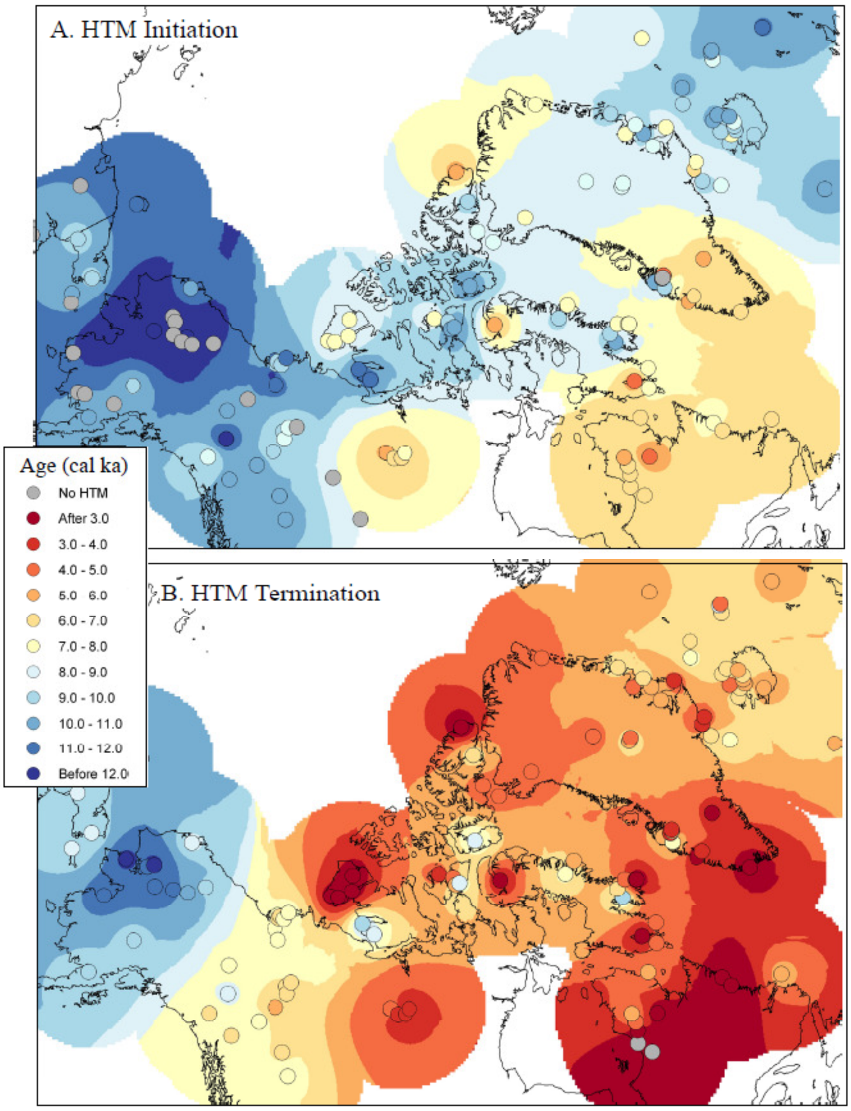


**Fig. 15: This map presents the spatio-temporal pattern of the Holocene thermal maximum (HTM) in the western Arctic, (a) Initiation and (b) termination of the HTM. Gray dots indicate equivocal evidence for the HTM. Dot colors indicate bracketing ages of the HTM, which are contoured using the same color scheme.**

The period between 8 and 9 ka BP is still a period of severe climatic disruption (Mayewski et al., 2004). There is a marked cooling and change in atmospheric circulation in Scandinavian and Iceland areas (Hald et al., 2007; Karlén and Kuylenstierna, 1996; Knudsen et al., 2004), which is occurring during a time of high IRD flux in the North Atlantic (Bond et al., 1997). In the northeast Atlantic (west of Reykjanes Ridge) there is an opposing trend, and temperatures reach their maximum during this period (de Vernal et al., 2006; Solignac et al., 2008). This is also the time that rapid melting of the Laurentide Ice Sheet (LIS) occurs (Barber et al., 1999) and that the East Mediterranean experiences very humid conditions (Arz et al., 2003).

Around 8,2 ka BP there is a major shift in both oceanic and atmospheric circulation patterns due to the draining of the Canadian glacial Lakes Agassiz and Ojibway in the NE Atlantic (Alley et al., 1997). This 8,2 ka event lasted for about 200 year and had the largest impact in Greenland (temperature drop of about 5 °C), but also influenced the whole North Atlantic region and possibly elsewhere in the Northern Hemisphere (Alley and Ágústsdóttir, 2005; Rohling and Palike, 2005). There is for example a marked dry period between 8,4 and 7,6 ka in the tropics. This event also created the setting compatible with LSW production (de Vernal et al., 2006; Hillaire-Marcel et al., 2001) state that the LSW became established mainly after 7 ka BP.

Between 8 and 7 ka BP some major changes occurred in the NW Atlantic due to insolation induced strengthening in the westerlies (Sachs, 2007). These stronger winds cool the slope waters by increasing convection in the Labrador Sea and the export of cold water via the Labrador Current, reinforcing the subpolar gyre, and creating opposing sea ice anomalies in the Labrador and Greenland Seas (Curry and McCartney, 2001). A link is suggested between the cooling of the slope waters and the initiation of deep convection in the Labrador Sea (Sachs, 2007). An alternative mechanism for cooling of the slope waters is a southward migration of the GS path, which is supported by the data.

The overall Atlantic overturning circulation shows no trend in the long-term (Bauch et al., 2001; Oppo et al., 2003). Still proxy records indicate a weakening of the NE Atlantic Deep Water production throughout the Holocene. This is probably related to a slight increase of sea ice variability and average seasonal duration (Solignac et al., 2004). It suggests a progressive enhancement of the western branch of the Atlantic Meridional Overturning with respect to its northeastern route (de Vernal et al., 2006).

*Mid-late Holocene transition*

Large scale changes in the atmospheric and oceanic circulation mark the transition between mid and late Holocene between 7 and 5,4 ka BP (deMenocal et al., 2000; Solignac et al., 2004). This time interval corresponds with the exhaustion of the meltwater supplies from decaying ice sheets (Dyke et al., 2003), a minimum in sea ice (de Vernal et al., 2006) and a sharp increasing trend in summer insolation (Berger and Loutre, 1991).

The period from 5 to 6 ka is one of worldwide glacier expansions and cooling in the North Atlantic (Denton and Karlén, 1973; Mayewski et al., 2004). A shift is observed in drift ice input from regions under the influence of the North Atlantic Drift towards sites influenced by the cold EGC (Moros et al., 2006). Also the area of the Faroe-Shetland ridge experienced an increase in IRD and SSTs around 5,4 ka BP, which has been related to a more dominant SC and a weakening in NAC (Solignac et al., 2004). In Northern Africa, the African Humid Period came suddenly to an end at about 5,4 ka BP, which has been associated with gradual insolation changes and strong non-linear feedback processes (Claussen et al., 1999).

*Late Holocene*

Alkenone derived SSTs in the North Atlantic realm show a continuous SST decrease in the NE and NW Atlantic towards the end of the Holocene, while a persistent warming occurs over the western subtropical Atlantic, the eastern Mediterranean Sea and the northern Red Sea (Kim et al., 2004; Sachs, 2007). Summer based SST records indicate a long-term trend of southward displacement of the oceanographic Polar Front in the Denmark Strait region initiating around 5-4 ka BP. This trend may be related to reduced Northern Hemisphere summer insolation (Andresen and Bjorck, 2005; Moros et al., 2004). The long-term trend around Iceland is characterized by a decrease in temperature and an increase in ice rafting between about 6,7 and 3,7 ka BP (Andersson et al., 2003; Bendle and Rosell-Mele, 2007; Birks and Koç, 2002; Marchal et al., 2002; Moros et al., 2004). Since the decline of temperatures, the amplitude of the short-term climate variations has increased (Moros et al., 2004; Risebrobakken et al., 2003), which is consistent with the onset of neoglaciation (Nesje et al., 2000). An unstable but generally warmer period occurs in the NA between 3,7 and 2 ka BP. The period from 2 until 0,5 ka BP is marked by a second neoglaciation trend, along with an increase in snow precipitation (Andersson et al., 2003; Birks and Koç, 2002; Moros et al., 2004; Risebrobakken et al., 2003). According to Moros et al. (2004) the temperature instability between 3700 and 2000 can be associated with a late Holocene increase in winter insolation at high northern latitudes.

The increased climate variability is connected to a decrease in winter precipitation in Scandinavia during the cold events (Nesje et al., 2001) and to an increase in Arctic sea-ice cover derived from diatom records (Koc and Jansen, 1994). Records in the EGC and NIC show warming winter SSTs and diminishing trends of sea ice extent in this area during the late Holocene period. This is probably related to a strengthening of the IrC (Solignac et al., 2004).

Model experiments suggest that interactions between the Nordic Seas and the Labrador Sea, during these last few kyr of high variability, could have resulted in oscillations of the overturning circulation of the Atlantic Ocean at multi-centennial-to-millennial timescales (Schulz et al., 2007). A continuous freshwater input into the Labrador Sea can push the large-scale ocean circulation into a bi-stable regime, which is characterized by phases of active and inactive deep-water formation in the Labrador Sea. In contrast, deep-water formation in the Nordic Seas is active during all phases of the oscillations.

### *3.4.2 Periodicity during the Holocene*

Many studies put forward a certain degree of cyclity during the Holocene on a centennial to millennial timescale (Bond et al., 1997; Chapman and Shackleton, 2000; Schulz et al., 2004).

The worldwide expansion of glaciers between 8-9; 5-6; 3,8-4,2; 2,5-3,5; 1-1,2 and 0,15-0,6 ka BP made Denton & Karlen (Denton and Karlén, 1973) conclude that glacier advances occurred about every 2,5 kyr. They also suggest that these events are related to solar variability. A similar periodicity in dust deposition over Greenland and a ~780 yr periodicity in the East Asian monsoon regime has also been correlated to this 2,5 kyr periodicity.

The study of ice rafted debris IRD (hematite-stained grains, Icelandic volcanic glass shards, and detrital carbonates) in North Atlantic cores lead to the discovery of a 1470±500 year cycle, which has been linked to solar activity and is much similar to the glacial period related Dansgaard-Oeschger Cycles ((Bond et al., 1997), 2001). About every 1500 year, cool, ice-bearing waters from north of Iceland were advected as far south as the latitude of Britain. At about the same times, the atmospheric circulation above Greenland changed abruptly. These enhanced concentrations of IRD occur around 11,1; 10,3; 9,4; 8,1; 5,9; 4,2; 2,8; 1,4 and 0,4 ka BP. These events have also been discovered in many other studies (Bianchi and McCave, 1999; Chapman and Shackleton, 2000; Solignac et al., 2004; Viau et al., 2002).

Variations in sediment lightness, a proxy for changes in North Atlantic Deep Water (NADW) circulation, in a North Atlantic sediment core indicate high-frequency fluctuations with periodicities equivalent to 550 and 1000 yr as well as a <1600-yr cyclicity comparable to the Bond cycles over the past 11,5 kyr (Chapman and Shackleton, 2000). Cross-spectral analysis suggests that these periodicities in NADW circulation were coherent with fluctuations in atmospheric conditions over Greenland and may have been linked to short-term variations in atmospheric $^{14}C$. Their results imply that the pattern of NADW production has been a significant factor affecting centennial-to millennial-scale Holocene climate variability in the North Atlantic region.

Proxies of atmospheric temperature and humidity from Greenland and northern/central Europe show evidence for 900-y climate oscillations between 3 and 8,5 ka BP (Schulz et al., 2004). They suggest that negative salinity anomalies in the North Atlantic are the immediate cause of these cold spells, by means of reduced northward heat transport via thermohaline circulation. A decrease in North Atlantic sea-surface salinity, predicted by climate models for a future greenhouse climate (Wood et al., 1999), may restart this climate oscillator.

### *3.4.3 North Atlantic Oscillation variability*

One of the challenges in Holocene climate research is how to reconstruct “modes of variability” (Oldfield, 2005), like ENSO, AO, NAO, Pacific Decadal Oscillation and Atlantic Multi-decadal. This study focuses on the NAO, as the North Atlantic is the main study area.

There has been a lot of discussion regarding the Holocene trend of the NAO. In the early 2000s, most studies and model experiments suggest a trend towards a negative NAO during the Holocene (Gladstone et al., 2005; Rimbu et al., 2003; Rimbu et al., 2004). Model simulations are mainly compared with alkenone based temperature reconstructions around Europe, which also imply a positive NAO during the mid Holocene (Kim et al., 2004). This trend towards a negative NAO is contested by precipitation patterns in the Mediterranean and Scandinavian areas (Jalut et al., 2000; Nesje et al., 2001).

Recently, some important dinocyst and alkenone based temperature reconstructions have been published (de Vernal et al., 2006; Sachs, 2007; Solignac et al., 2008). Records from the NW Atlantic indicate an increased meridional SST gradient and a 4-10°C cooling (Sachs, 2007; Solignac et al., 2006), while in the NE Atlantic there is only a 1-3°C cooling (Kim et al., 2004; Marchal et al., 2002).

## 3.5 Holocene forcings on millennial and centennial timescales

The relative importance of external forcings like orbital forcing, solar variability, and volcanic activity, and the complex interactions between these factors and their impacts on the global climate system are not fully understood (Bradley et al., 2003; Oldfield, 2005). These forcings induce small perturbations, which trigger a chain of secondary reactions. These reactions can either amplify the primary change (positive feedback) or reduce the change (negative feedback). A brief summary on the orbital and solar activity forcings discussing how they were reconstructed and how they affected the climate is noted below.

### *3.5.1 Orbital forcing*

Variance in insolation is driven by orbital changes, due to alterations in the relative position of Sun and Earth in space determined by eccentricity, obliquity and precession (Milankovitch, 1920; Milankovitch, 1941). Orbital forcing is slow on a Holocene timescale, but change in insolation over the past 12 kyr is considerable and cannot be neglected (Eystein et al., 2008). The change in insolation can amount to 54 W/m² (37 W/m² for the Holocene) at high latitudes (Beer and Geel, 2008). Orbital forcing is the only forcing that is fully understood, and can be calculated for past and future (Berger and Loutre, 2004). A graph representing insolation at 65°N is shown in figure 16.

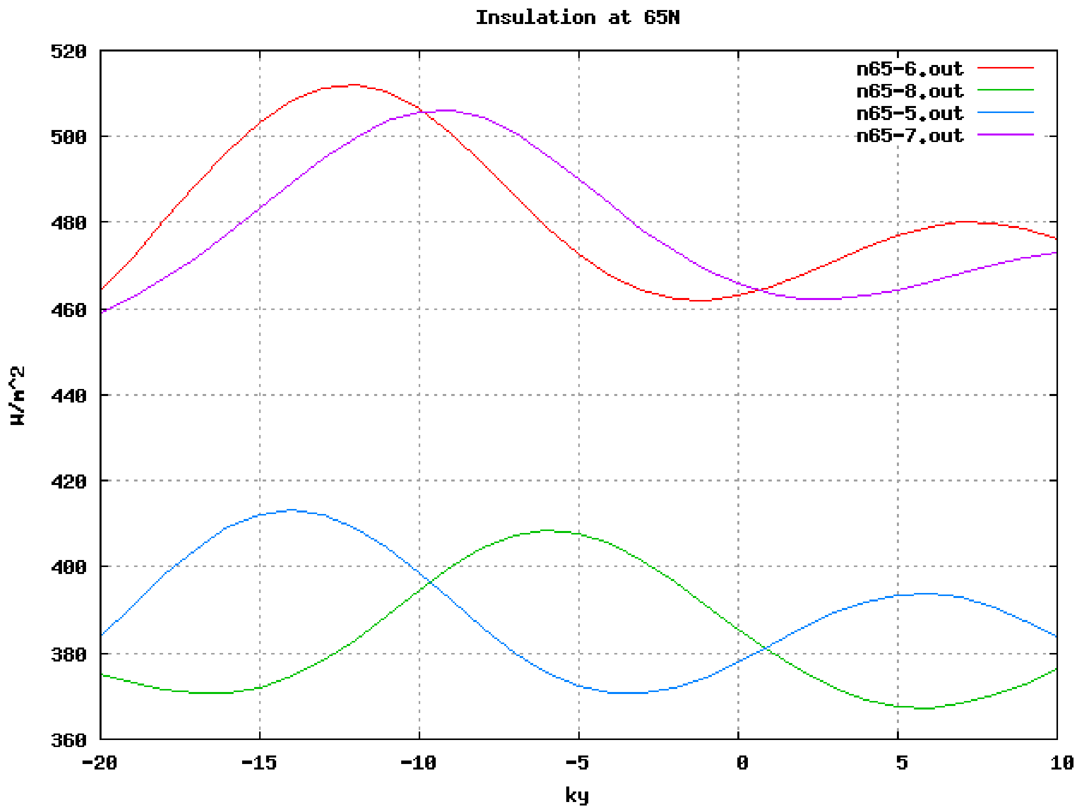


**Fig 16: The insolation (W/m²) at 65°N for the two months after and the two months before the summer solstice from 20 ka BP before present to 10 ka AP, calculated with the program insola from Laskar et al. 2004.**

Most records and model experiments indicate that changing orbital parameters are the main forcing for Holocene climate evolution on an annual as well as seasonal basis (Claussen et al., 1999; Liu et al., 2003; Moros et al., 2004; Sachs, 2007).

### *3.5.2 Solar activity and solar forcing*

The Sun is an active star showing considerable cyclic changes in its magnetic activity, as expressed in the sunspot number. The solar radiation arriving at the top of the atmosphere, also called Total Solar Irradiance (TSI), fluctuates in phase with the magnetic activity of the Sun (Beer and Geel, 2008).

Observations of sunspots, which are a good measure for solar activity are available for the last four centuries. Indirect proxy data, derived from measurements of the cosmogenic nuclides $^{10}Be$ and $^{14}C$ in ice cores and tree rings, have been proven to be a relatively good alternative for solar activity estimates prior to these observations (Beer et al., 1990; Muscheler et al., 2004; Stuiver et al., 1991). These nuclides are produced through interaction of nitrogen and oxygen with galactic cosmic rays, whose intensity is determined by solar activity and the geomagnetic field (Masarik and Beer, 1999). The physics of the production processes in the atmosphere are well understood, but the transport from the atmosphere into archive is rather complex, and is still not clarified (Beer et al., 2002).

The solar component is extracted from the signal by removing the geomagnetic effect. This results in a record of the solar modulation function Φ, where 0 means a completely quiet sun and 1000 MeV corresponds to an active sun (Vonmoos et al., 2006). Such a modulation function records has been reconstructed between 9,3 and 0,3 ka BP. There are three well known cyclic features present in this reconstruction, which show periodicities of ~11 yrs (Schwabe cycle), ~80 yrs (Gleisberg cycle), ~205 yrs (de Vries or Suess cycle), and 2,2 kyr (Hallstatt cycle) (Stuiver and Braziunas, 1993).

Due to problems of filtering the geomagnetic field, TSI reconstruction for the entire Holocene on the long-term were not trustworthy. However, recent findings of the relationship between total solar irradiance and the open solar magnetic field created the possibility to derive TSI values from the solar modulation function (Steinhilber et al., 2009).

The effect of changes in solar activity remains debated, because solar irradiance changes are assumed to be relatively small and amplifying mechanisms are required (Rind, 2002) to account for the magnitude of the observed climate changes (0,5 -1°C in Europe during the last 500 year (Luterbacher et al., 2004). Fact is that a lot of studies show marked correlations between climate and solar variability (Andresen and Bjorck, 2005; Denton and Karlén, 1973; Magny, 1993))

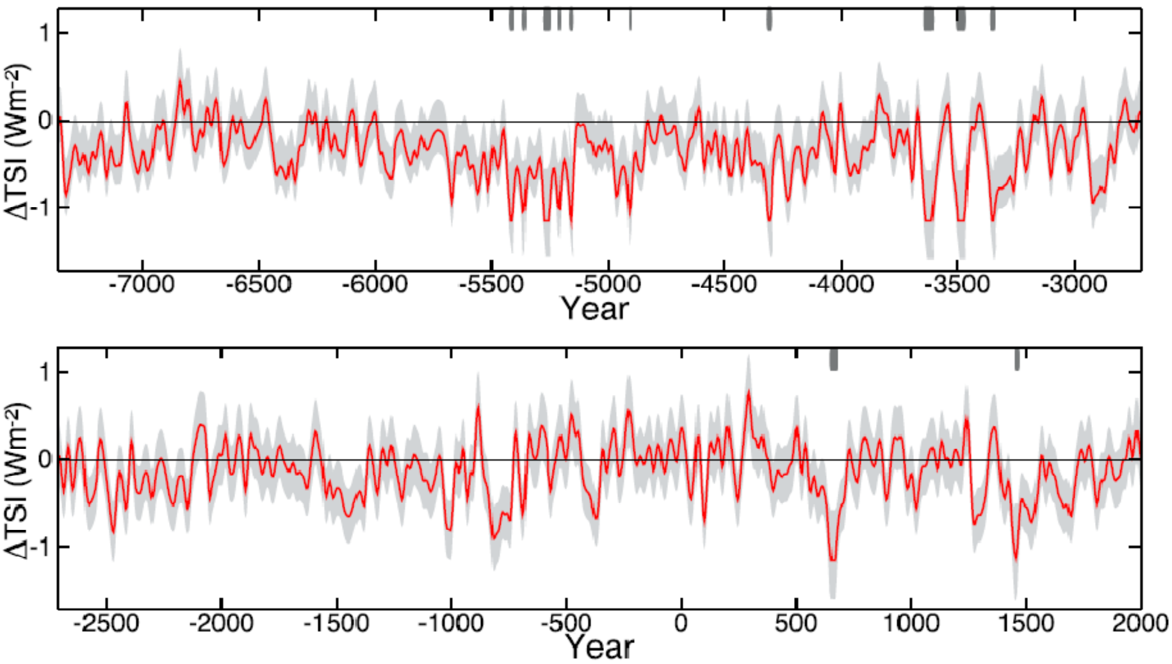


**Fig 17: 40-year (cycle) averaged TSI for the past 9,3 ka BP based on its relationship with the open magnetic field ($B_r$) relative to the value of the PMOD composite (Fröhlich et al., 2006) during the solar minimum of the year 1986 (1365,57 W/m²). The shaded band is the 1 σ uncertainty considering the uncertainties of the TSI-$B_r$ calibration and of the reconstruction of $B_r$. The bars in top of the plot mark periods when TSI reaches the minimum value of 1364,64 W/m² corresponding to Φ = 0 MeV and $B_r$ = 0 nT. During these periods the uncertainty is not defined and was set to 0,5 W/m²**

### 3.6 Proxy comparisons

A general comparison between the five proxies during the Holocene has not been published yet, but there are some articles comparing two or three proxies. In most of the articles, the proxy comparison is also limited to one location or region. Only recently, a first article has been published on a global scale comparison between the alkenone and Mg/Ca proxies (Leduc et al., 2010). The most important findings from different proxy comparisons are stated below.

Jansen et al. (2008) compared several proxies in a core in the Norwegian Sea and notices that proxies cluster in two groups. A first one with a distinct Holocene thermal maximum (diatoms and alkenones) and a second one which shows an opposing warming trend towards the late Holocene and more high amplitude changes at century to millennial time-scales after about 4 ka (foraminiferal-based). There is also no reason to distrust these temperature reconstructions, so other factors like seasonality of the forcing, the habitat of the biological proxy indicators, and the seasonality of the vertical structure of the upper layers of the high-latitude should cause these striking differences (Jansen et al., 2008). The fact that certain planktonic foraminifera occur mostly around the thermocline is suggested to play an important role in this discrepancy (Risebrobakken et al., 2003),. Therefore, planktonic foraminifera based records from high latitude areas should be considered as primarily representing thermocline temperatures (Hald et al., 2007; Jansen et al., 2008).

Intercomparison between planktonic foraminifera and dinocysts yield conflicting paleotemperatures estimates, notably in the subpolar North Atlantic (de Vernal et al., 1997; Eynaud et al., 2004)). Changes in surface salinity and structure of upper water masses are involved to explain the distinct response of dinocysts and foraminifera. Conflicting past temperature estimates based on different proxies are relatively numerous and point to the fact that there are no unequivocal transfer functions (de Vernal et al., 1997).

The comparison of alkenone and Mg/Ca based records indicates significant differences between the two, and suggests that regional paleoceanographic dynamics interacting with phytoplankton and zooplankton ecological behavior affect SST records with a strong seasonal imprint in the geological record (Leduc et al., 2010). This implies that one should be careful interpreting multi-proxy based SST maps. Upwelling and nearby rivers are also known to cause substantial differences between alkenone and Mg/Ca records (Elderfield and Ganssen, 2000; Weldeab et al., 2007)

# 4. Model development and results

## 4.1 Introduction

### *4.1.1 History of climate modeling*

Climate modelling has known a rapid evolution over the past three decades after having started in 1979 (Imbrie and Imbrie, 1980). These climate models can be made for reconstructing the past climate, but more important also to predict the future climatic changes. Because of anthropogenic impact, a better understanding of the climate system and feedbacks within the climate system is crucial. The importance of understanding past climate change in order to predict future climate scenarios is stressed by the Intergovernmental Panel on Climate Change (IPCC).

The first climate models, atmosphere general circulation models (AGCM), evolved from numerical weather prediction models during the 1960s and became very important to climate science during the 1970s. In the beginning the focus was only on the LGM, because of the difference from today's climate and the availability of proxy data (CLIMAP_Project_members, 1976); summary in Crowley (2000).

In the 1980s, the first ocean general circulation models (OGCMs) were created. It was soon after the first OGCMs appeared that the importance of poleward oceanic heat transport in climate change and variability was discovered (Manabe and Bryan, 1985). The foundation of a second global project, Cooperative Holocene Mapping Project (COHMAP), came in the late 1980s. The goal of this project was to reconstruct climate conditions at successive 3,000 yr intervals from 18,000 BP to present (Cohmap, 1988).

A final breakthrough came with the consideration of biogeochemical cycles as a crucial component of the climate system in the early 1990s, whereas before the main focus was on physical feedbacks between ocean, atmosphere and sea ice.

### *4.1.2Today's climate models*

Climate models can be divided in two main categories: conceptual and numerical models. Only the numerical models are considered as conceptual models give no quantitative results. These numerical models are very complex due to the interaction of the different subsystems (Crucifix, 2008). The numerical models can be divided in two main groups of models: the general circulation models (GCMs) and the earth system models of intermediate complexity (EMICs). Only GSMs are shortly discussed as all the models considered in this study belong to this group of models.

Global GCMs provide the most comprehensive results and suit better than regional models as boundary data for paleoclimatic simulations tend to contain large uncertainties (Crucifix, 2008).

Models can run in an uncoupled mode, but then rely on reconstructed data specifying the boundary conditions. The coupled ocean-atmosphere models are a better approach, but still not satisfying as they consider a constant heat transport, limiting simulations to comparable climates (Bice et al., 2000). At the moment, the most complex models are coupled atmosphere-ocean-vegetation general circulation models (AOVGCMs), where it is now also possible to include biosphere, carbon cycle and atmospheric chemistry.

#### *4.1.3 Active climate projects*

At the moment, there are many project groups working on different aspects of the climate system. The more reputable groups include Paleoclimate Modelling Intercomparison Project (PMIP), Past Global Changes (PAGES), Rapid Climate Change (RAPID) and the Coupled Carbon Cycle Climate Model Intercomparison Project (C4MIP). The PMIP is discussed more in depth as this project deals with the modeling of the mid to late Holocene period.

The PMIP was launched back in 1992, and its first phase was based on the analysis and comparison of AGCMs. In 2002 a second phase was initialized due to the development of the more complex OAVGCMs (Harrison and Prentice, 2003). The focus of this project has been mainly on the LGM (21 ka BP) and mid Holocene (6 ka BP). One of the goals of the PMIP 2 is maintaining a database of model results in which long-term means and individual year are archived.

a) *Role of proxy data*

Proxy data are very important for the construction of these climate models as they can be used for data assimilation (models help to physically interpret the local proxies in a global context), for integration in the models and for testing and evaluating models.

b) *Limitations of modeling*

The ocean-atmosphere-cryosphere-biosphere system is a complex system with different time and space scale interactions, which are generally nonlinear and unstable making it very difficult to model the system over a long time path. Therefore, many of these models need flux adjustments to balance surface fluxes at the ocean-atmosphere interface to avoid numerical drifts (Kanamitsu et al., 2002). These flux adjustments are based on the present climate, and are therefore not very reliable for past climates.

## 4.2 Factors causing climate variability during the Holocene

According to climate model studies, orbitally forced changes in insolation are the key factor to cause long-term climate variations during the Holocene (Braconnot et al., 2000; Crucifix et al., 2002; Gallimore and Kutzbach, 1989; Hewitt and Mitchell, 1998; Weber, 2001; Weber et al., 2004; Weber and Oerlemans, 2003). Other important factors are internal feedbacks from which ice-albedo and taiga-tundra feedbacks play a major role, as they significantly influence the surface albedo (Foley et al., 1994; Kerwin et al., 1999).

An important limitation is that most climate models assume that the climate has been in equilibrium with 9 or 6 kyr BP as a boundary condition. Because of the constantly changing orbital forcing and the melting of ice sheets during the early Holocene (Brovkin et al., 2002; Claussen et al., 1999; Wang et al., 2004), this equilibrium can be questioned. That's why several groups (Crucifix et al., 2002; Weber, 2001) have recently simulated the Holocene climate evolution using earth system models of intermediate complexity (EMIC's, Claussen et al. (2002)). According to these studies, the coupled system clearly participates and interacts in the Holocene.

## 4.3 ECBilt-CLIO-VECODE model

### *4.3.1 Introduction*

ECBILT-CLIO-VECODE is a three-dimensional OAVGCM (Goosse et al., 2005; Renssen et al., 2005). The atmospheric component is ECBILT2 (Opsteegh et al., 1998), a quasi-geostrophic model with simple parameterizations for diabatic heating processes. The oceanic component is CLIO3 (Fichefet and Morales Maqueda, 1997; Goosse and Fichefet, 1999), which is made up of a 3°×3°, ocean general circulation model coupled to a comprehensive thermodynamic-dynamic sea ice model. ECBILT-CLIO is coupled to VECODE, a global vegetation model that simulates the dynamics of two main terrestrial plant functional types (trees and grass) as well as desert (Brovkin et al., 2002; Brovkin et al., 1998). The importance of the vegetation part in modeling the climate changes between 0 and 6 ka BP is especially important in northern Africa, as "green" conditions were present in these regions during the mid Holocene (Renssen et al., 2003).
This model is an updated and improved version simulating the climate closer to modern observations. This is especially due to a new land surface scheme that includes the heat capacity of the soil, and the use of isopycnal diffusion and represents the effect of meso-scale eddies in the ocean (Gent and McWilliams, 1990). The sensitivity of the model is about 0,5°C/(W/m²), which is better than most coupled climate models (between 0,5-1°C/(W/m²)) (Cubasch et al., 2001).

The main objectives of this model are to estimate Holocene climate variability at northern high latitudes, as this variability can be explained by a response of the coupled climate system caused by slow changes in external forcings (Renssen et al., 2004).

#### *4.3.2 Model experiments and comparison with proxy data*

a) *Millennial scale variations*

The last 9 kyr have been simulated with the ECBILT-CLIO-VECODE model taking into account the annual varying insolation (Berger et al., 1978) and trends of atmospheric concentrations of $CO_2$ and $CH_4$ (Raynaud et al., 2000). The effects of high frequency changes of volcanic and solar activity have not been taken into account in this simulation.

The reason why the experiment only starts at 9 kyr BP is due to the lack of a dynamical ice-sheet model. Such a model could simulate the melting of the Laurentide and Scandinavian Ice Sheets earlier in the Holocene. Because the Laurentide Ice Sheet only disappeared at ~7 kyr BP, the simulation was divided in two sections called ICE (9-6 kyr BP) and MAIN. The only difference between the two simulations is that in the ICE experiment an additional residual Laurentide Ice Sheet was included between 9 and 7 kyr BP that was instantly removed at 7 kyr BP. Overall Atlantic overturning is kept constant throughout the experiment, but a strengthening in heat release has been assigned to the Labrador Sea and a weakening to the Nordic Seas (corresponding to proxy data) (Renssen et al., 2005). The averaged temperature results for both simulations are shown in figure x.

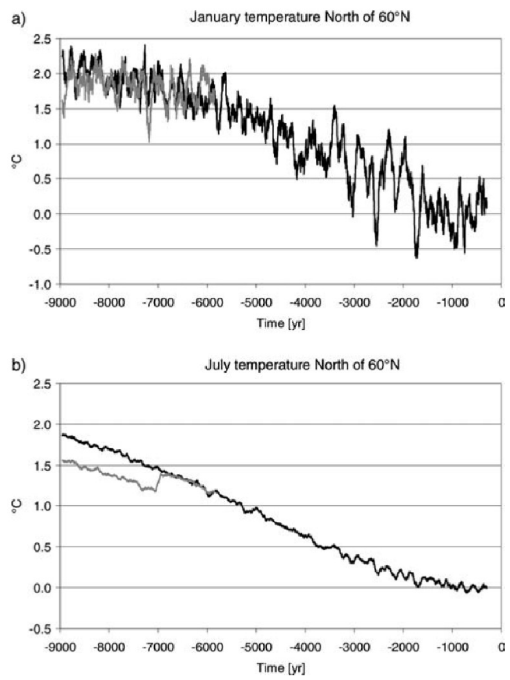


**Fig. 18: Simulated time series (100-point running means) of surface temperature (°C) averaged over the north of 60°N, shown as deviations from the preindustrial mean (1000-250 yr BP), a) January and b) July. The black line represents MAIN, the gray line ICE. The preindustrial mean for January and July temperatures are -27,5 and 8,8 °C, respectively (Renssen et al., 2005).**

The results of this experiment are in agreement with the long-term summer cooling at high latitudes due to changes in orbital forcing. The average temperature depression of 1-3°C (fig. 18) is similar to earlier OAGCM simulations (Renssen et al., 2005).

A number of other important changes during the Holocene are also indicated by this model. The first important one is a weakening in overturning strength and convection in the Nordic Seas, and an opposing change in the Labrador Sea, which is confirmed by results of proxy data (Hillaire-Marcel et al., 2001; Solignac et al., 2004). A second one is the evolution towards more climate variability in the higher latitudes due to cooling and advancing sea ice (Goosse et al., 2003; Goosse and Renssen, 2004). These results are consistent with high resolution records (Andersen et al., 2004; Andersson et al., 2003; Lauritzen and Lundberg, 1999).). A last important finding is a decrease in zonality, which indicates a reduction of the North Atlantic Oscillation. This is supported by certain proxy studies (Andersen et al., 2004; Hammarlund et al., 2002)), but there are also a number of articles suggesting a trend towards a positive NAO, and thus a more zonal trend (Marchal et al., 2002; Sachs, 2007)).

*b) Centennial scale variations*

This experiment uses the same model, with the same assumptions as the above, but now the high frequency effects of changes in solar activity are included (Renssen and Goosse, 2006). The long term trend in the solar modulation parameter is removed to avoid introducing an artificial trend, due to the uncertainties connected to the data, long term changes in solar activity (Muscheler et al., 2005)), and a linear trend is assumed between the solar modulation function and TSI based on Lean (2000).

This experiment reveals four interesting trends. The simulation suggests a link between TSI reductions and a local shutdown of deep convection, an increase in chance to have a convection failure towards the end of the Holocene, an extension of the cooling by about 50 year after long lasting negative TSI anomalies, and a consistency between the results and proxy evidence (Renssen and Goosse, 2006).

## 4.4 PMIP2: average model results

### *4.4.1 Surface temperature and precipitation changes*

The average results of PMIP1 and PMIP2 models regarding surface temperature and precipitation change between 6 and 0 ka are presented in fig. 19. The explanation for major changes between 6 and 0 ka is attributed to an enhanced seasonal cycle in the northern hemisphere, which is simulated by all models (Braconnot et al., 2007). This favors continental warming during summer, which deepens the thermal low over land and intensifies the low level winds and moisture transport from the tropical ocean to the continent. The result is an amplification of the monsoon system in the tropical regions (Joussaume et al., 1999). In winter the major changes correspond to a large continental cooling with maximum values within the subtropical regions where the change in insolation is the largest. This contributes to strengthen the winter monsoon, so that the northern hemisphere continents experience drier conditions, whereas precipitation is reinforced over the ocean (Battarbee et al., 2004; Cane et al., 2006). The models generate similar large-scale patterns, but there are major differences in the magnitude of the warming between different OA simulations.

From these findings we can thus conclude that high latitude areas have experienced major changes in temperature and seasonality, while low latitude areas experienced major shifts in precipitation and overall hydrologic regime.

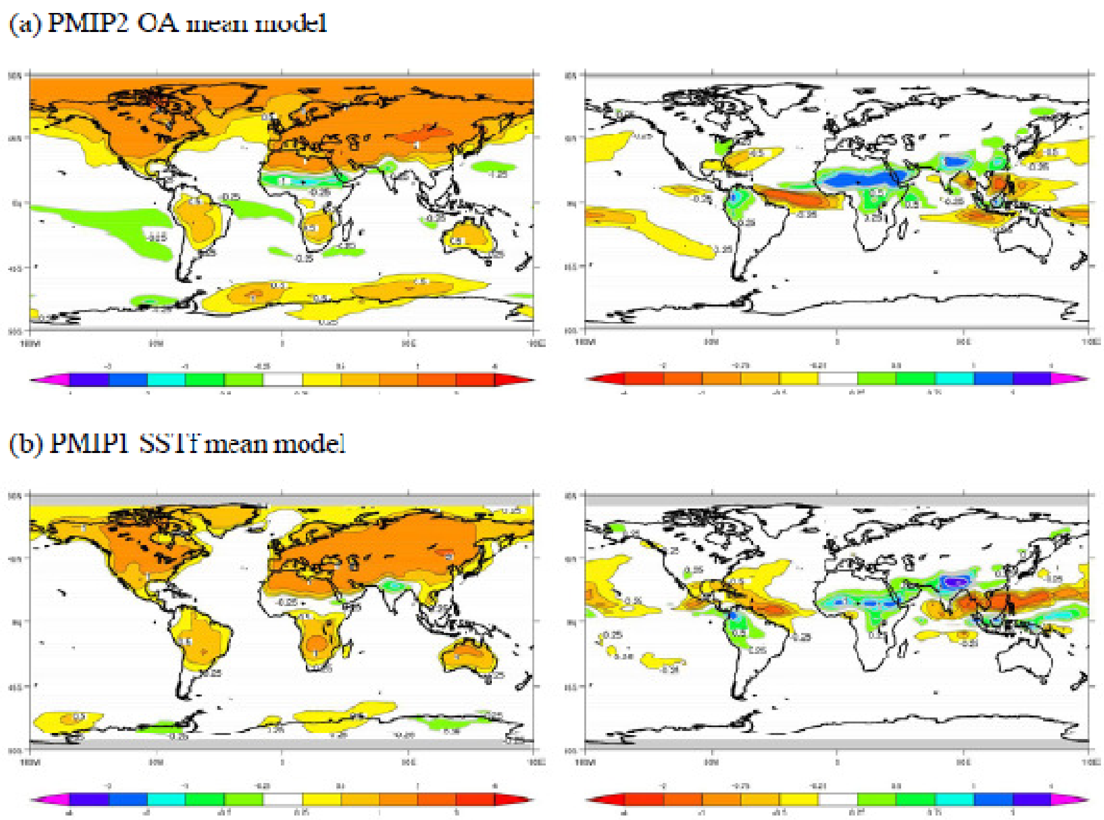


**Fig. 19: JJAS mean surface air temperature (°C) and precipitation (mm/d) differences between mid Holocene and preindustrial for (a) the ensemble mean of PMIP2 simulations and (b) the ensemble mean of PMIP1 simulations (Braconnot et al., 2007)**

### *4.4.2 SST changes*

Figure x show the average sea surface temperature results of eleven different models. A study on SST results from the PMIP2 has not been published yet. If compared to the surface temperatures, the SST changes indicate a same trend and are generally more subtle.

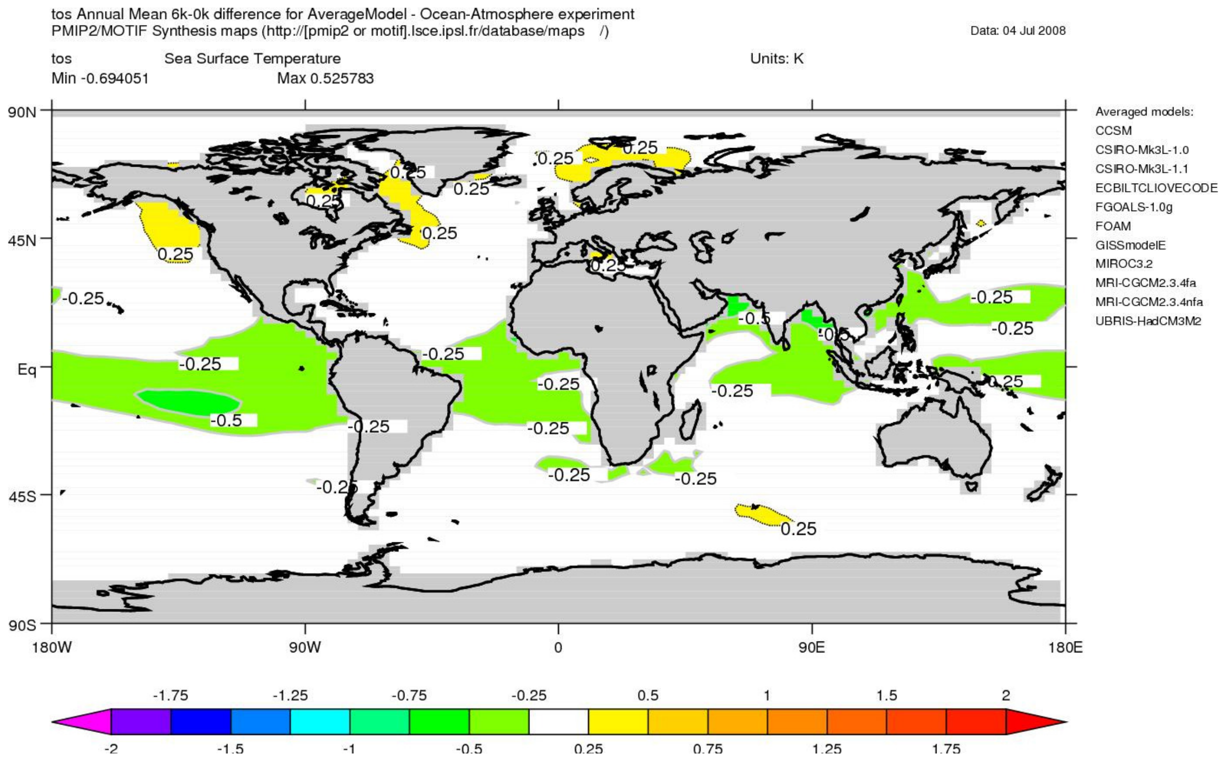


**Fig. 20: 11 OA model average of annual mean SST change between 0 and 6 ka BP (Synthesis maps – http://pmip2.lsce.ipsl.fr/database/maps)**

# II Material and methods

## 1. Data collecting

In the interest of this study, as much as possible SST data from the Atlantic Ocean and Mediterranean Sea spanning at least 1,5 kyr BP of the Holocene have been gathered.

The datasets and graphics are collected from online databases as the PaleoNetwork for Geological and Environmental Data (PANGEA) database (Diepenbroek et al., 2002) (www.pangaea.de).

A second major source on the internet for data from paleoclimatic research is the World Data Center-A (WDC-A) (http://www.ncdc.noaa.gov/paleo/data.html) and coordinated by the **International Geosphere-Biosphere Programme** (**IGBP**) and the Past Global Changes (PAGES). The data in these databases are stored in a consistent format together with the related meta-information for their understanding. For all five temperature proxies, the PANGAEA and WDC-A database were searched for useful datasets.

As the aim was to collect as much data as possible, there is variability in data storage formats. For most of the data the reference article and data tables are available, but there is also an important amount of data, where only the article is available and a minor amount where only the data table could be collected. Data tables and graphics from articles are all stored and arranged in excel files to form a well structured database. The database is available on cd-rom.

## 2. Database construction

Now some words on the database construction. The final version of the proxy database contains five excel files, wherefrom each one of them contains all temperature reconstructions of one of the five proxies. All five excel files have the following structure. A first sheet gives some key information of all temperature reconstructions, including location, time span, resolution and applied method. Then there are three sheets summarizing each record in numbers to easily notice similarities and differences between the graphs. Finally follow all the raw data and graphs, where every record takes one sheet and contains at least a graph of the temperature reconstruction. The order of the records is based on the direction of flow of the modern ocean surface currents, which relies on the Mariano Global Surface Velocity Analysis (MGSVA) (Rosenthiel School of Marine and Atmospheric Science (RSMAS, Miami University), http://oceancurrents.rsmas.miami.edu/index.html). The ocean current system in the Atlantic starts at the Benguela Current, and after going through the South Subtropical Gyre, North Subtropical Gyre, North Atlantic Current system and Subpolar Gyre, finally finishes at the Labrador Current.

## 3. Data presentation

### *3.1 Data tables*

All data are arranged primarily by proxy and secondary according to ocean surface currents. It contains the following variables: location (ocean current, geographical and 3D coordinates (longitude, latitude and depth), core name, resolution (in yr), reference (article and/or database), transfer function method or calibration, seasonal period of SST (only for transfer function methods), uncertainty of prediction, time cover of Holocene, and for possible remarks.

### *3.2 Data maps*

A map is created for each of the five proxy methods with the location of their datasets. Besides these separated maps, there is also a general map with data points from all proxies. These location maps are put together with Generic Mapping Tool (GMT). Thanks to these maps it is easy to discuss the geographical spread of the proxies. The low latitude or tropical data are the datasets between 30°S and 30°N, the middle (subtropical) and high latitude areas are from 30°N to 80°N.

### *3.3 Original studies*

As there are so many data, it is impossible to give a short summary of the original studies of the records. For most data, more information can be found in the database where the articles are ordered by proxy and by name of the author. If the article is not included, an abstract has been enclosed in a word document.

## 4. Data results

In order to easily compare the graphs in the database, three sheets of data tables have been constructed giving useful information on the temperature records. All these tables were produced by visually estimating temperature changes (±0,5°C) or ages (±0,1 kyr BP). The first one contains information on the millennial to Holocene timescale temperature variability of the graphs. These tables include the average Holocene temperature and temperature change, overall Holocene temperature maxima and minima over a period of at least 500 yr, the overall Holocene temperature variability (max Holocene temperature – min Holocene temperature), average temperature difference between early to late, and mid to late Holocene, average seasonality difference if summer and winter temperatures are available, and finally some information on the Holocene Thermal Maximum (5,5-9,5 ka BP), and Mid Holocene Dip(s) if present. The second set of data tables treats the centennial Holocene temperature variability. Only datasets with at least intermediate (>300 yr) resolution are considered. These tables contain the average short term variability (100-500 yr), timing of minimum and maximum temperature peaks during the Holocene, with special attention for the 8,2 ka event and centennial scale events during the last 2,5 ka BP including the Late Iron Cold period (2,5-2,1 ka BP – LICP), Roman Warm Period (2,1-1,7 ka BP – RWP), Dark Ages Cold Period (1,7-1,1 ka BP – DACP), Medieval Warm Period (1,1-0,7 ka BP – MWP) and Little Ice Age (0,7-0,1 ka BP – LIA) (these events show some degree of overlap), and at last an estimate of possible short term cycles during the Holocene. The third set of data tables describes the temperature changes of the most reoccurring temperature changes on a short timescale.

From the most valuable data tables, maps have been created with GMT. Graphs have been produced in Excel from the raw data tables. Certain temperature graphs have been put together with Corel Draw for comparison on a centennial timescale.

## 5. Model results

The ECBilt-CLIO-VeCode model was used to make a NetCDF database containing ocean and climate data for the last 8000 year. Air temperature maps and graphs are constructed with a "Grid Analysis and Display System", better known as GrADS. Only annual temperatures are considered. The created maps and graphs are also stored in the database. It should be stressed that these temperatures are air temperatures and no sea surface temperatures. This should also be taken into consideration in the results and discussion.

Maps have been constructed for the North Atlantic averaged over 500 year for the last 8000 year with contour lines every 2°C. Then maps have also been created, where temperature is averaged over the Holocene Thermal Maximum (5,5-8 ka BP), Late Holcene and Latest Holocene (0-2,5 ka). A last set of maps averages temperatures over the LICP, RWP, DACP, MWP and LIA periods. Besides the SST maps, SST versus age graphs have been constructed based on the available proxy data. In these graphs, temperatures are a moving average over 50 year to filter temperature extremes. In total 58 graphs have been produced. All these maps and graphs are included in the database.

Apart from the maps and graphs created with GrADS, two maps have been constructed with GMT representing the extent of the positive or negative temperature evolution of model and data during the last 8 kyr.

# III Data presentation

## 1. Data facts and remarks

A total of 159 temperature reconstructions have been collected. Alkenone based records are most abundant in the database with 68 datasets. Second important proxy is the planktonic foraminifera transfer function method contributing 35 temperature reconstructions to the database. Then there is the dinocyst proxy with 25 datasets, where temperatures are also calculated through transfer functions. A fourth group of 22 temperature reconstructions is based on the calibration of Mg/Ca values found in certain planktonic foraminifera. The smallest group of datasets is based on diatom transfer functions adding only 9 temperature records.

The resolution varies from a few data points to about 10 yr, and is divided in five categories. The following terms for time resolutions of the datasets are applied in this study:

- Very low: few data points (use: recognize a general Holocene trend)
- Low: 700-350 year resolution (use: millennial trend)
- Intermediate: 350-160 yr resolution (use: temperature extremes & millennial cycle)
- High: 160-50 yr resolution (use: centennial trend & centennial cycle)
- Very high: 50-10 yr resolution (use: very short term temperature changes & cycles)

In total there are 25 datasets with very low resolution, 28 with a low resolution, 41 with an intermediate resolution, 48 with a high resolution, and 17 with a very high resolution. The numbers for the five categories are present in the data table for each separate proxy.

The Mg/Ca and alkenone calibrations give both annual temperatures, but the SSTs from proxies based on transfer function methods are seasonal temperatures. About half of the planktonic foraminifera datasets and almost all dinocyst based records have winter and summer (February and August) temperatures. The planktonic foraminifera data with temperature reconstructions of cold and warm season will be considered winter and summer season, although there is some minor difference in the transfer function between them. Most of the other half of the planktonic foraminifera data and all but one diatom based record only contain summer temperatures. Some planktonic foraminifera data include another season and there is one annual based record.

In the remarks data column, the possible influence of rivers, glaciers, irregular resolutions and the reference of the modern database for the transfer function methods (if available) are mentioned. If the dataset is not calibrated to calendar age, it is also included, but more than 90 procent of the datasets has been calibrated. The reason to include coast, river and/or melt water (glacier) influence in the data table is to easily spot temperature reconstructions, which might be deviating due to one of the above factors. Temperature reconstructions derived from cores taken nearshore are indicated by marking the water depth in the summary table in red. The reason to pay attention to the proximity of the coast is that temperatures tend to vary a lot more near shore than offshore. Also local processes and coastal currents play a larger role near the coast leading to anomalous data.

An overview of the data is too large to include in the text, and can be found in Appendix 2.

## 2. Data map

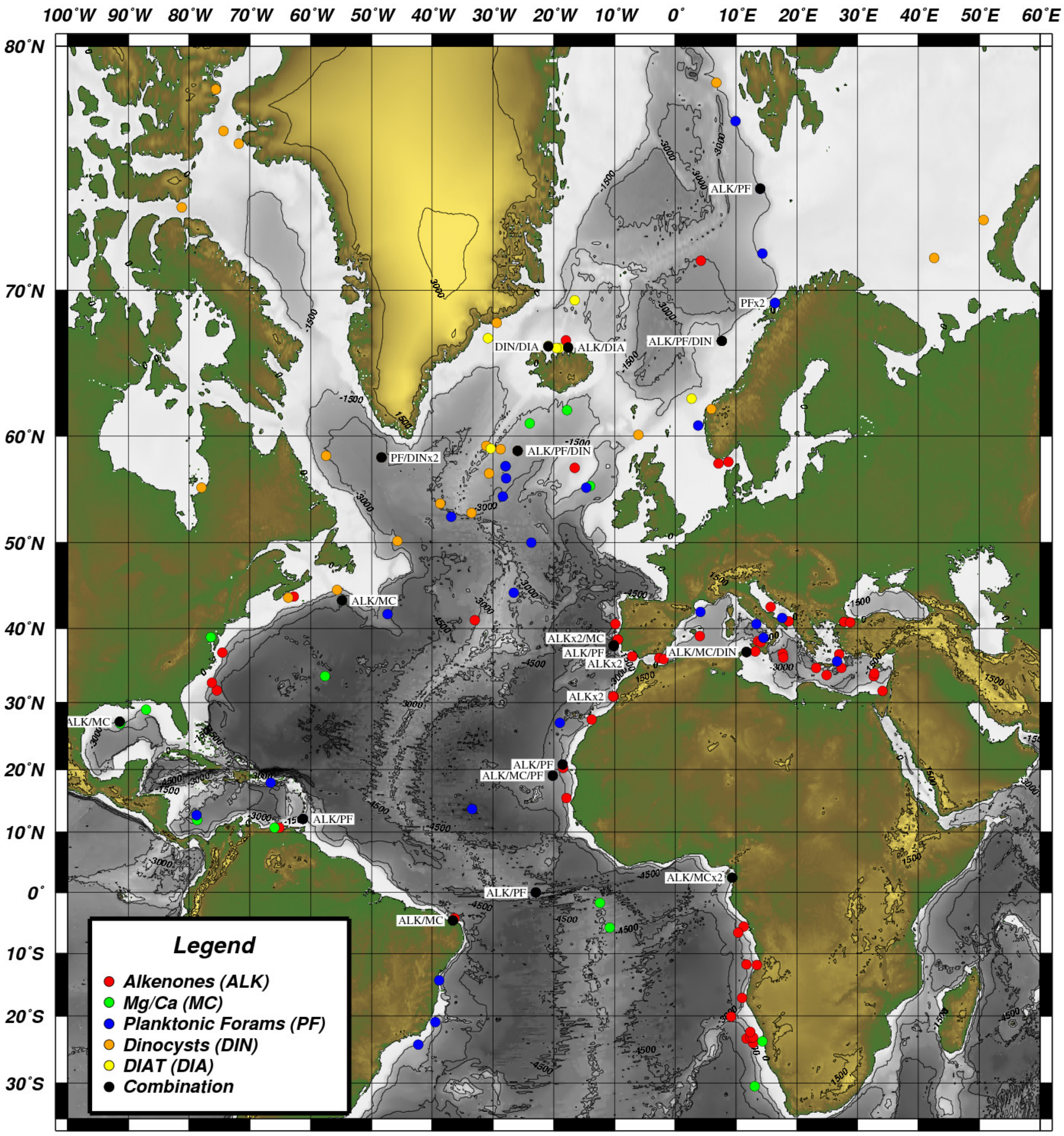


**Fig 21: Geographical spread of all temperature records for each proxy. If more than one proxy record is available from the same core, a text box has been added with the names of the proxies.**

The map in figure 21 shows the geopraphical spread of all the proxies. Maps with core locations and names for each individual proxy are available in the database. The majority of the alkenone and Mg/Ca based temperature reconstructions are situated in the tropical to subtropical latitudes, while the diatom and dinocyst based reconstructions can only be found in the high latitudes. The planktonic foraminifera transfer function based temperature reconstructions are quite regularly spread over the Atlantic region. Almost all records are situated near continents (shelf and slope) and on the Mid Atlantic Ridge. This is quite logical as these areas are easy to access, have high sedimentation rates and are key regions in the ocean current system.

## 3. Differences in transfer function methods/calibration analysis for a same proxy

Knowing the variability within a same proxy (due to several transfer function and calibration techniques) is useful before comparing the calibration methods of the proxies with each other. In addition it is important of being aware of the regional limitations and uncertainty levels of the different methods. These different methods can sometimes be compared as some datasets contain more than one temperature reconstruction method. Datasets with different reconstruction techniques in the same region and influenced by a same surface current can also be compared.

### *3.1 Alkenones*

For alkenones, there are five methods being used for calibration: the Prahl et al. (1988), the Müller et al. (1998), the Prahl & Wakeham (1987), the Rosell-Melé et al. (1995) and Sikes & Volkman (1993) calibration methods. The Prahl & Wakeham (1987) calibration was the first designed method, but was one year later slightly adjusted to the more accepted Prahl et al. (1988) calibration. The Prahl et al. (1988) and Müller et al. (1998) calibrations are used for the majority of the temperature reconstructions. The first one can be applied globally, while the second one gives faulty results for the polar regions. The other calibration methods are only used in one or a few datasets. The Rosell-Melé et al. (1995) and Sikes & Volkman (1993) calibrations were developed specifically for the northern and southern polar regions, but have not been used extensively due to the alternative of other and better proxies in these regions. The temperature limits for the methods range from about 4 to 28°C and the calibrations become less reliable at the extremes. The standard errors vary from 1,5°C for the global method to 1°C for the Müller et al. (1998) calibration and 0,7°C for the Rosell-Melé et al. (1995).

The temperature record results for the Müller et al. (Müller et al., 1998) and Prahl et al. (1988) calibration methods are in good agreement with each other. The other calibrations cannot be compared well, due to the lack of datasets.

### *3.2 Mg/Ca*

Most Mg/Ca based records are reconstructed through measurements on the *G. ruber* species, and calibrated with the Dekens et al. (2002). method or the slightly adjusted Anand et al. (2003) method. The other calibration techniques, which are based on other foraminifera as *G. sacculifer, N. pachyderma, G. bulloides* and *G. inflata*, are only used in one or two datasets and are not discussed. The standard errors of about all these calibration methods vary between 1 and 1,2°C.

As there is only one dominant calibration method, it is not possible to compare the different calibrations. In general the Mg/Ca based temperature records display large temperature variability, but in most datasets temperatures remain rather stable on average (mostly slight decrease).

### *3.3 Planktonic foraminifera*

There are nine transfer function methods applied on planktonic forams counting: I&K (Imbrie and Kipp, 1971), F13' (Kipp, 1976), MAT (Hutson, 1978; 1980), WA-PLS (Braak and Juggins, 1993), SIMMAX-MAT (Pflaumann et al., 1996), M&M (Morey et al., 2005), RAM (Waelbroeck et al., 1998), ANN (Malmgren et al., 2001), ML (Birks and Koç, 2002). With 17 datasets, the MAT is by far the most applied. The SIMMAX-MAT, RAM, ML, WA-PLS and I&K methods are used in 5 or 6 datasets, F13', ANN and M&M in 1 or 2. The standard errors for most methods vary around 1°C, with the RAM and ANN method having the lowest standard error, followed by SIMMAX-MAT and MAT. The I&K and F13' methods, which are the most old ones, along with the WA-PLS and ML methods, have estimated errors of 1,3 to 1,9°C. In spite of the larger errors for ML and WA-PLS, these methods are less biased by spatial autocorrelation in the training set (lack of independence of spatially close sites), while the cross-validation estimates of the root mean square error for most other techniques are overoptimistic (Hald et al., 2007). Except for these different transfer function methods, also the modern databases, on which the transfer functions are based, differ from region to region and have also evolved in time. These differences cause artificial differences between the regions.

Compared to the other techniques, the MAT technique shows the least centennial and millennial variability (about half). In the data for the Norwegian Current, it is also clear that the MAT underestimates the latitudinal temperature change compared to WA-PLS and ML methods, which give similar results. The F13' and I&K method are also much alike. Data indicate that these methods tend to underestimate temperatures changes in the low latitudes and overestimate them in the higher ones, and also the temperature variability is mostly higher than for the other techniques. ANN and RAM have more outliers, but all in all the remaining methods show same variability and average Holocene temperatures. The Holocene temperature trend differences between all the techniques are mostly minor.

### *3.4 Dinocysts*

The dinocyst based temperature records are all reconstructed by applying a modern analogue transfer function technique (Guiot, 1990) initially used for pollen records, and slightly adjusted for dinocysts. The modern database upon which this technique relies was gradually extended by Rochon (1999) and de Vernal et al. (2001, 2005, 2006). This implies that the accuracy of the temperature reconstructions also improved during the establishment of the database. One of the first databases had estimated errors of prediction of 1,8 and 1,3 °C during August and February, while these errors are only 1,5 and 1,1 °C in the most recent database (de Vernal and Hillaire-Marcel, 2006).

As all data use the same transfer function technique, it has no use to discuss differences caused by varying temperature reconstruction methods. The only things that are worth noting is that these dinocyst records indicate a lot of variability and that regional variability seems to play a major role in the polar waters, as there are enormous local differences. There is one dataset where also ANN (Malmgren et al., 2001) is applied and this one indicates more seasonality difference compared to the MAT.

### *3.5 Diatoms*

For the diatom data, WA-PLS and I&K transfer function methods are mostly applied, and give very similar results. Other methods have been tested, but were not so successful (Andersen et al., 2004); (Justwan et al., 2008). Standard errors are 1,5 °C for August and 1 °C for February for most of the data (Koç and Schrader, 1990). All data based on diatoms are coming from the polar latitudes, as there is a wide variety of species living in these areas, making it possible to estimate temperatures more correctly. Temperature records seem to be more or less in agreement on a millennial time scale.

### *3.6 Conclusion*

The uncertainty of many proxy methods did decrease during the last year thanks to expanding the modern databases and refining the transfer functions and calibrations. Most methods have uncertainties of 1 to 1,5°C. Uncertainties are generally higher at high latitudes and for summer temperatures. This is rather convenient as the summer temperature variability is higher than the winter temperature variability, and temperatures for higher latitudes vary more than temperatures at low latitudes.

# IV Results

A first goal of this thesis is to uncover the general differences between the proxies. This is important towards the next steps in this study of trying to reconstruct the Holocene climate changes in the Atlantic on a millennial and centennial timescale, and to compare the proxy data with climate models.

Several maps indicating temperature change are included in the results (figs. . One must be careful interpreting these, as all diatom records and about half the planktonic foraminifera records show only summer temperature trends. As the seasonal trends are not always like the annual trends, this can lead to faulty interpretations. For specific records of the planktonic foraminifera, one should advise the data table (appendix 1) to check whether dealing with only summer or both winter and summer temperatures. For the dinocyst and other planktonic foraminifera records, an average between winter and summer temperatures is displayed. If these averages are compared with the calibration based proxies (alkenones and Mg/Ca), it should also be kept in mind that these calibrations display merely the temperature during production.

## 1. General trend differences between the proxy methods

The comparison of the proxy methods focuses mainly on the long term Holocene changes. Frequently recurring differences in average Holocene temperatures, total Holocene temperature amplitude and temperature evolution (particularly based on mid to late Holocene temperature evolution) are discussed. Also the timing of the Holocene maxima is mentioned for the different proxies. From the short term temperature changes, only the variance in short term variability (100-500 yr) is mentioned. The focus is only on general differences between the five proxies, as it is not the intention to make a detailed study of each deviating record. Regionally the attention goes mostly to latitudinal differences. A clear distinction is made between tropical and high latitudinal records.

The average Holocene temperatures for the five proxies indicate some constant trends. The most pronounced trend is that alkenone based records are showing higher temperatures than the other proxies in the higher latitudes (alkenones: 1-4°C) (fig. 22). In the tropical latitudes the opposite is true and some alkenone records tend to underestimate temperatures a bit (0,5-1.5°C). From all proxies, the Mg/Ca is least consistent with respect to average Holocene temperatures, thus no real trend exists. The three transfer function based proxies are most of the time in good agreement with each other. The only marked difference is that the planktonic foraminfera based winter temperatures are clearly higher than the dinocyst winter temperatures (averagely 2-3°C). If compared with current winter temperatures, the dinocyst winter temperatures are more trustworthy than the planktonic foraminifera ones. This also means that dinocysts records indicate larger seasonality differences than planktonic foraminifera based records.

| Current | Alkenones | Mg/Ca | P. Forams (S) | P. Forams (W) | Dinocysts (S) | Dinocysts (W) | Diatoms (S) | Modern annual |
|---|---|---|---|---|---|---|---|---|
| NAC | - | - | 12; 16-16,5 | 10,5 | 10-13 | 5-7 | 11-11,5 | 7-13 |
| IrC | 11,5-12 | 7,5-10,5 | 12-14 | 9-10 | 11-14 | 2-7 | - | 9-11 |
| NIC | 7,5-8 | - | - | - | 8 | 2 | 10,5-11 | 2-7 |
| NAD | 13,5-14 | 10-10,5 | - | - | - | - | - | 9-11 |
| SC | - | - | 13,5-14 | - | 11-11,5 | 5,5-6 | - | 10-14 |
| NS | 13-13,5 | - | - | - | - | - | - | 9-11 |
| NC | 12 | - | 11-14 | - | 12,5-13 | 5-6 | 12 | 7-9,5 |
| WSC | 6-6,5 | - | 4,5-5,5 | 2-2,5 | - | - | - | 1-4 |
| MC | - | - | - | - | 8 | - | - | 5-7 |
| EGC | - | - | - | - | 7,5-8 | 0-0,5 | 6-8,5 | 0-6 |
| WGC | - | - | 7-7,5 | 2,5-3 | 8,5-9 | 2-2,5 | - | 4-5 |
| BaC | - | - | - | - | 2-2,5 | - | - | -2 to 1 |
| HB | - | - | - | - | 6,5-7 | -(0,5-1) | - | 4-6 |
| LaC | 12,5-13 | 14,5-15 | - | - | 8-17,5 | 1,5-4 | - | 2-10 |

**Fig 22: Average Holocene temperatures (°C) for each proxy in different current regions (see appendix 1 for abbreviations). As a reference, estimates of modern average annual temperatures have been added. Alkenone temperatures are almost equal to summer temperatures at high latitudes (S: Summer; W: Winter).**

The overall Holocene temperature amplitude for alkenone records is especially in the central Atlantic lower than for the other proxies. Only in the Mediterranean region, North Icelandic Current and Labrador Current the overall temperature variability is in agreement with the other proxies. Dinocyst based reconstructions indicate clearly higher summer amplitude than planktonic foraminifera records (up to 10°C more), while the difference in winter variability between the proxies is only minor. The winter Holocene temperature amplitude in the tropical latitudes is clearly higher than during the summer, while this trend is opposite in the higher latitudes. This high latitude difference in amplitude is clearly more distinct for dinocyst records than for the planktonic foraminifera ones, and is most pronounced along the path of the North Atlantic Current.

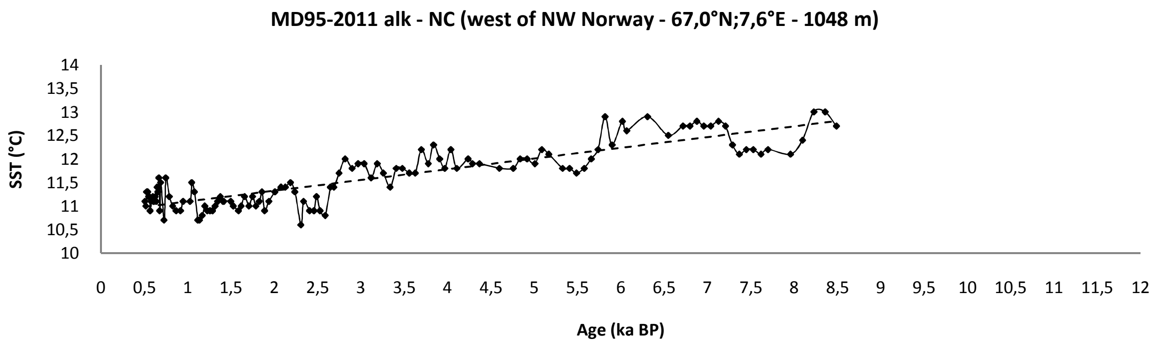


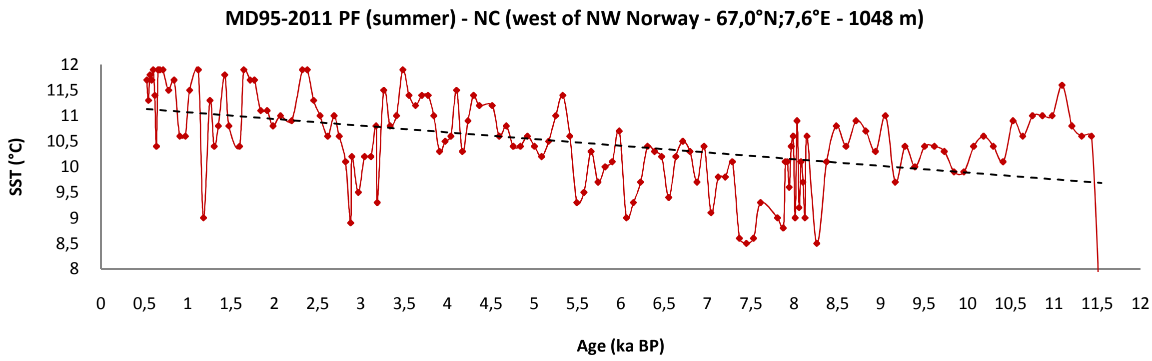


**Fig. 23: These two graphs in the Nordic Seas typically indicate the difference in Holocene temperature evolution between alkenone and diatom records and planktonic foraminifera records (also Mg/Ca). The low temperature variability of the alkenone record on centennial timescale is also present. (Kim et al., 2004; Hald et al., 2007)**

The Holocene temperature evolution for the different proxies shows some major differences. Although it is difficult to compare the proxies without analyzing them thoroughly, it is possible to find one striking fact immediately. Apparently there is a marked difference between the long term temperature evolution based on diatoms and alkenones on one side, and Mg/Ca and planktonic foraminifera on the other side (fig. 23). This is clearly demonstrated if one has a closer look at the timing of the Holocene maximum at high latitudes. The majority of the alkenone and all diatom based data indicate a mid Holocene maximum, while the Mg/Ca and planktonic foraminifera proxies suggest dominantly early and late Holocene maxima. The dinocyst summer temperature evolution follows in most regions the alkenone and diatom temperature trends, but for the winter temperatures it follows clearly the Mg/Ca and planktonic foraminifera temperature evolution. A last remark is on the diatom temperature evolution. Although they follow the same trend as the alkenone records, the diatom based records show a far bigger temperature decrease between mid and late Holocene as the alkenone records (3-5°C for diatoms versus 1-2°C for alkenones).

The short term or centennial variability is clearly lowest for alkenone records (<0,5-1°C) (fig. 23), except for North Icelandic Current and the Mediterranean Sea area (0,5-4°C), and highest for the dinocyst records (mostly up to 4-6°C for summer and 3-4°C for winter). The other three proxies show similar variability somewhere in between the alkenone and dinocyst temperature variability. Another trend that can be noticed is the consistently larger variability for summer temperatures than for winter temperatures in the dinocyst records, but this is less pronounced or even non-existent for the planktonic foraminifera records.

## 2. Holocene temperature variability according to the proxy data

### *2.1 Millennial timescale evolution and general centennial variability*

There is a clear Holocene temperature trend for the South and Central Atlantic. Both regions show early Holocene temperature rise of about 1-2°C. The South Atlantic temperatures reach their maximum between 5,5 and 7 ka BP, and then gradually decrease by 0,5-1°C. Central Atlantic temperature evolution of the late Holocene is more variable, but averagely temperatures seem to remain rather stable. Temperature evolution in the North Atlantic region is far more variable and local, which makes it very hard to give a general temperature trend during the Holocene. The best way to compare the different regions and proxies is to divide the Holocene in several periods according to millennial scale temperature shifts occurring in the different Atlantic regions. Four clear periods can be distinguished in the records. The first one starts at the end of the Younger Dryas and finishes around the 9,4 ka BP Bond event, the next period ends roughly at the 8,2 ka BP event, the third one is terminated around the 5,9 ka event, and the last one runs until recent. These periods can for example be recognized in figure 23.

The mid to late Holocene temperature change, a general analysis of the four periods and the regional variability of the Holocene maximum in relation to the periods form a first part of this section. A second one briefly discusses the evolution of seasonality differences. A final part focuses on the complex Mediterranean Sea temperature evolution, as there is a great deal of local variability in this region.

#### *2.1.1 Holocene temperature evolution in the Atlantic – four periods*

Before analyzing the temperature trends more into detail, the aim is to already have an idea of the general evolution during the whole Holocene. From earlier studies it is known that there has been a Holocene Thermal Maximum (HTM) during the mid Holocene (9,5-5,5 ka BP) and a neoglaciation during the late Holocene (Kaufmann et al., 2004; Knudsen et al., 2003). A map displaying the average temperature change between mid and late Holocene has been created to see in which areas this trend applies for the Atlantic (fig 24).

The mid to late Holocene temperature change map indicates a serious temperature drop between mid and late Holocene for many Atlantic regions. The areas with the largest temperature decrease are the northeast US coastal area and the northwestern part of the North Atlantic Current (3 to 6°C). Also the alkenone and diatom based records in the Mediterranean and GIN area display serious temperature drops, but these are not consistent with the other methods which mostly indicate slight temperature rises. This map thus uncovers the major issues in the different temperature reconstructing methods. In spite of the contradictions in some areas, it is fair to say that the mid Holocene was on average clearly warmer than the late Holocene. Only the central North (east) Atlantic and tropical areas show dominantly slight temperature rises.

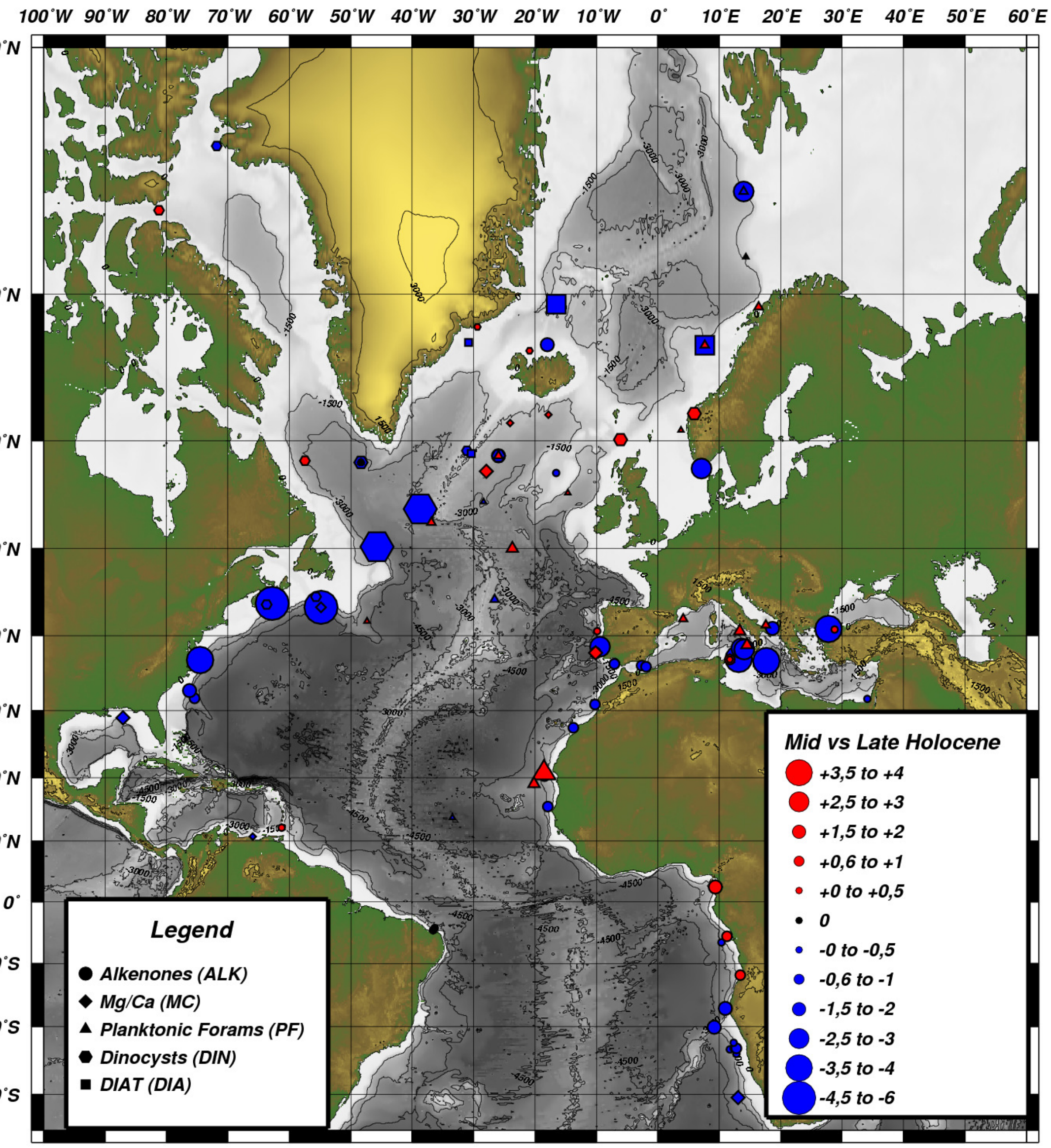


**Fig. 24: Average temperature changes of the different records between MH and LH.**

1. *Younger Dryas/Holocene transition until 9,4 ka BP Bond event (11,8-11,1 ka BP to 9,6-8.9 ka BP) (fig. 25)*

Most records do not go back 11-12 ka, so it is difficult to give a detailed reconstruction of what happened during the Younger Dryas – Holocene transition. The transition occurs not everywhere at the same time. The timing of the first temperature boosts in the Gulf Stream (past Cape Hatteras) already appear at 11,7-11,9 ka BP. This temperature rise occurs also in the southern Labrador Current and western Irminger Current. Temperature reconstructions in the Mediterranean Sea area are not consistent regarding the timing of the end of the Younger Dryas, but some of them extend the Younger Dryas to 11,1-10,9 ka BP, while some data already show high temperatures around 11,8-12,0 ka BP. This is not consistent with temperature reconstructions from most other places, which date the end of the Younger Dryas at about 11,55 ka BP (Hughen et al., 2000). There are also some regions where no temperature anomaly occurs during the Younger Dryas period. This is the case for the northwest North Atlantic Current, north Labrador Current and west Greenland Current.

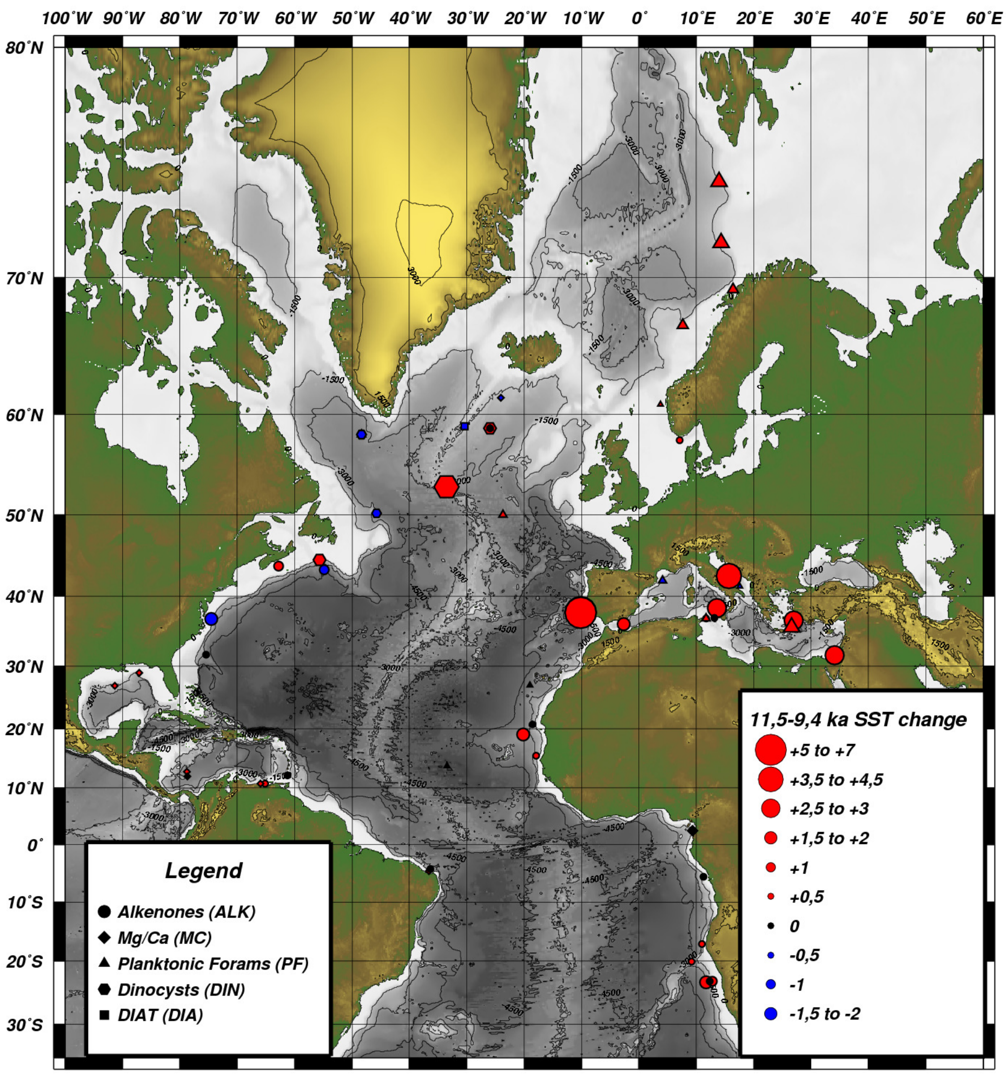


**Fig. 25: temperature evolution of all records during the first 2 kyr of the Holocene**

Except for the Benguela Current and southern part of the Angola Current (~1°C increase), the South Subtropical Gyre shows a slight temperature decrease during this period (~0,5°C). North Brazil Current, Guyana Current and Caribbean Current, which form the connection to the Gulf Stream and North Atlantic Current, all indicate rising temperatures (0,5-1°C). Temperatures near the eastern US coast remain averagely stable after a 2°C decrease around 11,1 ka BP (fig. 30). In the Mediterranean Sea and Portugal Current area, the temperature evolution is variable, but most reconstructions show a temperature rise of several degrees during the first 500-1000 yr and afterwards a slight cooling. Temperatures in the Canary Current area are stable or show a slight temperature increase (0,5-1°C). Records in the Northeast Atlantic display a slight to significant temperature rise (0,5-3°C). In the Northwest and North Atlantic Ocean there is not much change on average. Though, the temperature variability during summer (one location even up to 16°C! (fig. 26)) and in a lesser extent during winter is very high. Variability is most pronounced in the northwest Atlantic and Central Irminger Current region and reaches its Holocene maximum during this period. Also in many tropical areas there is a Holocene maximum in variability. This maximum in variability lasts for most datasets until the end of the next period.

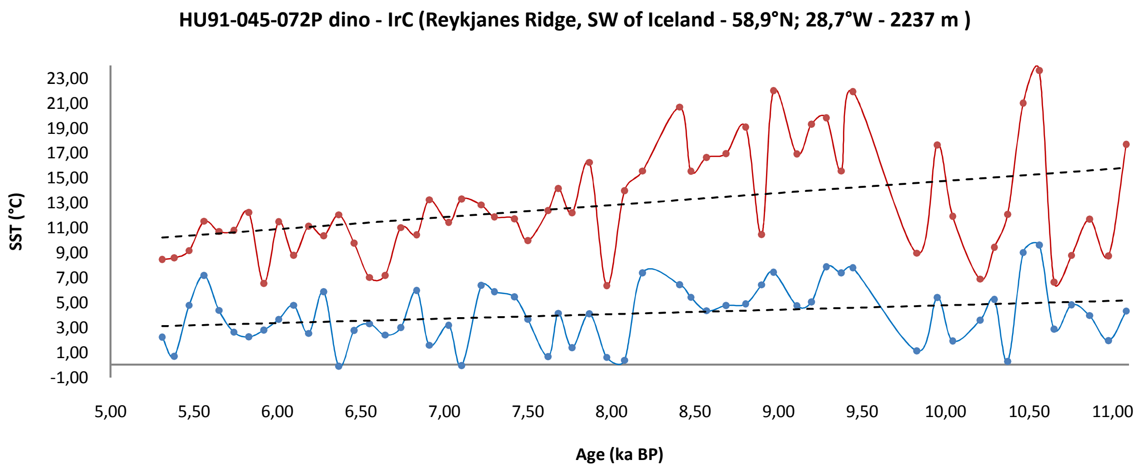


**Fig. 26: This temperature record from the Irminger Current region indicates large variability during the early Holocene (winter SST: blue; summer SST: red) (de Vernal and Hillaire-Marcel et al., 2000)**

2. *9,4 ka BP Bond event until 8,1 ka BP Bond event (9,6-8,9 ka BP until 8,5-7,5 ka BP) (fig 27)*

The period around the 9,4 ka BP event marks the start of major temperature rises and decreases in many datasets across the Atlantic, and especially in the central to northwestern Atlantic. The turning point is not everywhere at the same time. In most regions the trend change occurs around 9,3-9,4 ka BP or sometimes around 9,6 ka BP. There is one region (Central North Atlantic) where most data put the temperature shift around 8,9-9,0 ka BP. This region includes the Irminger Current, North Icelandic Current and East Greenland Current areas.

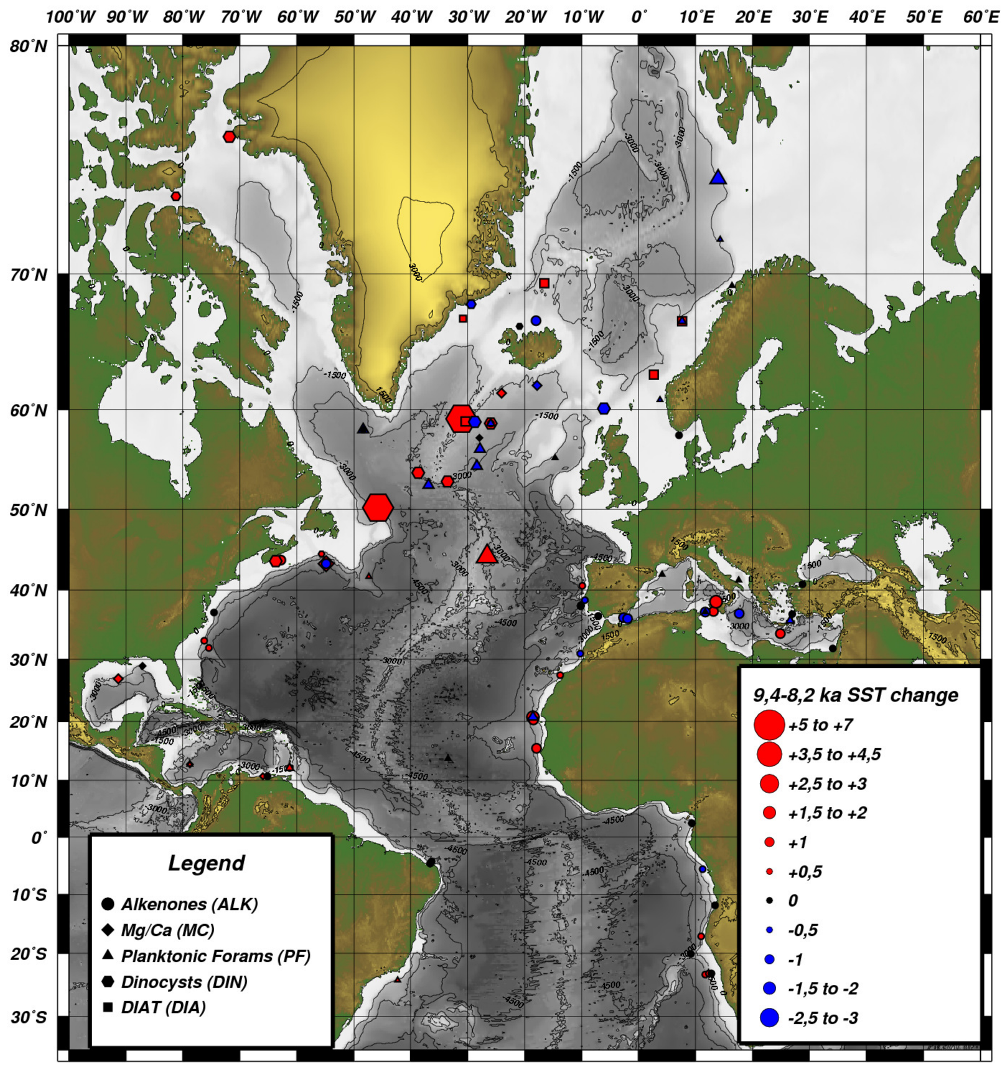


**Fig. 27: temperature evolution of all records during the early-mid Holocene**

Most regions display relatively small temperature changes. The Gulf Stream and Canary Current areas show slight temperature rises (averagely 1°C), the dataset near the Azores indicates a larger temperature increase (about 4 °C). Most Mediterranean Sea and northeastern Atlantic and utter North Atlantic (south of Iceland) records display slight temperature decreases (mostly between 0,5 and 1,5°C, except for the diatoms records which all show a slight temperature rise). Only the most northern situated record (West of Spitsbergen) indicates a larger temperature decrease of about 3°C. The regions that draw most attention during this time frame are the northwest and central North Atlantic. Temperatures show a large increase in the northwestern part of the North Atlantic Current and Irminger Current regions (2-6°C) and a clear cooling for the southeastern part of these currents (1-3°C). This temperature rise and fall are accompanied by an increase and a decrease in seasonality. The both Greenland Current areas show not much temperature change, although there is a slight decrease in seasonality. The records in the Nares Strait (strait between Greenland and Canada) point towards a temperature increase of about 2°C. One of the most striking results in all the temperature records during this period is the incredibly high temperature variability in one of the two cores southwest of Greenland, with maxima and minima about every 100-200 yr, and summer and winter temperature variability of 4 to 12°C and 1 to 4°C (fig. 28). A second important observation is a temperature dip between more or less 8,8 and 9,2 ka BP in most datasets from Labrador Current, East Greenland and North Icelandic Current. A final remark is the contradiction between the very high temperatures in the northwest Atlantic and the temperature dip in many records from the Mediterranean region (fig. 28 versus fig. 33).

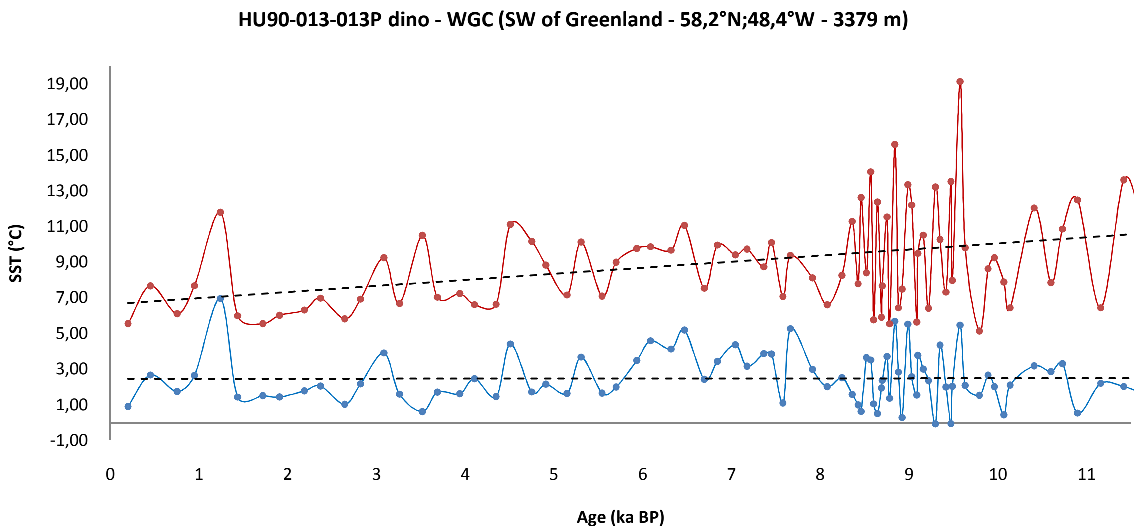


**Fig. 28: This record situated south of Greenland indicates large temperature variability between 9,5 and 8,5 ka BP Holocene (winter SST: blue; summer SST: red) (Hillaire-Marcel et al., 2001)**

*3. 8,1 ka BP Bond event until 5,9 ka BP Bond event (8,5-7,5 ka BP to 6,7-5,5/4,8 ka BP) (fig. 29)*

The period of transition from the second to the third period runs from about 8,5 to 7,4 ka BP. Many records put the trend change at 8,1-8,2 ka BP, but there are also a fair share that estimate it around 8,4 ka BP and 7,5-7,6 ka BP. From these three, the 7,5-7,6 ka BP is the only one which is regionally bound. It comes across in most Labrador Current records and some records in the Irminger Current and Mediterranean area. One alkenone and several dinocyst temperature based reconstructions in central Irminger Current, Labrador Current and East Greenland Current suggest a sudden temperature drop during the transition phase.

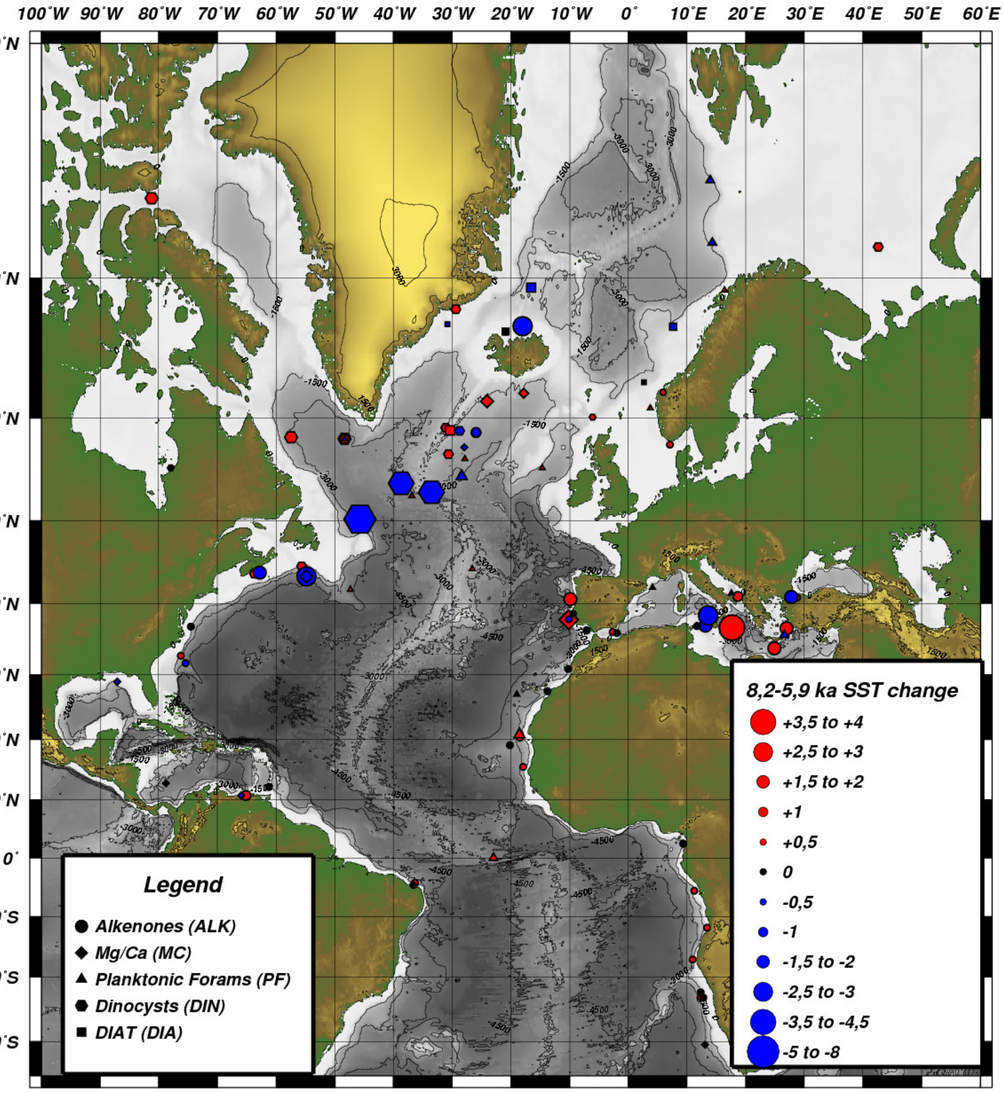


**Fig. 29: temperature evolution of all records during the late-mid Holocene**

Records indicate a slight warming in the lower latitudes (up to 1°C) and a somewhat larger temperature rise in the Mediterranean Sea (averagely 2°C, but lots of variability). Also Slope Current, North Sea and Norway Current waters show a slight temperature increase, while the utter northeast Atlantic and North Icelandic Current regions experience temperature decrease of 1 to 3°C. Similar to the second period, the northeast and central North Atlantic areas are most dynamic. Several records in the northeastern Atlantic (south Labrador Current and northeast North Atlantic Current) suggest a major temperature decrease of 4 to locally 8°C (e.g. fig. 26), while the northern Labrador Sea and Baffin Bay records display a significant temperature rise (about 2°C). The temperature trend change in records from the Irminger Current area is variable. On average the temperature change is about zero, but the Mg/Ca records suggest that the upper north part of the Irmiger Current and North Atlantic Drift waters slightly warmed. Also there seems to be a trend towards a temperature rise in the eastern part of the Irminger Current and a temperature drop in the western part. The centennial variability during this period is for most areas lower than in the other periods. Only records from the GIN area display a peak in variability. Towards the end of this period, many records from different regions indicate a serious temperature dip. These regions include the West Mediterranean Sea, east Irminger Current and the GIN area (except for the East Greenland Current).

*4. 5,9 ka BP Bond event until recent (6,7-5,5 (4,8) ka BP until 0,15 ka BP) (fig. 32)*

The timing of the final widespread temperature shift varies a lot between records and regions. The majority of the records suggest a transition between 6,3 and 5,7 ka BP. A few temperature reconstructions, particularly the ones from the Portugal Current region, signify an earlier shift at about 6,7 ka BP. Still two other, more recent transition dates appear in a significant amount of data. The first one is around 5,5 ka BP, and occurs in all but the alkenone proxy records from the Canary Current, NAD, Slope Current and Norwegian Current (fig. 23 & 31). This shift is unique as it is accompanied by a sudden temperature rise of 1 to 2°C during winter and 1 to 5°C during summer. The second even later shift takes place around 4,8 ka BP. This event appears as a maximum in many Mediterranean temperature reconstructions, but it is also a winter temperature maximum in records from the central Labrador Sea and Irminger Current. A last remarkable occurrence during the timeframe of all these transitions (6,7-4,8 ka BP), is a maximum in centennial temperature variability in a core just north of Cape Hatteras (central East US coast) (fig. 30).

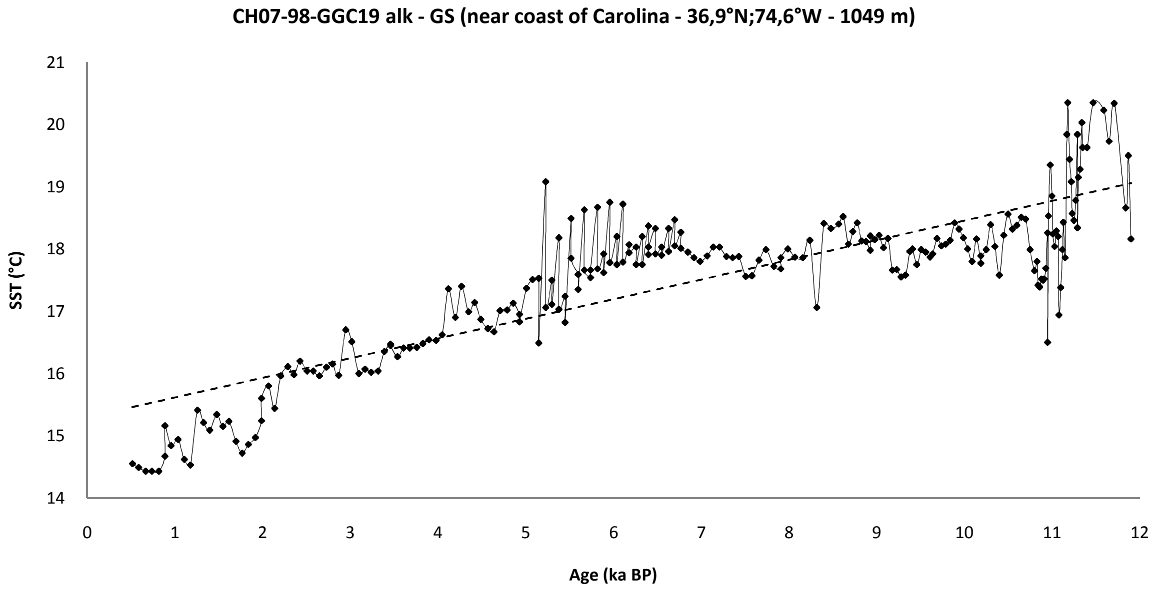


**Fig. 30: Temperature reconstruction north of Cape Hatteras (central East US coast) showing a lot of tempertature variability during the transition phase, and a ~3°C temperature drop during the last 6 ka BP (Sachs et al., 2007)**

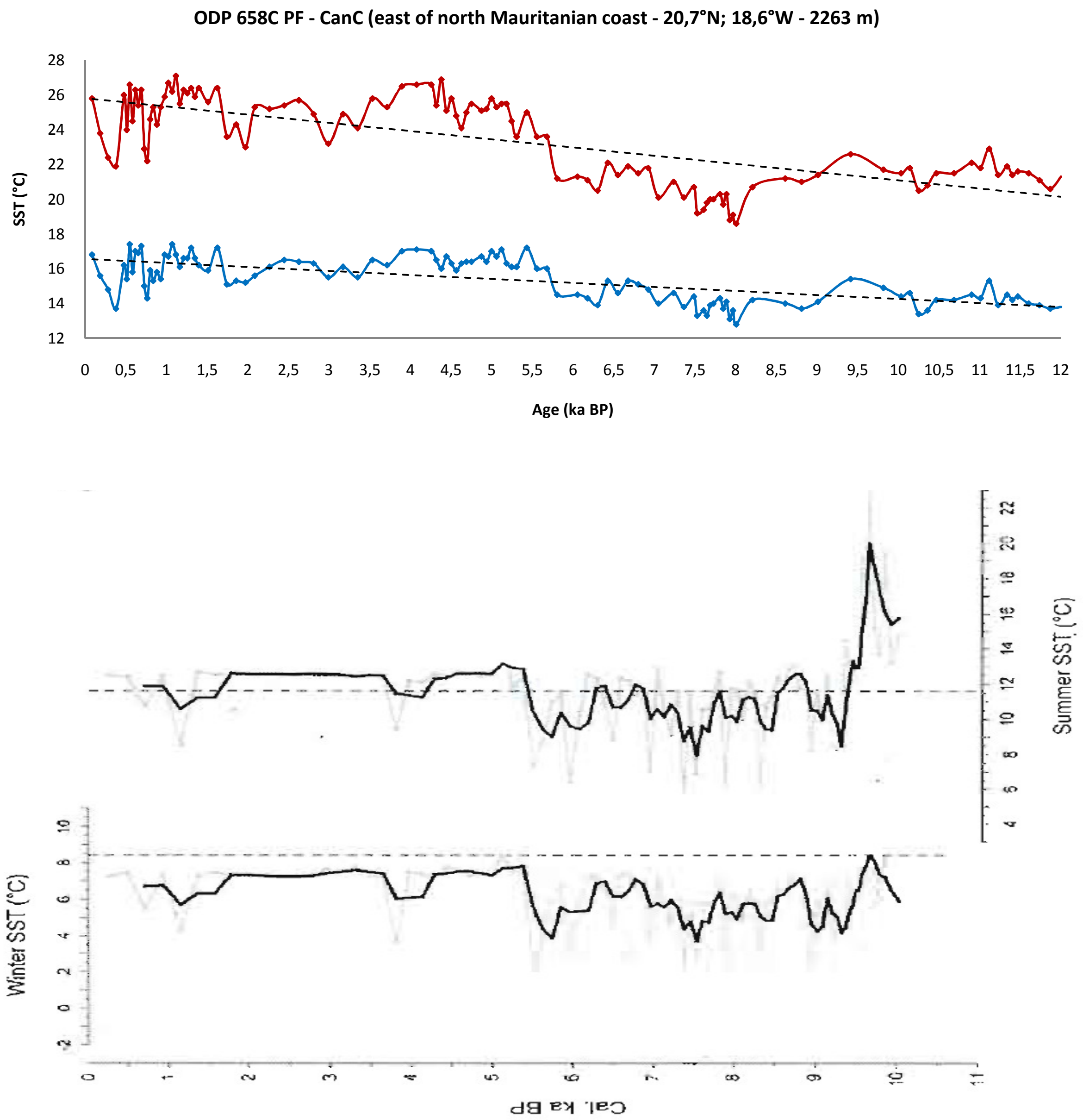


**Fig. 31: Winter and summer SST records from the Canary Current and Slope Current areas indicating a 2-3°C temperature shift. (blue: winter; red: summer) (deMenocal et al., 2000; copied from Solignac et al., 2008)**

This last period, also known as neoglaciation, is almost everywhere marked by a clear temperature decrease. There are only two significant regions where temperatures remain stable or even increase a little bit. These regions are the tropical areas and the central North Atlantic. Some records in other areas are also displaying a temperature rise. Most of them are based on planktonic foraminifera, and as they are on their own in many of the areas, the correctness of these reconstructions is questioned. In the area north of Iceland and east of central Greenland, temperature trends are inconsistent, but on average the temperature change is about zero. Then there are also two alkenone based records in the utter eastern Mediterranean Sea and one record in the central Labrador Sea that display a small temperature increase. Of all the areas showing temperature decreases, records along the northeast US coast show the largest temperature decline (2 to 4°C). In the other regions the temperature decrease is mostly 0,5 to 2°C, and locally up to 3°C. The centennial variability reaches a high in the southern part of the Gulf Stream, the Mediterranean, Labrador Sea and Baffin Bay areas during this episode. In the majority of the record, the temperature change is fairly gradual and there are no clear temperature shifts during the last 5 kyr. The most recurring transition points during this period in some records are around 4,5 ka BP, 4,1 ka BP , 2,8 ka BP and about 0,5-0,6 ka BP.

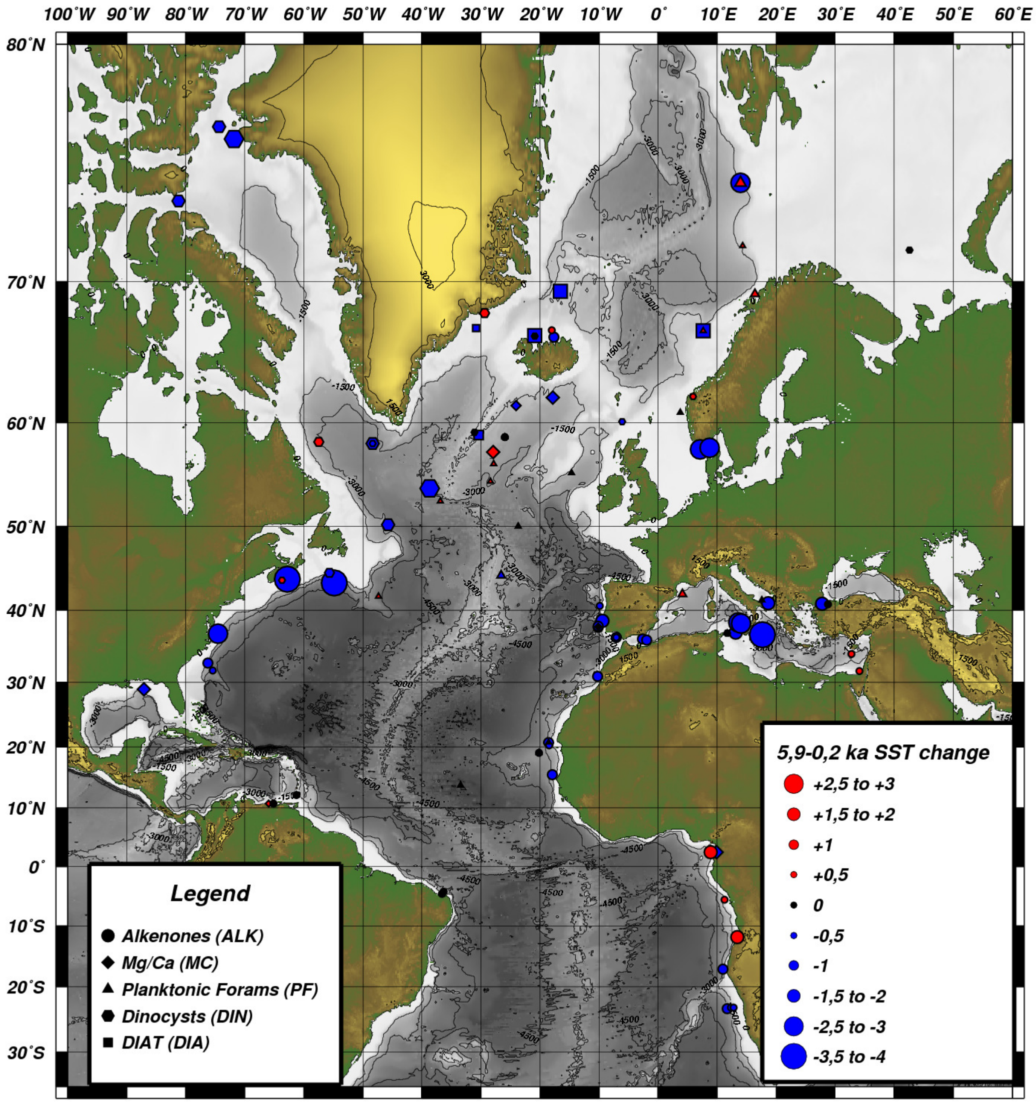


**Fig. 32: temperature evolution of all records during the late Holocene**

*Regional differences in timing of Holocene maximum*

In order to analyze regional trends in the timing of the Holocene maximum, a map has been created in GMT representing the timing of the temperature maxima during the Holocene for each record (fig. 33). The most obvious trend that can be deduced from the map is that high latitude areas generally have an early Holocene to early mid Holocene maximum, while low latitude areas have a mid

Holocene to Late Holocene maximum. This transition occurs quite gradually. In the central and eastern North Atlantic there is a lot of variability amongst the different proxies, with diatom and alkenone records suggesting an early to mid Holocene maximum and the other proxies displaying a late Holocene maximum. The Mediterranean Sea region also indicates a trend from an early Holocene maximum in the Portugal Current area to a late Holocene maximum in the utter east of the Mediterranean Sea. A peculiarity in dinocyst based winter temperature reconstructions in the both Greenland Currents and Labrador Current regions is a late Holocene winter maximum.

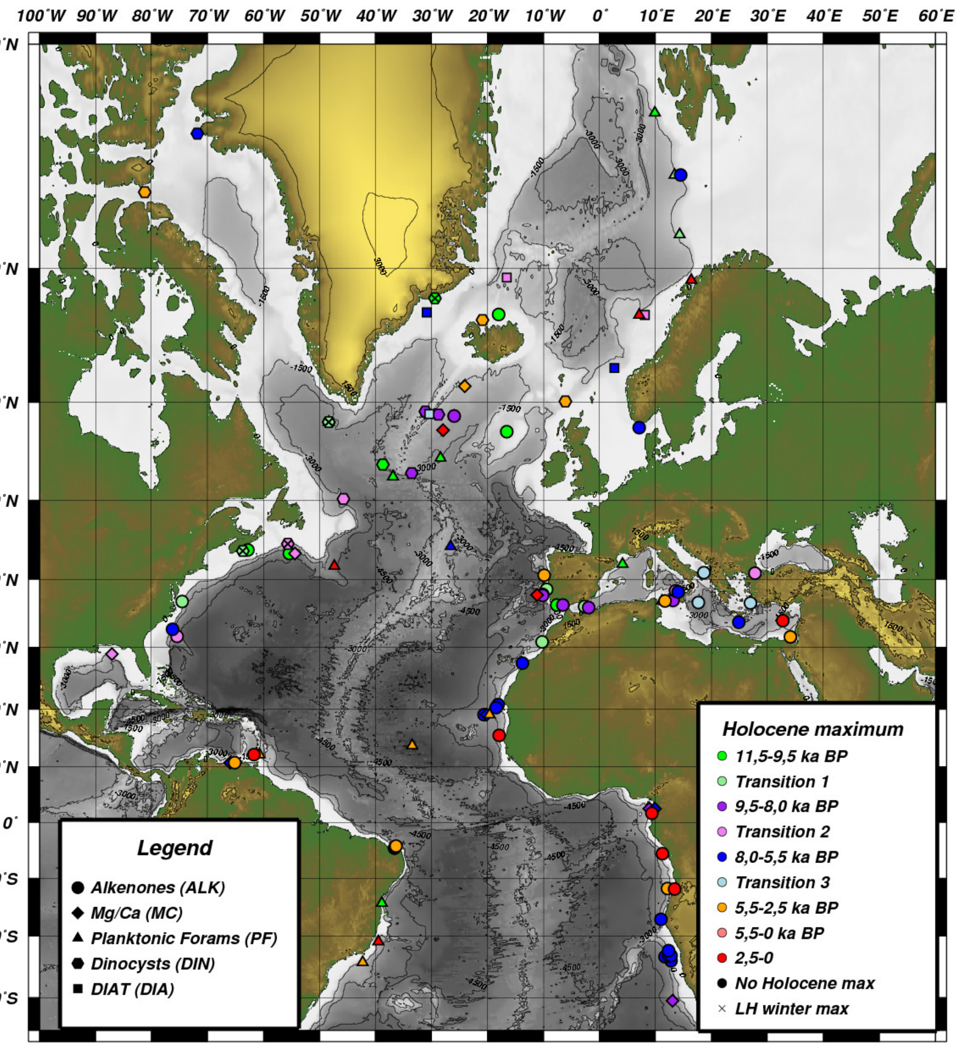


**Fig. 32: Period of Holocene temperature maximum for all records during the late Holocene. The cross in some high latitudinal dinocyst records highlights that there is a late Holocene winter maximum, but that there is an overall cooling. There is a clear trend from high latitudinal records having an early or early-mid Holocene maximum and of low latitudinal records having a late-mid to late Holocene maximum.**

### *2.1.2 Seasonality evolution during the Holocene*

Most dinocyst and planktonic foraminifera records in the North Atlantic suggest a clear decrease in seasonality during the Holocene (e.g. fig. 26). In most cases this corresponds with an overall temperature decrease. The regions where seasonality did increase are the Slope Current (fig. 31), southeastern side of the North Atlantic Current, and Canary Current areas (fig. 31). These are also the regions displaying an overall temperature increase for dinocyst and planktonic foraminifera records during the Holocene. During the last 5-6 kyr of the Holocene, seasonality also increases in the central Irminger Current (fig. 43).

### *2.1.3 Analysis of the Mediterranean Sea region (fig. 33)*

There are several reasons to present the data of the Mediterranean region more thoroughly. First of all there are a lot of records available in the region. A second motive is the large variability among records and the occurrence of some specific temperature anomalies. The role of the Mediterranean temperature evolution regarding to the North Atlantic Oscillation forms a final reason.

*Younger Dryas-Holocene transition*

Already along the Portugal coastline, records indicate a great deal of variability regarding the YD. The temperature dip during the YD varies from 3-4°C in the most northern record to 6-8°C in the southern ones, while the temperature recovery is 4-5 kyr in the north and only about 1 kyr in the south. The Mediterranean Sea shows a Younger Dryas with a 4-7°C dip. Planktonic foraminifera records display a very fast temperature rise (100-500 yr) at the end of the Younger Dryas, while alkenone records indicate at least a 500 yr recovery time. A peculiarity is that the YD is even extended the by at least 500 yr for the alkenone records in the East Mediterranean Sea.

*Mid Holocene temperature dips*

There are two temperature dips that can be recognized in the Mediterranean records between about 10 and 6 ka BP. The first, longest and most distinct one occurs between about 7,6 and 9,9 ka BP. Only the alkenone records north of Sicily do not show this temperature anomaly and even display a temperature maximum. This temperature dip is more obvious in planktonic foraminifera (1-2°) records than in alkenone records (0,5-1°C). A second dip appears between about 6,4 and 7,4 ka BP,. Just like the first one, the anomaly is clearer in planktonic foraminifera based reconstructions. Now the alkenone records east of Italy are not consistent and indicate a temperature maximum.

*Neoglaciation period*

Except for the utter east Mediterranean area, all alkenone records display a temperature decrease of averagely 1°C. For some records near Italy this decline is up to 3-4°C. Planktonic foraminifera records on the contrary indicate stable temperatures or even a slight temperature increase during the last 5 ka.

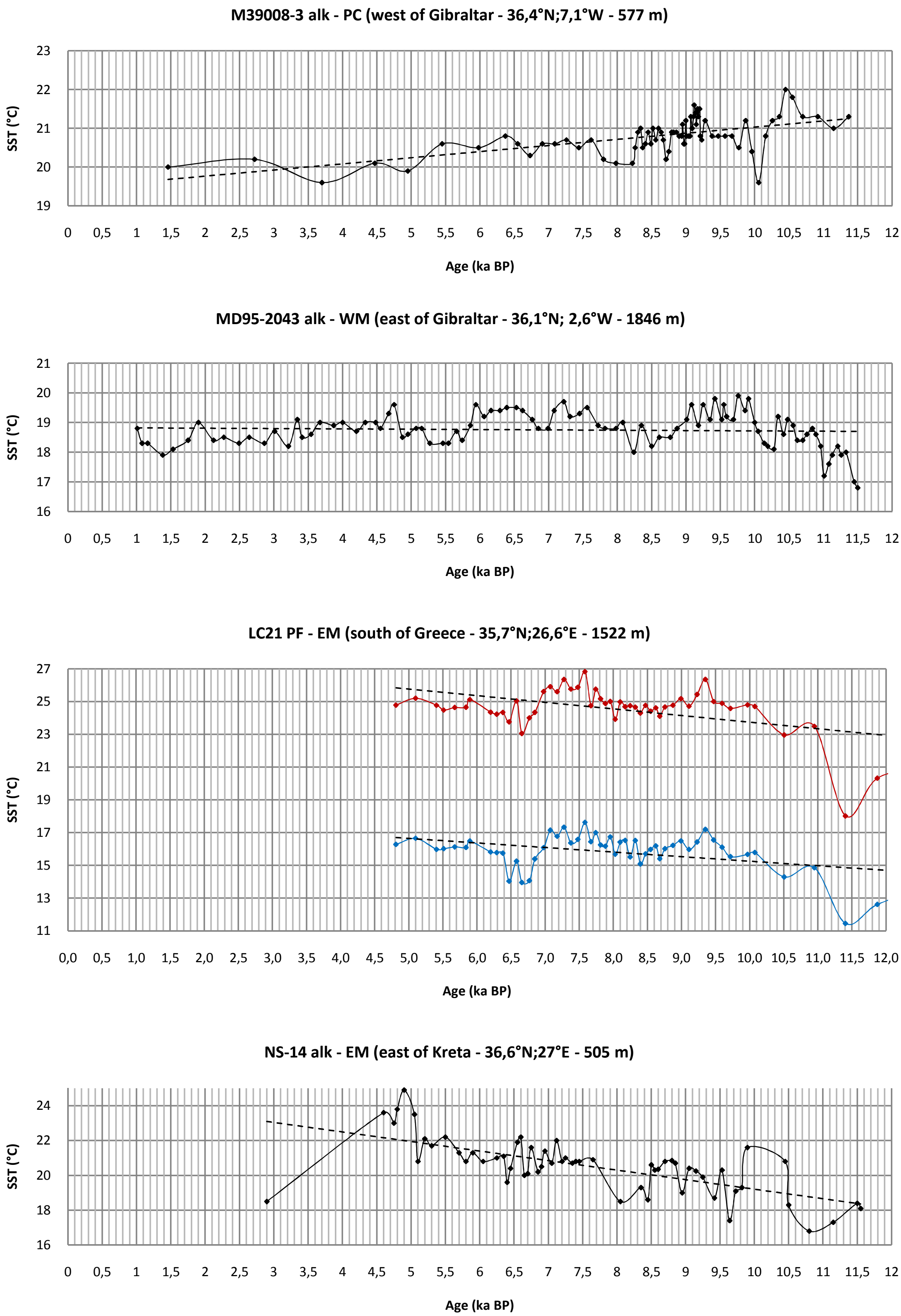


**Fig. 33: Four temperature records form the Mediterranean region (from west to east) showing the two mid Holocene negative temperature anomalies and the variance in temperature recovery after the YD. (black: annual; blue: winter; red: summer) (Cacho et al., 2001; Marino et al., 2009; Triantaphyllou et al., 2009)**

## 2.2 Centennial timescale evolution

This section of the results contains three parts. The first one discusses periodicity in the records. A second part focuses on the last 2,5 ka BP, in which several warm and cold episodes occur known as the Late Iron Cold Period (LICP ) (~2,5-2,1 ka BP), Roman Warm Period (RWP) (~2,1-1,6 ka BP), Dark Ages Cold Period (DACP) (~1,6-1,1 ka BP), Medieval Warm Period (MWP) (~1,1-0,65) and Little Ice Age (LIA) (~0,65-0,15)(Gil García et al., 2007; Jiang et al., 2005). Finally, a short remark is noted on centennial seasonal variability.

### *2.2.1 Cyclicity during the Holocene*

In order to find a certain periodicity, a first data table was reconstructed with the timing of clear temperature maxima and minima of the intermediate to very high resolution records (see database). It soon turned out that in most records the temperature minima are dominant over the maxima. After screening the minima for most datasets, not less than three periodicities appear. The first and most recurring one has a periodicity of 500±200 yr. A second one indicates more variability and occurs about every 150-200 yr in many of the high to very high resolution records. In the records with highest resolution (5-15 yr) there is also a 30-40 yr periodicity. After discovering these cycles, a second set of data tables was produced. This data table contains specific information for each record showing one or more of these periodicities. The latter data table is also added in the database. A summary for each of the three cycles is reported below. Figures are presented in the discussion.

*a) 500 yr cycle*

The cycle has been well recognized in about 40-45 records from all different proxies, which is about half the amount of intermediate to very high resolution records. This cycle appears about everywhere and shares mostly the same timing for the minima. Only along the Greenland coast, the cycle is not very distinct and maxima are dominant over the minima. The periodicity varies between 400 and 600 yr, but is mostly around 500 yr. Actually, it is better to speak of a 500-1000-1500 yr cycle, as there are often missing minima. Another remark is that the cycle tends to be less clear or non-existent near continents.

*b) 150-200 yr cycle*

The periodicity is found in about 35 records from all five proxies, which is more than half the amount of high to very high resolution records. In many records, this cycle is only visible during a certain part of the Holocene. The cycle may average 150-200 yr, but in fact it ranges from about 80 to 250 yr. Because of standard dating errors, it is difficult to check whether the timing of the minima correspond for the different records.

*c) 30-40 yr cycle*

In 5 very high resolution records, there also seems to be a 30 to 40 yr periodicity. As there are not many records with this kind of resolution and it is actually a cycle on a decadal timescale, it will not be further discussed.

*2.2.2 Cold and warm periods during the last 2,5 ka BP*

The different warm and cold episodes occurring during the last 2,5 ka are present in many of the high resolution records, but these different periods are noticeably overlapping each other and are not occurring everywhere in the same extent. The mid latitudes and especially the North Atlantic Current path experience highest temperature fluctuations during these events. The DACP, MWP and LIA are generally more significant than the LICP and RWP. An analysis of these five periods indicates that these periods are not constant cold or warm periods, but that they should be seen as periods with high temperature variability containing more cold extremes in the case of LICP, DACP and LIA, and more warm extremes in the case of the RWP and MWP. The 150-200 year cycle plays a significant role in these cold and warm peaks. Most clear cold peak during the LICP is around 2,3 ka BP, but around 2,1 and 2,5 ka BP there is also a temperature minimum in several datasets. The Roman Warm Periods clearest maxima are around 2,05 and 1,8 ka BP. For the DACP there is a very good agreement between the proxies on the timing of a temperature dip around 1,3 ka BP. MWP and LIA clearly display several temperature peaks. There are maxima during the MWP around 1,1, 0,9 and 0,7 ka BP. The minima during the LIA are mostly appearing around 0,65; 0,45 and 0,3 ka BP.

*2.2.3 Remark on seasonality variation*

A peculiarity in seasonality for dinocyst based datasets in the central and western Irminger Current is that winter and summer temperature trends are as good as opposite on a centennial scale. This means that winter minima correspond with summer maxima and the other way round. There are two records coming from other areas that also suggest opposite seasonality. The first one is located near the St-Lawrence estuary (south Labrador Current region) and the second one just north of Iceland (North Iceland Current).

## 3. Model output and comparison with proxy records

### Surface temperature evolution according to the ECBilt-CLIO-VeCode model (0-8 ka BP)

Comparing the different Holocene air temperature maps produced from the ECBilt-CLIO-VeCode model, uncovers that the overall temperature change during the last 8 kyr is too small to easily compare the maps. The temperature versus age graphs were proven to be more helpful, as they show the temperature trends on specific places. From these graphs a map was produced with temperature change during the last 8 kyr. Along with the temperature change, the average temperatures during the last 8 kyr are also displayed on the map (fig. 35). The average temperatures are superficially compared with recent air temperatures to check in what areas the model performs questionable. Then, the model temperature changes are compared with the proxy data temperature change of the last 8 kyr. In order to do this, there was also a map created with 8 kyr temperature evolution for the proxy records (fig. 36). The consequences of comparing air temperatures with sea surface temperatures are considered in the discussion.

Modern air temperatures (fig. 33) suggest that the model overestimates the temperatures along the West African coast (Angola and Guinea Basin) and along the northeast US coast towards the northern central Atlantic by averagely 5°C. Modern temperatures indicate also that temperatures at the highest latitudes are generally underestimated by several degrees (up to 8°C west of Spitsbergen). Subtropical and most tropical regions do not show major deviations.

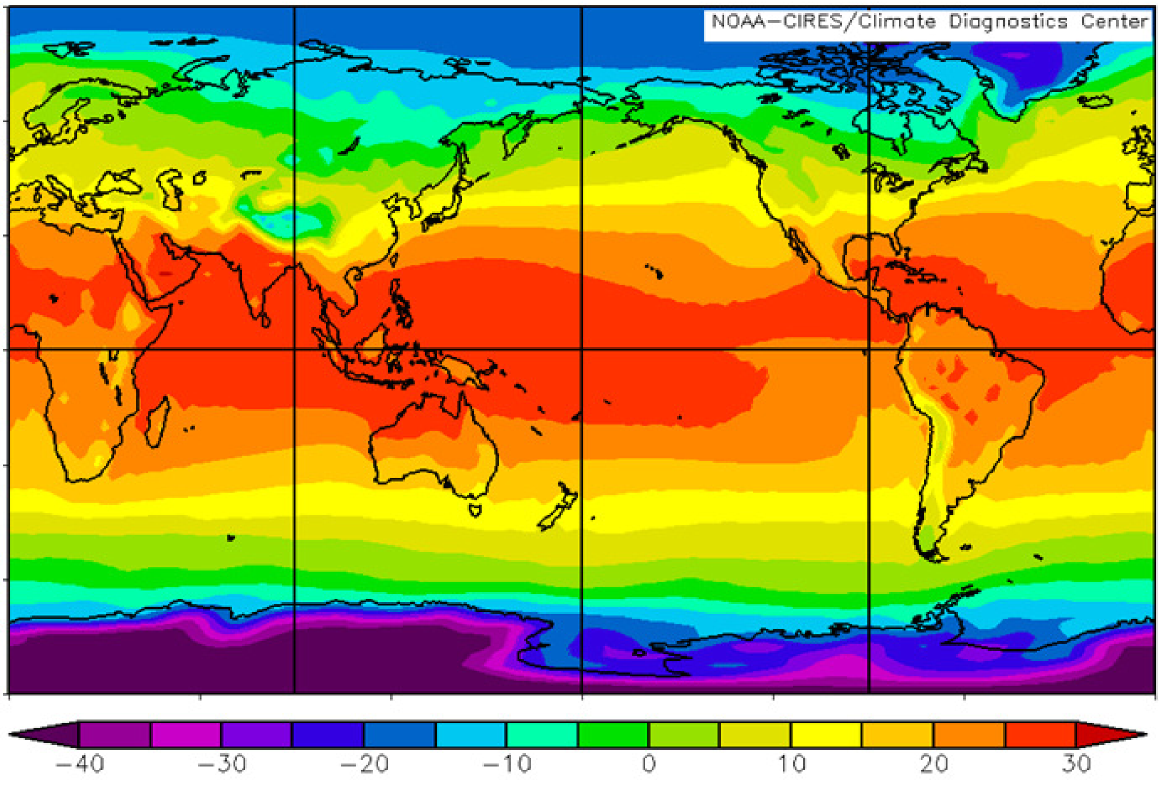


**Fig. 34: Global annual mean surface air temperatures 1968-1996 (NOAA-CIRES Climate Diagnostic Center (http://www.esrl.noaa.gov/psd/))**

Notice that the temperature change maps of data and model have different scales (fig. 35 versus fig. 36), as the temperature change is in general far lower according to the model output than to the proxy reconstructions. For the model output, there is a slightly positive trend for temperature evolution in the tropics and the east US coast (Gulf Stream and Southern Labrador Current). All other Atlantic regions show a decrease in temperature becoming stronger towards the pole (up to -4°C). The temperature trend for the proxy data in the tropics is much alike the model. The most striking difference between the proxy data and model output is the temperature trend along the northeast US coast. The data indicate a decrease of 3 to 6°C, while the model suggests even a slight temperature increase (0-0,5°C). Although the proxy data are not entirely consistent in the Mediterranean Sea and Canary Current region, there is a dominant decreasing trend, which is in agreement with the model. According to the proxy data, there is large localized variability for the temperature trend in the Central North Atlantic region, which is almost nonexistent in the model results. Temperature trends in other areas are mostly consistent with the model, only there is no strengthening of the temperature decrease towards the pole.

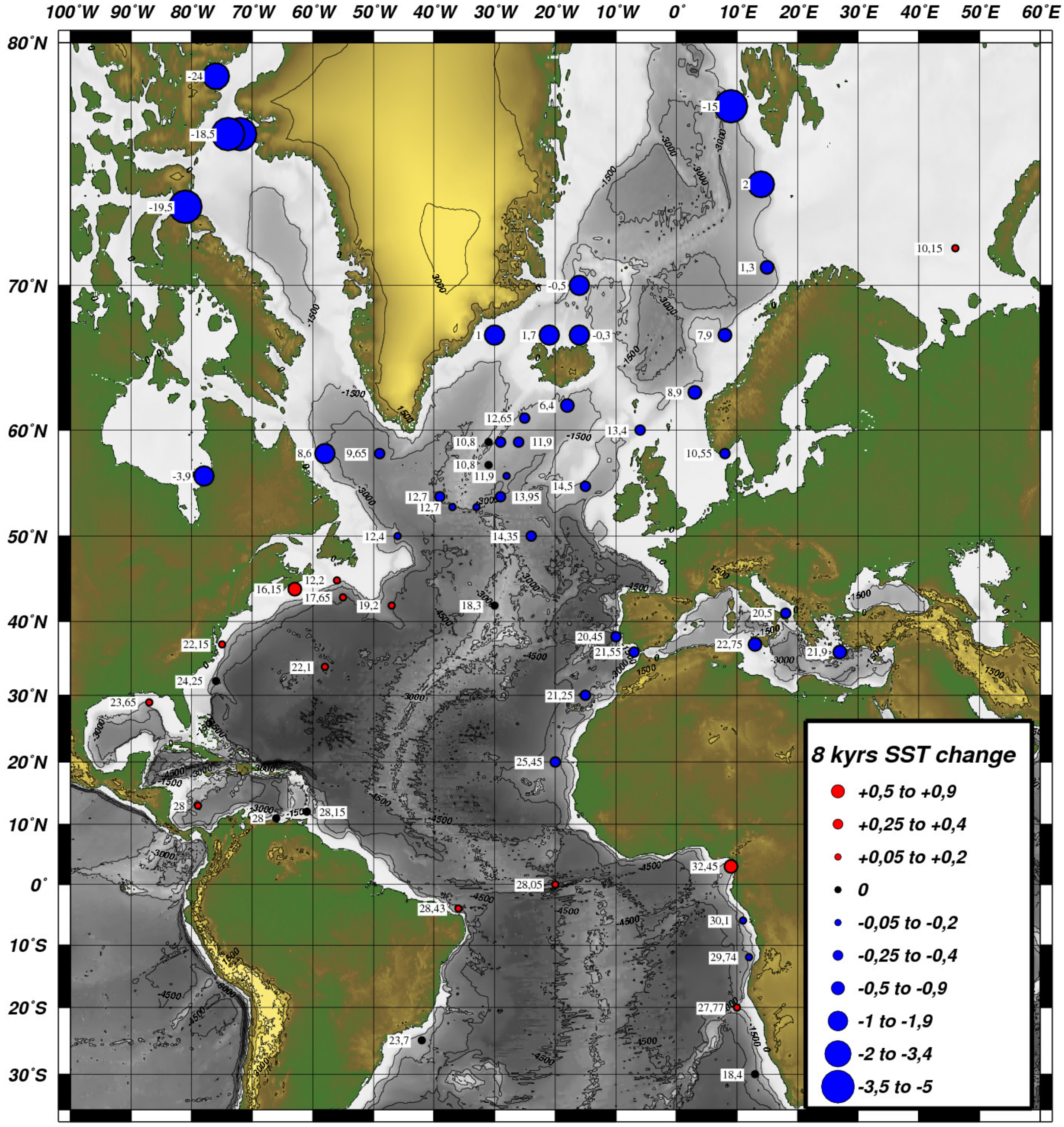


**Fig. 35: Surface air temperature change between 0 and 8 ka BP according to an experiment with the ECBILT-CLIO-VECODE model. The data in the added text boxes show the average air temperatures (°C) from the last 8 kyr from the model output.**

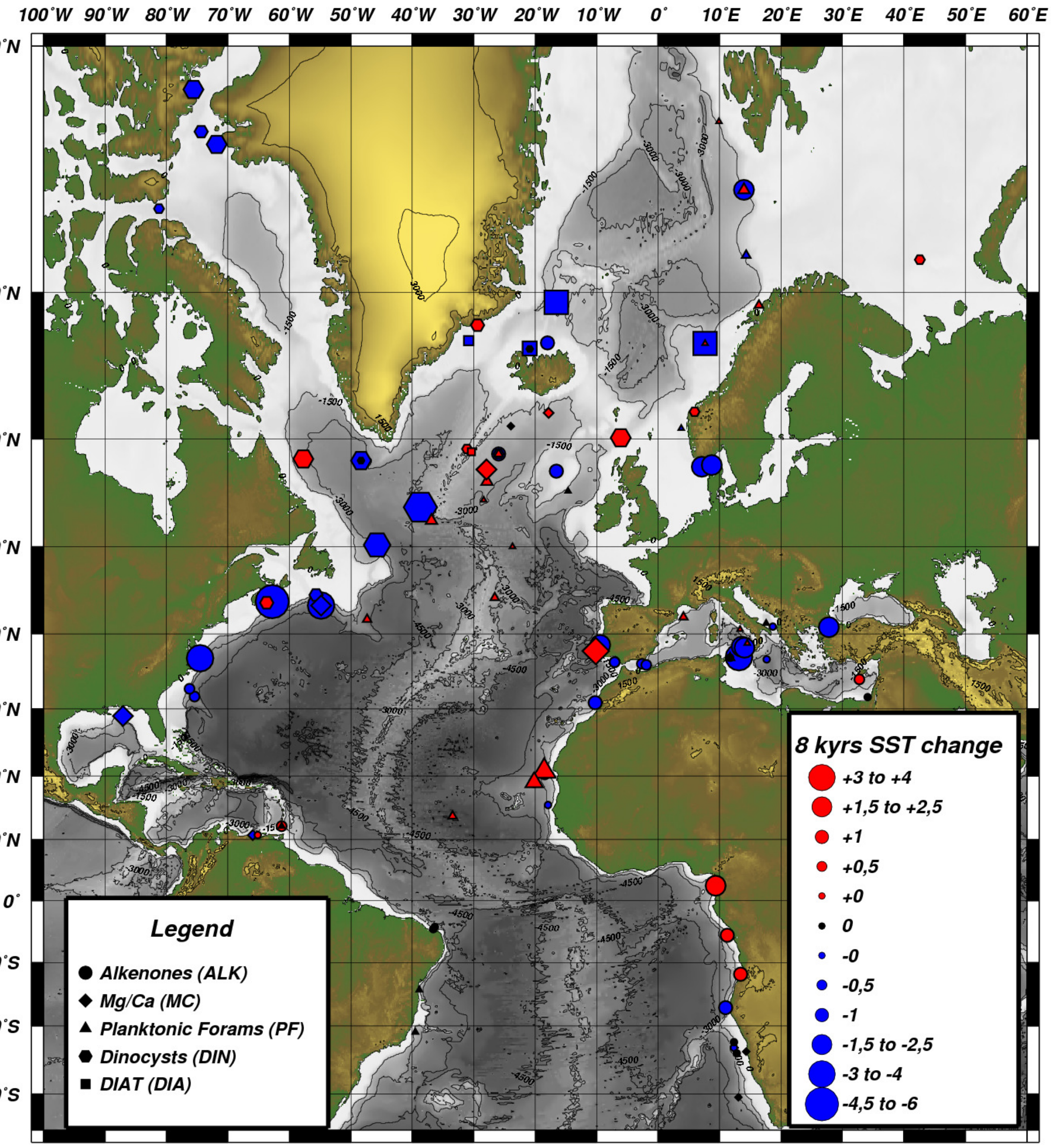


**Fig. 37: temperature change during the last 8 kyr according to proxy records**

# V Discussion

## 1. Variation between proxies

### 1.1 Hypotheses on consistent proxy data differences

There are only a few possible explanations for widely occurring proxy differences. These include vertical distribution of the micro-fauna, dominant growth season of E. Huxleyi and planktonic foraminifera (regarding the calibrations based methods) and sensitivity of the micro fauna to temperature extremes (de Vernal et al., 1997; Jansen et al., 2008). All three reasons are discussed below.

#### *1.1.1 Living depth variations*

The high centennial variability and especially the high seasonality gap in the dinocyst records suggest a living habitat of the dinoflagellates very near the surface, as only the top water layer is so susceptible to temperature changes. This confirms that the maximum abundance depth is situated in the upper meters of the photic zone (Taylor, 1987; de Vernal et al., 2000). The alkenone based records indicate least centennial temperature variability, which could suggest another living habitat of the E. Huxleyi than dinocysts. Measurements of habitat depths of the E. Huxleyi though indicate that the alkenone production occurs mainly near the surface (Jordan and Chamberlain, 1997; Okada and Honjo, 1973) (Müller et al., 1998). This probably means that another effect creates the differences in temperature variability. Not many studies exist on diatom habitat distribution, but it is generally accepted that they are also mainly living in the upper few meters of the surface water (Armstrong and Brasier, 2005a). A detailed study on vertical distribution of planktonic foraminifera indicates that there are major regional and species related differences regarding the living depth (Fairbanks, 1978). The inter variability between the different planktonic foraminifera species regarding the habitat depth can be an explanation for the inconsistencies in the different Mg/Ca records, as there are several species used for Mg/Ca temperature reconstructions.

The conclusion from the above is that only the planktonic foraminifera are clearly deviating from the other micro-fauna regarding the living depth. The fact that planktonic foraminifera have a lower average living depth could mean that temperature reconstructions are significantly influenced by the thermocline. This seems especially to be the case in higher latitudes, where the mixed layer depth only extends to around 30 m. This theory has already been proposed by Came et al. (2007), and model simulations (Liu et al., 2003) back this hypothesis up. In this study, the hypothesis is supported by several facts. The seasonal temperature differences for planktonic foraminifera based records are estimated too low and especially the summer temperature variability is clearly lower than for the dinocyst records. Also the fact that Mg/Ca and planktonic foraminifera records display similar temperature evolution as the winter temperature evolution of the dinocyst records, suggests that records based on planktonic foraminifera are influenced by the thermocline (fig. 38). The fact that the average Holocene summer temperatures are estimated rightly can be explained by the tuning that is used for the transfer function method.

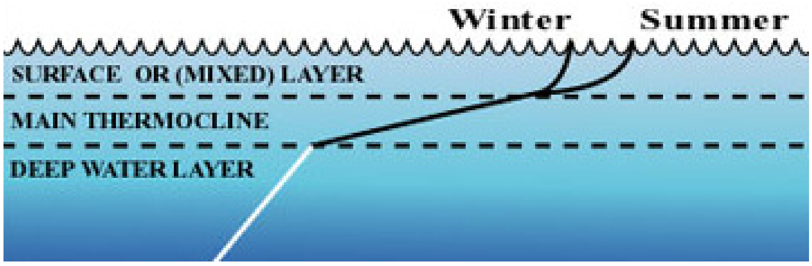


**Fig. 38: The temperature trend in the ocean surface layer. (adapted from http://www.onr.navy.mil)**

### *1.1.2 <u>Preference in seasonal growth or productivity</u>*

The alkenone and Mg/Ca based temperature reconstructions are dependent on the growth season of the E. Huxleyi and the planktonic foraminifera. The average Holocene temperatures suggest a clear overestimation of the alkenone temperatures in the high latitudes, which would mean that the dominant growth season is rather summer than spring. This theory is enhanced by the fact that the deviation becomes higher towards the pole. The results of this study are consistent with earlier results (Brown and Yoder, 1994), which suggest that the dominant growth season of the E. Huxleyi varies from summer to early autumn in the higher latitudes of the North Atlantic. This also implies that alkenone temperature trends in the high latitudes are mostly summer dominated (Leduc et al., 2010; Lorenz et al., 2006).

### 1.1.3 *<u>Sensitivity of the micro-fauna</u>*

General differences in centennial variability could not be explained by habitat depth variations. Another possibility is that temperature extremes might have different consequences for E. Huxleyi, planktonic foraminifera, diatom and dinocyst assemblages. A similar remark is noted in a study on a proxy comparison during the last glacial maximum (de Vernal et al., 2006).

## *1.2 Regional proxy data variance*

Several area-specific phenomenons can have diverse effects on records from same cores based on different proxies. The records suggest that the two most important ones are upwelling and the influx of fresh water through rivers or drift ice. An example of upwelling related temperature differences between a Mg/Ca and alkenone record is situated in the Canary Basin (Elderfield and Ganssen, 2000). Near Cameroon, two records based on Mg/Ca and alkenones suggest the effect of river influence (Weldeab et al., 2007).

## 2. Holocene temperature evolution related to changes in the ocean system and NAO

In the results of the temperature evolution, the Holocene has been divided in 4 periods. The relation between temperature evolution and the ocean system during these four periods and the YD-Holocene transition are discussed below. Also the trend changes regarding the North Atlantic Oscillation are mentioned keeping in mind the seasonality of the proxies.

*Younger Dryas-Holocene transition*

The first signs of a temperature recovery after the Younger Dryas are found in northwest Atlantic records around 11,8 ka BP, which is about 200 to 300 year earlier as the sudden temperature increase seen in most other regions. This suggests that the northwest Atlantic has been the key area during the start of the Holocene. The warming is especially visible in the Gulf Stream north of Cape Hatteras (fig. 30) suggesting that the northern branch of the Gulf Stream became stronger and more warm water started to flow to the (north)east thanks to the westerlies. These winds were probably enhanced by the increased north south temperature gradient, due to higher summer insolation (de Vernal et al., 2006). Warmer waters then gradually started to penetrate further into the northeast Atlantic. At about 11,6 ka BP, MOC is triggered in the GIN area, due to the cooling of the warm salty waters transported to this area (McManus et al., 2004). This overturning water initiated a convection cycle or conveyor belt, pulling warm surface water to the northeast Atlantic, and transporting cold deep water towards the south. The sudden temperature increase in many areas shows the vigor of this process (fig. 39). In the Azores and central Portugal Current region, but also in some reconstruction from the East Mediterranean, records suggest that the Younger Dryas ends 500 to even 1000 year later (fig. 39). The temperature recovery in the Azores and central Portugal Current region is also very slow (3-4 kyr), especially for the alkenone records (fig. 39). The prolongation and even strengthening of the Younger Dryas in these areas suggests a weak southern branch of the Gulf Stream. Local effects as fresh water input from melting glaciers could also have attributed to the extension of the YD in the Mediterranean area. From the information above, one can imply that the North Atlantic Current was really strong and took a very northern track during the initial stages of the Holocene.

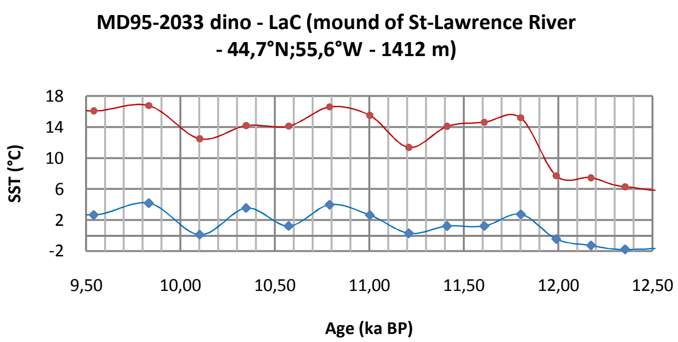

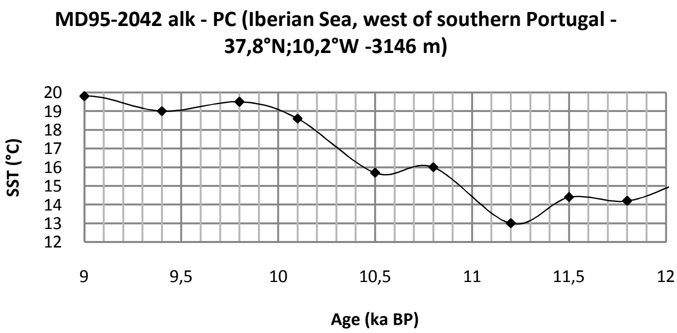


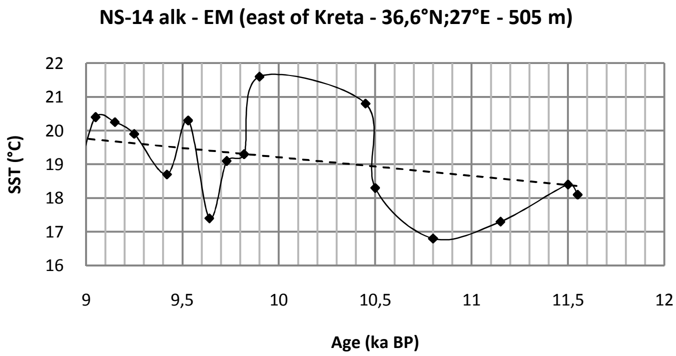


**Fig. 39: Records indicate the difference in temperature recovery after the Younger Dryas. The graph from the Labrador Current region shows a very fast and early recovery, while the ones from the Portugal Current and East Mediterranean region show a delay or a very slow recovery. (de Vernal and Hillair-Marcel, 2006; Pailler and Bard 2002; Triantaphyllou et al., 2009)**

1. *11,5-9,4 ka BP – Start of THC & MOC in GIN area*

The slight cooling in the Equatorial Current regions and warming in the connection to the North Subpolar Gyre between 11,5 and 9,5 ka BP (fig. 25) are a significant indication for more heat transfer to the north indicating a strengthening thermohaline circulation. The extent of short term temperature variability in the northwest Atlantic and central Irminger Current region suggest that the thermohaline circulation was not very stable during the first 2 kyr of the Holocene (fig. 26). Temperature changes during this period indicate a slight southward correction and a strengthening of the North Atlantic Current, which is consistent with the late temperature rises in the Mediterranean region. An explanation for the high temperature variability in the central and northwest Atlantic during this period can be attributed to the effect of periodic large fresh water influxes from meltwater from the arctic, leading periodically to significant weakening of the thermohaline circulation (Björck et al., 2001). It is difficult to estimate whether real conveyor belt shutdowns occurred during this period, but if they took place, they could not have lasted for decades as temperature drops during this periods cold events are far too small compared to the Younger Dryas.

The fact that strong temperature increases occur in the (north)eastern part of the Atlantic, and that there is even a slight temperature decrease in certain northwest Atlantic records (fig. 25) suggest an evolution towards a positive trend in NAO during winter and summer. This is related to the strengthening of the thermohaline circulation, creating a more zonal trend due to strong westerlies.

2. *9,4-8,1 ka BP – Large temperature shift in NE Atlantic*

After one or two cold events around 9,4 and 8.9 ka BP, wherefrom the first one marks one of the IRD events described by Bond et al. (1997), temperatures rise in most Atlantic areas during the following 1000 to 1500 year. The major temperature changes in the North Atlantic indicate that much more heat is going to the northwestern side of the Atlantic, which is consistent with the rapid melting of the Canadian ice sheets during this period (Alley et al., 1997). Also the temperature decrease in the GIN area (at least during the winter) and the first Mid Holocene temperature dip in the Mediterranean suggest a change in heat distribution. A decrease in ice surface in combination with high summer insolation can be the explanation for a reorganization of surface currents. The triggers for the heat shifting towards the western side of the Atlantic are probably the 9,4 and 8,9 ka BP cold events, which suggest a weaker thermohaline circulation in the GIN area. The warm North Atlantic Current could then probably split due to weaker current speeds. Another factor that could have had an important effect is the large freshwater influxes from the fast melting Laurentide Ice Sheet. This fresh water would make the surface layer of the Labrador Sea less salty and easily create sea-ice during winter. A known consequence of winter sea ice in these areas is the occurrence of strong northern winds along the southern tip of Greenland (Lippsett, 2009). The periodic maxima in the record southwest of Greenland indicate that warm Atlantic water started to periodically penetrate the Labrador Sea (fig. 28).

The regional temperature trends during this timeframe indicate a general change towards a negative NAO. Especially the high temperatures in the NW Atlantic are a good indicator that there is a trend towards a negative NAO, but also cold period in the Scandinavian area confirms this (Hald et al., 2007; Karlén and Kuylenstierna, 1996)

3. *8,1-5,9 ka BP – Labrador MOC and its effect on the GS-NAC System*

The start of the third shift in temperature trend coincides in many regions with the 8,2 ka event, which is accepted to be caused by the drainage of the Agassiz melting lake into the Atlantic Ocean via the Great Lakes and Saint-Lawrence river (Alley et al., 1997, 2005). Temperature increases in the central Labrador Sea, west Irminger Current and West Greenland Current regions, along with the temperature decrease in Labrador Current (especially dinocyst data), southwest GIN area and North Icelandic Current clearly indicate that heat draining from the latter to the first regions occurs. This change in heat distribution is evidence for the start of the Labrador Sea Water formation (Hillaire-Marcel et al., 2001). The extensive temperature decrease in the northern North Atlantic Current (fig. 40) starts approximately at the same time as the initiation of the Labrador Sea Water formation suggesting a link between the two. Two hypotheses have been proposed by Sachs (2007) for the more southern track of the North Atlantic Current. The first one is based on intensified westerlies, which originate due to increasing convection and the export of cold water via the Labrador Current. This process strengthens the subpolar gyre and creates opposing sea ice anomalies in the Labrador and Greenland seas (Curry & McCartney, 2001), which means that the area with the largest temperature gradient shifts southward. A second theory is a gradual southward migration of the Gulf Stream path. Data suggest a combination of both hypotheses and it is possible that the first one helped to trigger the second one. A decrease in summer insolation probably helps to sustain the gradual southward shift (Sachs, 2007). The more southward track of the North Atlantic Current is also consistent with slight temperature rises in the North Sea, Norwegian Sea and Slope Current areas, and a cooling in the more north situated North Cape Current and West Spitsbergen Current regions. The initiation of the Labrador Sea Water formation was probably only possible after the Laurentide ice sheet melting, as fresh water from those ice masses prohibited the start of overturning in the Labrador Sea (Hillaire-Marcel et al., 2001; de Vernal et al., 2006).

The temperature decrease in the northwest Atlantic and the temperature increase in the Mediterranean correspond with a trend towards a positive NAO. This shift from negative to positive NAO is in the same range as the change in the 9,4-8,2 ka BP period, but in opposite direction. This trend has also been described in Sachs (2007).

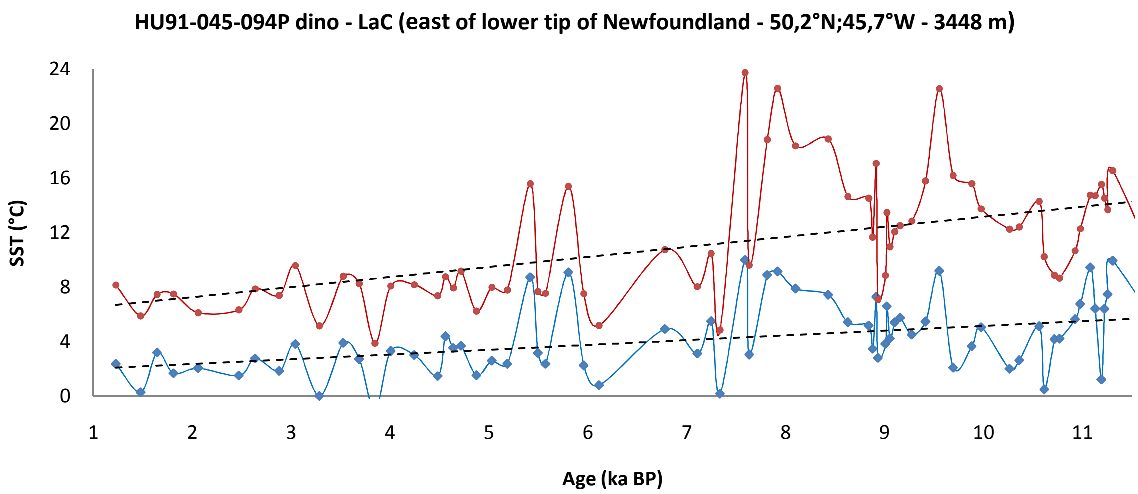


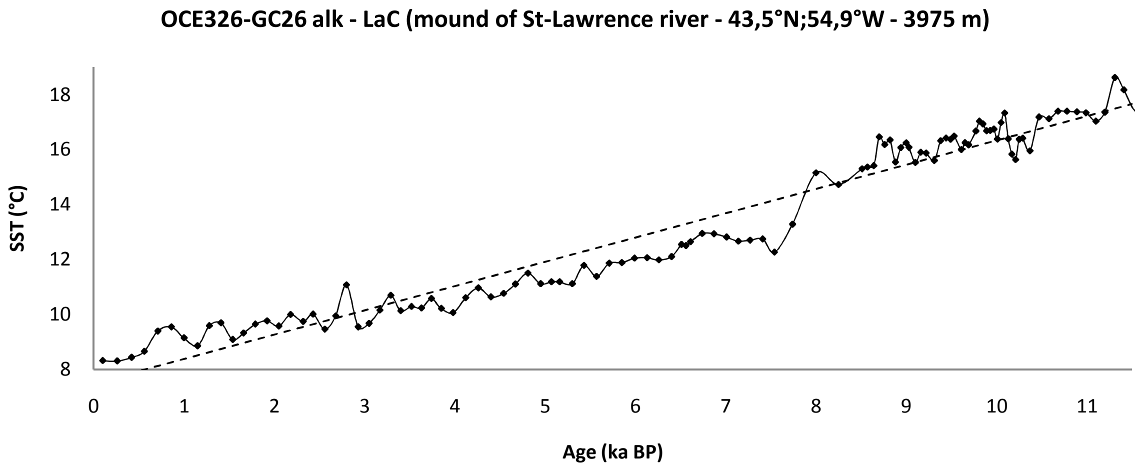


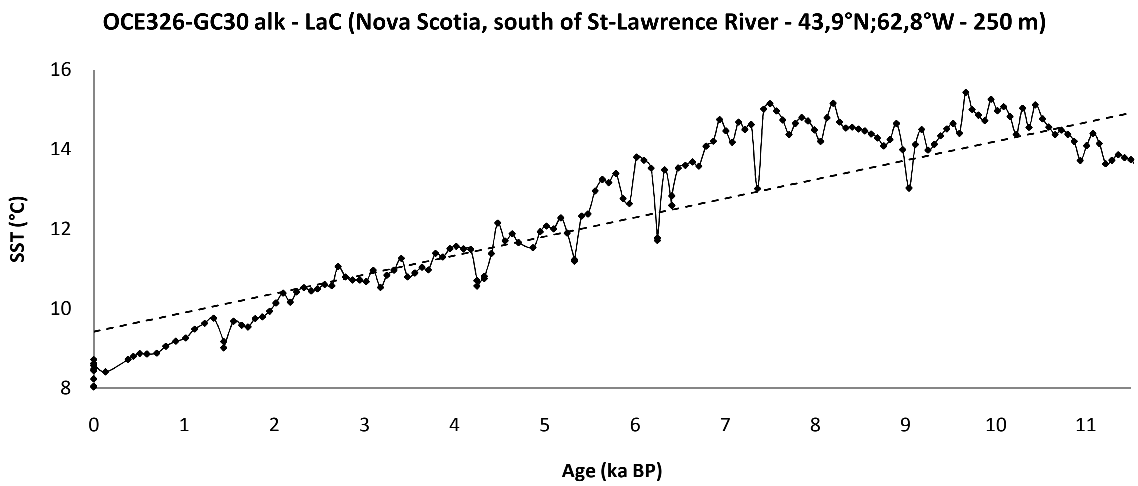


**Fig. 40: Temperature reconstructions from north to south along the NE US coast showing a sudden temperature shift in the north and a more gradual shift in the south due to the cooling of the Labrador Current slope waters. These temperature trends suggest that the initial change was very fast, but after finding equilibrium the temperature change became gradual. (de Vernal et al., 2006; Sachs, 2007)**

*4. 5,9 ka BP until recent – Strengthening of the Labrador MOC*

The end of the previous period and start of the last major temperature trend shift is marked by a period of unstable climate between 6,7 and 4,8 ka BP. The 5,9 ka BP Bond event, also correlated with the melt of the last remnants of the Laurentide ice sheet (Dyke et al., 2003), occurs in the middle of this period, and is in many records well discernable. A remarkable temperature shift is the one at 5,5 ka BP, which is accompanied by a sudden temperature rise. This age corresponds approximately with the end of the African Humid Period (de Menocal et al., 2000), with the penetration of the slope waters (south Labrador Current) towards Cape Hatteras (fig. 30), and with a change in distribution of IRD (Moros et al., 2006). This event is indicated in dinocyst records as well as in planktonic foraminifera ones. For the North Atlantic, Solignac (2008) proposed a decoupling of the NAC and SC, which are influencing the Faroe-Shetland Channel. This hypothesis is also supported be the gradual southward shift of the GS and NAC. The temperature rise in the Canary Current area is attributed to nonlinear positive feedbacks linking a sudden decrease in regional precipitation, vegetation cover loss, and increasing albedo (Claussen et al., 1999). The regional variability of the 4,8 ka BP (e.g. fig. 33) event suggest a clear link with a negative NAO phase.

The ocean system remains dominantly stable during this period, as no temperature shifts occur in the same range of the prior ones. Although temperatures decrease about everywhere, dinocyst records indicate that the winter temperatures increase in many high latitude areas due to the increase of winter insolation (e.g. fig. 26) (de Vernal et al., 2006). The discussion on proxy difference showed that planktonic foraminifera summer records probably display rather Holocene winter trends instead of the summer ones. The fact that there is a clear opposing seasonal trend in many areas probably means that alkenone records are overestimating the temperature change as they dominantly represent summer temperature trends due to their preference in growth season. The localization of records with maximum temperature variability during this time frame suggests that the gradual southward shift of the North Atlantic Current continues. The large variability during this period north of Cape Hatteras indicates the start of cold Labrador Current water (slope water) penetrating further south (fig. 30), as from 5 ka BP onwards temperatures decrease by several degrees in the northwest Atlantic (fig. 32). This slower temperature decrease in the alkenone records southwest of Newfoundland (Canada) are related to the fast temperature decrease observed during the previous period in dinocyst records just north of the alkenone ones. This is again proof of the GS and NAC shifting further southward (Sachs, 2007). Stable average temperatures in the central and northeast Atlantic suggest only minor changes in current paths during the last 5 ka.

There is a lot of debate about the NAO evolution from mid to late Holocene (Rimbu et al., 2003, 2004; Sachs, 2007; Solignac et al., 2008). The major cause for the controversy can be attributed to the fact that the NAO is mostly a seasonal index. Because of the opposing winter and summer trends in certain areas, it is thus difficult to estimate the annual trend. The summer temperatures suggest a trend towards a positive NAO, due to a strong decrease in slope water temperatures. The NAO evolution during winter is not so clear, but slightly rising winter temperatures in the northwest Atlantic (fig. Holocene maxima) suggest a neutral to negative NAO. As the temperature trends in summer are mostly dominant over the winter, the overall trend is probably towards a positive NAO. The theory of a positive trend in NAO is also supported by an evolution towards dryer conditions in the West Mediterranean (Jalut et al., 2000). The overall positive NAO trend is also stated in Sachs (2007), but Rimbu et al. (2003) suggests a negative trend in NAO.

## 3.1 The effect of forcings on Holocene climate evolution

### *3.1 Insolation*

There are only a few forcings which can have major influence on millennial and centennial scale climate change. The most important one on millennial and certainly on Holocene (10 kyr) timescale is the Milankovic cycle related to orbital changes (Berger, 1988). This cycle represents latitudinal differences in insolation regarding to seasonality. The reconstructed insolation intensity suggests a 65°N summer maximum between 9 and 10 ka BP (fig. 41).

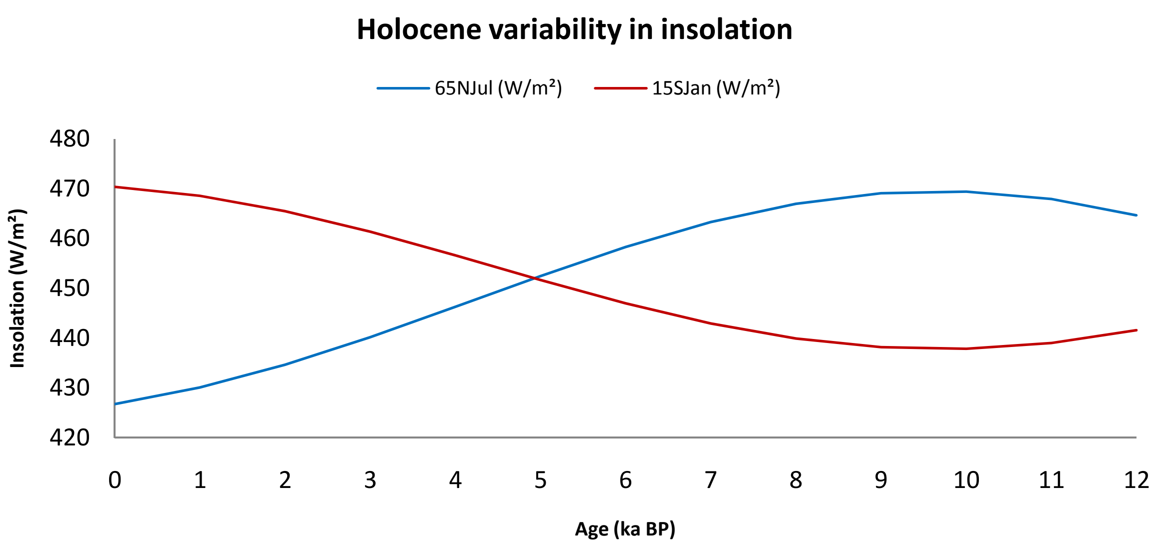


**Fig. 41: Insolation changes during the Holocene period (NOAA database)**

A simple way to show that there is a good correlation between the seasonal Holocene insolation and the proxy records is to analyze the timing of the Holocene maxima (fig. 32). The fact that these maxima gradually shift from high latitudes during the early Holocene towards low latitudes at the end of the Holocene, proves that there is a strong correlation between temperatures and summer insolation. Also the decrease in seasonality in many of the high latitude records can be at least partially explained by the decrease in summer and increase in winter insolation. The theory that planktonic foraminifera records in high latitude locations present rather winter temperature than summer temperature trends is also strengthened by the influence of insolation.

The fact that the Holocene maximum in most of the North Atlantic regions is already reached between 11,5 and 8 ka BP suggests that there is no or at least not much delay between ocean temperatures and insolation. This is in contrast with many continental records in the high latitudes which show a delay in Holocene maximum due to the presence of ice masses in the early and first part of middle Holocene.

### *3.2 Solar activity and IRD*

The effect of solar activity on centennial climate evolution has already been suggested to be the main forcing with regards to the Little Ice Age (Mauquoy et al., 2002). Variability in solar activity has also been proposed as trigger for the Younger Dryas (Renssen et al., 2000) and 8,2 ka BP event (Muscheler et al., 2004), but the most important correlation that has been found is the one with percentages of ice rafted debris deposited in the North Atlantic due to arctic ice melt about every 1500 year (Bond et al., 2001). Therefore both IRD deposits and solar activity are considered together.

Three cycles were found in this study. The 150-200 yr cycle and ~500 yr cycle are compared with solar activity during the Holocene. The reconstruction of the solar modulation function (measure of solar activity), is based on the cosmogenic radionuclides $^{10}Be$ and $^{14}C$ (Vonmoos et al., 2006). The 150-200 year cycle that is found consistently in the records might be linked to the known ~205-year de Vries solar cycle. The 400-600 year periodicity is not really a known cycle, but as already mentioned in the results, it can also be seen as a 500-1000-1500 yr cycle, which suggest a relation to the Bond cycle.

A graph with varying solar activity during the last 9,3 ka BP (Vonmoos et al., 2006) combined with averaged percentages of IRD from 3 sediment cores (Bond et al., 2001) is displayed in figure x. The IRD peaks represent mostly the Bond events. Some remarks can be made on the IRD reconstruction. There is a sudden decrease in IRD deposits after 5,2 ka BP, which corresponds nicely with the end of the last transition period. This trend is also consistent with a stabilization of the ocean system and a decrease in seasonality difference (and temperatures). The maxima in IRD are related with minima in solar activity due to more ice growth during winter (Bond et al., 2000). Along with the minima, the amplitude of the solar activity also seems to play a role. After 5 ka BP, the maxima in IRD percentages occur mostly during a rise in solar activity suggesting that there is a positive trend in ice growth during periods of low solar activity.

There is a lot of centennial scale variability, but there seems to be some periodicity in the curve. The two cycles in relation to IRD and solar activity are discussed below. Also a short summary is given on the findings of the. As there was also found an opposing correlation between the first two Holocene Mediterranean temperature dips, this will be also shortly discussed.

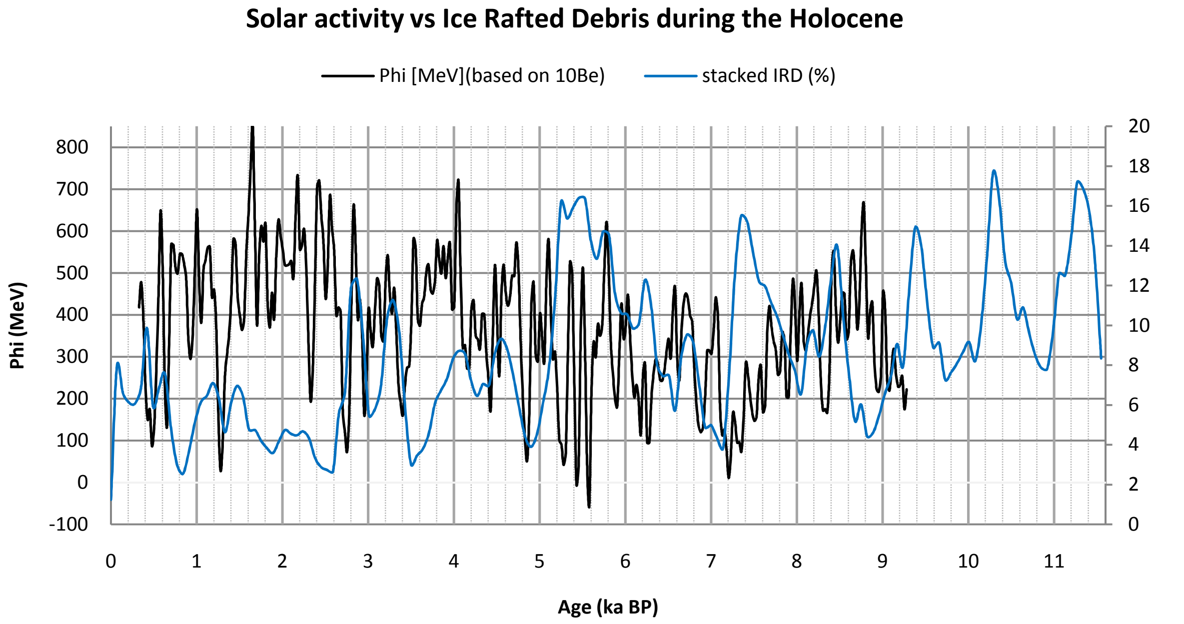


**Fig. 42: A combined graph of solar activity and IRD events. There is a clear relation between low solar activity and high IRD flux. The reason why the IRD flux decreases after 5,2 ka BP is a change in the ice rafting path. (Bond et al., 2001; Vonmoos et al., 2006)**

1. *500-1000-1500 yr cycle*

The most recurring minima in the records related to the Bond events are dated at 10,4-10,3; 9,5-9,3; 8,2-8,1; 5,9-5,8; 4,1-3,8; 3,0-2,7 and 1.4-1,3 ka BP. The reason why the minima of the 4,1 and 2,8 ka BP are spread over a few hundred year is because there are two dominant minima occurring around these ages. Another remark is that the 8,2 ka BP event occurred during a minor IRD increase and a solar maximum. This indicates another origin for this event, which has been found to be the draining of two major Canadian melt lakes into the northwest Atlantic (Alley et al., 1997). Other minima that are frequently present in the records and which are also intimately related to a high IRD flux and a low solar activity can be found at 8,5-8,4; 7,6-7,4; 6,5-6,3; 5,5-5,3; 4,5-4,4; 3,5-3,4 and 0,3-0,4 ka BP. The link of these temperature anomalies with IRD as well as solar activity suggest that the 1500 yr cycle should be reviewed. There is still a last group of minima which are occurring during solar activity minima, but where no significant correlation is present with IRD deposits. These minima have an age of about 9,9; 8,9; 7,0-6,9; 5,0-4,9; 2,4-2,3; 1,9-1,8 and 0,8 ka BP. The reason that there are no major ice drifts during these certain minima might be explained either by the fact that the solar minima are not profound enough or that there was not much ice present during these specific minima, and as a consequence ice had to expand again before major melting could originate. This theory is verified by the fact that these minima occur mainly after a very large IRD event, which suggest an ice minimum. Another reason to believe this hypothesis is that during a rise in solar activity afterwards, the IRD flux suddenly rises.

If all these minima are considered, a periodicity of 400 to 600 year during the entire Holocene appears. The fact that solar variability, proxy records, and in a large extent IRD deposits all agree, strengthens the theory of this periodicity. Also the fact that these temperature anomalies can be found in most regions and in all proxies is reassuring. These results look similar to the 550 and 1000, as well as >1600-yr cyclicity proposed by Chapman & Skackleton 2000, which again justifies these findings. The records in figure 44 clearly indicate that all events do not occur in every record and certainly not everywhere in the same extent.

The few regions (Labrador Current and Greenland Current regions) where these events are not clear have in common that they all transport ice towards the south. This suggests that a freshwater influence might alter the temperatures. Another observation that strengthens this hypothesis are the opposing seasonality trends in the Irminger Current (fig. 43). Although Eynaud et al. (2004) denied a link between the IRD events and the temperature trends, there is a very good correlation between the two. During times of high IRD fluxes, the seasonality decreases drastically. This effect can only be seen in the dinocyst records and not in the planktonic foraminifera ones, which suggest that the decreasing seasonality trend only occurs at the surface. A possible explanation for the cold summer temperatures is the advection of cold ice rich fresh water from the East Greenland Current. The fact that winter temperatures increase could be linked to fast ice growth between Greenland and Iceland due to the large amounts of fresh water. This ice formation triggers a negative NAO phase, which strengthens the Irminger Current and weakens the North Atlantic Current.

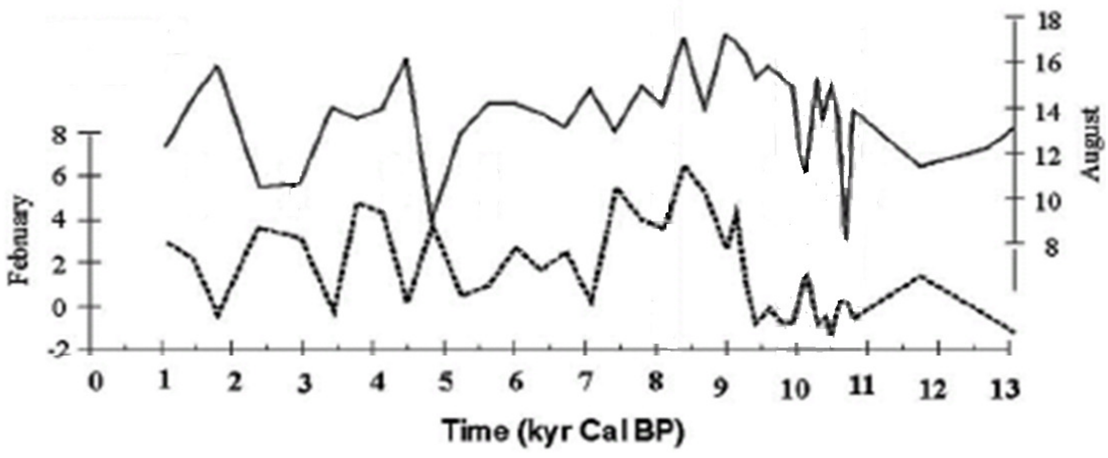


**Fig. 43: Dinocyst based summer and winter temperatures in the Irminger Current area (58°N;28°W) showing opposing seasonality trend. There is also an increase in seasonality during the last 6 kyr (adapted from Eynaud et al. (2004))**

The fact that such organized cold events occur every 500 year suggests higher climate variability during the Holocene than previously thought. Due to the regularity of these events, it might also be possible to tune records on these events.

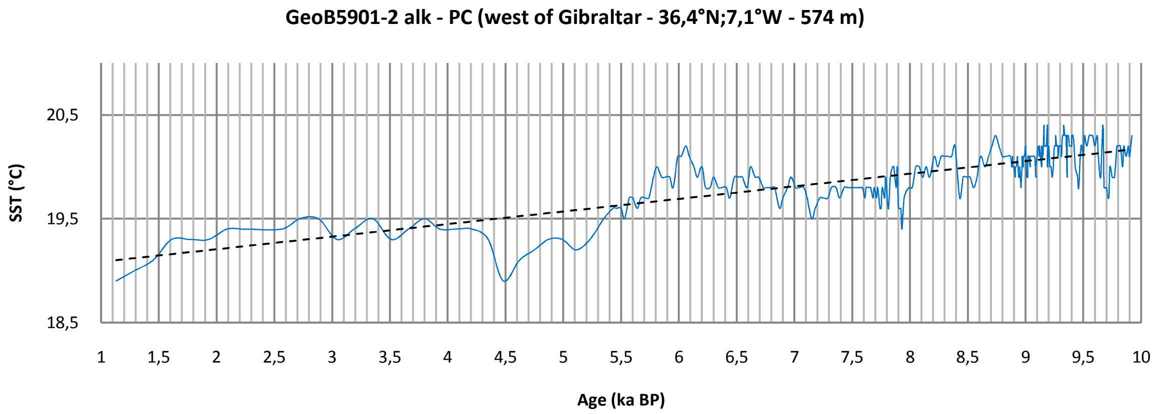


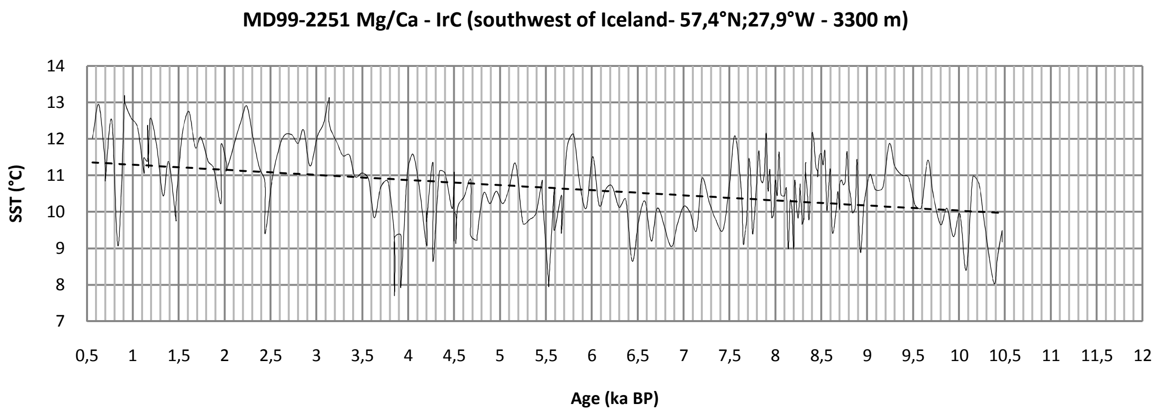


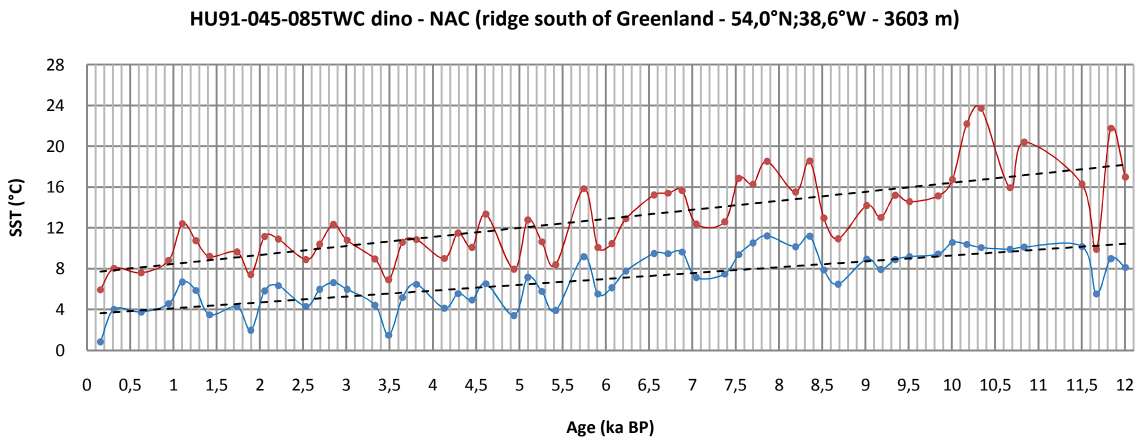


**Fig. 44: Temperature graphs of three different proxies, which indicate during most of the Holocene the ~500 yr cycle. For more examples and graphs is referred to the database. (Kim et al., 2004; Farmer et al., 2008; de Vernal and Hillaire-Marcel, 2000)**

*2. 150-200 yr cycle*

The solar activity graph indicates indeed a variability of about 150-200 year. The best way to verify this is to count the minima per 1000 yr. This frequency is between 5 and 7 (8) and the timing between the minima varies from just less than a 100 year to a little more than 200 yrs, but most of the times it is around 200, which is consistent with the de Vries cycle. The very small amplitude minima are mostly the low frequency ones, and are possible linked to the 80-90 yr Gleissberg cycle. A stack of some examples from different proxy records and regions are presented in figure 45.

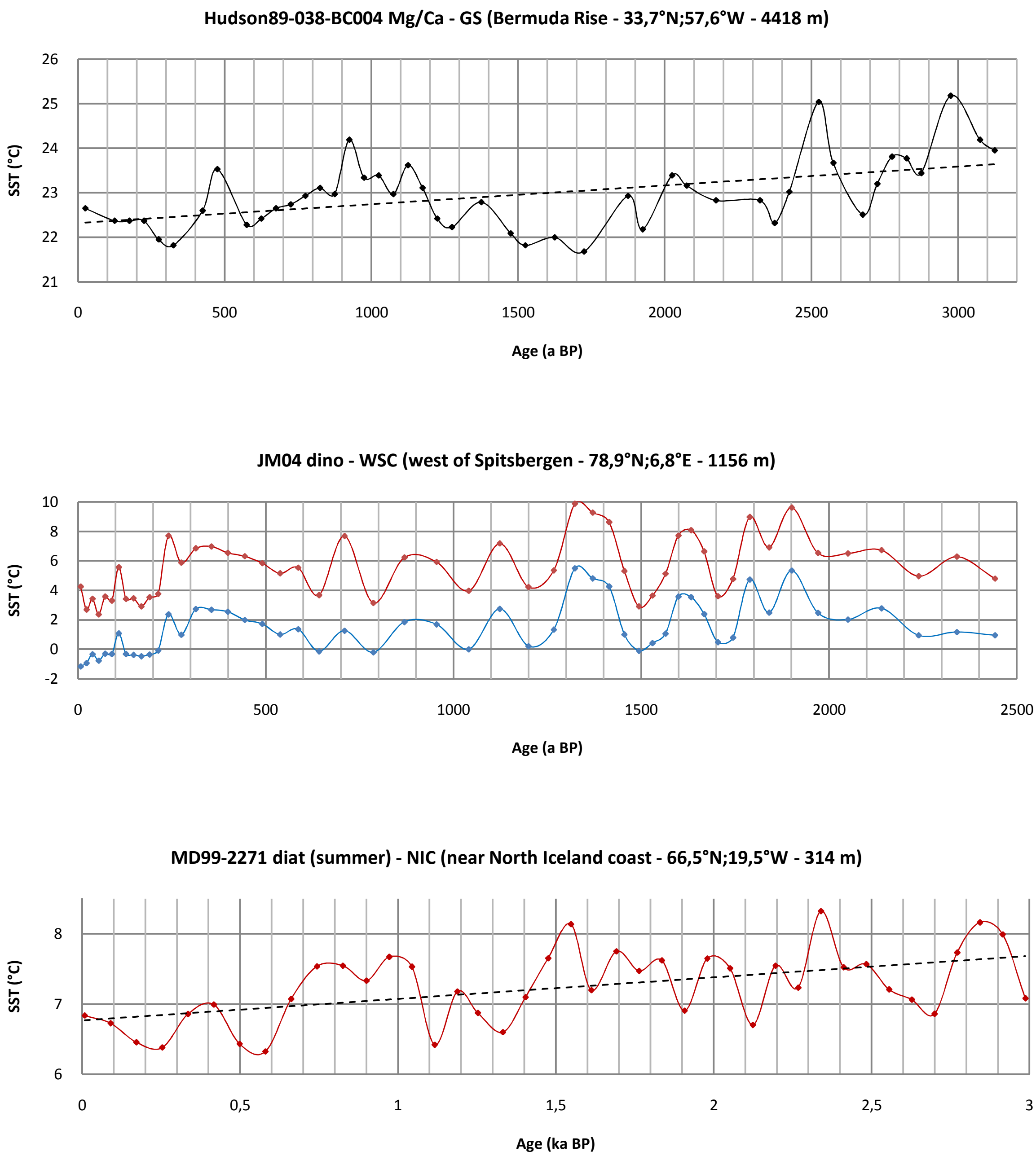


**Fig. 45: Three records of three different proxy methods of the last 2,5-3 kyr BP showing a dominantly 150-200 yr cycle. The first and third graph also indicate the different cold and warm periods during the last 2,5 ka BP. (Keigwin, 1996; Bonnet et al., 2010; Jiang et al., 2007)**

*3. Cold and warm periods during the last 2,5 ka BP*

The observed minima during LIA, DACP and LICP, and maxima during MWP and RWP are in good agreement with solar activity. Also the approximately 200 year frequency of these minima and maxima suggest a strong link with solar activity (fig. 45).

*4. The mid Holocene temperature dips in the Mediterranean*

The periods with negative temperature anomalies from about 9,4 to 7,6, ka BP and 7,4 to 6,3 ka BP in the Mediterranean region occur during high solar activity phases (fig. 33). These temperature trends are thus not consistent with solar activity and the NAO trend, which is suggested to be in a negative mode due to a more humid climate during the mid Holocene in the Mediterranean region, Middle East and northwest Africa (Parker et al., 2006; Jung et al., 2004; Migowski et al., 2006). A possible explanation for these cooling events is a change in intermediate water circulation in the Mediterranean Sea due to large influxes of fresh water (Rohling et al., 2006). This explanation is also consistent with low salinities, low oxygen isotope values and sapropel deposition during these periods (Vidal et al., 2010). Also the Black Sea draining into the Mediterranean Sea was probably a major fresh water source (Sperling et al., 2003). The last mid Holocene dip occurs during the period with highest solar variability and is linked to a final widespread Holocene sapropel deposition in the Mediterranean Sea (Tryantaphyllou et al., 2009).

## 4. Discussion on model-data differences

### *4.1 ECBilt-CLIO-VeCode surface temperatures during last 8 kyr*

The fact that model based surface temperatures are compared with SST records has some implications. Especially along continental margins, differences between surface temperatures and SSTs can occur due to advection of either warm/cold air from continents and warm/cold water from surface currents. A comparison of current air and sea surface temperatures indicates that these differences are mostly marginal on an annual basis, which suggests that a general comparison between these temperatures can be made. At the highest latitudes, where ice is regularly present on the ocean surface, it is though impossible to compare sea surface temperatures with surface air temperatures.

The comparison of modern air temperatures with the model temperatures suggests that the model is significantly overestimating the temperatures along the northern part of the SE-NW path of the GS-NAC. The anomalously high temperatures in this area indicate that the model has difficulties in picking up the southward shift of the GS. Sachs (2007) already mentions that only lower resolution models have managed to predict this shift. Another remark is that the temperatures seem averagely too high. This could be one of the reasons why the model fails to simulate the GS shift.

The fact that the temperature change in the model prediction at mid latitudes is very low in comparison to the proxy records might be related to several causes. A first one is the low resolution of the model, which leads to a flattening trend. This means that most local phenomena are not generated by the model. Another reason can be the fact that most proxy records indicate seasonal trends instead of annual ones (Leduc et al., 2010). Errors through mistakes in initial conditions and parameterization are a third factor. The variation in ice surface might also have its effects, but this is more important on a short time scale, as seen in the experiment related to solar activity (Renssen et al., 2006).

The temperature change in mid latitudinal areas is underestimated by the model. The model also fails to predict the right trends on a regional scale. These findings indicate that the model fails to simulate a southward shift of the Gulfstream. This is the reason why the model prediction indicates a trend from a positive NAO during the mid Holocene towards a negative NAO during the late Holocene (Rimbu et al., 2003, 2004).

### *4.2 PMIP2: 6 ka SST synthesis maps*

The results from the ECBILT-CLIO-VECODE surface temperatures are not so promising, as they fail to predict the temperature evolution in some key areas of the North Atlantic. Therefore the data have also been compared with the 6 ka SST synthesis maps of the ECBilt-Clio-VeCode and all other PMIP-2 models to see whether some of them give better correlations with the proxy records.On the PMIP-2 website, there are 12 SST synthesis maps available from all developed OA and OAV models. These synthesis maps contain the annual temperature change over the last 6 kyr, and have been added in the database. The model produced maps have all been compared with the temperature changes according to the proxy data (fig. 47). Of the 12 models, there is only one that manages to really generate similar results as the proxy data. This particular model is the 'CSIRO-Mk3L-1.1' OA model (Phipps et al., 2008). The synthesis map of this model and of the ECBilt-CLIO-VeCode model are shown in fig 46. Note that the temperature maps indicate the difference in function of 0 ka! The 6 kyr SST synthesis map of the ECBilt-CLIO-VeCode model shows mostly similar temperature changes as the 8 kyr surface temperatures. Most models give similar results as the ECBilt-CLIO-VeCode model.

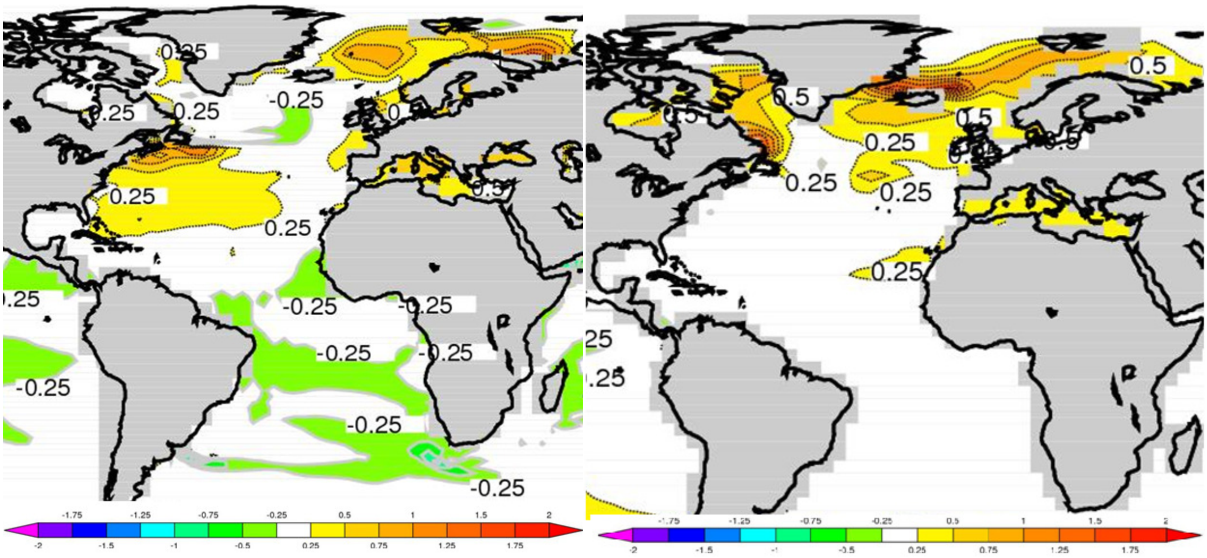

**Fig. 46: Annual mean SST change between 0 and 6 ka BP for the CSIRO-Mk3L-1.1 (left) ocean-atmosphere model experiment and the ECBILT-CLIO-VECODE (right) vegetation-ocean-atmosphere model experiment. Be aware that temperatures change is indicated from 0 ka BP! (http://pmip2.lsce.ipsl.fr/pmip2/database/maps/db_maps_6k.shtml)**

The CSIRO-Mk3L-1.1 model manages to be in agreement with the proxy data in practically all regions where the ECBilt-CLIO-VeCode model fails to do that. The two most striking differences are the correct prediction of the northeast US cooling and the slight Irminger Current warming.

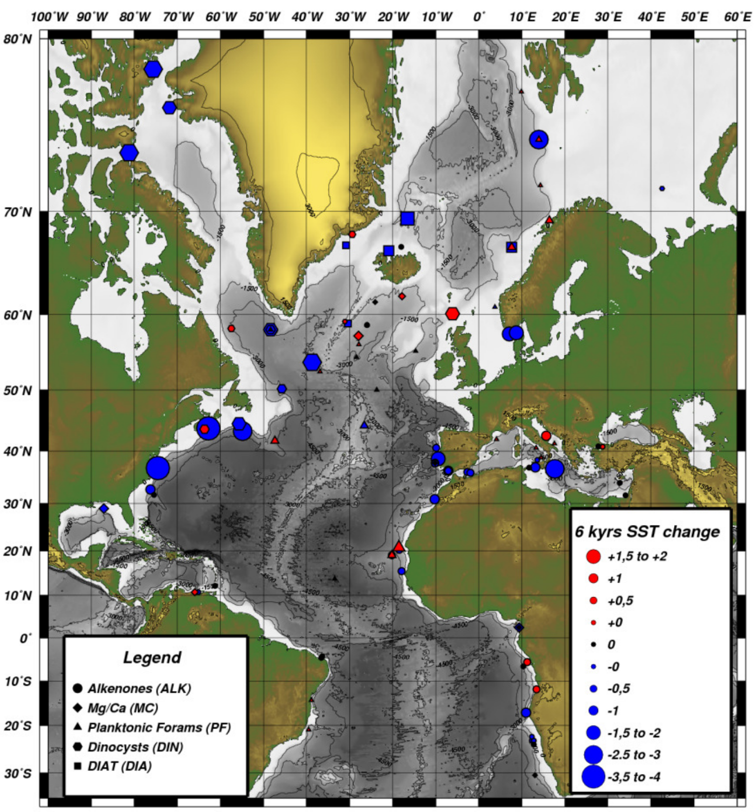


**Fig. 47: Map showing the temperature change of all proxy data between 6 and 0 ka BP.**

# V Conclusion

This is the first study to compare all important temperature proxies in such a wide study area. The different proxy records have been compared for several purposes. A first part analyses the differences between the five proxies. These reveal that one must be careful in combining and comparing several proxies with each other. Recurring differences between the proxy records indicate that particularly variability in living depth and in seasonal productivity can have major effects on temperature reconstructions. The preference in growth season of *E. huxleyi* towards the summer in higher latitudes is present in all alkenone based temperature reconstructions (1-4°C). Planktonic foraminifera based records suggest a major influence of thermocline temperatures. These findings suggest that the interpretation of alkenone and planktonic foraminifera temperature reconstructions should be reconsidered.

The second part discussed the millennial timescale temperature evolution of the Atlantic. The most important findings are that summer as well as winter temperature evolution relate well to summer and winter insolation. Also the path of the Gulf Stream System seems to be significantly influenced by insolation changes during the Holocene. Records show that this Gulf Stream System can suddenly change at certain threshold points. Regarding the long term evolution, four clear events of a reorganization of the ocean currents are present. A first one occurs at the YD-Holocene transition, due to initiation of MOC in the GIN area. Then a second one appears around 9,5 ka BP, probably triggered by a maximum in summer insolation forcing and strong northerly winds between Canada and Greenland. These strong winds could originate due to a strong temperature gradient between the warm Atlantic waters and the cold Laurentide Ice Sheet. A third shift occurs around 8 ka BP, and is related to the initiation of Labrador Sea Water formation. Increased westerlies were able to cool the slope waters of the Labrador Current (Sachs, 2007). Further south, these cold slope waters come in touch with the warm Atlantic water which could then mix, and force the Gulfstream southward. This process was probably sustained by a decrease in summer insolation. Around 5,5 ka BP a (for now) final reoganization seems to have taken place (Solignac et al., 2008). Records along the east US coast and near the Faroe-Shetland ridge suggest a sudden southward shift.

In a third part, the centennial climate variability was linked to solar avctivity. Two periodicities of 150-200 yr (80-250 yr) and about 500 yr (400-600 yr) could be found in the data, and then especially in the temperature minima. Similar trends are present in the solar activity. This could mean that solar acitivity is the most important factor in centennial climate variability.

A last part compares the proxy data with the surface air temperatures of the ECBILT-CLIO-VECODE model. Results indicate that this model fails to correctly predict regional temperature changes during the Holocene. Therefore, synthesis maps of other climate models have also been compared. From the twelve models there was only one that was able to reproduce the most important regional trends.

# VI References

Aagaard, K., Swift, J.H. and Carmack, E.C., 1985. Thermohaline Circulation in the Arctic Mediterranean Seas. J. Geophys. Res., 90(C3): 4833-4846.
Alley, R.B. and Ágústsdóttir, A.M., 2005. The 8k event: cause and consequences of a major Holocene abrupt climate change. Quaternary Science Reviews, 24(10-11): 1123-1149.
Alley, R.B. et al., 1997. Holocene climatic instability: A prominent, widespread event 8200 yr ago. Geology, 25(6): 483-486.
Alley, R.B., 2000. The Younger Dryas cold interval as viewed from central Greenland. Quaternary Science Reviews, 19(1-5): 213-226.
Alverson, J., Bundle, S.F., Sohaskey, C.D., Lybecker, M.C. and Samuels, D.S., 2003. Transcriptional regulation of the ospAB and ospC promoters from Borrelia burgdorferi. Molecular Microbiology, 48(6): 1665-1677.
Anand, P., 2005. Variability of Mg/Ca and Sr/Ca between and within the planktonic foraminifera *Globigerina bulloides* and *Globorutolia truncatulinoides*. Geochemistry Geophysics Geosystems, 6(Q11D15).
Anand, P., Elderfield, H. and Conte, M.H., 2003. Calibration of Mg/Ca thermometry in planktonic foraminifera from a sediment trap time series. Paleoceanography, 18(2): 15.
Andersen, C., Koç, N. and Moros, M., 2004. A highly unstable Holocene climate in the subpolar North Atlantic: evidence from diatoms. Quaternary Science Reviews, 23(20-22): 2155-2166.
Anderson, D.M. and Archer, D., 2002. Glacial-interglacial stability of ocean pH inferred from foraminifer dissolution rates. Nature, 416(6876): 70-73.
Andersson, C., Risebrobakken, B., Eystein, J. and Dahl, S.O., 2003. Late Holocene surface ocean conditions of the Norwegian Sea (Voring Plateau). Paleoceanography, 18(2).
Andreev, A. A., Klimanov, V. A., and Sulerzhitsky, L. D. (2001). Vegetation and climate history of the Yana River lowland, Russia, during the last 6400 yr. Quaternary Science Reviews **20,** 259-266.
Andresen, C.S. and Bjorck, S., 2005. Holocene climate variability in the Denmark Strait region - a land-sea correlation of new and existing climate proxy records. Geografiska Annaler: Series A, Physical Geography, 87(1): 159-174.

Arctic and Alpine Research, 5(4): 347-372.

Armstrong, H.A. and Brasier, M.D., 2005a. Diatomea, Microfossils. Blackwell, pp. 200-209.
Armstrong, H.A. and Brasier, M.D., 2005b. Dinoflagellates and ebridians, Microfossils. Blackwell, pp. 80-95.

Armstrong, H.A. and Brasier, M.D., 2005c. Foramninfera, Microfossils. Blackwell, pp. 142-187.
Arz, H.W., Lamy, F., Patzold, J., Muller, P.J. and Prins, M., 2003. Mediterranean Moisture Source for an Early-Holocene Humid Period in the Northern Red Sea. Science, 300(5616): 118-121.
Balsam, W.L. and McCoy, F.W., Jr., 1987. Atlantic Sediments: Glacial/Interglacial Comparisons. Paleoceanography, 2.
Barber, K.E. et al., 1999. Proxy records of climate change in the UK over the last two millennia: documented change and sedimentary records from lakes and bogs. Journal of the Geological Society, 156(2): 369-380.
Bard, E., 2001. Paleoceanographic Implications of the Difference in Deep-Sea Sediment Mixing Between Large and Fine Particles. Paleoceanography, 16.
Barker, S., Cacho, I., Benway, H. and Tachikawa, K., 2005. Planktonic foraminiferal Mg/Ca as a proxy for past oceanic temperatures: a methodological overview and data compilation for the Last Glacial Maximum. Quaternary Science Reviews, 24(7-9): 821-834.
Bartlein, P.J. and Colin, I., 1986. Climatic Response Surfaces from Pollen Data for Some Eastern North American Taxa. Journal of Biogeography, 13(1): 35-57.
Battarbee, R.W. et al., 2004. Evaluation of PMIP coupled ocean-atmosphere simulations of the Mid-Holocene, Past Climate Variability through Europe and Africa. Developments in Paleoenvironmental Research. Springer Netherlands, pp. 515-533.
Bauch, H.A. et al., 2001. A multiproxy reconstruction of the evolution of deep and surface waters in the subarctic Nordic seas over the last 30,000 yr. Quaternary Science Reviews, 20(4): 659-678.

Bé, A.W.H. and Tolderlund, D.S., 1971. Distribution and ecology of living foraminifera in surface water of the Atlantic and Indian Oceans. In: Funnel, B.M., Riedel, W.R. (Eds.), The micropaleontology of oceans, Cambridge University Press, Cambridge, pp. 105–149.
Beer, J. and Geel, B.v., 2008. Holocene climate change and the evidence for solar and other forcings. Blackwell.
Beer, J. et al., 1990. Use of 10Be in polar ice to trace the 11-year cycle of solar activity. Nature, 347(6289): 164-166.
Beer, J. et al., 2002. Cosmogenic nuclides during Isotope Stages 2 and 3. Quaternary Science Reviews, 21(10): 1129-1139.
Bendle, J. and Rosell-Melé, A., 2004. Distributions of $U^{k37}$ and $U^{k37'}$ in the surface waters and sediments of the Nordic Seas: Implications for paleoceanography. Geochemistry Geophysics Geosystems, 5.
Bendle, J.A.P. and Rosell-Mele, A., 2007. High-resolution alkenone sea surface temperature variability on the North Icelandic Shelf: implications for Nordic Seas palaeoclimatic development during the Holocene. The Holocene, 17(1): 9-24.
Benthien, A. and Müller, P.J., 2000. Anomalously low alkenone temperatures caused by lateral particle and sediment transport in the Malvinas Current region, western Argentine Basin. Deep Sea Research Part I: Oceanographic Research Papers, 47(12): 2369-2393.
Bentov, S. and Erez, J., 2005. Novel observations on biomineralization processes in foraminifera and implications for Mg/Ca ratio in the shells. Geology, 33(11): 841-844.
Bentov, S. and Erez, J., 2006. Impact of biomineralization processes on the Mg content of foraminiferal shells: A biological perspective. Geochemistry Geophysics Geosystems, 7.
Berger, A. and Loutre, M.F., 1991. Insolation values for the climate of the last 10 million years. Quaternary Science Reviews, 10(4): 297-317.
Berger, A. and Loutre, M.F., 2004. Astronomical theory of climate change. J. Phys. IV France, 121: 1-35.
Berger, A., eacute and L, 1978. Long-Term Variations of Daily Insolation and Quaternary Climatic Changes. Journal of the Atmospheric Sciences, 35(12): 2362-2367.
Berger, W.H., 1969. Ecologic patterns of living planktonic foraminifera: Deep-sea research. 16(1-24).
Bersch, M., 1995. On the circulation of the northeastern North Atlantic. Deep Sea Research Part I: Oceanographic Research Papers, 42(9): 1583-1607.
Bersch, M., Meincke, J. and Sy, A., 1999. Interannual thermohaline changes in the northern North Atlantic 1991-1996. Deep Sea Research Part II: Topical Studies in Oceanography, 46(1-2): 55-75.
Bianchi, G.G. and McCave, I.N., 1999. Holocene periodicity in North Atlantic climate and deep-ocean flow south of Iceland. Nature, 397(6719): 515-517.
Bice, K.L., Scotese, C.R., Seidov, D. and Barron, E.J., 2000. Quantifying the role of geographic change in Cenozoic ocean heat transport using uncoupled atmosphere and ocean models. Palaeogeography, Palaeoclimatology, Palaeoecology, 161(3-4): 295-310.
Bigg, E.K., Leck, C. and Nilsson, E.D., 1996. Sudden changes in arctic atmospheric aerosol concentrations during summer and autumn. Tellus B, 48(2): 254-271.
Birks, C.J.A. and Koç, N., 2002. A high-resolution diatom record of late-Quaternary sea-surface temperatures and oceanographic conditions from the eastern Norwegian Sea. Boreas, 31(4): 323 - 344.
Birks, H.J.B., 2008. Holocene climate research - progress, paradigms, and problems. In: R.W. Battarbee and H.A. Binney (Editors), Natural Climate Variability and Global Warming: A Holocene Perspective. John Wiley and Sons, Ltd., Publication, New York, pp. 7-57.
Bischof, B., Marino, A.J. and Ryan, E.H., 2003. "The North Atlantic Drift Current." Ocean Surface Currents.
Björck, S. et al., 2001. High-resolution analyses of an early Holocene climate event may imply decreased solar forcing as an important climate trigger. Geology, 29(12): 1107-1110.
Blanz, T., Emeis, K.-C. and Siegel, H., 2005. Controls on alkenone unsaturation ratios along the salinity gradient between the open ocean and the Baltic Sea. Geochimica et Cosmochimica Acta, 69(14): 3589-3600.
Boersma, A. and Silva, I.P., 1983. Paleocene Planktonic Foraminiferal Biogeography and the Paleooceanography of the Atlantic Ocean. Micropaleontology, 29(4): 355-381.
Bond, G. et al., 1997. A Pervasive Millennial-Scale Cycle in North Atlantic Holocene and Glacial Climates. Science, 278(5341): 1257-1266.

Braak, C.J.F. and Juggins, S., 1993. Weighted averaging partial least squares regression (WA-PLS): an improved method for reconstructing environmental variables from species assemblages. Hydrobiologia, 269-270(1): 485-502.
Braconnot, P. et al., 2007. Results of PMIP2 coupled simulations of the Mid-Holocene and Last Glacial Maximum – Part 1: experiments and large-scale features. Climate Past, 3: 261-277.
Braconnot, P., Joussaume, S., de Noblet, N. and Ramstein, G., 2000. Mid-Holocene and Last Glacial Maximum African monsoon changes as simulated within the Paleoclimate Modelling Intercomparison Project. Global and Planetary Change, 26(1-3): 51-66.
Bradley, R.S., 1999. Paleoclimatology. Reconstructing Climates of the Quaternary. Academic Press, San Diego, 610 pp.
Bradley, R.S., Hughes, M.K. and Diaz, H.F., 2003. CLIMATE CHANGE: Climate in Medieval Time. Science, 302(5644): 404-405.
Brassel, S.C. et al., 1986. Palaeoclimatic signals recognized by chemometric treatment of molecular stratigraphic data. Organic geochemistry, 10(4-6): 649-660.
Broecker, W., Matsumoto, K., Clark, E., Hajdas, I. and Bonani, G., 1999. Radiocarbon Age Differences Between Coexisting Foraminiferal Species. Paleoceanography, 14.
Broecker, W.S. and Peng, T.-H., 1982. Tracers in the Sea , . Lamont-Doherty Geological Observatory, Palisades, N.Y., 690 pp.
Brovkin, V. et al., 2002. Carbon cycle Vegetation and Climate Dynamics in the Holocene Experiments with the CLIMBER Model. Global Biogeochemical Cycles, 16(4): 1139.
Brovkin, V., Claussen, M., Petoukhov, V. and Ganopolski, A., 1998. On the stability of the atmosphere-vegetation system in the Sahara/Sahel region. J Geophys Res, 103(D24): 31613-31624.
Brown, C.W. and Yoder, J.A., 1994. Coccolithophorid blooms in the global ocean. J. Geophys. Res., 99(C4): 7467-7482.
Brown, E. et al., 2001. Ocean Circulation. The Open University, Walton Hall, Milton Keynes, UK.
Brown, S.J. and Elderfield, H., 1996. Variations in Mg/Ca and Sr/Ca Ratios of Planktonic Foraminifera Caused by Postdepositional Dissolution: Evidence of Shallow Mg-Dependent Dissolution. Paleoceanography, 11(5): 543-551.
Bryan, F., 1986. High-latitude salinity effects and interhemispheric thermohaline circulations. Nature, 323: 301-304.
Came, R.E., Oppo, D.W. and McManus, J.F., 2007. Amplitude and timing of temperature and salinity variability in the subpolar North Atlantic over the past 10 k.y. Geology, 35(4): 315-318.
Cane, M.A. et al., 2006. Progress in Paleoclimate Modeling*. Journal of Climate, 19(20): 5031-5057.
CAPE_project_members. (2001). Holocene paleoclimate data from the Arctic: testing models of global climate change. Quaternary Science Reviews **20,** 1275-1287.
Castañeda, I.S. et al., 2010. Millennial-scale sea surface temperature changes in the eastern Mediterranean (Nile River Delta region) over the last 27,000 year. Paleoceanography, 25(1): PA1208.
Chapman, M.R. and Shackleton, N.J., 2000. Evidence of 550-year and 1000-year cyclicities in North Atlantic circulation patterns during the Holocene. The Holocene, 10(3): 287-291.
Claussen, M. et al., 1999. Simulation of an abrupt change in Saharan vegetation in the mid-Holocene. Geophys. Res. Lett., 26(14): 2037.
Claussen, M., Brovkin, V., Ganopolski, A., Kubatzki, C. and Petoukhov, V., 2002. Climate Change in Northern Africa: The past is not the future. Climatic Change, 57: 99-118.
CLIMAP_Project_members, 1976. The surface of the ice age earth. Science, 191: 1131-1137.
CLIMAP_Project_members, 1976. The surface of the ice age earth. Science, 191: 1131-1137.
Cohmap, M., 1988. Climatic changes of the last 18,000 years: observations and model simulations. Science 241 (4869): 1043–1052.
Conte, M.H. and Eglinton, G., 1993. Alkenone and alkenoate distributions within the euphotic zone of the eastern North Atlantic: correlation with production temperature. Deep Sea Research Part I: Oceanographic Research Papers, 40(10): 1935-1961.
Conte, M.H. et al., 2006. Global temperature calibration of the alkenone unsaturation index (U-37(K ')) in surface waters and comparison with surface sediments. Geochemistry Geophysics Geosystems, 7: 22.
Conte, M.H., Thompson, A., Eglinton, G. and Green, J.C., 1995. Lipid biomorker diversity in the coccolithophorid *E. Huxleyi* (Prymnesiophyceae) and the related species *G. oceanica*., 31(2): 272-282.

Conte, M.H., Thompson, A., Lesley, D. and Harris, R.P., 1998a. Genetic and Physiological Influences on the Alkenone/Alkenoate Versus Growth Temperature Relationship in Emiliania huxleyi and Gephyrocapsa Oceanica. Geochimica et Cosmochimica Acta, 62(1): 51-68.
Conte, M.H., Weber, J.C. and Ralph, N., 1998b. Episodic particle flux in the deep Sargasso Sea: an organic geochemical assessment. Deep Sea Research Part I: Oceanographic Research Papers, 45(11): 1819-1841.
Conte, M.H., Weber, J.C., King, L.L. and Wakeham, S.G., 2001. The alkenone temperature signal in western North Atlantic surface waters. Geochimica et Cosmochimica Acta, 65(23): 4275-4287.
Craig, H. and Gordon, L.I., 1965. Deuterium and oxygen-18 variations in the ocean and marine atmospheres. In: E. Tongiorgi (Editor), Proceedings of a Conference on StableStable Isotopes in Oceanographic Studies and Palaeotemperatures. Lischi and Figli, Pisa, Italy.
Crosta, X. and Koç, N., 2007. Diatoms: from micropaleontology to isotope chemistry. Book: Proxies in late cenozoic paleoceanography 327-369.
Crosta, X., Koç, N., Claude, H.-M. and Anne De, V., 2007. Chapter Eight Diatoms: From Micropaleontology to Isotope Geochemistry, Developments in Marine Geology. Elsevier, pp. 327-369.
Crowley, T.J., 2000. CLIMAP SSTs re-revisited. Climate Dynamics, 16(4): 241-255.
Crucifix, Loutre, Tulkens, Fichefet and Berger, 2002. Climate evolution during the Holocene: a study with an Earth system model of intermediate complexity. Climate Dynamics, 19(1): 43-60.
Crucifix, M., 2008. Modeling the climate of the Holocene. In: R.W. Battarbee and H. Binney (Editors), Natural Climate Variability and Global Warming: a Holocene Perspective. Wiley-Blackwell, Chichester, pp. 123-139.
Cubasch, U. et al., 2001. Projections of Future Climate Change. Related Information: Climate Change 2001: Working Group I: The Scientific Basis, 525-582, Medium: ED; Size: HTML pp.
Cuny, J., Rhines, P.B., Niiler, P.P. and Bacon, S., 2002. Labrador Sea Boundary Currents and the Fate of the Irminger Sea Water. Journal of Physical Oceanography, 32(2): 627-647.
Curry, R.G. and McCartney, M.S., 2001. Ocean Gyre Circulation Changes Associated with the North Atlantic Oscillation*. Journal of Physical Oceanography, 31(12): 3374-3400.
Dahl, S.O. and Nesje, A., 1996. A new approach to calculating Holocene winter precipitation by combining glacier equilibrium-line altitudes and pine-tree limits: a case stud from Hardangerjokulen, central southern Norway. The Holocene, 6(4): 381-398.
Dale, B., 1976. Cyst formation, sedimentation, and preservation: Factors affecting dinoflagellate assemblages in recent sediments from Tronsheimsfjord, Norway. Review of Palaeobotany and Palynology, 22: 39-60.
De Sève, M.A., 1999. Transfer function between surface sediment diatom assemblages and sea-surface temperature and salinity of the Labrador Sea. Marine Micropaleontology, 36(4): 249-267.
de Vernal, A. and Hillaire-Marcel, C., 2006. Provincialism in trends and high frequency changes in the northwest North Atlantic during the Holocene. Global and Planetary Change, 54(3-4): 263-290.
de Vernal, A. and Marret, F., 2007. Organnic-walled dinoflagellate cysts: tracers of sea-surface conditions. In C. Hillaire-Marcel and A. de Vernal: Proxies in Late Cenozoic paleoceanography. 371-408.
de Vernal, A. et al., 1992. Quaternary organic-walled dinoflagellate cysts of the North Atlantic Ocean and adjacent seas; ecostratigraphy and biostratigraphy. In Head M.J.
de Vernal, A. et al., 2005. Reconstruction of sea-surface conditions at middle to high latitudes of the Northern Hemisphere during the Last Glacial Maximum (LGM) based on dinoflagellate cyst assemblages. Quaternary Science Reviews, 24(7-9): 897-924.
de Vernal, A. et al., 2006. Comparing proxies for the reconstruction of LGM sea-surface conditions in the northern North Atlantic. Quaternary Science Reviews, 25(21-22): 2820-2834.
de Vernal, A., Guiot, J. and Turon, J.L., 1993. Late and Postglacial Paleoenvironments of the Gulf of St. Lawrence: Marine and Terrestrial Palynological Evidence. Géographie physique et Quaternaire, 47(2): 167-180.
de Vernal, A., Henry, M, Jens Matthiessen, Peta J. Mudie, André Rochon, Karin P. Boessenkool, Frédérique Eynaud, Kari GrØsfjeld, Joël Guiot, Dominique Hamel, Rex Harland, Martin J. Head, Martina Kunz-Pirrung, Elisabeth Levac, Virginie Loucheur, Odile Peyron, Vera Pospelova, Taoufik

Radi, Jean-Louis Turon, Elena Voronina, 2001. Dinoflagellate cyst assemblages as tracers of sea-surface conditions in the northern North Atlantic, Arctic and sub-Arctic seas: the new lsquo<I>n</I> = 677rsquo data base and its application for quantitative palaeoceanographic reconstruction. Journal of Quaternary Science, 16(7): 681-698.
de Vernal, A., Hillaire-Marcel, C. and Bilodeau, G., 1996. Reduced meltwater outflow from the Laurentide ice margin during the Younger Dryas. Nature, 381(6585): 774-777.
de Vernal, A., Rochon, A., Turon, J.-L. and Matthiessen, J., 1997. Organic-walled dinoflagellate cysts: Palynological tracers of sea-surface conditions in middle to high latitude marine environments. Geobios, 30(7): 905-920.
de Vernal, A., Turon, J.L. and Guiot, J., 1994. Dinoflagellate cyst distribution in high-latitude marine environments and quantitative reconstruction of sea-surface salinity, temperature, and seasonality. Canadian Journal of Earth Sciences, 31(1): 48-62.
de Villiers, S., 2005. Foraminiferal shell-weight evidence for sedimentary calcite dissolution above the lysocline. Deep Sea Research Part I: Oceanographic Research Papers, 52(5): 671-680.
Dekens, P.S., Lea, D.W., Pak, D.K. and Spero, H.J., 2002. Core top calibration of Mg/Ca in tropical foraminifera: Refining palaeotemperaturs estimation. Geochem. Geophys. Geosyst., 3(4).
deMenocal, P., Ortiz, J., Guilderson, T. and Sarnthein, M., 2000. Coherent High- and Low-Latitude Climate Variability During the Holocene Warm Period. Science, 288(5474): 2198-2202.
Denton, G.H. and Karlén, W., 1973. Lichenometry: Its Application to Holocene Moraine Studies in Southern Alaska and Swedish Lapland
Devillers, R. and de Vernal, A., 2000. Distribution of dinoflagellate cysts in surface sediments of the northern North Atlantic in relation to nutrient content and productivity in surface waters. Marine Geology, 166: 103-124.
Dickson, R.R., Meincke, J. and Malmberg, S.A., 1984. The great salinity anomaly in the northern North Atlantic, 1968-82. Progress In Oceanography, 20: 103-151.
Diepenbroek, M. et al., 2002. PANGAEA--an information system for environmental sciences. Computers & Geosciences, 28(10): 1201-1210.
Dodge, J.D. and Marshall, H.G., 1994. Biogeographic analysis of the armored planktonic dinoflagellate 'Ceratium' in the North Atlantic and adjacent seas. Journal of Phycology, 30(6): 905-922.
Duplessy, J.-C., Ivanova, E., Murdmaa, I., Paterne, M. and Labeyrie, L., 2001. Holocene paleoceanography of the northern Barents Sea and variations of the northward heat transport by the Atlantic Ocean. Boreas, 30(1): 2 - 16.
Dyke, A.S., Moore, A. and Roberson, L., 2003. Deglaciation of North America.Geological Survey of Canada Geological Survey of Canada.
Eggins, S., De Deckker, P. and Marshall, J., 2003. Mg/Ca variation in planktonic foraminifera tests: implications for reconstructing palaeo-seawater temperature and habitat migration. Earth and Planetary Science Letters, 212(3-4): 291-306.
Eglinton, G. and Calvin, M., 1967. Chemical fossils. Scientific American, 261: 32-43.
Elderfield, H. and Ganssen, G., 2000. Past temperature and $d^{18}O$ of surface ocean waters inferred from foraminiferal Mg/Ca ratios. Nature, 405(6785): 442-445.
Elderfield, H., Vautravers, M. and Cooper, M., 2002. The relationship between shell size and Mg/Ca, Sr/Ca, d18O, and d13C of species of planktonic foraminifera. Geochemistry Geophysics Geosystems, 3.
Erez, J., 2003. The Source of Ions for Biomineralization in Foraminifera and Their Implications for Paleoceanographic Proxies. Reviews in Mineralogy and Geochemistry, 54(1): 115-149.
Eynaud, F. et al., 2002. Norwegian sea-surface palaeoenvironments of marine oxygen-isotope stage 3: the paradoxical response of dinoflagellate cysts. Journal of Quaternary Science, 17: 349-359.
Eynaud, F., Turon, J.L. and Duprat, J., 2004. Comparison of the Holocene and Eemian palaeoenvironments in the South Icelandic Basin: dinoflagellate cysts as proxies for the North Atlantic surface circulation. Review of Palaeobotany and Palynology, 128(1-2): 55-79.
Eystein, J. et al., 2008. The early to mid-Holocene thermal optimum in the North Atlantic. In: R.W. Battarbee and H. Binney (Editors), Natural Climate Variability and Global Warming: a Holocene Perspective. Wiley-Blackwell, Chichester, pp. 123-144.
Fairbanks, R.G. et al., 2005. Radiocarbon calibration curve spanning 0 to 50,000 years BP based on paired 230Th/234U/238U and 14C dates on pristine corals. Quaternary Science Reviews, 24(16-17): 1781-1796.

Fensome, R.A. et al., 1993. A classification of living and fossil dinoflagellates. American museum of natural history. Micropaleontology, Special publications number 7: 1-351.
Fichefet, T. and Morales Maqueda, M.A., 1997. Sensitivity of a global sea ice model to the treatment of ice thermodynamics and dynamics. J Geophys Res, 102: 12609–12646.
Fitzwater, S.E., Coale, K.H., Gordon, R.M., Johnson, K.S. and Ondrusek, M.E., 1996. Iron deficiency and phytoplankton growth in the equatorial Pacific. Deep Sea Research Part II: Topical Studies in Oceanography, 43(4-6): 995-1015.
Foley, J.A., Kutzbach, J., Coe, M.T. and Levis, S., 1994. Feedbacks between climate and boreal forests during the Holocene epoch. Nature, 371: 52-54.
Fritts, H.C., Blasing, T.J., Hayden, B.P. and Kutzbach, J.E., 1971. Multivariate techniques for specifying tree-growth and climate relationships and for reconstructing anomalies in paleoclimate. Journal of Applied Meteorology, 10: 854-864.
Gallimore, R.G. and Kutzbach, J.E., 1989. Effects of soil moisture on the sensitivity of a climate model to earth orbital forcing at 9000 yr BP. Climatic Change, 14(2): 175-205.
Garcin, Y., Vincens, A., Williamson, D., Buchet, G. and Guiot, J., 2007. Abrupt resumption of the African Monsoon at the Younger Dryas--Holocene climatic transition. Quaternary Science Reviews, 26(5-6): 690-704.
Gehlen, M., Bassinot, F., Beck, L. and Khodja, H., 2004. Trace element cartography of Globigerinoides ruber shells using particle-induced X-ray emission. Geochem. Geophys. Geosyst., 5(12): Q12D12.
Gent, P.R. and McWilliams, J.C., 1990. Isopycnal Mixing in Ocean Circulation Models. Journal of Physical Oceanography, 20(1): 150-155.
Gil García, M. et al., 2007. Late holocene environments in Las Tablas de Daimiel (south central Iberian peninsula, Spain). Vegetation History and Archaeobotany, 16(4): 241-250.
Giraudeau, J., Cremer, M., Manthé, S., Labeyrie, L. and Bond, G., 2000. Coccolith evidence for instabilities in surface circulation south of Iceland during Holocene times. Earth and Planetary Science Letters, 179(2): 257-268.
Gladstone, R.M. et al., 2005. Mid-Holocene NAO: A PMIP2 model intercomparison.
Godwin, H., 1962. Half-life of Radiocarbon. Nature, 195(4845): 984-984.
Goosse, H. and Fichefet, T., 1999. Importance of ice-ocean interactions for the global ocean circulation: a model study. J Geophys Res, 104: 23337–23355.
Goosse, H. and Renssen, H., 2004. Exciting natural modes of variability by solar and volcanic forcing: idealized and realistic experiments. Climate Dynamics, 23(2): 153-163.
Goosse, H., Renssen, H., Timmermann, A. and Bradley, R.S., 2005. Internal and forced climate variability during the last millennium: a model-data comparison using ensemble simulations. Quaternary Science Reviews, 24(12-13): 1345-1360.
Goosse, Selten, Haarsma and Opsteegh, 2003. Large sea-ice volume anomalies simulated in a coupled climate model. Climate Dynamics, 20(5): 523-536.
Grimalt, J.O. et al., 2000. Modifications of the C37 alkenone and alkenoate composition in the water column and sediment: Possible implications for sea surface temperature estimates in paleoceanography. Geochemistry Geophysics Geosystems, 1.
Guiot, J. and de Vernal, A., 2006. Proxies in Late Cenozoic paleoceanography: Transfer functions. Book: 523-563.
Guiot, J., Cheddadi, R., Prentice, I.C. and Jolly, D., 1996. A method of biome and land surface mapping from pollen data: Application to Europe 6000 year ago. Paleoclimates: Data and modelling, 1: 311-324.
Guisan, A., Edwards, T.C. and Hastie, T., 2002. Generalized linear and generalized additive models in studies of species distributions: setting the scene. Ecological Modelling, 157(2-3): 89-100.
Gulliksen, S., Birks, H.H., Possnert, G.r. and Mangerud, J., 1998. A calendar age estimate of the Younger Dryas-Holocene boundary at Krakenes, western Norway. The Holocene, 8(3): 249-259.
Hackett, B. and Røed, L.P., 1998. A numerical study of the slope current northwest of the British Isles. Continental Shelf Research, 18(1): 1-30.
Hald, M. et al., 2007. Variations in temperature and extent of Atlantic Water in the northern North Atlantic during the Holocene. Quaternary Science Reviews, 26(25-28): 3423-3440.
Hall, I.R., Bianchi, G.G. and Evans, J.R., 2004. Centennial to millennial scale Holocene climate-deep water linkage in the North Atlantic. Quaternary Science Reviews, 23(14-15): 1529-1536.

Hammarlund, D., Barnekow, L., Birks, H.J.B., Buchardt, B.r. and Edwards, T.W.D., 2002. Holocene changes in atmospheric circulation recorded in the oxygen-isotope stratigraphy of lacustrine carbonates from northern Sweden. The Holocene, 12(3): 339-351.
Hansen, B. and Østerhus, S., 2000. North Atlantic-Nordic Seas exchanges. Progress In Oceanography, 45(2): 109-208.
Harrison, S.P. and Prentice, C.I., 2003. Climate and CO2 controls on global vegetation distribution at the last glacial maximum: analysis based on palaeovegetation data, biome modelling and palaeoclimate simulations. Global Change Biology, 9(7): 983-1004.
Hastings, D.W., Russell, A.D. and Emerson, S.R., 1998. Foraminiferal magnesium in *Globeriginoides sacculifer*. Paleoceanography, 13(2): 161-169.
Haugan, P.M., 1999. Structure and heat content of the West Spitsbergen Current. Polar Research, 18(2): 183-188.
Haugan, P.M., Evensen, G., Johannessen, J.A., Johannessen, O.M. and Pettersson, L.H., 1991. Modeled and Observed Mesoscale Circulation and Wave-Current Refraction During the 1988 Norwegian Continental Shelf Experiment. J. Geophys. Res., 96(C6): 10487-10506.
Hay, M.B., Smol, J.P., Pipke, K.J. and Lesack, L.F.W., 1997. A Diatom-Based Paleohydrological Model for the Mackenzie Delta, Northwest Territories, Canada. Arctic and Alpine Research, 29(4): 430-444.
Hayes, A., Kucera, M., Kallel, N., Sbaffi, L. and Rohling, E.J., 2005. Glacial Mediterranean sea surface temperatures based on planktonic foraminiferal assemblages. Quaternary Science Reviews, 24(7-9): 999-1016.
Head, M.J., 1996. Modern dinofllagellate cysts and their biological affinities. In J. Jansonius, & D. C. McGregor (Eds), Palynology: Principles and applications (Vol. 3, pp. 1197-1248). Salt Lake City, UT: American Association of Stratigraphic Palynologists Foundation.
Hewitt, C.D. and Mitchell, J.F.B., 1998. A fully coupled GCM simulation of the climate of the mid‐Holocene. Geophys. Res. Lett., 25(3): 361-364.
Hillaire-Marcel, C., de Vernal, A., Bilodeau, G. and Weaver, A.J., 2001. Absence of deep-water formation in the Labrador Sea during the last interglacial period. Nature, 410(6832): 1073-1077.
Hopkins, T.S., 1991. The GIN Sea--A synthesis of its physical oceanography and literature review 1972-1985. Earth-Science Reviews, 30(3-4): 175-318.
Horner, R.A., 1985. Ecology of sea ice microalgae., Sea Ice Biota. CRC Press, Bocan Raton, FL, pp. 83-104.
Hughen, K. et al., 2004. Marine04 Marine radiocarbon age calibration, 26-0 ka BP. Journal Name: Radiocarbon; Journal Volume: 46; Journal Issue: 3: Medium: ED; Size: PDF-file: 37 pages; size: 0.7 Mbytes.
Hughen, K.A., Southon, J.R., Lehman, S.J. and Overpeck, J.T., 2000. Synchronous Radiocarbon and Climate Shifts During the Last Deglaciation. Science, 290(5498): 1951-1954.
Huntley, B., 1994. Late Devensian and Holocene palaeoecology and palaeoenvironments of the Morrone Birkwoods, Aberdeenshire, Scotland. Journal of Quaternary Science, 9(4): 311-336.
Hurrel, J.W., 1995. Decadal trends in the North Atlantic Oscillation: Regional Temperatures. Science, 269(5224): 676-679.
Hurrel, J.W., Kushnir, Y. and Visbeck, M., 2001. The North Atlantic Oscillation. Science, 291: 603-605.
Hurrell, J.W. and Van Loon, H., 1997. Decadal variations in climate associated with the North Atlantic Oscillation. Climatic Change, 36(3): 301-326.
Hutson, W.H., 1978. Application of transfer functions to Indian Ocean planktonic Foraminifera. Quaternary Research, 9(1): 87-112.
Hutson, W.H., 1980. The Agulhas Current During the Late Pleistocene: Analysis of Modern Faunal Analogs. Science, 207(4426): 64-66.
Imbrie, J. and Imbrie, J.Z., 1980. Modeling the Climatic Response to Orbital Variations. Science, 207(4434): 943-953.
Imbrie, J. and Kipp, N.G., 1971. A new micropaleontological method for quantitative paleoclimatology: Application to a Late Pleistocene Carribean core. The late cenozoic glacial ages: 71-181.
Jalut, G., Esteban Amat, A., Bonnet, L., Gauquelin, T. and Fontugne, M., 2000. Holocene climatic changes in the Western Mediterranean, from south-east France to south-east Spain. Palaeogeography, Palaeoclimatology, Palaeoecology, 160(3-4): 255-290.

Jansen, E. et al., 2008. Holocene climate research - progress, paradigms, and problems. In: R.W. Battarbee and H. Binney (Editors), Natural Climate Variability and Global Warming: a Holocene Perspective. Wiley-Blackwell, Chichester, pp. 123-139.
Jiang, H., Eiriksson, J., Schulz, M., Knudsen, K.-L. and Seidenkrantz, M.-S., 2005. Evidence for solar forcing of sea-surface temperature on the North Icelandic Shelf during the late Holocene. Geology, 33(1): 73-76.
Jordan, R.W. and Chamberlain, A.H.L., 1997. Biodiversity among haptophyte algae. Biodiversity and Conservation, 6(1): 131-152.
Joussaume, S. et al., 1999. Monsoon changes for 6000 years ago: Results of 18 simulations from the Paleoclimate Modeling Intercomparison Project (PMIP). Geophys. Res. Lett., 26(7): 859-862.
Justwan, A., Koç, N. and Jennings, A.E., 2008. Evolution of the Irminger and East Icelandic Current systems through the Holocene, revealed by diatom-based sea surface temperature reconstructions. Quaternary Science Reviews, 27(15-16): 1571-1582.
Kamatani, A., Ejiri, N. and Treguer, P., 1988. The dissolution kinetics of diatom ooze from the Antarctic area. Deep Sea Research Part A. Oceanographic Research Papers, 35(7): 1195-1203.
Kanamitsu, M. et al., 2002. NCEP DOE AMIP-II Reanalysis (R-2). Bulletin of the American Meteorological Society, 83(11): 1631-1643.
Kaplan, M. R., Wolfe, A. P., and Miller, G. H. (2002). Holocene Environmental Variability in Southern Greenland Inferred from Lake Sediments. Quaternary Research **58,** 149-159.
Karlén, W. and Kuylenstierna, J., 1996. On solar forcing of Holocene climate: evidence from Scandinavia. The Holocene, 6(3): 359-365.
Kaufman, D.S. et al., 2004. Holocene thermal maximum in the western Arctic (0-180°W). Quaternary Science Reviews, 23(5-6): 529-560.
Kerwin, M.W. et al., 1999. The Role of Oceanic Forcing in Mid-Holocene Northern Hemisphere Climatic Change. Paleoceanography, 14(2): 200-210.
Kim, J.-H. et al., 2004. North Pacific and North Atlantic sea-surface temperature variability during the Holocene. Quaternary Science Reviews, 23(20-22): 2141-2154.
Kim, J.-H., Schouten, S., Hopmans, E.C., Donner, B. and Sinninghe Damsté, J.S., 2008. Global sediment core-top calibration of the TEX86 paleothermometer in the ocean. Geochimica et Cosmochimica Acta, 72(4): 1154-1173.
Kipp, N.G., 1976. New transfer function for estimating past sea surface conditions from seabed distribution of planktonic forminiferal assemblages in the North Atlantic. In: R.M. Cline, Hays, J.D. (Editor), Investigation of Late Quaternary Paleoceanography and Paleoclimatology. Geological Society of America, Boulder, pp. 3-41.
Knudsen, K.L. et al., 2004. Environmental changes off North Iceland during the deglaciation and the Holocene: foraminifera, diatoms and stable isotopes. Marine Micropaleontology, 50(3-4): 273-305.
Koc, N. and Jansen, E., 1994. Response of the high-latitude Northern Hemisphere to orbital climate forcing: Evidence from the Nordic Seas. Geology, 22(6): 523-526.
Koç, N., Jansen, E. and Haflidason, H., 1993. Paleoceanographic reconstructions of surface ocean conditions in the Greenland, Iceland and Norwegian seas through the last 14 ka based on diatoms. Quaternary Science Reviews, 12(2): 115-140.
Koc, N., Jansen, E., Hald, M., and Labeyrie, L. (1996). Late glacial-Holocene sea surface temperatures and gradients between the North Atlantic and the Norwegian Sea: implications for the Nordic heat pump. Geological Society, London, Special Publications 111**,** 177-185.
Koç, N.K. and Schrader, H., 1990. Surface Sediment Diatom Distribution and Holocene Paleotemperature Variations in the Greenland, Iceland and Norwegian Sea. Paleoceanography, 5.
Kokinos, J.P. et al., 1998. Characterization of a highly resistant biomacromolecular material in the cell wall of a marine dinoflagellate resting cyst. Organic Geochemistry, 28(5): 265-288.
Korhola, A., Weckström, J., Holmström, L. and Erästö, P., 2000. A Quantitative Holocene Climatic Record from Diatoms in Northern Fennoscandia. Quaternary Research, 54(2): 284-294.
Krauss, W. and Ning, C.W., 1987. Lagrangian properties of eddy fields in the northern North Atlantic as deduced from satellite-tracked buoys. Journal of Marine Research, 45: 259-291.
Krauss, W., 1995. Currents and mixing in the Irminger Sea and in the Iceland Basin. J. Geophys. Res., 100(C6): 10851-10871.
Krauss, W., Fahrbach, E., Aitsam, A., Elken, J. and Koske, P., 1987. The North Atlantic current and its

associated eddy field southeast of Flemish Cap. Deep Sea Research Part A. Oceanographic Research Papers, 34(7): 1163-1185.
Krauss, W., Se, R.H.K. and Hinrichsen, H.H., 1990. The Branching of the Gulf Stream Southeast of the Grand Banks. J. Geophys. Res., 95(C8): 13089-13103.
Kucera, M. and Darling, K.F., 2002. Cryptic species of planktonic foraminifera: their effect on palaeoceanographic reconstructions. Philosophical Transactions of the Royal Society of London. Series A: Mathematical, Physical and Engineering Sciences, 360(1793): 695-718.
Kucera, M. et al., 2005. Reconstruction of sea-surface temperatures from assemblages of planktonic foraminifera: multi-technique approach based on geographically constrained calibration data sets and its application to glacial Atlantic and Pacific Oceans. Quaternary Science Reviews, 24(7-9): 951-998.
Lauritzen, S.-E. and Lundberg, J., 1999. Calibration of the speleothem delta function: an absolute temperature record for the Holocene in northern Norway. The Holocene, 9(6): 659-669.
Lazier, J.R.N. and Wright, D.G., 1993. Annual Velocity Variations in the Labrador Current. Journal of Physical Oceanography, 23(4): 659-678.
Lea, D.W., Mashiotta, T.A. and Spero, H.J., 1999. Controls on magnesium and strontium uptake in planktonic foraminifera determined by live culturing. Geochimica et Cosmochimica Acta, 63(16): 11.
Lean, J., 2000. Evolution of the Sun's Spectral Irradiance Since the Maunder Minimum. Geophys. Res. Lett., 27(16): 2425-2428.
Lear, C.H., Elderfield, H. and Wilson, P.A., 2000. Cenozoic Deep-Sea Temperatures and Global Ice Volumes from Mg/Ca in Benthic Foraminiferal Calcite. Science, 287(5451): 269-272.
Leduc, G., Schneider, R., Kim, J.H. and Lohmann, G., 2010. Holocene and Eemian sea surface temperature trends as revealed by alkenone and Mg/Ca paleothermometry. Quaternary Science Reviews, 29(7-8): 989-1004.
Levac, E. and De Vernal, A., 1997. Postglacial changes of terrestrial and marine environments along the Labrador coast: palynological evidence from cores 91-045-005 and 91-045-006, Cartwright Saddle. Canadian Journal of Earth Sciences, 34(10): 1358-1365.
Levac, E., 2001. High resolution Holocene palynological record from the Scotian Shelf. Marine Micropaleontology, 43(3-4): 179-197.
Levac, E., de Vernal, A. and Weston Blake, J., 2001. Sea-surface conditions in northernmost Baffin Bay during the Holocene: palynological evidence. Journal of Quaternary Science, 16(4): 353-363.
Levandowsky, M. and Kaneta, P., 1987. Behaviour in dinoflagellates. In: F. J. R. Taylor (Ed.), *The biology of dinoflagellates*. 330-397.
Leventer, A., 1991. Sediment trap diatom assemblages from the northern Antarctic Peninsula region. Deep Sea Research Part A. Oceanographic Research Papers, 38(8-9): 1127-1143.
Licursi, M., Sierra, M.V. and Gómez, N., 2006. Diatom assemblages from a turbid coastal plain estuary: Río de la Plata (South America). Journal of Marine Systems, 62(1-2): 35-45.
Lippsett, L., 2009. Ocean Conveyor's 'Pump' Switches Back On, Oceanus magazine.
Liu, Z., Otto-Bliesner, B., Kutzbach, J., Li, L. and Shields, C., 2003. Coupled Climate Simulation of the Evolution of Global Monsoons in the Holocene*. Journal of Climate, 16(15): 2472-2490.
Lohmann, G.P., 1995. A Model for Variation in the Chemistry of Planktonic Foraminifera Due to Secondary Calcification and Selective Dissolution. Paleoceanography, 10.
Lorenz, S.J., Kim, J.-H., Rimbu, N., Schneider, R.R. and Lohmann, G., 2006. Orbitally driven insolation forcing on Holocene climate trends: Evidence from alkenone data and climate modeling. Paleoceanography, 21.
Luterbacher, J., Dietrich, D., Xoplaki, E., Grosjean, M. and Wanner, H., 2004. European Seasonal and Annual Temperature Variability, Trends, and Extremes Since 1500. Science, 303(5663): 1499-1503.
Macdonald, A.M. and Wunsch, C., 1996. An estimate of global ocean circulation and heat fluxes. Nature, 382: 436-439.
MacDonald, G. M., Velichko, A. A., Kremenetski, C. V., Borisova, O. K., Goleva, A. A., Andreev, A. A., Cwynar, L. C., Riding, R. T., Forman, S. L., Edwards, T. W. D., Aravena, R., Hammarlund, D., Szeicz, J. M., and Gattaulin, V. N. (2000). Holocene Treeline History and Climate Change Across Northern Eurasia. Quaternary Research **53,** 302-311.
Magny, M., 1993. Solar Influences on Holocene Climatic Changes Illustrated by Correlations between Past Lake-Level Fluctuations and the Atmospheric 14C Record. Quaternary Research, 40(1): 1-9.

Malmgren, B.A. and Nordlund, U., 1996. Application of Artificial Neural Networks to Chemostratigraphy. Paleoceanography, 11: 505-512.
Malmgren, B.A., Kucera, M., Nyberg, J. and Waelbroeck, C., 2001. Comparison of Statistical and Artificial Neural Network Techniques for Estimating Past Sea Surface Temperatures from Planktonic Foraminifer Census Data. Paleoceanography, 16.
Manabe, S. and Bryan, J.K., 1985. $CO_2$-induced Change in a Coupled Ocean-Atmosphere Model and its Paleoclimatic Implications. Journal of Geophysical Research, 90(C6): 11689-11707.
Mann, C.R., 1967. The termination of the Gulf Stream and the beginning of the North Atlantic Current. Deep Sea Research and Oceanographic Abstracts, 14(3): 337-359.
Marchal, O. et al., 2002. Apparent long-term cooling of the sea surface in the northeast Atlantic and Mediterranean during the Holocene. Quaternary Science Reviews, 21(4-6): 455-483.
Marchal, O. et al., 2002. Apparent long-term cooling of the sea surface in the northeast Atlantic and Mediterranean during the Holocene. Quaternary Science Reviews, 21(4-6): 455-483.
Marlowe, I.T. et al., 1984b. Long chain (n-C37-C39) alkenones in the Prymnesiophyceae, distribution of alkenones and other lipids and their taxonomic significance. British Phycological Journal, 19(3): 203-216.
Marlowe, I.T., Brassell, S.C., Eglinton, G. and Green, J.C., 1984. Long chain unsaturated ketones and esters in living algae and marine sediments. Organic Geochemistry, 6: 135-141.
Marlowe, I.T., Brassell, S.C., Eglinton, G. and Green, J.C., 1990. Long-chain alkenones and alkyl alkenoates and the fossil coccolith record of marine sediments. Chemical geology, 88(3-4): 349-375.
Marret, F., de Vernal, A., Benderra, F. and Harland, R., 2001. Late Quaternary sea-surface conditions at DSDP Hole 594 in the southwest Pacific Ocean based on dinoflagellate cyst assemblages. Journal of Quaternary Science, 16(7): 739-751.
Masarik, J. and Beer, J., 1999. Simulation of particle fluxes and cosmogenic nuclide production in the earth's atmoshpere. Journal of Geophysical Research, D104(10): 12099-13012.
Mashiotta, T.A., Lea, D.W. and Spero, H.J., 1999. Glacial-interglacial changes in Subantarctic sea surface temperature and [delta]18O-water using foraminiferal Mg. Earth and Planetary Science Letters, 170(4): 417-432.
Matthiessen, J. et al., 2005. Modem organic-walled dinoflagellate cysts in arctic marine environments and their (paleo-) environmental significance. Paläontologische Zeitschrift, 79(1): 3-51.
Mayewski, P.A. et al., 2004. Holocene climate variability. Quaternary Research, 62(3): 243-255.
McManus, J.F., Francois, R., Gherardi, J.M., Keigwin, L.D. and Brown-Leger, S., 2004. Collapse and rapid resumption of Atlantic meridional circulation linked to deglacial climate changes. Nature, 428(6985): 834-837.
Milankovitch, M., 1920. Théorie Mathématique des Phénomènes Thermiques Produits par la Radiation Solaire. . Académie Yougoslave des Sciences et des Arts de Zagreb, Gauthiers-Villiers, Paris.
Milankovitch, M., 1941. Kanon der Erdbestrahlung und seine Anwendung auf das Eiszeitenproblem, 133. Academie Royale Serrbe, 633 pp.
Morey, A.E., Mix, A.C. and Pisias, N.G., 2005. Planktonic foraminiferal assemblages preserved in surface sediments correspond to multiple environment variables. Quaternary Science Reviews, 24(7-9): 925-950.
Moros, M. et al., 2004. Sea surface temperatures and ice rafting in the Holocene North Atlantic: climate influences on northern Europe and Greenland. Quaternary Science Reviews, 23(20-22): 2113-2126.
Moros, M., J. T. Andrews, D. D. Eberl, and E. Jansen, 2006. Holocene history of drift ice in the northern North Atlantic: Evidence for different spatial and temporal modes. Paleoceanography, 21(PA2017).
Moros, M., Jensen, K.G. and Kuijpers, A., 2006. Mid-to late-Holocene hydrological and climatic variability in Disko Bugt, central West Greenland. The Holocene, 16(3): 357-367.
Müller, P.J., Kirst, G., Ruhland, G., von Storch, I. and Rosell-Melé, A., 1998. Calibration of the alkenone paleotemperature index U37K' based on core-tops from the eastern South Atlantic and the global ocean (60°N-60°S). Geochimica et Cosmochimica Acta, 62(10): 1757-1772.
Murray, J., 1897. Balfour Shoal: A submarine elevation in hte Coral sea. Scottish Geographical Journal, 13(3): 120-134.
Murray, J., 1897. Balfour Shoal: A submarine elevation in hte Coral sea. Scottish Geographical Journal, 13(3): 120-134.

Muscheler, R., Beer, J. and Vonmoos, M., 2004. Causes and timing of the 8200 yr BP event inferred from the comparison of the GRIP 10Be and the tree ring [Delta]14C record. Quaternary Science Reviews, 23(20-22): 2101-2111.
Muscheler, R., Joos, F., Muller, S.A. and Snowball, I., 2005. Climate: How unusual is today's solar activity? Nature, 436(7050): E3-E4.
Neori, A. and Holm-Hansen, O., 1982. Effect on temperature on rate of photosynthesis in Antarctic phytoplankton. Polar Biology, 1: 33-38.
Nesje, A., Lie, Ø. and Dahl, S.O., 2000. Is the North Atlantic Oscillation reflected in Scandinavian glacier mass balance records? Journal of Quaternary Science, 15(6): 587-601.
Nesje, A., Matthews, J.A., Dahl, S.O., Berrisford, M.S. and Andersson, C., 2001. Holocene glacier fluctuations of Flatebreen and winter-precipitation changes in the Jostedalsbreen region, western Norvay, based on glaciolacustrine sediment records. The Holocene, 11(3): 267-280.
Nürnberg, D., Bijma, J. and Hemleben, C., 1996. Assessing the reliability of magnesium in foraminiferal calcite as a proxy for water mass temperatures. Geochimica et Cosmochimica Acta, 60(5): 803-814.
Ohkouchi, N., Eglinton, T.I., Keigwin, L.D. and Hayes, J.M., 2002. Spatial and Temporal Offsets Between Proxy Records in a Sediment Drift. Science, 298(5596): 1224-1227.
Okada, H. and Honjo, S., 1973. The distribution of oceanic coccolithophorids in the Pacific. Deep Sea Research and Oceanographic Abstracts, 20(4): 355-364, IN3-IN4, 365-374.
Oldfield, F., 2005. Environmental change: key issues and alternative perspectives. University Press, United Kingdom, Camebridge.
Oppo, D.W., McManus, J.F. and Cullen, J.L., 2003. Palaeo-oceanography: Deepwater variability in the Holocene epoch. Nature, 422(6929): 277-277.
Opsteegh, J.D., Haarsma, R.J., Selten, F.M. and Kattenberg, A., 1998. ECBILT: a dynamic alternative to mixed boundary conditions in ocean models. Tellus B, 50A: 348–367.
Perkin, R.G. and Lewis, E.L., 1984. Mixing in the West Spitsbergen Current. Journal of Physical Oceanography, 14(8): 1315-1325.
Peyron, O. and de Vernal, A., 2001. Application of artificial neural networks (ANN) to high-latitude dinocyst assemblages for the reconstruction of past sea-surface conditions in Arctic and sub-Arctic seas. Journal of Quaternary Science, 16(7): 699-709.
Pflaumann, U., Duprat, J., Pujol, C. and Labeyrie, L.D., 1996. SIMMAX: A Modern Analog Technique to Deduce Atlantic Sea Surface Temperatures from Planktonic Foraminifera in Deep-Sea Sediments. Paleoceanography, 11.
Pickart, R.S., Spall, M.A., Ribergaard, M.H., Moore, G.W.K. and Milliff, R.F., 2003. Deep convection in the Irminger Sea forced by the Greenland tip jet. Nature, 424(6945): 152-156.
Pokras, E.M. and Molfino, B., 1986. Oceanographic control of diatom abundances and species distributions in surface sediments of the tropical and southeast Atlantic. Marine Micropaleontology, 10(1-3): 165-188.
Prahl, F.G. and Wakeham, S.G., 1987. Calibration of unsaturation patterns in long-chain ketone compositions for palaeotemperature assessment. Nature, 330(6146): 367-369.
Prahl, F.G., Muehlhausen, L.A. and Zahnle, D.L., 1988. Further evaluation of long-chain alkenones as indicators of paleoceanographic conditions. Journal Name: Geochimica et Cosmochimica Acta; (USA); Journal Volume: 52:9: Medium: X; Size: Pages: 2303-2310.
Prahl, F.G., Wolfe, G.V. and Sparrow, M.A., 2003. Physiological impacts on alkenone paleothermometry. Paleoceanography, 18(2).
Prahl, F.G., Wolfe, G.V. and Sparrow, M.A., 2003. Physiological impacts on alkenone paleothermometry. Paleoceanography, 18(2).
Racca, J.M., Gregory-Eaves, I., Pienitz, R. and Prairie, Y.T., 2004. Tailoring palaeolimnological diatom-based transfer functions. Canadian Journal of Fisheries & Aquatic Sciences, 61(12): 15.
Ragueneau, O. et al., 2000. A review of the Si cycle in the modern ocean: recent progress and missing gaps in the application of biogenic opal as a paleoproductivity proxy. Global and Planetary Change, 26(4): 317-365.
Raynaud, D. et al., 2000. The ice record of greenhouse gases: a view in the context of future changes. Quaternary Science Reviews, 19(1-5): 9-17.
Renssen, H. and Goosse, H., 2006. Coupled climate model simulation of Holocene cooling events: oceanic feedback amplifies solar forcing. Climate Past, 2: 79-90.

Renssen, H. et al., 2004. Simulating the Holocene climate evolution at northern high latitudes using a coupled atmosphere-sea ice-ocean-vegetation model. Climate Dynamics, 24(1): 23-43.
Renssen, H., Brovkin, V., Fichefet, T. and Goosse, H., 2003. Holocene climate instability during the termination of the African Humid Period. Geophys. Res. Lett., 30(4): 1184.
Renssen, H., Goosse, H., Fichefet, T., Brovkin, V., Driesschaert, E., and Wolk, F. (2004). Simulating the Holocene climate evolution at northern high latitudes using a coupled atmosphere-sea ice-ocean-vegetation model. Climate Dynamics **24,** 23-43.
Rhein, M., Stramma, L. and Send, U., 1995. The Atlantic Deep Western Boundary Current: Water masses and transports near the equator. J. Geophys. Res., 100(C2): 2441-2457.
Riebesell, U., Revill, A.T., Holdsworth, D.G. and Volkman, J.K., 2000. The effects of varying CO2 concentration on lipid composition and carbon isotope fractionation in Emiliania huxleyi. Geochimica et Cosmochimica Acta, 64(24): 4179-4192.
Rimbu, N., Lohmann, G., Kim, J.H., Arz, H.W. and Schneider, R., 2003. Arctic/North Atlantic Oscillation signature in Holocene sea surface temperature trends as obtained from alkenone data. Geophys. Res. Lett., 30.
Rimbu, N., Lohmann, G., Lorenz, S.J., Kim, J.H. and Schneider, R.R., 2004. Holocene climate variability as derived from alkenone sea surface temperature and coupled ocean-atmosphere model experiments. Climate Dynamics, 23(2): 215-227.
Rind, D., 2002. The Sun's Role in Climate Variations. Science, 296(5568): 673-677.
Risebrobakken, B., Eystein, J., Andersson, C. and Eirik, M., 2003. A high-resolution study of Holocene paleoclimatic and paleoceanographic changes in the Nordic Seas. Paleoceanography, 18(1): 1017.
Rogers, J.C., 1984. The Association between the North Atlantic Oscillation and the Southern Oscillation in the Northern Hemisphere. Monthly Weather Review, 112(10): 1999-2015.
Rohling, E.J. and Palike, H., 2005. Centennial-scale climate cooling with a sudden cold event around 8,200 years ago. Nature, 434(7036): 975-979.
Rosell-Melé, A., Eglinton, G., Pflaumann, U. and Sarnthein, M., 1995. Atlantic core-top calibration of the U37K index as a sea-surface palaeotemperature indicator. Geochimica et Cosmochimica Acta, 59(15): 3099-3107.
Rosell-Melé, W.S.K.J., 1998. Variability of the Arctic front during the last climatic cycle: application of a novel molecular proxy. Terra Nova, 10(2): 86-89.
Rosenthal, Y. and Boyle, E.A., 1993. Factors controlling the fluoride content of planktonic foraminifera: An evaluation of its paleoceanographic applicability. Geochimica et Cosmochimica Acta, 57(2): 335-346.
Rosenthal, Y. and Lohmann, G.P., 2002. Accurate estimation of sea surface temperatures using dissolution-corrected calibrations for Mg/Ca paleothermometry. Paleoceanography, 17.
Rosenthal, Y., Boyle, E.A. and Slowey, N., 1997. Temperature control on the incorporation of magnesium, strontium, fluorine, and cadmium into benthic foraminiferal shells from Little Bahama Bank: Prospects for thermocline paleoceanography. Geochimica et Cosmochimica Acta, 61(17): 3633-3643.
Rosenthal, Y., Lear, C.H., Oppo, D.W. and Braddock, K.L., 2006. Temperature and carbonate ion effects on Mg/Ca and Sr/Ca ratios in benthic foraminifera: Aragonitic species *Hoeglundina elegans*. Paleoceanography, 21(PA1007).
Rossby, T., 1996. The North Atlantic Current and surrounding waters: At the crossroads. Rev. Geophys., 34(4): 463-481.
Round, F.E., Crawford, R.M. and Mann, D.G., 1990. The diatom: Biology and mofology of the genera. Press Syndicate of the University of Cambridge.
Russell, A.D., Hönisch, B., Spero, H.J. and Lea, D.W., 2004. Effects of seawater carbonate ion concentration and temperature on shell U, Mg, and Sr in cultured planktonic foraminifera. Geochimica et Cosmochimica Acta, 68(21): 4347-4361.
Sachs, H.M., Webb, T. and Clark, D.R., 1977. Paleoecological Transfer Functions. Annual Review of Earth and Planetary Sciences, 5(1): 159-178.
Sachs, J.P. et al., 2000. Alkenones as paleoceanographic proxies. Geochemistry Geophysics Geosystems, 1(2000GC000059).
Sachs, J.P., 2007. Cooling of Northwest Atlantic slope waters during the Holocene. Geophys. Res. Lett., 34(L03609).

Sadekov, A.Y., Eggins, S.M. and De Deckker, P., 2005. Characterization of Mg/Ca distributions in planktonic foraminifera species by electron microprobe mapping. Geochemistry Geophysics Geosystems, 6.
Sætre, R., 1999. Features of the central Norwegian shelf circulation. Continental Shelf Research, 19(14): 1809-1831.
Saloranta, T.M. and Haugan, P.M., 2004. Northward cooling and freshening of the warm core of the West Spitsbergen Current. Polar Research, 23(1): 79-88.
Sarnthein, M. et al., 2003. Centennial-to-millennial-scale periodicities of Holocene climate and sediment injections off the western Barents shelf, 75°N. Boreas, 32(3): 447-461.
Savin, S.M. and Douglas, R.G., 1973. Stable Isotope and Magnesium Geochemistry of Recent Planktonic Foraminifera from the South Pacific. Geological Society of America Bulletin, 84(7): 2327-2342.
Schlichtholz, P. and Houssais, M.-N.l., 1999. An Investigation of the Dynamics of the East Greenland Current in Fram Strait Based on a Simple Analytical Model. Journal of Physical Oceanography, 29(9): 2240-2265.
Schmidt, D.N., Renaud, S., Bollmann, J., Schiebel, R. and Thierstein, H.R., 2004. Size distribution of Holocene planktic foraminifer assemblages: biogeography, ecology and adaptation. Marine Micropaleontology, 50(3-4): 319-338.
Schouten, S., Forster, A., Panoto, F.E. and Sinninghe Damsté, J.S., 2007. Towards calibration of the TEX86 palaeothermometer for tropical sea surface temperatures in ancient greenhouse worlds. Organic Geochemistry, 38(9): 1537-1546.
Schrader, H.-J., 1971. Fecal Pellets: Role in Sedimentation of Pelagic Diatoms. Science, 174(4004): 55-57.
Schulz, H.-M., Schöner, A. and Emeis, K.-C., 2000. Long-chain alkenone patterns in the Baltic sea--an ocean-freshwater transition. Geochimica et Cosmochimica Acta, 64(3): 469-477.
Schulz, M., Paul, A. and Timmermann, A., 2004. Glacial-interglacial contrast in climate variability at centennial-to-millennial timescales: observations and conceptual model. Quaternary Science Reviews, 23(20-22): 2219-2230.
Schulz, M., Prange, M. and Klocker, A., 2007. Low-frequency oscillations of the Atlantic Ocean meridional overturning circulation in coupled climate model. Climate of the Past, 3: 97-107.
Schwander, J., Eicher, U. and Ammann, B., 2000. Oxygen isotopes of lake marl at Gerzensee and Leysin (Switzerland), covering the Younger Dryas and two minor oscillations, and their correlation to the GRIP ice core. Palaeogeography, Palaeoclimatology, Palaeoecology, 159(3-4): 203-214.
Shemesh, A., Burckle, L.H. and Froelich, P.N., 1989. Dissolution and preservation of Antarctic diatoms and the effect on sediment thanatocoenoses. Quaternary Research, 31(2): 288-308.
Sherwin, T.J., Turrell, W.R., Jeans, D.R.G. and Dye, S., 1999. Eddies and a mesoscale deflection of the slope current in the Faroe-Shetland Channel. Deep Sea Research Part I: Oceanographic Research Papers, 46(3): 415-438.
Siegenthaler, U. and Sarmineto, J.L., 1993. Atmospheric carbon dioxide and the ocean. Nature, 365: 119-125.
Sikes, E.L. and Volkman, J.K., 1993. Calibration of alkenone unsaturation ratios (Uk'37) for paleotemperature estimation in cold polar waters. Geochimica et Cosmochimica Acta, 57(8): 1883-1889.
Simonsen, R., 1979. The diatom system: ideas on phylogeny, Bacillaria, pp. 9-71.
Simonsen, R., 1979. The diatom system: ideas on phylogeny, Bacillaria, pp. 9-71.
Skinner, L.C. and Elderfield, H., 2005. Constraining ecological and biological bias in planktonic foraminiferal Mg/Ca and δ18Occ: A multispecies approach to proxy calibration testing. Paleoceanography, 20(1): PA1015.
Smetacek, V.S., 1985. Role of sinking in diatom life-history cycles: ecological, evolutionary and geological significance. Marine Biology, 84(3): 239-251.
Smetacek, V.S., 1985. Role of sinking in diatom life-history cycles: ecological, evolutionary and geological significance. Marine Biology, 84(3): 239-251.
Smtih, E.H., Soule, F.M. and Mosby, O., 1937. The Marion and General Green expeditions to Davis Strait and the Labrador Sea. Bull. U.S. Coast Guard, 19: 259.
Solignac, S. et al., 2008. Reorganization of the upper ocean circulation in the mid-Holocene in the

northeastern Atlantic. Canadian Journal of Earth Sciences, 45: 1417-1433.
Solignac, S., de Vernal, A. and Giraudeau, J., 2006. Changes of mixed-layer depth and upper water column stratification during the Holocene in the eastern North Atlantic, Fall meeting 2006. American Geophysical Union.
Solignac, S., de Vernal, A. and Hillaire-Marcel, C., 2004. Holocene sea-surface conditions in the North Atlantic--contrasted trends and regimes in the western and eastern sectors (Labrador Sea vs. Iceland Basin). Quaternary Science Reviews, 23(3-4): 319-334.
Sournia, A., 1995. Red tide and toxic marine phytoplankton of the world ocean: An inquiry into biodiversity. In: P. Lassus, G. Arzul, E. Erard, P. Gentien & B. Marcaillou (Eds). Harmful marine algal blooms: 103-112.
Steinhilber, F., Beer, J. and Fröhlich, C., 2009. Total solar irradiance during the Holocene. Geophys. Res. Lett., 36(L19704).
Stott, L. et al., 2004. Decline of surface temperature and salinity in the western tropical Pacific Ocean in the Holocene epoch. Nature, 431(7004): 56-59.
Stuiver, M. and Braziunas, T.F., 1993. Sun, ocean, climate and atmospheric $^{14}CO_2$ : an evaluation of causal and spectral relationships. The Holocene, 3(4): 289-305.
Stuiver, M., Braziunas, T.F., Becker, B. and Kromer, B., 1991. Climatic, solar, oceanic, and geomagnetic influences on late-glacial and holocene atmospheric 14C/12C change. Quaternary Research, 35(1): 1-24.
Taylor, K.C. et al., 1997. The Holocene-Younger Dryas Transition Recorded at Summit, Greenland. Science, 278(5339): 825-827.
Teece, M.A., Getliff, J.M., Leftley, J.W., Parkes, R.J. and Maxwell, J.R., 1998. Microbial degradation of the marine prymnesiophyte Emiliania huxleyi under oxic and anoxic conditions as a model for early diagenesis: long chain alkadienes, alkenones and alkyl alkenoates. Organic Geochemistry, 29(4): 863-880.
ter Braak, C.J.F. and Prentice, I.C., 1988. A theory of gradient analysis. Advances in ecological research, 18: 271-317.
ter Braak, C.J.F. and Prentice, I.C., 1988. A theory of gradient analysis. Advances in ecological research, 18: 271-317.
ter Braak, C.J.F., 1985. Correspondence Analysis of Incidence and Abundance Data: Properties in Terms of a Unimodal Response Model. Biometrics, 41(4): 859-873.
ter Braak, C.J.F., 1986. Canonical Correspondence Analysis: A New Eigenvector Technique for Multivariate Direct Gradient Analysis. Ecology, 67(5): 1167-1179.
ter Braak, C.J.F., 1987. The analysis of vegetation-environment relationships by canonical correspondence analysis. Plant Ecology, 69(1): 69-77.
Thomsen, C., Schulz-Bull, D.E., Petrick, G. and Duinker, J.C., 1998. Seasonal variability of the long-chain alkenone flux and the effect on the U37k'-index in the Norwegian Sea. Organic Geochemistry, 28(5): 311-323.
van Klinken, G.J. and Hedges, R.E.M., 1998. Chemistry strategies for organic $^{14}C$ samples = Stratégies chimiques pour les échantillons de $^{14}C$ organiques. Radiocarbon, 401-2: 51-56.
Versteegh, G.J.M. and Blokker, P., 2004. Resistant macromolecules of extant and fossil microalgae. Phycological Research, 52(4): 325-339.
Viau, A.E., Gajewski, K., Fines, P., Atkinson, D.E. and Sawada, M.C., 2002. Widespread evidence of 1500 yr climate variability in North America during the past 14â€Š000 yr. Geology, 30(5): 455-458.
Vink, A., 2004. Calcareous dinoflagellate cysts in South and equatorial Atlantic surface sediments: diversity, distribution, ecology and potential for palaeoenvironmental reconstruction. Marine Micropaleontology, 50(1-2): 43-88.
Vink, A., Brune, A., Holl, C., Zonneveld, K.A.F. and Willems, H., 2002. On the response of calcareous dinoflagellates to oligotrophy and stratification of the upper water column in the equatorial Atlantic Ocean Palaeogeography, Palaeoclimatology, Palaeoecology 178(1-2): 53-66.
Volkman, J.K., Eglinton, G., Corner, E.D.S. and Sargent, J.R., 1980. Novel unsaturated straight chain $C_{37}$-$C_{39}$ methyl and ethyl ketones in marine sediments and coccolithophore *Emiliana huxleyi*. In: A.G. Douglas & J. R. Maxwell (Eds). Advances in organic chemistry 1979: 219-227.
Vonmoos, M., Beer, J. and Muscheler, R., 2006. Large variations in Holocene solar activity: Constraints from $^{10}Be$ in the Greenland Ice Cor Project ice cor. Journal of Geophysical Research, 111(A10105).

Voronina, E., Polyak, L., Vernal, A.D. and Peyron, O., 2001. Holocene variations of sea-surface conditions in the southeastern Barents Sea, reconstructed from dinoflagellate cyst assemblages. Journal of Quaternary Science, 16(7): 717-726.
Waelbroeck, C. et al., 1998. Improving Past Sea Surface Temperature Estimates Based on Planktonic Fossil Faunas. Paleoceanography, 13.
Walczak, B. and Wegscheider, W., 1994. Calibration of non-linear analytical systems by a Neuro-Fuzzy approach. Chemometrics and Intelligent Laboratory Systems, 22: 199-207.
Wang, G., Eltahir, E.A.B., Foley, J.A., Pollard, D. and Levis, S., 2004. Decadal variability of rainfall in the Sahel: results from the coupled GENESIS-IBIS atmosphere-biosphere model. Climate Dynamics, 22(6): 625-637.
Webb, T. and Bryson, R.A., 1972. Late- and postglacial climatic change in the northern Midwest, USA: Quantitative estimates derived from fossil pollen spectra by multivariate statistical analysis. Quaternary Research, 2(1): 70-115.
Weber, S.L. and Oerlemans, J., 2003. Holocene glacier variability: three case studies using an intermediate-complexity climate model. The Holocene, 13(3): 353-363.
Weber, S.L., 2001. The impact of orbital forcing on the climate of an intermediate-complexity coupled model. Global and Planetary Change, 30(1-2): 7-12.
Weber, S.L., Crowley, T.J. and der Schrier, G., 2004. Solar irradiance forcing of centennial climate variability during the Holocene. Climate Dynamics, 22(5): 539-553.
Weldeab, S., Schneider, R. and Müller, P.J., 2007. Comparison of Mg/Ca- and alkenone-based sea surface temperature estimates in the fresh water–influenced Gulf of Guinea, eastern equatorial Atlantic. Geochemistry Geophysics Geosystems, 8(5): 10.
Wenn J.H. (eds), *Neogene and Quaternary dinoflagellate cysts and acritarchs*: 289-328. Publishers Press.
Wilkes, C., 1859. On the circulation of the oceans. University Microfilms.
Winter, A., Jordan, R.A. and Roth, P., 1994. Biogeography of living coccolithophores in ocean waters. In: A. Winter and W.G. Sieser, Editors, *Coccolithophores*, Cambridge University Press
Wood, R.A., Keen, A.B., Mitchell, J.F.B. and Gregory, J.M., 1999. Changing spatial structure of the thermohaline circulation in response to atmospheric CO2 forcing in a climatemodel. Nature, 399: 572-575.
Woodgate, R.A., Fahrbach, E. and Rohardt, G., 1999. Structure and transports of the East Greenland Current at 75°N from moored current meters. J. Geophys. Res., 104(C8): 18059-18072.

## Appendix 1: Abbreviations

AAIW : Antarctic Intermediate Waters

AABW : Antarctic Bottom Water

AGCM : atmosphere general circulation models

AHP = African Humid Period

Alk = alkenones

AMS : accelerator mass spectrometry

ANN : artificial neural networks

AO: Arctic Oscillation

C4MIP : Coupled Carbon Cycle Climate Model Intercomparison Project

CA : correspondence analysis

CCA : canonical correlation analysis

CCD : calcite compensation depth

CLIMAP : Climate Mapping, Analysis and Prediction

COHMAP : Co-operative Holocene Mapping Project

DACP = Dark Ages Cold Period

Dia = diatoms

DIC : dissolved inorganic carbon

Din = dinocysts

EH = Early Holocene (11,5-9,5 ka BP)

EMIC: Earth system Model of Intermediate Complexity

ENSO : El Niño/La Niña-Southern Oscillation

GCM: Global Circulation Model

GIN : Greenland-Iceland-Norwegian

GIN: Greenland Iceland Norway

HTM = Holocene Thermal Maximum

IPCC : Intergovernmental Panel on Climate Change

IRD : ice rafted debris

IRD: Ice Rafted Debris

Latest Holocene (2,5-0 ka BP)

LGM : Last Glacial Maximum

LH = Late Holocene (5,5-0 ka BP)

LIA = Little Ice Age

LICP = Late Iron Cold Period

LIS: Laurentide Ice Sheet

LSW: Labrador Sea Water

MAT : modern analogue technique

MC = Mg/Ca

MH = Mid Holocene (9,5-5 ka BP)

MOC: Meridional Overturning Circulation

MOW : Mediterranean Overflow Water

MWP = Medieval Warm Period

NADW : North Atlantic Deep Water

NAO: North Atlantic Oscillation

NBS : National Bureau of Standards

OA model: Ocean-Atmosphere model

OAV model: Ocean-Atmosphere-Vegetation model

OGCM : ocean general circulation models

PCA : principal component analysis

PDB : Pee Dee Belemnite carbonate

PF = planktonic foraminifera

PLS : partial least square analysis

PMIP 1: Paleoclimate Modeling Intercomparison Project (Phase I)

PMIP 2: Paleoclimate Modeling Intercomparison Project (Phase II)

PSS :Practical Salinity Scale

RAM : revised analogue method

RSAT : response surface analogue technique (

RWP = Roman Warm Period

S = summer

SIMMAX : similarity maximum

SMOW : Standard Mean Ocean Water

Solar activity:

SSS: Sea Surface Salinity

SST: Sea Surface Temperature

SST: Sea Surface Temperatures

THC: thermohaline circulation

TSI: Total Solar Irradiance

TSI: Total Solar Irradiance

W = winter

WA-PLS : Weighted averaging partial least squares regression

YD = Younger Dryas

**Ocean Currents**

AnC = Angola Current

AzC = Azores Current

BB & BC = Baffin Bay & Baffin Current

BeC = Benguela Current

BrC = Brazil Current

CanC = Canary Current

CarC = Caribbean Current

DWBC = Deep Western Boundary Current

EGC = East Greenland Current

EIC = East Icelandic Current

EM = East Mediterranean Sea

GOM = Gulf of Mexico

GS = Gulf Stream

GuiC = Guinea Current

GuyC = Guyana Current

HB = Hudson Bay

IrC = Irminger Current

LaC = Labrador Current

LoC = Loop Current

MC = Murman Current

NAC = North Atlantic Current

NAD = North Atlantic Drift

NBC = North Brazil Current

NC = Norwegian Current

NCC = North Cape Current

NIC = North Iceland Current

North Atlantic Drift Current (NADC)

NS = North Sea

PC = Portugal Current

PML = Polar Mixed Layer

SC = Slope Current

SEC = South Equatorial Current

SECC = South Equatorial Counter Current

WGC = West Greenland Current

WM = West Mediterranean Sea

WSC = West Spitsbergen Current

# Appendix 2: Data tables

| ALKENONES | | | | | | | | | | | |
|---|---|---|---|---|---|---|---|---|---|---|---|
| Region | Lon | Lat | Depth(m) | Core name | Resolution | Season | Reference article(s) | Reference database | Calibration method | Time Span | Remarks |
| Central South Atlantic | 8,80 | -41,31 | 4981 | TN057-21PC | High | Annual | Pahnke and Sachs, 2006<br>Sachs and Anderson, 2003 | Leduc et al., 2010 (PANGAEA) | Prahl et al. (1988) | ~6-10 ka BP | |
| Cape Basin (Namibia coast) | 12,77 | -24,11 | 1821 | IOW226660-5 (G660) | Low | Annual | Mollenhauer et al., 2003 | Mollenhauer, 2002b (PANGAEA) | Prahl et al. (1988) | ~1-12 ka | Not calibrated |
| Cape Basin (Namibia coast) | 11,70 | -23,43 | 2987 | GeoB1710-3 | Very low | Annual | Kirst et al., 1999 | Kirst & Müller, 2001b (PANGAEA) | Prahl et al. (1988) | ~2,5-12 ka BP | |
| Cape Basin (Namibia coast) | 12,38 | -23,32 | 1967 | GeoB1711-4 | Low | Annual | Kirst et al., 1999 | Kirst & Müller, 2001a (PANGAEA) | Prahl et al. (1988) | Holocene | |
| Cape Basin (Namibia coast) | 12,81 | -23,26 | 998 | GeoB1712-4 | Low | Annual | Kirst et al., 1999 | Kirst & Müller, 2001c (PANGAEA) | Prahl et al. (1988) | ~2-12 ka BP | |
| Cape Basin (Namibia coast) | 12,36 | -22,45 | 1683 | IOW226920-3 (G920) | Low | Annual | Mollenhauer et al., 2003 | Mollenhauer, 2002a (PANGAEA) | Prahl et al. (1988) | ~0,5-11,5 ka | Not calibrated |
| Cape Basin (Namibia coast) | 9,19 | -20,10 | 2209 | GeoB10285 | Very low | Annual | Schneider et al., 1995(NP) | Schneider, 2005c (WDCP-A) | Prahl et al. (1988) | ~3-12 ka BP | |
| Angola Basin | 11,01 | -17,16 | 1978 | GeoB1023-5 | Intermediate | Annual | Kim et al., 2002<br>Schefuss et al., 2005 | Kim, 2002 (PANGAEA) | Müller et al. (1998) | Holocene | |
| Central South Atlantic Ridge | -23,00 | 0,00 | 3870 | 86014-12PC51 | Very low | Annual | Sikes and Keigwin, 1994 (NP) | Sikes, 1994 (PANGAEA) | Prahl et al. (1988) | ~7-12 ka | Not calibrated |
| Guinea Basin | 9,39 | 2,50 | 1328 | GeoB4905-4 | Intermediate | Annual | Weldeab et al., 2007 | Weldeab, 2006b (PANGAEA) | Müller et al. (1998) | Holocene | River |
| Angola Basin | 11,22 | -5,59 | 962 | GeoB6518-1 | High | Annual | Schefuss et al., 2005 | Schefuss, 2005 (PANGAEA) | Müller et al. (1998) | Holocene | River |
| Angola Basin | 10,32 | -6,58 | 3124 | GeoB10083 | Very low | Annual | Schneider et al., 1995(NP) | Schneider, 2005a (WDCP-A) | Prahl et al. (1988) | Holocene | |
| Angola Basin | 11,68 | -11,77 | 3411 | GeoB1016-3 | Very low | Annual | Müller et al., 1994 (NP)<br>Andersen et al., 1999 | Müller & Schneider, 1998 (PANGAEA) | Prahl et al. (1988) | ~1,5-12 ka BP | |
| Angola Basin | 13,40 | -11,92 | 426 | 175-1078C | Intermediate | Annual | Kim et al., 2003 | Leduc et al., 2010 (PANGAEA) | Müller et al., 1998 | ~0-10,5 ka BP | |
| Brazil Basin | -36,35 | -4,25 | 2362 | GeoB3910-2 | Low | Annual | Jaescke et al., 2007 (NP) | Jaeschke et al., 2007 (PANGAEA) | Prahl et al. (1988) | ~1,5-12 ka BP | |
| Brazil Basin | -36,64 | -4,61 | 830 | GeoB3129-1 | Intermediate | Annual | Leduc et al., 2010 | Leduc et al., 2010 (PANGAEA) | Prahl et al. (1988) | ~0-10,5 ka BP | |
| Caribbean Sea | -61,24 | 12,09 | 1299 | M35003-4 | Intermediate | Annual | Ruhlemann et al., 1999 | Rühlemann, 2006 (PANGAEA) | Müller et al. (1998) | Holocene | River |
| Caribbean Sea | -65,17 | 10,71 | 893 | ODP 1002C | Low | Annual | Herbert & Schuffert, 2000<br>Peterson et al., 2000 | Kim et al., 2004 (GHOST Project) | Prahl et al. (1988) | ~0,5-11 ka BP | |
| Gulf of Mexico | -91,41 | 27,19 | 2259 | 96-619 | Very low | Annual | Jasper & Gagosian, 1989 (NP) | Leduc et al., 2010 (PANGAEA) | Prahl & Wakeham (1987) | ~1,5-8,5 ka BP | |
| NW Atlantic (Blake Ridge) | -75,42 | 31,67 | 2975 | KNR140-39GGC | Low | Annual | Kneeland et al., 2004 | Kneeland et al., 2004 (Thesis) | Prahl et al. (1988) | ~1,5-12 ka BP | |
| NW Atlantic (Carolina Slope) | -76,29 | 32,78 | 1790 | KNR140-51GGC | High | Annual | Kneeland et al., 2004 | Kneeland et al., 2004 (Thesis) | Prahl et al. (1988) | ~0-9,5 ka BP | |
| NW Atlantic (Virginia Slope) | -74,57 | 36,87 | 1049 | CH07-98-GGC19 | High | Annual | Sachs, 2007 | Sachs et al., 2007 (Pers comm) | Prahl et al. (1988) | ~0,5-12 ka BP | |
| Azores Plateau | -32,96 | 41,00 | 3413 | 306-U1313B | Very low | Annual | Stein et al., 2009 | Stein et al., 2009 (PANGAEA) | Müller et al. (1998) | ~2,5-12 ka BP | |

| | | | | | | | | | | | |
|---|---|---|---|---|---|---|---|---|---|---|---|
| Iberian Sea | -9,86 | 40,58 | 2465 | MD95-2040 | Low | Annual | Pailler and Bard, 2002 | Pailler & Bard, 2003a (PANGAEA) | Prahl et al. (1988) | ~0,5-12 ka BP | |
| Iberian Sea | -9,51 | 38,63 | 102 | GeoB8903-1 | Very high | Annual | Alt-Epping, 2008 (NP) | Alt-Epping, 2009 (WDCP-A) | ? | ~0-2,5 ka BP | River |
| Iberian Sea | -9,45 | 38,63 | 85 | D13882 | High | Annual | Rodrigues et al., 2009 | Leduc et al., 2010 (PANGAEA) | Müller et al., 1998 | ~0,5-10,5 | River |
| Iberian Sea | -10,18 | 37,88 | 2925 | MD01-2443 | High | Annual | Martrat et al., 2007 | Leduc et al., 2010 (PANGAEA) | Müller et al., 1998 | ~0-10,5 | |
| Iberian Sea | -10,17 | 37,80 | 3146 | MD95-2042 | Intermediate | Annual | Pailler and Bard, 2002 | Pailler & Bard, 2003b (PANGAEA) | Prahl et al. (1988) | ~0,5-12 ka BP | |
| Iberian Sea | -10,18 | 37,77 | 3155 | SU81-18 | Low | Annual | Bard et al., 2000 | Bard, 2006 (PANGAEA) | 3 methods | ~0,5-12 ka BP | |
| Iberian Sea (Gibraltar) | -7,07 | 36,38 | 574 | GeoB5901-2 | Very high | Annual | Kim et al., 2004 | Kim & Rühlemann, 2006 (PANGAEA) | Prahl et al. (1988) | ~1-10 ka BP | Gibraltar |
| Iberian Sea (Gibraltar) | -7,07 | 36,38 | 577 | M39008-3 | High | Annual | Cacho et al., 2001(NP) | Cacho & Grimalt, 2006a (PANGAEA) | Müller et al. (1998) | ~1,5-11,5 ka BP | Gibraltar |
| Mediterranean Sea (Gibraltar) | -2,62 | 36,14 | 1841 | MD95-2043 | High | Annual | Cacho et al., 2001(NP) | Cacho & Grimalt, 2006b (PANGAEA) | Müller et al. (1998) | ~1-11,5 ka BP | |
| Mediterranean Sea (Gibraltar) | -1,96 | 36,03 | 1984 | 161-977 | Very low | Annual | Martrat et al., 2004 | Leduc et al., 2010 (PANGAEA) | Müller et al., 1998 | ~0-10,5 | |
| Mediterranean Sea | 4,02 | 38,99 | 1897 | M40/4 SL87 | Very low | Annual | Emeis et al., 2003(NP) | Leduc et al., 2010 (PANGAEA) | Müller et al., 1998 | ~0,5-10 | |
| Mediterranean Sea | 11,67 | 36,95 | 771 | MD04-2797 CQ | Intermediate | Annual | Essallami et al., 2007 (NP); Rouis-Zargouni et al., 2009 | NP | ? | ~0,5-12 ka BP | |
| Mediterranean Sea | 13,19 | 37,04 | 467 | M40-4-SL78 | High | Annual | Emeis et al., 2003(NP) | Emeis et al., 2006c (PANGAEA) | Müller et al. (1998) | Holocene | |
| Mediterranean Sea | 13,58 | 38,41 | 1489 | BS79-38 | Intermediate | Annual | Cacho et al., 2001 | Cacho & Grimalt, 2006c (PANGAEA) | Müller et al. (1998) | ~1-11,5 ka BP | |
| Mediterranean Sea | 14,03 | 38,26 | 1282 | BS79-33 | Low | Annual | Cacho et al., 2001 | Cacho & Grimalt, 2006d (PANGAEA) | Müller et al. (1998) | ~1-11 ka BP | |
| Mediterranean Sea | 15,67 | 42,67 | 77 | RF 93-30 | Intermediate | Annual | Oldfield et al., 2003 | NP | Müller et al. (1998) | ~0-7 ka BP | Adriatic Sea |
| Mediterranean Sea | 17,72 | 36,75 | 3376 | RL 11 | Intermediate | Annual | Emeis et al., 2000 | Kim et al., 2004 (GHOST Project) | Müller et al. (1998) | Holocene | |
| Mediterranean Sea | 17,74 | 36,25 | 3640 | KC01 | High | Annual | Doose, 1999 (NP) | Doose et al., 2001a (PANGAEA) | Prahl & Wakeham (1987) | 7-8,2 ka | Not calibrated |
| Mediterrenea Sea | 18,64 | 40,87 | 844 | AD91-17 | Intermediate | Annual | Giunta et al., 2001(NP) | Kim et al., 2004 (GHOST Project) | Müller et al. (1998) | ~2-11,5 ka BP Hyat: 9-11 ka BP | Adriatic Sea |
| Mediterrenea Sea | 23,19 | 34,81 | ? | M40/4 SL71 | Very low | Annual | Emeis et al., 2003(NP) | Leduc et al., 2010 (PANGAEA) | Müller et al. (1998) | ~3,5-9,5 | |
| Mediterrenea Sea | 24,88 | 33,84 | 2201 | 160-969E | Intermediate | Annual | Emeis et al., 2003)(NP) | Leduc et al., 2010 (PANGAEA) | Müller et al. (1998) | ~5-10,5 | |
| Mediterrenea Sea | 27,01 | 36,65 | 505 | NS-14 | High | Annual | Triantaphyllou et al., 2009 | NP | Müller et al. (1998) | ~3-12 ka BP | |
| Mediterrenea Sea | 27,30 | 34,81 | 2157 | M40/4 SL67 | Very low | Annual | Emeis et al., 2003(NP) | Leduc et al., 2010 (PANGAEA) | Müller et al. (1998) | ~3-9,5 ka BP | |
| Marmara Sea | 27,76 | 40,84 | 566 | M44/1 KL71 | Intermediate | Annual | Sperling et al., 2003 | Kim et al., 2004 (GHOST Project) | Müller et al. (1998) | Holocene | Bosporus |
| Marmara Sea | 28,77 | 40,78 | 1142 | M44/1 74KL | Intermediate | Annual | Kim et al., 2004 | Leduc et al., 2010 (PANGAEA) | Prahl et al. (1988) | ~0-10,5 | Bosporus |
| Mediterranean Sea | 32,71 | 33,68 | 882 | KC20B | Intermediate | Annual | Doose, 1999 (NP) | Doose et al., 2001b (PANGAEA) | Prahl & Wakeham (1987) | 8,4-9,7 ka | Not calibrated |

| | | | | | | | | | | | |
|---|---|---|---|---|---|---|---|---|---|---|---|
| Mediterranean Sea | 32,73 | 34,07 | 2551 | ODP 967D | High | Annual | Emeis et al., 2000 | Kim et al., 2004 (GHOST Project) | Müller et al. (1998) | ~0-7 ka BP | |
| Mediterranean Sea | 34,07 | 31,65 | 562 | GeoB7702-3 | Intermediate | Annual | Castenada et al., 2010 | NP | Prahl et al. (1988) | Holocene | River |
| Canary Basin | -10,10 | 30,85 | 355 | GeoB6008-1 | Very high | Annual | McGregor et al., 2007 | McGregor et al., 2007 (PANGAEA) | Prahl et al. (1988) | ~0-2,5 ka BP | |
| Canary Basin | -10,27 | 30,85 | 900 | GeoB6007-2 | Very high | Annual | Kim et al., 2007 | Leduc et al., 2010 (PANGAEA) | Müller et al. (1998) | ~0-10,5 | |
| Canary Basin | -13,74 | 27,54 | 1172 | GeoB5546-2 | Intermediate | Annual | Freudental, unpublished | Leduc et al., 2010 (PANGAEA) | Prahl et al. (1988) | ~3-10,5 | |
| Canary Basin | -18,58 | 20,75 | 2262,9 | ODP 658C | High | Annual | Zhao et al., 1995(NP) deMenocal et al., 2000 | Kim et al., 2004 (GHOST Project) | Prahl et al. (1988) | Holocene | |
| Canary Basin | -18,45 | 20,21 | 2500 | GeoB7926-2 | Low | Annual | Romero et al., 2008 | Romero, 2008 (PANGAEA) | Müller et al. (1998) | Holocene | |
| Canary Basin | -20,16 | 19,00 | 3300 | BOFS31/1K | Low | Annual | Zhao et al., 1995(NP) Chapman et al., 1996(NP) | Zhao et al., 1997 (PANGAEA) | Prahl et al. (1988) | ~0,5-12 ka BP | |
| Canary Basin | -17,95 | 15,50 | 2384 | GeoB9508-5 | Low | Annual | Niedermeyer et al., 2009 | Niedermeyer et al., 2010 (PANGAEA) | Prahl & Wakeham (1987) | ~1,5-12 ka BP | |
| Iceland Basin (Reykjanes Ridge) | -25,96 | 58,76 | 2630 | MD95-2015 | High | Annual | Marchal et al., 2002 | Grimalt & Marchal, 2006 (PANGAEA) | Prahl et al. (1988) | ~0,5-11 ka BP | |
| Icelandic Shelf | -17,96 | 67,00 | 420 | JR51-GC35 | High | Annual | Bendle et al., 2007 | Leduc et al., 2010 (PANGAEA) | Müller et al. (1998) | ~0-10 ka BP | Glaciers |
| Icelandic Shelf | -17,68 | 66,55 | 470 | MD99-2275 | Very high | Annual | (Sicre et al., 2008) | NP | Prahl et al. (1988) | ~0-4,5 ka BP | Glaciers |
| Rockall Rise | -16,52 | 57,31 | 1135 | ODP982A | Very low | Annual | (Lawrence et al., 2009) | Lawrence, 2009 (WDCP-A) | ? | Holocene | |
| North Sea | 7,09 | 57,67 | 293 | IOW225517 | High | Annual | (Emeis et al., 2003)(NP) | Emeis et al., 2006a (PANGAEA) | Müller et al. (1998) | ~2-11,5 ka BP | |
| North Sea | 8,70 | 57,84 | 420 | IOW225514 | Very high | Annual | (Emeis et al., 2003)(NP) | Emeis et al., 2006b (PANGAEA) | Müller et al. (1998) | ~0,5-6,5 ka BP | |
| Norwegian Sea | 7,64 | 66,97 | 1048 | MD95-2011 | Very high | Annual | (Calvo et al., 2002) | Grimalt & Calvo., 2006 (PANGAEA) | Prahl et al. (1988) | ~0,5-8,5 ka BP | |
| Arctic Sea | 13,97 | 75,00 | 1768 | GIK23258-2 | Low | Annual | (Marchal et al., 2002) (Sarnthein et al., 2003) | Kim et al., 2004 (GHOST Project) | Rosell-Melé et al. (1995) | ~1-9 ka BP | |
| NW Atlantic (Laurentian Fan) | -54,87 | 43,48 | 3975 | OCE326-GGC26 | High | Annual | (Sachs, 2007) | Sachs et al., 2007 (Pers comm) | Prahl et al. (1988) | Holocene | River |
| NW Atlantic (Emerald Basin) | -62,80 | 43,88 | 250 | OCE326-GGC30 | High | Annual | (Sachs, 2007) | (Sachs, 2010) (Pers comm) | Prahl et al. (1988) | Holocene | River |

| Mg/Ca | | | | | | | | | | | |
|---|---|---|---|---|---|---|---|---|---|---|---|
| **Region** | **Lon** | **Lat** | **Depth(m)** | **Core number** | **Resolution** | **Season** | **Reference article(s)** | **Reference database** | **Calibration method** | **Time span** | **Remarks** |
| Cape Basin (west of South Africa) | 13,03 | -30,51 | 1992 | ODP1084B | High | Annual | Farmer et al., 2005 | Farmer et al., 200 (WDCP-A) | Mashiotta et al. (1999) on G. Bulloides | Holocene | |
| Southern Mid Atlantic Ridge | -10,75 | -5,77 | 3122 | GeoB1112-4 | Very low | Annual | (Nürnberg et al., 2000)(NP) | Nürnberg et al., 2000 (WDCP-A& PANGAEA) | Nägler et al. (2000) & Hippler et al. (2003) G. Sacculifer | 1-12 ka BP | |
| Southern Mid Atlantic Ridge | -12,43 | -1,67 | 3225 | Core1105-3/4 | Very low | Annual | (Nürnberg et al., 2000)(NP) | Nürnberg et al., 2000 (WDC-P & PANGAEA) | Nägler et al. (2000) & Hippler et al. (2003 G. Sacculifer | Holocene | |
| Guinea Basin | 9,39 | 2,50 | 1328 | GeoB4905-4 | Intermediate | Annual | (Weldeab et al., 2005) (Weldeab et al., 2007) | Weldeab, 2006b (PANGAEA) | Anand et al. (2003) on G. Ruber | Holocene | River |
| Guinea Basin | 9,39 | 2,50 | 1295 | MD03-2707 | Very high | Annual | (Weldeab et al., 2007) | NP | Dekens et al. (2002) on G.Ruber | Holocene | River |
| Brazil Basin (coast) | -36,64 | -4,61 | 830 | GeoB3129-1 | High | Annual | (Weldeab et al., 2006) | Weldeab, 2006a (PANGAEA) | Anand et al. (2003) on G. Ruber | Holocene | |
| Caribbean Sea (Cariaco Basin) | -65,94 | 10,70 | 790 | PL07-39PC | High | Annual | (Lea et al., 2003) | Lea, 2005 (WDCP-A) | Dekens et al. (2002) on G.Ruber | Holocene | |
| Caribbean Sea | -78,68 | 11,93 | 3623 | V28-122 | Low | Annual | (Schmidt et al., 2004) | Schmidt, 2004a (PANGAEA) | Dekens et al. (2002) on G.Ruber | 3-12 ka BP | |
| Caribbean Sea | -78,74 | 12,74 | 2828 | 165-999A | Low | Annual | (Schmidt et al., 2004) | Schmidt, 2004b (PANGAEA) | Dekens et al. (2002) on G.Ruber | 3-12 ka BP | |
| Gulf of Mexico | -91,36 | 26,94 | 2248 | MD02-2550 | Very high | Annual | LoDico et al., 2006 | NP | Anand et al. (2003) on G. Ruber | 7-10,5 ka BP | |
| Gulf of Mexico | -91,41 | 27,19 | 2259 | PBBC-1 | Very high | Annual | Richey et al., 2007 | Richey (pers comm) | Anand et al. (2003) on G. Ruber | 0-1,5 ka BP | |
| Gulf of Mexico | -91,33 | 26,95 | 2280 | EN32-PC6 | Intermediate | Annual | Flower et al., 2004 | Flower (pers comm) | Dekens et al. (2002) on G.Ruber | 8-12 ka BP | |
| Gulf of Mexico | -87,12 | 29,00 | 847 | MD02-2575 | Intermediate | Annual | (Ziegler et al., 2008) | Ziegler et al., 2008 (PANGAEA) | ? on G. Ruber | 1-12 ka BP | River |
| Bermuda Rise | -57,61 | 33,69 | 4417 | Hudson89 038-BC004 | High | Annual | (Sikes and Keigwin, 1996) | Keigwin, 1996 (WDCP-A) | ? on G. Ruber | 0-3 ka BP | |
| Chesapekae Bay | -76,39 | 38,88 | 26 | MD99-2209 | Very high | Annual | (Cronin et al., 2003) | Cronin et al., 2003 | ? on Loxoconcha | ~0-2,2 ka BP | |
| Iberian Sea | -10,17 | 37,80 | 3166 | MD99-2334 | Low | Annual | (Skinner and Elderfield, 2005) | Leduc et al., 2010 (PANGAEA) | Elderfield & Ganssen, 2000 | ~0-10 ka BP | |
| Canary Basin | -20,16 | 19,00 | 3300 | BOFS31/1K | Very low | Annual | (Elderfield and Ganssen, 2000) | Not Available | This study G. Ruber, N. Pachyderma, G. Bulloides | Holocene | |
| Iceland Basin (Reykjanes Ridge) | -27,91 | 57,45 | 2620 | MD99-2251 | Very high | Annual | Farmer et al., 2008 | Leduc et al., 2010 (PANGAEA) | Barker & Elderfield, 2002 | ~0,5-10,5 | |
| Iceland Basin (Reykjanes Ridge) | -24,08 | 61,43 | 1648 | 162-984 | High | Annual | Came et al., 2004 | Leduc et al., 2010 (PANGAEA) | Von Langen et al. (2005) N. Pachyderma | Holocene | |
| Iceland Basin (Reykjanes Ridge) | -17,82 | 62,09 | 1938 | RAPiD-12-1K | High | Annual | (Thornalley et al., 2009) | Thornalley, 2009 (WDCP-A) | This study on G. Bulloides & G. Inflata | Holocene | |
| NE Atlantic (Rockall Trough) | -13,99 | 55,65 | 2543 | ENAM9606 +M200309 | Very high | Annual | (Richter et al., 2009) | Richter et al., 2009 (WDCP-A) | Anand et al. (2003) on G. Bulloides | 0-2,3 ka BP | |
| NW Atlantic (Laurentian Fan) | -54,87 | 43,48 | 3975 | OCE326-GGC26 | Low | Annual | (Keigwin et al., 2005) | Leduc et al., 2010 (PANGAEA) | Elderfield & Ganssen (2000) | ~0,5-10,5 ka BP | |

| PLANKTONIC FORAMINIFERA | | | | | | | | | | |
|---|---|---|---|---|---|---|---|---|---|---|
| **Region** | **Lon** | **Lat** | **Depth(m)** | **Core number** | **Resolution** | **Season** | **Reference article(s)** | **Reference database** | **Time span** | **Remark** |
| Central South Atlantic Ridge | -23 | 0 | 3870 | 86014-12PC51 | Very low | Cold & Warm | Sikes and Keigwin, 1994(NP) | Sikes, 1997 (PANGAEA) | ~7-12 ka BP | |
| Central MAR | -33,48 | 1,37 | 3824 | v25-59w | Very low | Winter & Summer | Waelbroeck et al., 1998(NP) | Waelbroeck, 2005 (WDCP-A) | Holocene | |
| Brazil Basin | -38,82 | -14,4 | 965 | CMU-14 | Very low | Summer | Toledo et al., 2007 | NP | Holocene | |
| Brazil Basin | -39,52 | -20,95 | 1995 | ESP-08 | Very low | Summer | Toledo et al., 2007 | NP | Holocene | |
| Brazil Basin | -42,27 | -24,42 | 1682 | SAN-76 | Very low | Summer | Toledo et al., 2007 | NP | Holocene | |
| Caribbean Sea | -61,24 | 12,09 | 1299 | M35003-4 | Intermediate | Cold & Warm | Hüls and Zahn, 2000 (NP) | Hüls & Zahn, 2000 (PANGAEA) | Holocene | River |
| Caribbean Sea | -66,6 | 17,89 | 349 | PRB/PRP-12 | High | February-April & August-October | Nyberg, 2002 | Nyberg et al., 2002 (WDCP-A) | ~0-2 ka BP | |
| Caribbean Sea | -78,74 | 12,74 | 2828 | ODP165-999A | Very low | Annual | Martinez et al., 2007 | Martinez et al., 2007 (pers comm) | ~4-10,5 ka BP | |
| NW Atlantic (Newfoundland Basin) | -47,35 | 41,76 | 4100 | CH6909 | Intermediate | Summer | Waelbroeck et al., 1998(NP)<br>Labeyrie et al., 1999 (NP)<br>Marchal et al., 2002 | NP | ~0,5-10 ka BP | |
| Azores Plateau | -26,54 | 44,36 | 3050 | GIK15612-2 | Very low | Cold & Warm | Kiefer, 1998 (NP) | Kiefer & Sarnthein, 1998b (PANGAEA) | ~2-12 ka | Not calibrated |
| Iberian Sea | -10,18 | 37,77 | 3135 | SU81-18 | Low | Summer | Duplessy et al., 1992 (NP)<br>Waelbroeck et al., 1998(NP)<br>Marchal et al., 2002 | NP | ~0-10 ka BP | |
| Mediterranean Sea | 4,15 | 42,04 | 2100 | MD992346 | Low | April-May | Melki et al., 2009 | NP | Holocene | |
| Mediterranean Sea | 11,67 | 36,95 | 771 | MD04-2797 CQ | Intermediate | Winter & Summer | Essallami et al., 2007 (NP);<br>Rouis-Zargouni et al., 2009 | NP | Holocene | |
| Mediterranean Sea | 13,35 | 40,55 | 1920 | KET90-19 | Low | February & August + April-May | Kallel et al., 1997 | NP | Holocene | |
| Mediterranean Sea | 14,5 | 38,82 | 1900 | KET80-03 | Low | February & August + April-May | Kallel et al., 1997 | NP | Holocene | |
| Mediterranean Sea | 17,62 | 41,3 | 1010 | MD90-917 | Intermediate | Summer | Siani et al., 2001 | NP | ~1-12 ka BP | |
| Mediterranean Sea | 26,58 | 35,67 | 1522 | LC21 | High | Winter & Summer | Marino et al., 2009 | Rohling et al. (2002) Pers comm | ~4-12 ka BP | |
| Canary Basin | -18,99 | 27,01 | 3849 | GIK15637-1 | Low | Cold & Warm | Kiefer, 1998 (NP) | Kiefer & Sarnthein, 1998a (PANGAEA) | ~6-12 ka BP; Hyat: 8-10 ka BP | |
| Canary Basin | -18,58 | 20,75 | 2263 | ODP 658C | High | Cold & Warm | deMenocal et al., 2000 | NP | Holocene | |
| Canary Basin | -20,16 | 19 | 3300 | BOFS31/1K | Very low | Winter & Summer | Elderfield and Ganssen, 2000 | NP | Holocene | |

| | | | | | | | | | | |
|---|---|---|---|---|---|---|---|---|---|---|
| Central North Atlantic (Reykjanes Ridge) | -36,83 | 52,7 | ? | CH7702 | High | Summer | Marchal et al., 2002 | NP | ~0-10 ka BP | |
| West European Basin | -23,73 | 50 | 4053 | K708-1 | Very low | February & August | Imbrie et al., 1992 (NP) | SPECMAP contributors, 2005 (WDCP-A) | Holocene | |
| Central North Atlantic (Reykjanes Ridge) | -28,35 | 54,68 | ? | NEAP17K | High | Summer | Marchal et al., 2002 | NP | ~0-10 ka BP | |
| Central North Atlantic (Reykjanes Ridge) | -27,82 | 56,37 | ? | NEAP15K | Intermediate | Summer | Marchal et al., 2002 | NP | ~0-10 ka BP | |
| Central North Atlantic (Reykjanes Ridge) | -27,91 | 57,45 | 2620 | MD99-2251 | Very high | Winter & Summer | Ellison et al., 2006 | Ellison, 2006<br>(WDCP-A) | ~7,2-9,2 ka BP | |
| Iceland Basin (Reykjanes Ridge) | -25,96 | 58,76 | 2630 | MD95-2015 | Intermediate | February & August | Eynaud et al., 2004 | NP | ~1-12 ka BP | |
| Central North Atlantic (Rockall Rise) | -14,7 | 55,5 | ? | NA8722 | Low, High | Summer | Duplessy et al., 1992 (NP)<br>Marchal et al., 2002 | NP | ~0,5-10 ka BP | |
| North Sea | 3,73 | 60,87 | 345 | Troll8903/<br>28-02 | Intermediate | Summer | Klitgaard-Kristensen et al., 2001<br>Hald et al., 2007 | NP | Holocene | |
| Norwegian Sea | 7,64 | 66,97 | 1048 | MD95-2011 | High | Summer | Marchal et al., 2002<br>Risebrobakken et al., 2003<br>Andersson et al., 2003<br>(Hald et al., 2007 | NP | Holocene | |
| Norwegian Sea | 16,38 | 69,3 | 505 | T79-51/2 | Low | Summer | Hald et al., 2007; Hald et al., 1996 | NP | Holocene | |
| Norwegian Sea | 69,27 | 16,42 | 476 | JM99-1200 | Very high | ? | Hald et al., 2004 | Ebbesen & Hald, 2006<br>WDCP-A | ~10-12 ka BP | |
| Norwegian Sea | 14,36 | 71,99 | 1500 | T88-2<br>JM01-1199 | Intermediate | Summer | Hald and Aspeli, 1997<br>Hald et al., 2007 | NP | Holocene | |

| DINOCYSTS | | | | | | | | | | |
|---|---|---|---|---|---|---|---|---|---|---|
| Region | Lon | Lat | Depth(m) | Core number | Resolution | Season | Reference article(s) | Reference database | Time span | Remark |
| Mediterranean Sea | 11,67 | 36,95 | 771 | MD04-2797 CQ | Intermediate | Spring | Rouis-Zargouni et al., 2009 | NP | Hyat: ~9-10,5 ka BP | |
| Central North Atlantic (Reykjanes Ridge - Charlie Gibbs fracture) | -38,64 | 53,98 | 3603 | HU91-045-085TWC | Intermediate | Winter & Summer | de Vernal and Hillaire-Marcel, 2006 | de Vernal (Pers comm) | Holocene | |
| Central North Atlantic (Reykjanes Ridge - Charlie Gibbs fracture) | -33,53 | 53,05 | 3024 | HU91-045-080P | Low | Winter & Summer | de Vernal and Hillaire-Marcel, 2006 | de Vernal (Pers comm) | ~5-12 ka BP | |
| Central North Atlantic (Reykjanes Ridge) | -30,67 | 56,80 | 2440 | MD99-2254 | High | Winter & Summer | de Vernal and Hillaire-Marcel, 2006; Solignac et al., 2004 | de Vernal (Pers comm) | ~2-8 ka BP | |
| Iceland Basin (Reykjanes Ridge) | -31,10 | 59,20 | 1493 | LO09-14 | High | Winter & Summer | Solignac et al., 2008 | NP | Hyat: ~3,5-5,5 ka BP | |
| Iceland Basin (Reykjanes Ridge) | -28,73 | 58,93 | 2237 | HU91-045-072P | High | Winter & Summer | de Vernal and Hillaire-Marcel, 2006 | de Vernal (Pers comm) | ~5-12 ka BP | |
| Iceland Basin (Reykjanes Ridge) | -25,96 | 58,76 | 2630 | MD95-2015 | Intermediate | February & August | Eynaud et al., 2004 | NP | ~1-12 ka BP | |
| North icelandic Shelf | -20,85 | 66,62 | 365 | 2269/327 | High | February & August | Solignac et al., 2008 | NP | ~0-10 ka BP | |
| Faroer-Shetland channel | -6,07 | 60,11 | 1156 | HM03-133-25 | High | February & August | Solignac et al., 2008 | NP | ~0-10 ka BP | |
| Norwegian Sea | 5,97 | 62,17 | 698 | HM102-03 | Intermediate | February & August | Grøsfjeld et al., 1999 | NP | Holocene | fjord; Not calibrated |
| Fram Strait | 6,77 | 78,91 | 1497 | JM-06-WP-04-MCB | Very high | Winter & Summer | Bonnet et al., 2010 | Bonnet (pers comm) | 0-2,4 ka BP | |
| Barents Sea | 42,61 | 71,74 | 286 | PL-96-112 | Intermediate | Winter & Summer | Voronina et al., 2001 | de Vernal (Pers comm) | ~0-8 ka BP | |
| Barents Sea | 50,72 | 73,62 | 270 | PL-96-126 | High | August | Voronina et al., 2001 | NP | ~0-4,5 ka BP | |
| Denmark Strait | -29,35 | 68,10 | 404 | JM96-1207 | High | February & August | Solignac et al., 2008 | NP | ~0-10 ka BP | meltwater influence |
| Labrador Sea (south of Greenland) | -48,37 | 58,21 | 3379 | HU90-013-013P | Intermediate | Winter & Summer | Hillaire-Marcel et al., 2001 | de Vernal (Pers comm) | Holocene | |
| Labrador Sea (south of Greenland) | -48,37 | 58,21 | 3460 | MD99-2227 | High | Winter & Summer | Solignac et al., 2008 | de Vernal (Pers comm) | ~0,5-12 ka BP | |
| Baffin Bay | -71,86 | 76,81 | 823 | 91-039-012TWC/012P | Intermediate | Winter & Summer | Levac et al., 2001 | de Vernal (Pers comm) | ~1-8,5 ka BP | West Greenland Coast |
| Baffin Bay | -75,59 | 78,69 | 561 | LSSL2001-006 | Intermediate | February & August | Mudie et al., 2006 | NP | ~0-6,5 ka | Nares Strait; Not calibrated |
| Baffin Bay | -74,33 | 77,27 | 663 | 91-039-008P 91-039-007B | Intermediate | August | Levac et al., 2001 | de Vernal (Pers comm) | ~2,5-6,5 ka BP | Nares Strait |
| Baffin Bay | -81,19 | 74,19 | ? | 2004-804-009 PC | Intermediate | August | Ledu et al., 2008 | NP | Holocene? | Only 7 age points reconstructed |
| Hudson Bay (east side) | -77,97 | 55,48 | 165 | HU87-028-069P | High | Summer | Bilodeau et al., 1990(NP) de Vernal and Hillaire-Marcel, 2006 | de Vernal (Pers comm) | ~2,5-8,5 ka BP | |
| Labrador Sea (ne of Newfoundland | -57,50 | 58,37 | 2853 | HU84-030-021P | High | Winter & Summer | de Vernal, 2001 | NP | ~1-8,5 ka BP | near sinking spot |
| NW Atlantic (Orphan Knoll - E of Newfoundland) | -45,68 | 50,20 | 3448 | HU91-045-094P | High | Winter & Summer | de Vernal et al., 2000 Peyron and de Vernal, 200, Solignac et al., 2004 | de Vernal (Pers comm) | ~2-11 ka? | southeast of sinking spot |
| NW Atlantic (E of S Canada - Laurentian Fan) | -55,62 | 44,67 | 1412 | MD95-2033 | Intermediate | Winter & Summer | de Vernal and Hillaire-Marcel, 2006 | de Vernal (Pers comm) | ~1-12 ka BP | southeast of St.-Lawrence |
| NW Atlantic (Scotian Shelf) | -63,72 | 43,77 | 256 | 95-030-24 | Intermediate | February & August | Levac, 2001 | NP | Holocene? | |

| DIATOMS | | | | | | | | | | |
|---|---|---|---|---|---|---|---|---|---|---|
| Region | Lon | Lat | Depth(m) | Core number | Resolution | Season | Reference article(s) | Reference database | Time span | Remark |
| Iceland Basin (Reykjanes Ridge) | -30,41 | 58,94 | 1493 | LO09-14 | High | August | Andersen et al., 2004b | NP | Hyat: ~1,2-2,2 ka BP | |
| North Icelandic Shelf | -20,85 | 66,63 | 365 | MD99-2269 | High | August | Andersen et al., 2004a<br>Jón Eiríksson, 2000 | NP | ~0-10 ka BP | meltwater |
| North Icelandic Shelf | -19,50 | 66,50 | 143 | MD99-2271 | High | Summer | Jiang et al., 2007 | Jiang (Pers comm) | ~0-3 ka BP | meltwater |
| North Icelandic Shelf | -19,07 | 66,50 | ? | HM107-03 | High | Summer | Bonnet et al., 2010; Jiang et al., 2002<br>Solignac et al., 2008 | Jiang (Pers comm) | ~0-4,5 ka BP | meltwater |
| North Icelandic Shelf | -17,68 | 66,55 | ? | MD99-2275 | Very high | Winter & Summer | (Jiang et al., 2005) | Jiang (Pers comm) | ~0-2 ka BP | meltwater |
| Norwegian Sea | 2,70 | 62,97 | ? | HM796 | Intermediate | Summer | Koç & Jansen, 1992 (NP)<br>Marchal et al., 2002 | NP | ~4-10 ka BP | |
| Norwegian Sea | 7,64 | 66,97 | 1048 | MD95-2011; JM97-948/2A | High | August | Andersen et al., 2004a<br>Marchal et al., 2002<br>Birks and Koç, 2002 | NP | ~0,5-10 ka BP | |
| Denmark Strait (Greenland coast) | -16,53 | 69,46 | ? | PS21842 | Low | Summer | Koç et al., 1993(NP)<br>Koc and Jansen, 1994NP)<br>Marchal et al., 2002 | NP | ~0-10 ka BP | |
| Denmark Strait (Greenland coast) | -30,86 | 67,14 | 710 | HU93030-19A; BS88-06-5A | High | August | Andersen et al., 2004a | NP | ~0-9 ka BP | meltwater |

## References

Alt-Epping, Ulrich (2009): UK37 and sea surface temperatures of sediment core GeoB8903-1. doi:10.1594/PANGAEA.718843

Andersen, N et al. (1999): Paleotemperatures, stable isotopes and alkenones of samples from the South Atlantic. doi:10.1594/PANGAEA.728650, Supplement to: Andersen, Nils; Müller, Peter J; Kirst, Georg; Schneider, Ralph R (1999): Alkenone d13C as a Proxy for Past PCO2 in Surface Waters: Results from the Late Quaternary Angola Current. In: Fischer, G & Wefer, G (eds.), Use of Proxies in Paleoceanography - Examples from the South Atlantic, Springer, Berlin, Heidelberg, 469-488

Bard, Edouard (2006): Age, alkenone data and sea surface temperature records of sediment core SU81-18. doi:10.1594/PANGAEA.441524

Cacho, I. et al., 2001. Variability of the western Mediterranean Sea surface temperature during the last 25,000 years and its connection with the Northern Hemisphere climatic changes. Paleoceanography, 16.

Cacho, I et al. (2001): Alkenone-derived Holocene sea-surface temperature records of sediment core M39008-3. doi:10.1594/PANGAEA.438799, In Supplement to: Cacho, Isabel; Grimalt, Joan O; Canals, Miquel; Sbaffi, Laura; Shackleton, Nicholas J; Schönfeld, Joachim; Zahn, Rainer (2001): Variability of the Western Mediterranean sea surface temperatures during the last 25 000 years and its connection with the northern hemisphere climatic changes. Paleoceanography, 16(1), 40-52, doi:10.1029/2000PA000502

Cacho, I et al. (1999): Age determination and paleotemperatures of sediment core MD95-2042 in the Alboran Sea. doi:10.1594/PANGAEA.735759, Supplement to: Cacho, Isabel; Grimalt, Joan O; Pelejero, Carles; Canals, Miquel; Sierro, Francisco Javier; Flores, José Abel; Shackleton, Nicholas J (1999): Dansgaard-Oeschger and Heinrich event imprints in the Alboran Sea paleotemperature record. Paleoceanography, 14(6), 698-705, doi:10.1029/1999PA900044

Cacho, I et al. (2001): Alkenone-derived Holocene sea-surface temperature records of sediment core BS79-38. doi:10.1594/PANGAEA.438379, In Supplement to: Cacho, Isabel; Grimalt, Joan O; Canals, Miquel; Sbaffi, Laura; Shackleton, Nicholas J; Schönfeld, Joachim; Zahn, Rainer (2001): Variability of the Western Mediterranean sea surface temperatures during the last 25 000 years and its connection with the northern hemisphere climatic changes. Paleoceanography, 16(1), 40-52, doi:10.1029/2000PA000502

Cacho, I et al. (2001): Alkenone-derived Holocene sea-surface temperature records of sediment core BS79-33. doi:10.1594/PANGAEA.438371, In Supplement to: Cacho, Isabel; Grimalt, Joan O; Canals, Miquel; Sbaffi, Laura; Shackleton, Nicholas J; Schönfeld, Joachim; Zahn, Rainer (2001): Variability of the Western Mediterranean sea surface temperatures during the last 25 000 years and its connection with the northern hemisphere climatic changes. Paleoceanography, 16(1), 40-52, doi:10.1029/2000PA000502

Calvo, E., Grimalt, J.O. and Jansen, E., 2002. High resolution U-37(K) sea surface temperature reconstruction in the Norwegian Sea during the Holocene. Quaternary Science Reviews, 21(12-13): 1385-1394.

Chapman, M.R., Shackleton, N.J., Zhao, M. and Eglinton, G., 1996. Faunal and Alkenone Reconstructions of Subtropical North Atlantic Surface Hydrography and Paleotemperature Over The last 28 kyr. Paleoceanography, 11.

Cronin, T.M., Dwyer, G.S., Kamiya, T., Schwede, S. and Willard, D.A., 2003. Medieval Warm Period, Little Ice Age and 20th century temperature variability from Chesapeake Bay. Global and Planetary Change, 36(1-2): 17-29.

deMenocal, P., Ortiz, J., Guilderson, T. and Sarnthein, M., 2000. Coherent High- and Low-Latitude Climate Variability During the Holocene Warm Period. Science, 288(5474): 2198-2202.

Doose, Heidi (2001): (Table 2c) Alkenones, stable isotopes and sea surface temperature from sediment core KC01. doi:10.1594/PANGAEA.59762

Doose, Heidi (2001): (Table 2e) Alkenones, stable isotopes and sea surface temperature from sediment core KC20B. doi:10.1594/PANGAEA.59765

Elderfield, H. and Ganssen, G., 2000. Past temperature and [delta]18O of surface ocean waters inferred from foraminiferal Mg/Ca ratios. Nature, 405(6785): 442-445.

Emeis, K.-C., Struck, U., Blanz, T., Kohly, A. and Voss, M., 2003. Salinity changes in the central Baltic Sea (NW Europe) over the last 10000 years. The Holocene, 13(3): 411-421.
Emeis, K.-C. et al., 2000. Temperature and salinity variations of Mediterranean Sea surface waters over the last 16,000 years from records of planktonic stable oxygen isotopes and alkenone unsaturation ratios. Palaeogeography, Palaeoclimatology, Palaeoecology, 158(3-4): 259-280.
Emeis, K-C; Dawson, AG (2003): Age and alkenone-derived Holocene sea-surface temperature records of sediment core M40-4-SL78. doi:10.1594/PANGAEA.438795, Supplement to: Emeis, Kay-Christian; Dawson, Alastair G (2003): Holocene paleoclimate records over Europe and the North-Atlantic. The Holocene, 13, 305-309, doi:10.1191/0959683603hl622ed
Emeis, K-C et al. (2003): Age and alkenone-derived Holocene sea-surface temperature records of sediment core IOW225517. Baltic Sea Research Institute, Warnemünde, doi:10.1594/PANGAEA.438452,
In Supplement to: Emeis, Kay-Christian; Struck, Ulrich; Blanz, Thomas; Kohly, Alexander; Voß, Maren (2003): Salinity changes in the central Baltic Sea (NW Europe) over the last 10000 years. The Holocene, 13, 411-421, doi:10.1191/0959683603hl634rp
Giunta, S., Emeis, K.C. and Negri, A., 2001. Sea-surface temperature reconstruction of the last 16,000 years in the eastern Mediterrenean Sea. Sea. Riv Ital Paleont Stratigr, 107: 463-476.
Grimalt, Joan O; Marchal, Olivier (2006): Age and alkenone-derived Holocene sea-surface temperature records of sediment core MD95-2015. Physikalisches Institut, Universität Bern, doi:10.1594/PANGAEA.438814
Grimalt, Joan O; Calvo, E (2006): Age and alkenone-derived Holocene sea-surface temperature records of sediment core MD95-2011. Dept. of Environmental Chemistry, Inst. of Chemical and Environmental Research, doi:10.1594/PANGAEA.438810
Jaeschke, A et al. (2007): Determination of millennial-scale climate variability based on alkenones in the western Atlantic Ocean. doi:10.1594/PANGAEA.667499, Supplement to: Jaeschke, Andrea; Rühlemann, Carsten; Arz, Helge W; Heil, Gerrit M N; Lohmann, Gerrit (2007): Coupling of millennial-scale changes in sea surface temperature and precipitation off northeastern Brazil with high-latitude climate shifts during the last glacial period. Paleoceanography, 22, PA4206, doi:10.1029/2006PA001391
Jasper, JP; Gagosian, RB (1989): Alkenones and reconstructed sea surface temperature from sediment core 96-619 (Table 1). doi:10.1594/PANGAEA.52383, Supplement to: Jasper, John P; Gagosian, Robert B (1989): Alkenone molecular stratigraphy in an oceanic environment affected by glacial freshwater events. Paleoceanography, 4(6), 603-614, doi:10.1029/PA004i006p00603
Keigwin, L., Bice, M. and Copley, N., 2005. Seasonality and stable isotopes in planktonic foraminifera off Cape Cod, Massachusetts. Paleoceanography, 20(4): -.
Kim, J.-H. et al., 2007. Impacts of the North Atlantic gyre circulation on Holocene climate off northwest Africa. Geology, 35(5): 387-390.
Kim, J.-H., Schneider, R.R., Mulitza, S. and MÃ¼ller, P.J., 2003. Reconstruction of SE trade-wind intensity based on sea-surface temperature gradients in the Southeast Atlantic over the last 25 kyr. Geophys. Res. Lett., 30.
Kim, J.-H., Schneider, R.R., Müller, P.J. and Wefer, G., 2002. Interhemispheric comparison of deglacial sea-surface temperature patterns in Atlantic eastern boundary currents. Earth and Planetary Science Letters, 194(3-4): 383-393.
Kim, J-H et al. (2002): Sea-surface temperature reconstruction for sediment core GeoB1023-5. doi:10.1594/PANGAEA.735766, Supplement to: Kim, Jung-Hyun; Schneider, Ralph R; Müller, Peter J; Wefer, Gerold (2002): Interhemispheric comparison of deglacial sea-surface temperature patterns in Atlantic eastern boundary currents. Earth and Planetary Science Letters, 194(3-4), 383-393, doi:10.1016/S0012-821X(01)00545-3
Kim, J-H et al. (2003): Sea-surface temperature reconstruction of ODP Hole 175-1078C. doi:10.1594/PANGAEA.736601, Supplement to: Hüls, Matthias (2000): Millennial-scale SST variability as inferred from planktonic foraminifera sensus counts in the western subtropical Atlantic. GEOMAR Report, GEOMAR Research Center for Marine Geosciences, Christian Albrechts University in Kiel, 95, 118 pp
Kim, J-H et al. (2004): Age and alkenone-derived Holocene sea-surface temperature records of sediment core GeoB5901-2. doi:10.1594/PANGAEA.438384,

In Supplement to: Kim, Jung-Hyun; Rimbu, Norel; Lorenz, Stefan J; Lohmann, Gerrit; Schneider, Ralph R; Nam, Seung-Il; Schouten, Stefan; Sirocko, Frank; Rühlemann, Carsten (2004): North Pacific and North Atlantic sea-surface temperature variability during the Holocene. Quaternary Science Reviews, 23(20-22), 2141-2154, doi:10.1016/j.quascirev.2004.08.010

Kirst, G.J., Schneider, R.R., Müller, P.J., von Storch, I. and Wefer, G., 1999. Late Quaternary Temperature Variability in the Benguela Current System Derived from Alkenones. Quaternary Research, 52(1): 92-103.

Kirst, Georg; Müller, Peter J (2001): Total organic carbon, alkenones and sea surface temperature of sediment core GeoB1710-3. doi:10.1594/PANGAEA.58041

Kirst, Georg; Müller, Peter J (2001): Total organic carbon, alkenones and sea surface temperature of sediment core GeoB1711-4. doi:10.1594/PANGAEA.58042

Kirst, Georg; Müller, Peter J (2001): Total organic carbon, alkenones and sea surface temperature of sediment core GeoB1712-4. doi:10.1594/PANGAEA.58043

Labeyrie, Laurent; Cronin, Thomas M (2005): Physical properties of sediment core MD99-2209. doi:10.1594/PANGAEA.253565

Lawrence, K.T., Herbert, T.D., Brown, C.M., Raymo, M.E. and Haywood, A.M., 2009. High-amplitude variations in North Atlantic sea surface temperature during the early Pliocene warm period. Paleoceanography, 24: -.

Lea, D.W., Pak, D.K., Peterson, L.C. and Hughen, K.A., 2003. Synchroneity of Tropical and High-Latitude Atlantic Temperatures over the Last Glacial Termination. Science, 301(5638): 1361-1364.

Leduc, G., Schneider, R., Kim, J.H. and Lohmann, G., 2010. Holocene and Eemian sea surface temperature trends as revealed by alkenone and Mg/Ca paleothermometry. Quaternary Science Reviews, 29(7-8): 989-1004.

Leduc, G et al. (2010): Sea surface temperature reconstruction from sediment core TN057-21PC using alkenones. doi:10.1594/PANGAEA.737277

Leduc, G et al. (2010): Sea surface temperature reconstruction from sediment core GeoB3129-1 using Mg/Ca-ratios. doi:10.1594/PANGAEA.736989, In Supplement to: Leduc, Guillaume; Schneider, R; Kim, Jung-Hyun; Lohmann, Gerrit (2010): Holocene and Eemian Sea surface temperature trends as revealed by alkenone and Mg/Ca paleothermometry. Quaternary Science Reviews, 29, 989-1004, doi:10.1016/j.quascirev.2010.01.004

Leduc, G et al. (2010): Sea surface temperature reconstruction from sediment core CH07-98-GGC19 using alkenones. doi:10.1594/PANGAEA.737207, In Supplement to: Leduc, Guillaume; Schneider, R; Kim, Jung-Hyun; Lohmann, Gerrit (2010): Holocene and Eemian Sea surface temperature trends as revealed by alkenone and Mg/Ca paleothermometry. Quaternary Science Reviews, 29, 989-1004, doi:10.1016/j.quascirev.2010.01.004

Leduc, G et al. (2010): Sea surface temperature reconstruction from sediment core D13882 using alkenones. doi:10.1594/PANGAEA.737208, In Supplement to: Leduc, Guillaume; Schneider, R; Kim, Jung-Hyun; Lohmann, Gerrit (2010): Holocene and Eemian Sea surface temperature trends as revealed by alkenone and Mg/Ca paleothermometry. Quaternary Science Reviews, 29, 989-1004, doi:10.1016/j.quascirev.2010.01.004

Leduc, G et al. (2010): Sea surface temperature reconstruction from sediment core MD01-2443 using alkenones. doi:10.1594/PANGAEA.737243, In Supplement to: Leduc, Guillaume; Schneider, R; Kim, Jung-Hyun; Lohmann, Gerrit (2010): Holocene and Eemian Sea surface temperature trends as revealed by alkenone and Mg/Ca paleothermometry. Quaternary Science Reviews, 29, 989-1004, doi:10.1016/j.quascirev.2010.01.004

Leduc, G et al. (2010): Sea surface temperature reconstruction from sediment core 161-977 using alkenones. doi:10.1594/PANGAEA.737194, In Supplement to: Leduc, Guillaume; Schneider, R; Kim, Jung-Hyun; Lohmann, Gerrit (2010): Holocene and Eemian Sea surface temperature trends as revealed by alkenone and Mg/Ca paleothermometry. Quaternary Science Reviews, 29, 989-1004, doi:10.1016/j.quascirev.2010.01.004

Leduc, G et al. (2010): Sea surface temperature reconstruction from sediment core AD91-17 using alkenones. doi:10.1594/PANGAEA.737203, In Supplement to: Leduc, Guillaume; Schneider, R; Kim, Jung-Hyun; Lohmann, Gerrit (2010): Holocene and Eemian Sea surface temperature trends as revealed by alkenone and Mg/Ca paleothermometry. Quaternary Science Reviews, 29, 989-1004, doi:10.1016/j.quascirev.2010.01.004

Leduc, G et al. (2010): Sea surface temperature reconstruction from sediment core 160-969E using alkenones. doi:10.1594/PANGAEA.737193, In Supplement to: Leduc, Guillaume; Schneider, R; Kim, Jung-Hyun; Lohmann, Gerrit (2010): Holocene and Eemian Sea surface temperature trends as revealed by alkenone and Mg/Ca paleothermometry. Quaternary Science Reviews, 29, 989-1004, doi:10.1016/j.quascirev.2010.01.004

Leduc, G et al. (2010): Alkenone-derived Holocene Sea Surface Temperature database. doi:10.1594/PANGAEA.737301,
In Supplement to: Leduc, Guillaume; Schneider, R; Kim, Jung-Hyun; Lohmann, Gerrit (2010): Holocene and Eemian Sea surface temperature trends as revealed by alkenone and Mg/Ca paleothermometry. Quaternary Science Reviews, 29, 989-1004, doi:10.1016/j.quascirev.2010.01.004
Leduc, G et al. (2010): Sea surface temperature reconstruction from sediment core GeoB6007-2 using alkenones. doi:10.1594/PANGAEA.737217,
In Supplement to: Leduc, Guillaume; Schneider, R; Kim, Jung-Hyun; Lohmann, Gerrit (2010): Holocene and Eemian Sea surface temperature trends as revealed by alkenone and Mg/Ca paleothermometry. Quaternary Science Reviews, 29, 989-1004, doi:10.1016/j.quascirev.2010.01.004
Leduc, G et al. (2010): Sea surface temperature reconstruction from sediment core GeoB5546-2 using alkenones. doi:10.1594/PANGAEA.737214,
In Supplement to: Leduc, Guillaume; Schneider, R; Kim, Jung-Hyun; Lohmann, Gerrit (2010): Holocene and Eemian Sea surface temperature trends as revealed by alkenone and Mg/Ca paleothermometry. Quaternary Science Reviews, 29, 989-1004, doi:10.1016/j.quascirev.2010.01.004
Leduc, G et al. (2010): Sea surface temperature reconstruction from sediment core JR51-GC35 using alkenones. doi:10.1594/PANGAEA.737230,
In Supplement to: Leduc, Guillaume; Schneider, R; Kim, Jung-Hyun; Lohmann, Gerrit (2010): Holocene and Eemian Sea surface temperature trends as revealed by alkenone and Mg/Ca paleothermometry. Quaternary Science Reviews, 29, 989-1004, doi:10.1016/j.quascirev.2010.01.004
Leduc, G et al. (2010): Sea surface temperature reconstruction from sediment core GIK23258-2 using alkenones. doi:10.1594/PANGAEA.737227,
In Supplement to: Leduc, Guillaume; Schneider, R; Kim, Jung-Hyun; Lohmann, Gerrit (2010): Holocene and Eemian Sea surface temperature trends as revealed by alkenone and Mg/Ca paleothermometry. Quaternary Science Reviews, 29, 989-1004, doi:10.1016/j.quascirev.2010.01.004
Leduc, G et al. (2010): Sea surface temperature reconstruction from sediment core MD03-2707 using Mg/Ca-ratios. doi:10.1594/PANGAEA.736995,
In Supplement to: Leduc, Guillaume; Schneider, R; Kim, Jung-Hyun; Lohmann, Gerrit (2010): Holocene and Eemian Sea surface temperature trends as revealed by alkenone and Mg/Ca paleothermometry. Quaternary Science Reviews, 29, 989-1004, doi:10.1016/j.quascirev.2010.01.004
Leduc, G et al. (2010): Sea surface temperature reconstruction from sediment core PL07-39PC using Mg/Ca-ratios. doi:10.1594/PANGAEA.737007,
In Supplement to: Leduc, Guillaume; Schneider, R; Kim, Jung-Hyun; Lohmann, Gerrit (2010): Holocene and Eemian Sea surface temperature trends as revealed by alkenone and Mg/Ca paleothermometry. Quaternary Science Reviews, 29, 989-1004, doi:10.1016/j.quascirev.2010.01.004
Leduc, G et al. (2010): Sea surface temperature reconstruction from sediment core MD99-2334 using Mg/Ca-ratios. doi:10.1594/PANGAEA.737005,
In Supplement to: Leduc, Guillaume; Schneider, R; Kim, Jung-Hyun; Lohmann, Gerrit (2010): Holocene and Eemian Sea surface temperature trends as revealed by alkenone and Mg/Ca paleothermometry. Quaternary Science Reviews, 29, 989-1004, doi:10.1016/j.quascirev.2010.01.004
Leduc, G et al. (2010): Sea surface temperature reconstruction from sediment core MD99-2251 using Mg/Ca-ratios. doi:10.1594/PANGAEA.737004,
In Supplement to: Leduc, Guillaume; Schneider, R; Kim, Jung-Hyun; Lohmann, Gerrit (2010): Holocene and Eemian Sea surface temperature trends as revealed by alkenone and Mg/Ca paleothermometry. Quaternary Science Reviews, 29, 989-1004, doi:10.1016/j.quascirev.2010.01.004
Leduc, G et al. (2010): Sea surface temperature reconstruction from sediment core 162-984 using Mg/Ca-ratios. doi:10.1594/PANGAEA.736981,
In Supplement to: Leduc, Guillaume; Schneider, R; Kim, Jung-Hyun; Lohmann, Gerrit (2010): Holocene and Eemian Sea surface temperature trends as revealed by alkenone and Mg/Ca paleothermometry. Quaternary Science Reviews, 29, 989-1004, doi:10.1016/j.quascirev.2010.01.004
Leduc, G et al. (2010): Sea surface temperature reconstruction from sediment core OCE326-GGC26 using alkenones. doi:10.1594/PANGAEA.737258,
In Supplement to: Leduc, Guillaume; Schneider, R; Kim, Jung-Hyun; Lohmann, Gerrit (2010): Holocene and Eemian Sea surface temperature trends as revealed by alkenone and Mg/Ca paleothermometry. Quaternary Science Reviews, 29, 989-1004, doi:10.1016/j.quascirev.2010.01.004
Marchal, O. et al., 2002. Apparent long-term cooling of the sea surface in the northeast Atlantic and Mediterranean during the Holocene. Quaternary Science Reviews, 21(4-6): 455-483.
Martrat, B. et al., 2004. Abrupt temperature changes in the Western Mediterranean over the past 250,000 years. Science, 306(5702): 1762-1765.
McGregor, HV et al. (2007): Age, UK`37 and Sea Surface Temperatures of sediment core GeoB6008-1. doi:10.1594/PANGAEA.603183,

In Supplement to: McGregor, Helen V; Dima, Mihai; Fischer, Helmut W; Mulitza, Stefan (2007): Rapid 20th century increase in coastal upwelling off northwest Africa. Science, 315, 637-639, doi:10.1126/science.1134839
Mollenhauer, G. et al., 2003. Asynchronous alkenone and foraminifera records from the Benguela Upwelling System. Geochimica et Cosmochimica Acta, 67(12): 2157-2171.
Mollenhauer, Gesine; Müller, Peter J (2002): UK37 and alkenone sea surface temperatures of sediment core IOW226660-5. Baltic Sea Research Institute, Warnemünde, doi:10.1594/PANGAEA.80968
Mollenhauer, Gesine; Müller, Peter J (2002): UK37 and alkenone sea surface temperatures of sediment core IOW226920-3. Baltic Sea Research Institute, Warnemünde, doi:10.1594/PANGAEA.80806
Niedermeyer, Eva M; Prange, Matthias; Mulitza, Stefan (2010): Alkenone data of sediment core GeoB9508-5 from the continental slope off Senegal. doi:10.1594/PANGAEA.733699
Nürnberg, D., Müller, A. and Schneider, R.R., 2000. Paleo-Sea Surface Temperature Calculations in the Equatorial East Atlantic from Mg/Ca Ratios in Planktic Foraminifera: A Comparison to Sea Surface Temperature Estimates from U37Kâ€², Oxygen Isotopes, and Foraminiferal Transfer Function. Paleoceanography, 15.
Nürnberg, Dirk; Müller, A; Schneider, Ralph R (2008): Paleo-sea surface temperatures and Mg/Ca ratios of core GeoB1112-4. doi:10.1594/PANGAEA.710811
Pahnke, K. and Sachs, J.P., 2006. Sea surface temperatures of southern midlatitudes 0–160 kyr B.P. Paleoceanography, 21(PA2003).
Pailler, D. and Bard, E., 2002. High frequency palaeoceanographic changes during the past 140[punctuation space]000 yr recorded by the organic matter in sediments of the Iberian Margin. Palaeogeography, Palaeoclimatology, Palaeoecology, 181(4): 431-452.
Pailler, D; Bard, E (2002): Geochemistry and sea-surface temperature reconstruction for sediment cores of the Iberian Margin. doi:10.1594/PANGAEA.736599, Supplement to: Pailler, Delphine; Bard, Edouard (2002): High frequency palaeoceanographic changes during the past 140000 yr recorded by the organic matter in sediments of the Iberian Margin. Palaeogeography, Palaeoclimatology, Palaeoecology, 181(4), 431-452, doi:10.1016/S0031-0182(01)00444-8
Pailler, D; Bard, E (2002): (Table 1) Geochemical analytical data for sediment core MD95-2042. doi:10.1594/PANGAEA.96864, In Supplement to: Pailler, Delphine; Bard, Edouard (2002): High frequency palaeoceanographic changes during the past 140000 yr recorded by the organic matter in sediments of the Iberian Margin. Palaeogeography, Palaeoclimatology, Palaeoecology, 181(4), 431-452, doi:10.1016/S0031-0182(01)00444-8
Richter, T.O., Peeters, F.J.C. and van Weering, T.C.E., 2009. Late Holocene (0-2.4 ka BP) surface water temperature and salinity variability, Feni Drift, NE Atlantic Ocean. Quaternary Science Reviews, 28(19-20): 1941-1955.
Romero, O.E., Kim, J.-H. and Donner, B., 2008. Submillennial-to-millennial variability of diatom production off Mauritania, NW Africa, during the last glacial cycle. Paleoceanography, 23.
Romero, Oscar E (2008): Diatoms, opal, total organic carbon, calcium carbonate and sea surface temperature of sediment core GeoB7926-2. doi:10.1594/PANGAEA.701397
Ruhlemann, C., Mulitza, S., Muller, P.J., Wefer, G. and Zahn, R., 1999. Warming of the tropical Atlantic Ocean and slowdown of thermohaline circulation during the last deglaciation. Nature, 402(6761): 511-514.
Rühlemann, C et al. (1999): Sea surface temperature reconstruction based on alkenones of sediment core M35003-4. doi:10.1594/PANGAEA.734784, Supplement to: Rühlemann, Carsten; Mulitza, Stefan; Müller, Peter J; Wefer, Gerold; Zahn, Rainer (1999): Warming of the tropical Atlantic Ocean and slowdown of thermohaline circulation during the last deglaciation. Nature, 402(6761), 511-514, doi:10.1038/990069
Sachs, J.P., 2007. Cooling of Northwest Atlantic slope waters during the Holocene. Geophys. Res. Lett., 34(L03609).
Sachs, J.P., 2010.
Sarnthein, M. et al., 2003. Centennial-to-millennial-scale periodicities of Holocene climate and sediment injections off the western Barents shelf, 75°N. Boreas, 32(3): 447-461.
Schefuß, E et al. (2005): Sea surface temperature reconstruction of sediment core GeoB6518-1. doi:10.1594/PANGAEA.738200,

Supplement to: Schefuß, Enno; Schouten, Stefan; Schneider, Ralph R (2005): Climatic controls on central African hydrology during the last 20,000 years. Nature, 437, 1003-1006, doi:10.1038/nature03945
Schmidt, D.N., Renaud, S., Bollmann, J., Schiebel, R. and Thierstein, H.R., 2004. Size distribution of Holocene planktic foraminifer assemblages: biogeography, ecology and adaptation. Marine Micropaleontology, 50(3-4): 319-338.
Schmidt, MW et al. (2004): (Table SI-2) Stable oxygen isotope and Mg/Ca ratios of Globigerinoides ruber from sediment core V28-122. doi:10.1594/PANGAEA.716695,
In Supplement to: Schmidt, Matthew W; Spero, Howard; Lea, David W (2004): Links between salinity variation in the Caribbean and North Atlantic thermohaline circulation. Nature, 428, 160-163, doi:10.1038/nature02346
Schmidt, MW et al. (2004): (Table SI-2) Stable oxygen isotope and Mg/Ca ratios of Globigerinoides ruber from ODP Hole 165-999A.
doi:10.1594/PANGAEA.716694,
In Supplement to: Schmidt, Matthew W; Spero, Howard; Lea, David W (2004): Links between salinity variation in the Caribbean and North Atlantic thermohaline circulation. Nature, 428, 160-163, doi:10.1038/nature02346
Schneider, R.R., Müller, P.J. and Ruhland, G., 1995. Late Quaternary Surface Circulation in the East Equatorial South Atlantic: Evidence from Alkenone Sea Surface Temperatures. Paleoceanography, 10.
Sicre, M.A. et al., 2008. A 4500-year reconstruction of sea surface temperature variability at decadal time-scales off North Iceland. Quaternary Science Reviews, 27(21-22): 2041-2047.
Sikes, E.L. and Keigwin, L.D., 1994. Equatorial Atlantic Sea Surface Temperature for the Last 30 Kyr: A Comparison of U37 kâ€² , Î´18O and Foraminiferal Assemblage Temperature Estimates. Paleoceanography, 9.
Sikes, E.L. and Keigwin, L.D., 1996. A reexamination of northeast Atlantic sea surface temperature and salinity over the last 16 kyr. Paleoceanography, 11(3): 327-342.
Sikes, EL; Keigwin, LD (1994): Sea surface temperature estimation of sediment core 86014-12PC51. doi:10.1594/PANGAEA.729816,
Supplement to: Sikes, Elisabeth L; Keigwin, Lloyd D (1994): Equatorial Atlantic sea surface temperature for the last 30 kyr: A comparison of Uk37, d18O and foraminiferal assemblage temperature estimates. Paleoceanography, 9(1), 31-46, doi:10.1029/93PA02198
Skinner, L.C. and Elderfield, H., 2005. Constraining ecological and biological bias in planktonic foraminiferal Mg/Ca and Î´18Occ: A multispecies approach to proxy calibration testing. Paleoceanography, 20.
Sperling, M. et al., 2003. Black Sea impact on the formation of eastern Mediterranean sapropel S1? Evidence from the Marmara Sea. Palaeogeography, Palaeoclimatology, Palaeoecology, 190: 9-21.
Stein, R., Hefter, J., GrÃ¼tzner, J., Voelker, A. and Naafs, B.D.A., 2009. Variability of surface water characteristics and Heinrichâ€ like events in the Pleistocene midlatitude North Atlantic Ocean: Biomarker and XRD records from IODP Site U1313 (MIS 16â€“9). Paleoceanography, 24.
Stein, R et al. (2009): Alkenone, n-alkane and sea-surface temperature data determined at North Atlantic IODP Site U1313 (low-resolution record of MIS 1-5 and across terminations II and III). doi:10.1594/PANGAEA.714239,
In Supplement to: Stein, Ruediger; Hefter, Jens; Grützner, Jens; Voelker, Antje HL; Naafs, B David A (2009): Variability of surface water characteristics and Heinrich-like events in the Pleistocene midlatitude North Atlantic Ocean: Biomarker and XRD records from IODP Site U1313 (MIS 16 - 9). Paleoceanography, 24, PA2203, doi:10.1029/2008PA001639
Thornalley, D.J.R., Elderfield, H. and McCave, I.N., 2009. Holocene oscillations in temperature and salinity of the surface subpolar North Atlantic. Nature, 457(7230): 711-714.
Weldeab, S., Schneider, R. and Müller, P.J., 2007. Comparison of Mg/Ca- and alkenone-based sea surface temperature estimates in the fresh water–influenced Gulf of Guinea, eastern equatorial Atlantic. Geochemistry Geophysics Geosystems, 8(5): 10.

Weldeab, S., Schneider, R.R. and Kölling, M., 2006. Deglacial sea surface temperature and salinity increase in the western tropical Atlantic in synchrony with high latitude climate instabilities. Earth and Planetary Science Letters, 241(3-4): 699-706.

Weldeab, S., Schneider, R.R., Kolling, M. and Wefer, G., 2005. Holocene African droughts relate to eastern equatorial Atlantic cooling. Geology, 33(12): 981-984.

Weldeab, S et al. (2005): Mg/Ca ratios of Globigerinoides ruber of sediment core GeoB4905-4. doi:10.1594/PANGAEA.738242,
Supplement to: Weldeab, Syee; Schneider, Ralph R; Kölling, Martin; Wefer, Gerold (2005): Holocene African droughts relate to eastern equatorial Atlantic cooling. Geology, 33(12), 981-984, doi:10.1130/G21874.1

Weldeab, S et al. (2006): Sea surface temperature and salinity reconstruction of sediment core GeoB3129-1. doi:10.1594/PANGAEA.738284,
Supplement to: Weldeab, Syee; Schneider, Ralph R; Kölling, Martin (2006): Deglacial sea surface temperature and salinity increase in the western tropical Atlantic in synchrony with high latitude climate instabilities. Earth and Planetary Science Letters, 241, 699-706, doi:10.1016/j.epsl.2005.11.012

Zhao, M., Beveridge, N.A.S., Shackleton, N.J., Sarnthein, M. and Eglinton, G., 1995. Molecular stratigraphy of cores off northwest Africa: Sea surface temperature history over the last 80 ka. Paleoceanography, 10.

Zhao, M et al. (1997): (Table A2) Alkenones and calculated sea surface temperature of sediment core BOFS31/1K. doi:10.1594/PANGAEA.52712,
In Supplement to: Zhao, Meixun; Beveridge, N; Shackleton, Nicholas J; Sarnthein, Michael; Eglinton, Geoffrey (1995): Molecular stratigraphy, of cores off northwest Africa: Sea surface temperature history over the last 80 ka. Paleoceanography, 10(3), 661-675, doi:10.1029/94PA03354

Ziegler, M., Nurnberg, D., Karas, C., Tiedemann, R. and Lourens, L.J., 2008. Persistent summer expansion of the Atlantic Warm Pool during glacial abrupt cold events. Nature Geosci, 1(9): 601-605.

Ziegler, M et al. (2008): Paleorecords from MD02-2575 (Figure 2). doi:10.1594/PANGAEA.706301,
Supplement to: Ziegler, Martin; Nürnberg, Dirk; Karas, Cyrus; Tiedemann, Ralf; Lourens, Lucas J (2008): Persistent summer expansion of the Atlantic Warm Pool during glacial abrupt cold events. Nature Geoscience, 1, 601-605, doi:10.1038/ngeo277

Andersen, C., Koç, N., Jennings, A. and Andrews, J.T., 2004a. Nonuniform response of the major surface currents in the Nordic Seas to insolation forcing: Implications for the Holocene climate variability. Paleoceanography, 19.

Andersen, C., Koç, N., Jennings, A. and Andrews, J.T., 2004a. Nonuniform response of the major surface currents in the Nordic Seas to insolation forcing: Implications for the Holocene climate variability. Paleoceanography, 19: 16.

Andersen, C., Koç, N. and Moros, M., 2004b. A highly unstable Holocene climate in the subpolar North Atlantic: evidence from diatoms. Quaternary Science Reviews, 23(20-22): 2155-2166.

Bilodeau, G., de Vernal, A., Hillaire-Marcel, C. and Josenhans, H., 1990. Postglacial paleoceanography of Hudson Bay: stratigraphic, microfaunal, and palynological evidence. Canadian Journal of Earth Sciences, 27(7): 946-963.

Birks, C.J.A. and Koç, N., 2002. A high-resolution diatom record of late-Quaternary sea-surface temperatures and oceanographic conditions from the eastern Norwegian Sea. Boreas, 31(4): 323 - 344.

Bonnet, S., de Vernal, A., Hillaire-Marcel, C., Radi, T. and Husum, K., 2010. Variability of sea-surface temperature and sea-ice cover in the Fram Strait over the last two millennia. Marine Micropaleontology, 74(3-4): 59-74.

de Vernal, A., Henry, M, Jens Matthiessen, Peta J. Mudie, André Rochon, Karin P. Boessenkool, Frédérique Eynaud, Kari GrØsfjeld, Joël Guiot, Dominique Hamel, Rex Harland, Martin J. Head, Martina Kunz-Pirrung, Elisabeth Levac, Virginie Loucheur, Odile Peyron, Vera Pospelova, Taoufik Radi, Jean-Louis Turon, Elena Voronina, 2001. Dinoflagellate cyst assemblages as tracers of sea-surface conditions in the northern North Atlantic, Arctic and sub-Arctic seas: the new lsquo<I>n</I> = 677rsquo data base and its application for quantitative palaeoceanographic reconstruction. Journal of Quaternary Science, 16(7): 681-698.

de Vernal, A. and Hillaire-Marcel, C., 2006. Provincialism in trends and high frequency changes in the northwest North Atlantic during the Holocene. Global and Planetary Change, 54(3-4): 263-290.

de Vernal, A., Hillaire-Marcel, C., Turon, J.L. and Matthiessen, J., 2000. Reconstruction of sea-surface temperature, salinity, and sea-ice cover in the northern North Atlantic during the last glacial maximum based on dinocyst assemblages. Canadian Journal of Earth Sciences, 37(5): 725-750.

deMenocal, P., Ortiz, J., Guilderson, T. and Sarnthein, M., 2000. Coherent High- and Low-Latitude Climate Variability During the Holocene Warm Period. Science, 288(5474): 2198-2202.

Elderfield, H. and Ganssen, G., 2000. Past temperature and [delta]18O of surface ocean waters inferred from foraminiferal Mg/Ca ratios. Nature, 405(6785): 442-445.

Eynaud, F., Turon, J.L. and Duprat, J., 2004. Comparison of the Holocene and Eemian palaeoenvironments in the South Icelandic Basin: dinoflagellate cysts as proxies for the North Atlantic surface circulation. Review of Palaeobotany and Palynology, 128(1-2): 55-79.

Grøsfjeld, K. et al., 1999. Dinoflagellate cysts reflecting surface-water conditions in Voldafjorden, western Norway during the last 11 300 years. Boreas, 28(3): 403-415.

Hald, M. et al., 2007. Variations in temperature and extent of Atlantic Water in the northern North Atlantic during the Holocene. Quaternary Science Reviews, 26(25-28): 3423-3440.

Hald, M. and Aspeli, R., 1997. Rapid climatic shifts of the northern Norwegian Sea during the last deglaciation and the Holocene. Boreas, 26(1): 15-28.

Hald, M., Dokken, T. and Hagen, S., 1996. Palaeoceanography on the European arctic margin during the last deglaciation. Geological Society, London, Special Publications, 111(1): 275-287.

Hald, M. et al., 2004. Holocene paleoceanography and glacial history of the West Spitsbergen area, Euro-Arctic margin. Quaternary Science Reviews, 23(20-22): 2075-2088.

Hillaire-Marcel, C., de Vernal, A., Bilodeau, G. and Weaver, A.J., 2001. Absence of deep-water formation in the Labrador Sea during the last interglacial period. Nature, 410(6832): 1073-1077.

Hüls, M. and Zahn, R., 2000. Millennial-Scale Sea Surface Temperature Variability in the Western Tropical North Atlantic from Planktonic Foraminiferal Census Counts. Paleoceanography, 15.

Hüls, M; Zahn, R (2000): Sea surface temperature reconstruction for sediment core M35003-4 in the western tropical North Atlantic. doi:10.1594/PANGAEA.734153, Supplement to: Hüls, Matthias; Zahn, Rainer (2000): Millennial-scale sea surface temperature variability in the western tropical North Atlantic from planktonic foraminiferal census counts. Paleoceanography, 15(6), 659-678, doi:10.1029/1999PA000462

Jiang, H., Eiriksson, J., Schulz, M., Knudsen, K.-L. and Seidenkrantz, M.-S., 2005. Evidence for solar forcing of sea-surface temperature on the North Icelandic Shelf during the late Holocene. Geology, 33(1): 73-76.

Jiang, H., Ren, J., Knudsen, K., Eiríksson, J. and Ran, L., 2007. Summer sea-surface temperatures and climate events on the North Icelandic shelf through the last 3000 years. Chinese Science Bulletin, 52(6): 789-796.

Jiang, H., Seidenkrantz, M.-S., Knudsen, K.L. and Eriksson, J., 2002. Late-Holocene summer sea-surface temperatures based on a diatom record from the north Icelandic shelf. The Holocene, 12(2): 137-147.

Jón Eiríksson, K.L.K.H.H.J.H., 2000. Chronology of late Holocene climatic events in the northern North Atlantic based on AMS C dates and tephra markers from the volcano Hekla, Iceland. Journal of Quaternary Science, 15(6): 573-580.

Kallel, N., Paterne, M., Labeyrie, L., Duplessy, J.-C. and Arnold, M., 1997. Temperature and salinity records of the Tyrrhenian Sea during the last 18,000 years. Palaeogeography, Palaeoclimatology, Palaeoecology, 135(1-4): 97-108.

Kiefer, Thorsten; Sarnthein, Michael (1998): Stable isotope data of Cibicidoides wuellerstorfi of sediment core GIK15612-2. doi:10.1594/PANGAEA.55942

Kiefer, Thorsten; Sarnthein, Michael (1998): Age model of sediment core GIK15637-1. doi:10.1594/PANGAEA.203894

Koc, N. and Jansen, E., 1994. Response of the high-latitude Northern Hemisphere to orbital climate forcing: Evidence from the Nordic Seas. Geology, 22(6): 523-526.

Koç, N., Jansen, E. and Haflidason, H., 1993. Paleoceanographic reconstructions of surface ocean conditions in the Greenland, Iceland and Norwegian seas through the last 14 ka based on diatoms. Quaternary Science Reviews, 12(2): 115-140.

Levac, E., 2001. High resolution Holocene palynological record from the Scotian Shelf. Marine Micropaleontology, 43(3-4): 179-197.

Levac, E., de Vernal, A. and Weston Blake, J., 2001. Sea-surface conditions in northernmost Baffin Bay during the Holocene: palynological evidence. Journal of Quaternary Science, 16(4): 353-363.

Marchal, O. et al., 2002. Apparent long-term cooling of the sea surface in the northeast Atlantic and Mediterranean during the Holocene. Quaternary Science Reviews, 21(4-6): 455-483.

Martinez, J.I., Mora, G. and Barrows, T.T., 2007. Paleoceanographic conditions in the western Caribbean Sea for the last 560 kyr as inferred from planktonic foraminifera. Marine Micropaleontology, 64(3-4): 177-188.

Melki, T. et al., 2009. Abrupt climate change, sea surface salinity and paleoproductivity in the western Mediterranean Sea (Gulf of Lion) during the last 28 kyr. Palaeogeography Palaeoclimatology Palaeoecology, 279(1-2): 96-113.

Nyberg, J., 2002. Luminescence intensity in coral skeletons from Mona Island in the Caribbean Sea and its link to precipitation and wind speed. Philosophical Transactions of the Royal Society of London Series a-Mathematical Physical and Engineering Sciences, 360(1793): 749-766.

Peyron, O. and de Vernal, A., 2001. Application of artificial neural networks (ANN) to high-latitude dinocyst assemblages for the reconstruction of past sea-surface conditions in Arctic and sub-Arctic seas. Journal of Quaternary Science, 16(7): 699-709.

Siani, G. et al., 2001. Mediterranean Sea Surface Radiocarbon Reservoir Age Changes Since the Last Glacial Maximum. Science, 294(5548): 1917-1920.

Sikes, E.L. and Keigwin, L.D., 1994. Equatorial Atlantic Sea Surface Temperature for the Last 30 Kyr: A Comparison of $U^{k37'}$ , $\delta^{18}O$ and Foraminiferal Assemblage Temperature Estimates. Paleoceanography, 9.

Sikes, EL; Keigwin, LD (1994): Sea surface temperature estimation of sediment core 86014-12PC51. doi:10.1594/PANGAEA.729816, Supplement to: Sikes, Elisabeth L; Keigwin, Lloyd D (1994): Equatorial Atlantic sea surface temperature for the last 30 kyr: A comparison of Uk37, d18O and foraminiferal assemblage temperature estimates. Paleoceanography, 9(1), 31-46, doi:10.1029/93PA02198

Solignac, S., de Vernal, A. and Giraudeau, J., 2008. Comparison of coccolith and dinocyst assemblages in the northern North Atlantic: How well do they relate with surface hydrography? Marine Micropaleontology, 68(1-2): 115-135.

Solignac, S., de Vernal, A. and Hillaire-Marcel, C., 2004. Holocene sea-surface conditions in the North Atlantic--contrasted trends and regimes in the western and eastern sectors (Labrador Sea vs. Iceland Basin). Quaternary Science Reviews, 23(3-4): 319-334.

Toledo, F.A.L., Costa, K.B. and Pivel, M.A.G., 2007. Salinity changes in the western tropical South Atlantic during the last 30 kyr. Global and Planetary Change, 57(3-4): 383-395.

Voronina, E., Polyak, L., Vernal, A.D. and Peyron, O., 2001. Holocene variations of sea-surface conditions in the southeastern Barents Sea, reconstructed from dinoflagellate cyst assemblages. Journal of Quaternary Science, 16(7): 717-726.

Waelbroeck, C. et al., 1998. Improving Past Sea Surface Temperature Estimates Based on Planktonic Fossil Faunas. Paleoceanography, 13.